Northumbria Research Link

Northumbria University NEWCASTLE

University Library

CIRCULAR POLARISED MICROSTRIP ANTENNA DESIGN USING SEGMENTAL METHODS

ENG GEE LIM

Division of Electrical and Electronic Engineering

School of Engineering

University of Northumbria at Newcastle, U.K.

A thesis submitted in partial fulfilment

of the requirements of the

University of Northumbria at Newcastle

for the degree of Doctor of philosophy

August 2002

ABSTRACT

Research into the modelling and analysis of microstrip patch antenna have been reported in many studies. These include Transmission Line Modelling, Cavity Modelling, Coplanar Multiport Modelling and Full wave Modelling. Since the electromagnetic field elements are time harmonic, the phasor-form of the Maxwell field equations is used. In this thesis results are presented of the research that has been carried out into the segmental approach for the analysis of the microwave patch antennas. The segmental approach includes the "Segmentation" and the "Desegmentation" methods.

In the segmentation method two distinct structural forms have been identified, cascade and shunt types. In the cascade type all consecutive segment elements share a common boundary, while for the shunt type, all appended segment elements have no common boundary. In the case of the shunt type structure a generalised input impedance matrix formula, for any number of appended segment elements, has been obtained. For the desegmentation method a generalised input impedance for any number of deleted segment elements, has been obtained.

The above research studies have been applied in the design of a circular polarised two corner deleted square patch microstrip antenna with a single feed. For this structure the design involves both square and triangular patch geometries. The overall patch geometry for circular polarised is determined using perturbation analysis to determine the size of the deleted triangular segment elements.

New computationally efficient impedance coupling expressions for the interconnecting port impedances on a rectangle, and, on a right angled isosceles triangle shaped antenna patch have been derived. In the determination of the input impedance of the overall antenna structure the coupling impedances constitute the elements of the individual segment coupling matrices. The matrices are used in a general multiport matrix circuit analysis to obtain the input impedance formula. It is established that, where applicable, the desegmentation method is computationally more efficient than the segmentation method. The new results obtained have been applied to the design of a corner deleted square patch antenna, and, the design procedure is fully described.

The computer program implementation evaluates the perturbation quantity, and, the antenna input impedance. The structural properties of the coupling matrices, which are used for efficient computation, are described in detail. All the results from the above work show close agreement with full-wave software simulation and practical results.

SIGNIFICANT RESEARCH ACHIEVEMENTS:

❖ Both segmentation and desegmentation methods have been studied and it has been shown that the desegmentation approach, when applicable, is in general significantly more computationally efficient.

❖ In the segmentation method two structural forms, cascade and shunt have been identified. In the latter case a new generalised input impedance matrix formula has been obtained for any number of appended segment elements.

❖ A new generalised input impedance matrix formula has been obtained for any number of deleted segment elements in the desegmentation method.

❖ New computationally efficient expressions for the coupling impedances have been derived and used in test applications.

❖ New computationally efficient expressions for the offset input impedance of a linear polarised rectangular patch, and, an isosceles right-angled triangular patch have been derived and experimentally verified.

❖ A program implementing the design procedure for the corner-deleted truncated square patch circular polarised microstrip antenna has been constructed using MATHCAD programming.

The research carried out has produced the following original work. Seven refereed research papers in the area of microstrip antenna design have been published or accepted.

1. B.Aljibouri, E.G.Lim, H.Evans and A.Sambell, "Multiobjective genetic algorithm approach for a dual-feed circular polarised patch antenna design", Electronics Letters, Vol.36, No.12, pp.1005-1006, 8th Jun 2000.

2. H.Evans, E.G.Lim, P.Gale, B.Aljibouri, E.Korolkeiwicz and A.Sambell, "Application of simulated annealing to design of serial feed sequentially rotated 2x2 antenna array", Electronics Letters, Vol.36, No.24, pp.1987-1988, 23th Nov 2000.

3. B.Al-Jibouri, H.Evans, E.Korolkiewicz, E.G.Lim, A.Sambell and T.Vlasits,: "Cavity model of circularly polarised cross-aperture-coupled microstrip antenna", IEE Proceeding Microwave Antennas propagation, Vol.148, No.3, Pp.147-152, June 2001.

4. M.Mathian, E.Korolkewicz, P.Gale, E.G.Lim,: "Design of a Circularly Polarized 2×2 Patch Array 2.45 GHz ISM Band", Microwave Journal, May 2002.

5. E. G. Lim, E. Korolkiewicz, S. Scott, A. Sambell and B.Aljibouri,: "An Efficient Formula for the Input Impedance of a Microstrip Right-angled Isosceles Triangular Patch Antenna", IEEE Antenna and Wireless propagation letters (has been accepted, Feb 2002).

6. E. G. Lim, S. Scott and E. Korolkiewicz,: "An application of closed forms of infinite series", International Journal of Mathematical Education in Science and Technology (has been accepted, April 2002).

7. Yi Qin, E. G. Lim, E. Krolkiewicz,: "Design of a Microstrip Offset Feed Circular Polarized Nearly Square Patch Antenna Operating at 2.45GHz", IEE Electronics Letters(has been accepted, July 2002).

ACKNOWLEDGEMENTS

ABBREVIATIONS

AVA	Automatic Vehicle Access
RSU	Road Side Unit
OBU	On Board Unit
ASK	Amplitude Phase keying
PSK	Phase Shift Keying
IRM	Image Rejection Mixer
TLM	Transmission Line Model
c	$3 \times 10^{8}\ m/s$
μ_0	$4\pi \times 10^{-7}$
ε_0	8.854×10^{-12}
σ_c	Conductivity of Copper 5.7×10^{7} S/M
f_0	$2.45\ GHz$ Design Frequency
ε_r	Dielectric Constant
ε_{eff}	Effective Dielectric Constant
h	Thickness of Substrate
k_0	Wave Number in Free Space
Q	Unloaded Q - factor
W	Width of the Feed Line
T	Offset Feed Line Position
N	Number of Ports
$N1$	Upper Summation Limit of Infinite Series
$M1$	Upper Summation Limit of Infinite Series

TABLE OF CONTENTS

Chapter 5: COPLANAR MULTIPORT CIRCUIT ANALYSIS

Chapter 6: MULTIPORT SEGMENTATION AND DESEGMENTATION MODELLING OF COMPOSITE STRUCTURES

Chapter 7: DERIVATION OF EFFICIENT IMPEDANCE COUPLING FORMULAS BETWEEN PORTS ON A RECTANGULAR PATCH

CHAPTER 1

INTRODUCTION AND OVERVIEW OF THESIS

1.1 Introduction

The Centre for Communication System Research at the University of Northumbria at Newcastle is involved in the research and development of a microwave digital system to be used in a variety of traffic management systems. The main focus of the centre is in automatic tolling and automatic access for the vehicle to restricted areas.

In response to the integrated transport White Paper 2000, there is also a requirement for local authorities to restrict traffic in urban areas, and produce more pedestrianised city centres [1,2]. However, Automatic Vehicle Access (AVA) is still required for emergency vehicles, public transport, taxis and commercial deliveries. Consequently, there is a need for automatic control of vehicle access involving reliable and accurate vehicle identification, which is needed by universities, hotels, private businesses and local authorities.

As part of this research several detailed studies of the system and the antenna design have been carried out by the members of the Research Group. This research has included (a) the design of a short range digital data communication system between a moving vehicle and a Road-Side Unit(RSU) [3], (b) investigation into the integration of microwave patch antennas on vehicle windscreens[4], (c) the modelling of single feed slot antennas to be used in the vehicle On-Board Unit(OBU)[5] ,and, (d) the modelling of a cross-aperture coupled single feed patch antenna[6].

1

For vehicle to RSU communication the OBU normally is placed behind the vehicle windscreen. It is important that the antenna is small in profile and inexpensive to manufacture. These requirements are best achieved using a microstrip patch antenna structure in each of the above applications. The total unit consists of a microstrip antenna and the associated circuitry which is required for ASK demodulation and PSK modulation. Further, and, importantly, circular polarisation is essential so that the OBU can be placed in any orientation behind the vehicle's windscreen.

This thesis presents research carried out using perturbation analysis to determine the area of perturbation to achieve circular polarisation. Further the segmental approach is used to evaluate the input impedance of a composite microstrip antenna structure. In the segmental approach a coplanar multiport analysis is used to connect the impedances of the segments composing the structure with the overall impedance of the antenna.

New computationally efficient expressions have been derived for the elements of the interport coupling matrices in respect of both the rectangular patch and the right-angled isosceles triangle patch.

For both the segmentation and desegmentation methods new generalised input impedance expressions have been obtained for any number of appended/deleted segments.

The research presented covers the theoretical design analysis and practical measurements for a single feed truncated corners square patch circular polarised

antenna. An operation frequency of 2.45GHz has been used in the design of the microwave circuitry throughout this thesis. This operational frequency is used in the design of short range digital communication systems such as in traffic application.

The overview of the research carried out is presented in the following section.

1.2 Overview of thesis

In chapter two the basis of the short-range prototype microwave system developed for automatic debiting application in vehicle tolling and car park access is discussed. The operation of a microwave system to be used in traffic applications is described with block diagrams showing the communications operation between the RSU and the OBU. The circuit diagram of the wake-up tag is presented. A listing illustrating the possibilities with different remote identification technologies is tabulated.

In chapter three various modelling approaches and methods of analysis for the microstrip antenna are described. A new computationally efficient expression for the input impedance of the rectangle patch with offset feed is derived and applied to obtain impedance-frequency graphs, and, the variation of impedance with respect to feed location. A new computationally efficient expression for the input impedance of a microstrip right angled isosceles triangular patch antenna is derived and applied to obtain impedance values in respect of feed locations on both a vertical edge, and, on the hypotenuse edge. The electric field conditions for circular polarisation are given and possible feed arrangements required to generate circular polarised radiation are described.

In chapter four the perturbation analysis and the equivalent circuit model of Haneishi [7] are employed to determine the proportional amount of perturbation necessary for circular polarisation in respect of a truncated corner square patch antenna. The eigenvalues and eigenfunctions for a square patch are obtained. These are then applied in a variational analysis to obtain the dominant eigenvalues and normalised eigenfunctions of the corner truncated patch from which the dominant components of electric voltage are obtained. By means of an equivalent circuit of the antenna model the voltage amplitude and phase conditions necessary for circular polarisation are applied to obtain the amount of corner deleted perturbation required.

In chapter five a microstrip antenna patch is treated as a planar circuit on which the voltage at any point satisfies a non-homogeneous wave equation. The solution of the associated boundary value problem giving the voltage in terms of a probe feed current density is obtained using the eigenfunction expansion method. This introduces the Green's function of the patch geometry. It is shown that a perimeter microstrip feed is equivalent to a probe feed with the same line current density. The coupling impedance between two perimeter ports is defined and the general formula for the coupling impedance in terms of the associated Green's function is derived.

In chapter six the role of the multiport structure in preserving the overall surface current distribution on the antenna is discussed and it is shown that when the patch geometry is constructed from a combination of regular shapes, such as rectangles and some triangles, it is possible to determine the antenna input impedance analytically. This is possible because the Green's functions of the regular shaped component geometries are known analytically. The 'segmentation method' and 'desegmentation

method' are the two segmental methods, using the multiport modelling structure, which may be employed to obtained the feed input impedance of the antenna. In these methods connecting ports are introduced between the regular shaped segments and a multiport analysis applied to obtain the overall characteristic of the combined structure. Both methods and their analysis for the input impedance are presented in this chapter. In the segmentation method two distinct structural forms have been identified, cascade and shunt types. In the cascade-type all consecutive segment elements share a common boundary, while for the shunt-type, all appended segment elements have no common boundary. . In respect of the segmentation method explicit formulas for combining two and three cascade-type segments are derived. In the case of the shunt-type structure a generalised input impedance matrix formula, for any number of appended segment elements, has been obtained. For the desegmentation method a generalised input impedance for any number of deleted segment elements, has been obtained. These are an important new results. It is established that the 'desegmentation' approach, when applicable is computationally more efficient than the 'segmentation' approach.

In chapter seven closed forms of infinite series are used to obtain efficient impedance coupling expressions between the perimeter ports on a rectangular patch. Three cases are considered: (a) two ports on the same side (b) two ports on adjacent sides (c) two ports on opposite sides. In the derivation, the required term by term double integration of the Green's function gives, initially, an impedance formula which consists of a single term, two single infinite series, and, one double infinite series. The single infinite series are summed to closed form, while the double infinite series is reduced to a single infinite series. Numerical trials using the new expressions have shown that

in all the cases considered only one term of the series is required to give convergence to three significant figures. In the worst case convergence to five significant figures requires at most 4 terms of the series, and, for convergence to seven significant figures 10 terms at most are required. The result of test applications for each of the three configurations considered are given in this chapter, and, are found to be in good agreement with Ensemble™ (Full wave analysis software).

In chapter eight efficient impedance coupling expressions between the perimeter ports on a right angled isosceles triangle patch are obtained. Four cases are considered: (a) two ports on a vertical side, (b) two ports on adjacent vertical horizontal sides, (c) one port on a vertical side and one port on the hypotenuse, and (d) two ports on the hypotenuse. In the derivation, the required term by term double integration of the Green's function produces, initially, an impedance formula which consists of a constant term, and, several single and double infinite series. The single infinite series are summed to close form, while, for coupling ports not involving the hypotenuse the double series is reduces to a single infinite series. For coupling ports involving the hypotenuse the double infinite series cannot be reduced to a single infinite series. However, the double series can be economised by extracting the diagonal terms which can be summed to closed form. The remaining terms, by symmetry, can then be expressed in the form of semi-infinite double series for which the summation indices are $m \geq 1$, $n \geq m+1$. Numerical trials show that in the worst case convergence to seven significant figures an upper summation index of 9 at most, is required. The results of test applications for each of the four configurations considered are given in this chapter, and, are found to be in good agreement with Ensemble™.

In chapter nine a design procedure for a circular polarised microstrip antenna is described. A program for the desegmentation method applied to the corner deleted square patch is constructed to evaluate the perturbation $(\Delta S/S)$, and, the antenna input impedance (Zin). The structural properties of the coupling matrices involved are described and results are used to produce a computationally efficient program.

CHAPTER 2

REVIEW OF A TWO WAY COMMUNICATION SYSTEM FOR TRAFFIC APPLICATION

2.1 Introduction

The Centre for Communication System Research at the University of Northumbria at Newcastle is involved in the research and development of the microwave data-link for vehicle tolling and car park access. The main requirements in implementing a two-way short range communication system are the efficiency, reliability and size of the system. It is also necessary to satisfy the requirements of both the range and region of communication. Also in respect of above applications the system must be capable of checking on every vehicle to ensure that the appropriate fees are charged and it must also provide a method by which traffic violators may be identified.

2.2 System Requirements

For security reasons expensive control equipment, such as the host computer, could need to be housed remotely.

The user identification tag must be of reasonable size (50x40x50mm, approximately the size of a credit card) with acceptable battery life of about five years.

The system must be capable of interfacing with existing technologies and allowing for the possibility of retrofitting. For example in applications to vehicle barrier control systems.

The systems must be capable of supporting a variety of user and operator displays (monitor and LED display).

The control panel needs to inform the operator of the systems status as well as fault and alarm conditions. This panel must also provide an override facility capability. The system design must be adaptable to increases in both the number of uses, and , user activity.

The system may be required to control the flow of traffic both entering and leaving a restricted area. Physical entry and exit of vehicles to this area is controlled by various types of barriers including hydraulic bollards or sleeping policemen. User identification is achieved with the use of a tag from within the confines of the vehicle. This tag can be either manually operated with the use of a 'push button tag' or operated automatically with no user intervention, using a ' wake up tag'.

User authorisation must be obtained before access is granted. This will depend on the correct user identification and the fee-credit standing of the user. The system must be capable of integrating with other technologies to aid correct vehicle identification. In future the system may be required to cross check the On-Board-Unit (OBU) identifier with the vehicle number-plate.

The vehicle is controlled by traffic lights and by driver information shown on an LED dot display mounted above the road. This allows comprehensive information to be passed to the user. Such information includes:
- Please wait for the barrier to open
- Please proceed
- Access denied
- Car park full

If a vehicle approach speed is not controlled this could lead to a dangerous situation if access was unexpectedly denied. Therefore traffic calming measures, such as speed ramps, should be used to ensure that a safe approach speed is always maintained.

A typical scenario is illustrated in figure 2.2.1 below:
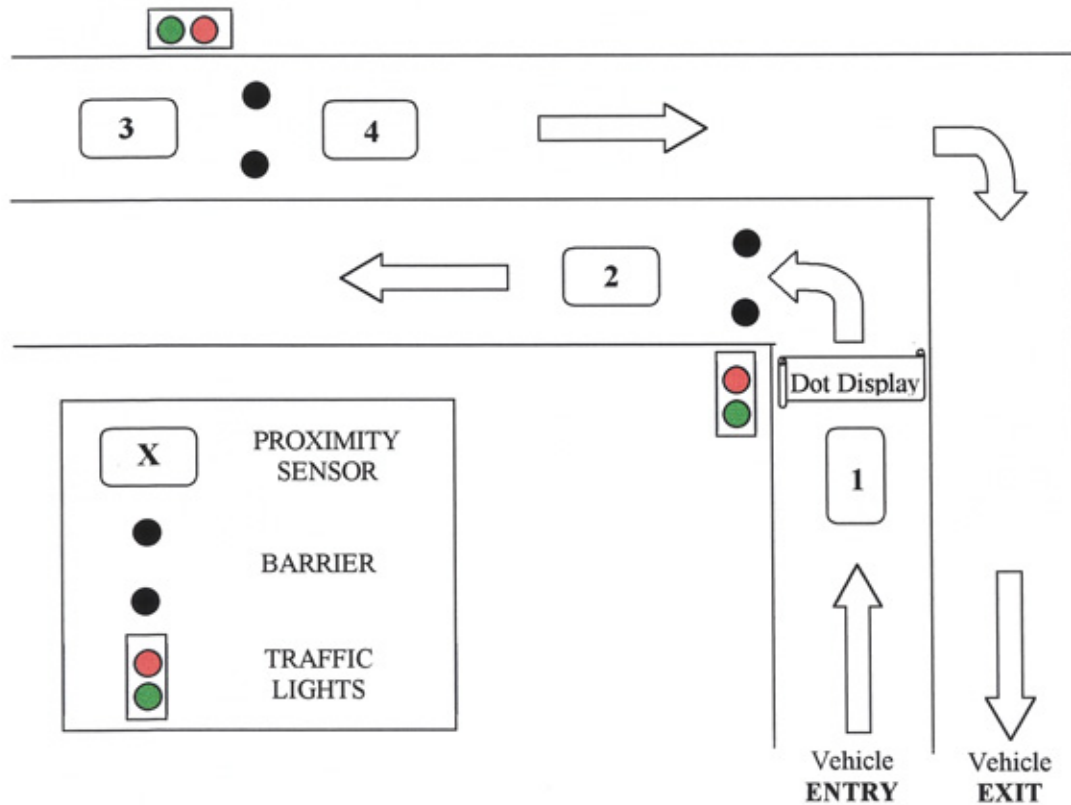
Figure 2.2.1: Typical layout for a car park Entrance/ Exit

To maintain safe operation the vehicle must wait for the barrier to have opened completely before passing. Therefore the traffic light must remain red until the barrier is fully open. Once green the traffic light must return to red as soon as the vehicle leaves the first entry sensor (sensor 1) to stop the vehicle behind from proceeding. Furthermore the vehicle must have fully passed over the barrier before it begins to close. This sequence must only recommence once the barrier has fully closed.

Consequently, for peak periods and emergencies, an override must be available to keep the barrier permanently open and the traffic lights green.

In respect of car parking the system must be able to record the immediate occupancy, the ID of each vehicle, and, the arrival and departure times. For general traffic movement the system must be able to log the traffic density and the total volume of traffic over given period. This information should be available to an operator both on screen and in the form of a hardcopy and hence it is proposed to use a PC rather than PLC as the host computer. The advantages of a PC also include:

- Interfacing with external data source

- Driving user display such as dot signs

- Maintaining comprehensive on site log/records

- The flexibility to offer optional operator-on-site control (display and keyboard)

- Can be remotely located up to 100m from site with a standard cable.

2.3 Operation of the microwave system

The microwave communication link between the vehicle and the reader is designed to produce an error free communication zone so that an ID number which is stored in the OBU can be received at the roadside-unit (RSU). It is essential that the OBU has a low profile so that it can be conveniently located behind the windscreen of the vehicle. Further it must be inexpensive and this is achieved by transferring the need for "OBU transmission power" from the OBU to the RSU. That is the RSU transmission both alerts the OBU, and, enables the OBU to re-radiate its communication signal up to the RSU as shown in figures 2.3.1.
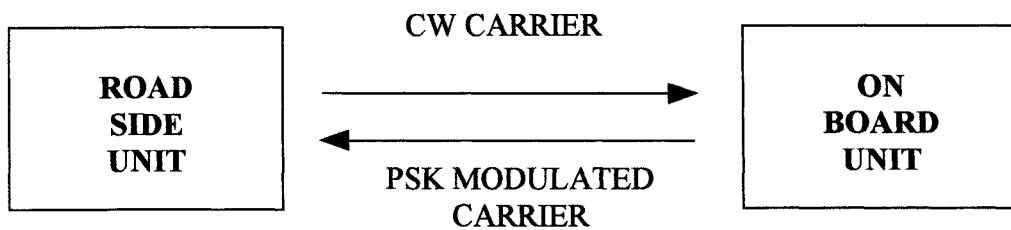
Figures 2.3.1: Operation of the microwave system

2.4 Design of the Road-Side Unit (RSU)

A block diagram of the RSU is shown in figure 2.4.1.
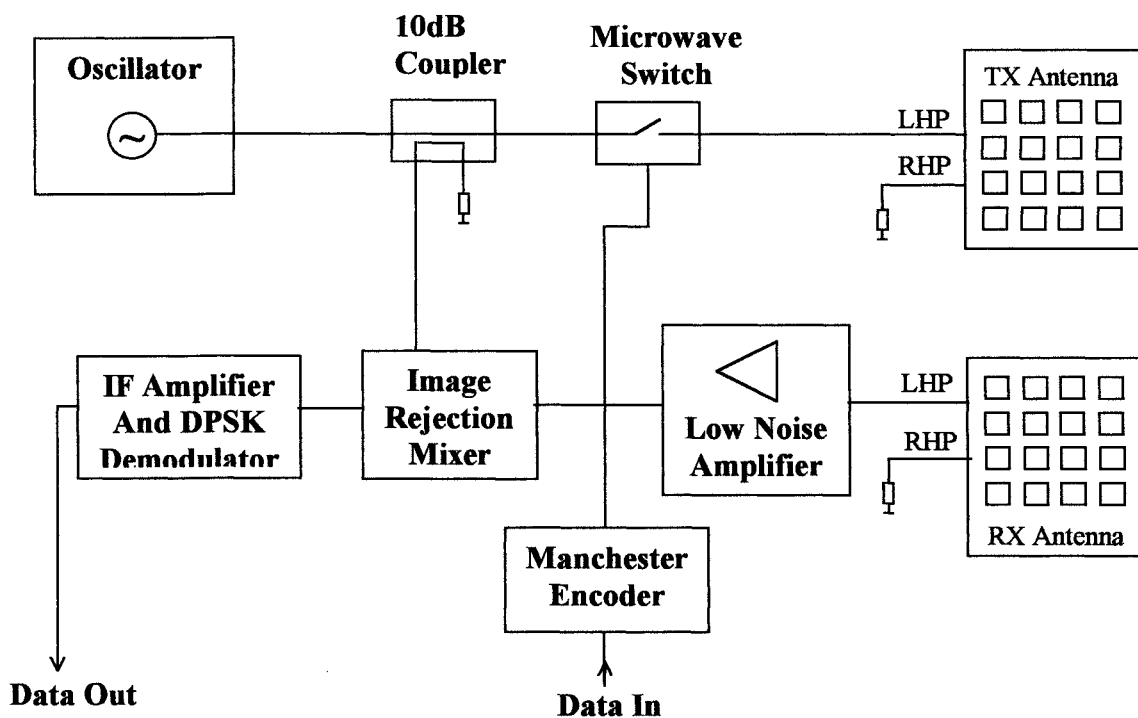
Figure 2.4.1: A block diagram of the RSU

A stable, low phase noise dielectric resonator oscillator is used as a microwave source

at the RSU in order to meet the European standards so as not to cause interference to

other systems using nearby frequencies. The RSU antenna consists of two, four by four microstrip antennas having a beam width of 16°.

Two antennas are required at the RSU, as one is used to transmit a Continuous carrier Wave (CW) carrier while the other is used to receive the PSK(Phase Shift Keying) modulated signal from the OBU. Circular polarisation is used to minimise the effects of multi-path reflections from the vehicle bonnet and to ensure that the physical orientation of the OBU behind the windscreen in not critical. Left-hand polarisation is used for both the CW signal and the PSK signal and this simplifies the design of the OBU antenna. In normal operation the microwave switch is closed so that the RSU transmits a CW signal which is PSK modulated at the OBU using a DPSK 1 MHz sub-carrier, before being re-radiated back to the RSU. The 1 MHz sub-carrier is used to reduce the effect of '1/f' flicker noise. At the RSU, the receivers PSK signal is initially amplified by a low-noise amplifier before been fed it to an Image Rejection Mixer (IRM). It is not possible to use a conventional mixer at the RSU as the phase of the incoming signal is constantly changing due to the movement of the vehicle. The IRM mixer rejects one of the side-bands and converts the other side-band to an IF frequency of 1 MHz which is then amplified and limited by the IF amplifier. The data is then coherently recovered with a squaring loop.

2.5 Design of the On Board Unit (OBU)

A block diagram of the OBU is in figure 2.5.1.
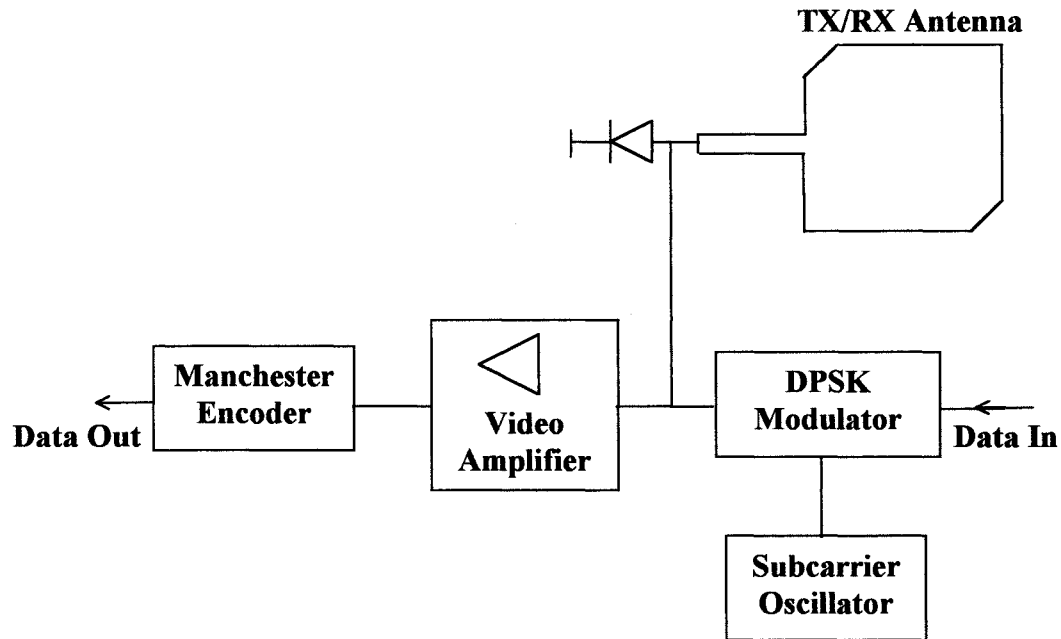
Figure 2.5.1: A block diagram of the OBU

The complexity of the OBU can be kept to a minimum using a single polarised TX/RX microstrip square patch antenna and a single diode for PSK modulation. Circular polarisation is currently achieved by feeding the square patch antenna with two signals 90° out of phase to generate two orthogonal modes in the patch. In this design the 90° phase shift is produced by a power splitter in which the length of lines differ by $\lambda/4$ as shown in figure 2.5.2. In the future, this antenna design will be replaced by a single fed two corner-deleted circular polarised microstrip square patch antenna as shown in figure 2.5.3. This antenna design can effectively reduce the dimension of the antenna and hence reduce the size of the OBU.
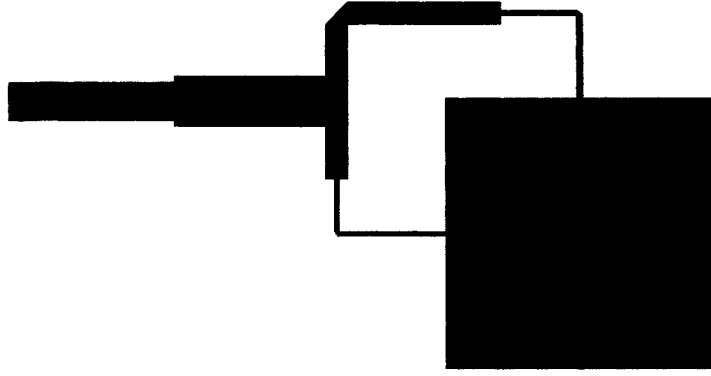
Figure 2.5.2: Current OBU antenna

Figure 2.5.3: New OBU antenna

2.6 Design of the Wake-up Tag

The circuits diagram of the wake-up tag is shown in figure 2.6.1 where the wake-up

CW signal received from the RSU is detected by one of the diodes, while the other

diode provides a reference voltage. The difference in the voltages across the two

diodes is then fed into an operation amplifier. The second reference diode is used to

overcome the problems of variation of temperature. Normally the Tag is in the sleep

mode using only a standby current of 10mA. When the tag receives a signal from

RSU, the voltage difference across the diode drops by 20mV, and the 3V CMOS

voltage level is generated by the operation amplifier comparator, and this wakes up

the PIC processor. The Tag also contains a manual wakeup switch as an alternative or

a back up process.

TX/RX Antenna
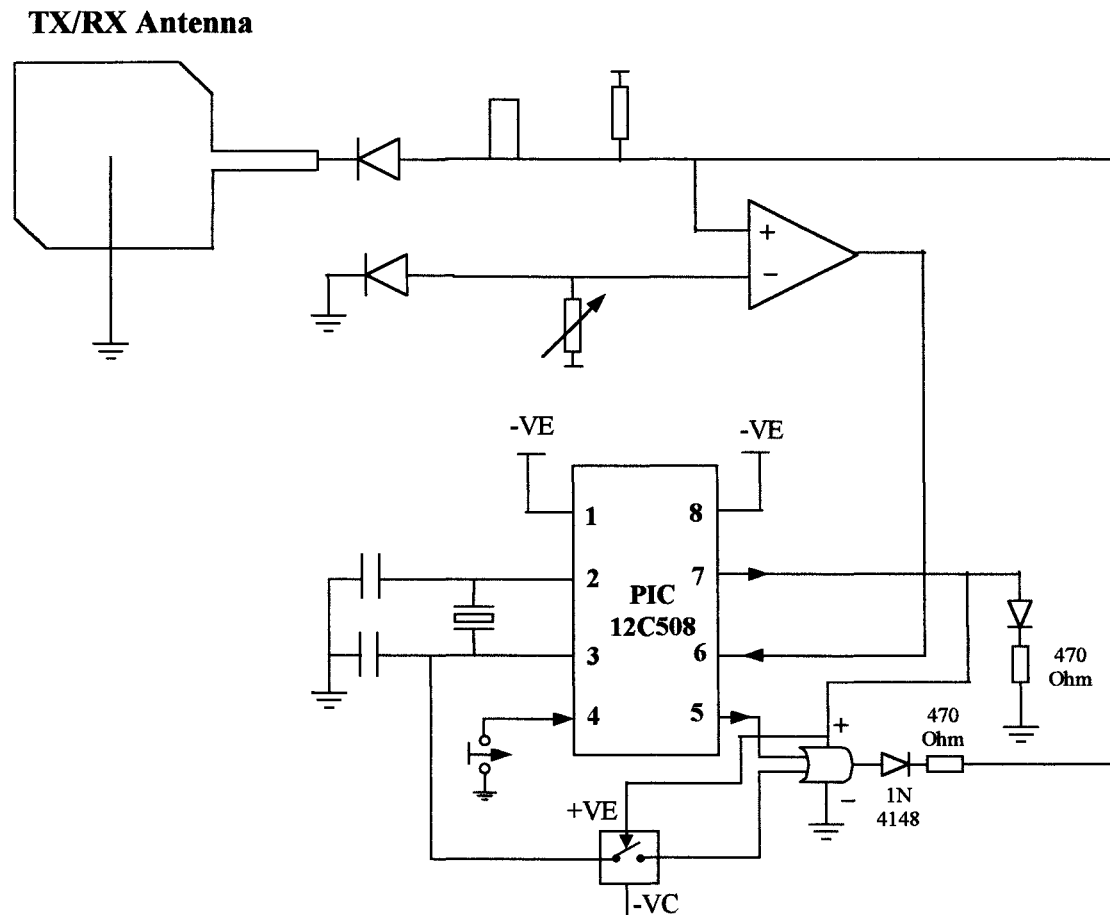
Figure 2.6.1: Circuit diagram of the wake-up tag

2.7 Contactless identification technologies

The following table illustrates a comparison of the possibilities with different remote

identification technologies. It should be noted that all manufacturers do not provide

every function.

Contactless ID technologies	high frequency (2.45 GHz)	low frequency (125 kHz, 13.5 MHz)	bar code (Code 39)	infrared ("TV remote control")
Parameter				
Reading range	very good	moderate	moderate	very good
Passage speed	very high	low	moderate	high
Read-write data carriers	yes	yes	no	yes
Directional readers	yes	no	yes	yes
Reads through glass, clothes, wood etc	yes	yes	no	no
Resistance against dirt	good	good	low	low
Resistance against wear	good	good	moderate	good
Resistance against interference	good	low	good	good
Reading of multiple data carriers	yes	yes	no	yes
Readers close to each other	yes	no	yes	no
Insensitive to metal mounting	yes	no	yes	yes
Reader cost	moderate	low	low	moderate
Data carrier cost	moderate	low	very low	high

Table 2.7.1: Comparison of the different remote identification technologies

Summary

The basis of the short-range prototype microwave system developed for automatic debiting application in the vehicle tolling and car park access has been discussed. The operation of a microwave system to be used in traffic applications is described. Block diagrams showing the communications operation between the RSU and OBU have been presented. The circuit diagram of the wake-up tag has been described. A listing illustrating the possibilities with different remote identification technologies has been tabulated.

CHAPTER 3

REVIEW FOR THE DESIGN AND MODELLING OF RECTANGULAR AND TRIANGULAR MICROSTRIP PATCH ANTENNAS

3.1 Introduction

A microstrip antenna is different from conventional antennas such as wire aerials and the waveguide configurations. The patch antenna consists of a metalised deposit on a plane dielectric substrate which allows for a very thin printed-conductor topology of any shape.

Microstrip antennas have several advantages compared to conventional microwave antennas and therefore are used in many applications over the broad frequency range. Some of the principal advantages of microstrip antennas compared to conventional microwave antennas are[1]:

- lightweight, compact, low profile planar configurations which can be made conformal

- low fabrication cost and amenable to mass production

- can be made ultra-thin, and hence, they do not perturb the aerodynamics of host aerospace vehicles

- the antennas may be easily mounted on missiles, rockets and satellites without major alterations

- linear, circular (left hand or right hand) polarisations are possible with simple changes in feed position

18

- simultaneous dual frequency antennas are easily made

- microstrip antennas are compatible with modular designs (solid state devices such as oscillators, amplifiers, variable attenuators, switches, modulators, mixers, phase shifters etc. which can be added directly to the antenna substrate board)

- feed lines and matching networks are fabricated simultaneously with the antenna structure

However, microstrip antennas also have some disadvantages compared to conventional microwave antennas including:

- narrow bandwidth (high Q factor)

- losses due to copper and dielectric, hence somewhat lower gain

- most microstrip antennas radiate into a half-plane

- practical limitations on the maximum gain (~ 20dB)

- poor isolation between the feed and the radiating elements which can be reduced using slot feed arrangement

- possibility of excitation of surface waves

- lower power handling capability

In this chapter, various modelling approaches and methods of analysis for the microstrip antenna are described in section 3.2. A new computationally efficient expression for the input impedance of the rectangle patch with offset feed is derived in section 3.3.1 and applied to obtain impedance-frequency graphs, and, the variation of impedance with respect to feed location. A new computationally efficient expression for the input impedance of a microstrip right angled isosceles triangular patch antenna is derived in

section 3.3.2 and applied to obtain impedance values in respect of feed locations on both

a vertical edge, and, on the hypotenuse edge. In section 3.4 the electric field condition for

circular polarisation is described together with possible feed arrangements required to

generate circular polarised radiation.

3.2 Antenna Modelling and Analysis

Various approaches, of varying complexity, for the analysis of microstrip patch antennas

have been reported and are discussed in the following sections. In the modelling analysis

involving the electromagnetic field structure of the antenna, since all the field elements

are time harmonic, the phasor-form of the Maxwell field equations is used throughout the

thesis.

3.2.1 Transmission Line Modelling

The basic Transmission line model(TLM) [2] is used for a rectangular antenna patch

structure with a microstrip feed restricted to a centre position on one of the sides as

shown in figure 3.2.1. The radiating function of the antenna is modelled by two slots on

opposite edges of the antenna, radiating into half-space and separated by a transmission

line of low characteristic impedance. The radiating slots are represented by self-

conductance (G) and self-susceptance (B) connected in parallel. Modifications to the

basic TLM have improved its accuracy and versatility [3] by taking into consideration

factors such as the mutual coupling (G_{12}) between the radiating edges, the surface

roughness of the copper, and, the width of the microstrip feed line. For the transmission

line model a closed form expression has been derived [4,5] for the total input impedance

of a rectangular patch antenna which includes the effect of radiation loss and mutual coupling between the radiation slots.

(a)

(b)
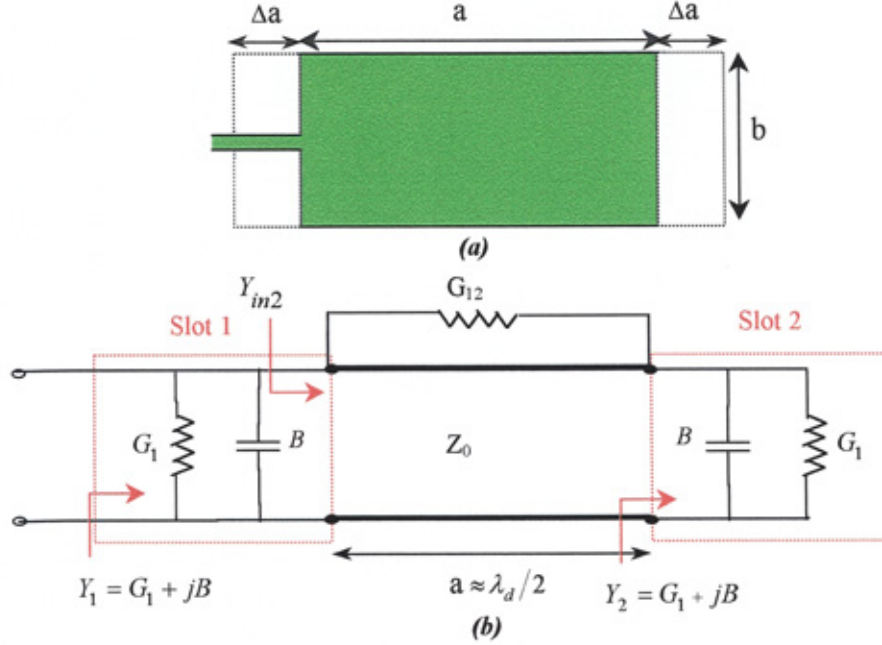
Figure 3.2.1: Transmission line equivalent circuit

The resonant frequency of the microstrip antenna is a function of its length. Usually the length 'a' is made slightly less than $\lambda_d/2$, where λ_d is the wavelength in the substrate, hence

$$Y_{in2} = G_1 - jB \qquad (3.2.1.1)$$

The conductance of a single slot, G_1, can be obtained by using the field expression derived by the cavity model. In general, the conductance is defined as

$$G_1 = \frac{2P_{rad}}{|V_0|^2} \qquad (3.2.1.4)$$

where, V_0 is the voltage across slot and P_{rad} is the radiated power [6].

Therefore the conductance G_1 in equation (3.2.1.4) can put into the form [6]

$$G_1 = \frac{I_1}{120\pi^2}$$ (3.2.1.5)

where

$$I_1 = \int_0^\pi \left[\frac{\sin\left(\frac{k_0 b}{2}\cos\theta\right)}{\cos\theta} \right]^2 \sin^3\theta \, d\theta$$ (3.2.1.6)

The mutual coupling between the radiating edges is modelled as a mutual conductance G_{12} given by [6]

$$G_{12} = \frac{1}{120\pi^2} \int_0^\pi \left[\frac{\sin\left(\frac{k_0 b}{2}\cos\theta\right)}{\cos\theta} \right] J_o(k_0 a \sin\theta)\sin^3\theta \, d\theta$$ (3.2.1.7)

The total input impedance at resonance is then given by

$$Z_{in} = \frac{1}{2(G_1 \pm G_{12})}$$ (3.2.1.8)

where the plus (+) sign is used for modes with an odd (antisymmetric) resonant voltage distribution beneath the patch and between the slots, while, the minus (-) sign is used for modes with an even (symmetric) resonant voltage distribution. The above expressions for I_1 and G_{12} must be evaluated numerically.

The effect of copper and dielectric losses on the input impedance are not taken into account which results in impedance values with errors of the order ten-per-cent. The input impedance for the dominant mode can be modelled by an equivalent parallel R-L-C circuit. In the present of the further modes then the input impedance is modelled by a

sequence of model parallel R-L-C circuit all connected in series as discussed in the next section.

3.2.2 Cavity Modelling

The rectangular microstrip patch is shown in figure 3.2.2.1 can be considered as a resonant cavity. In the model the microstrip antenna structure is considered as a resonant cavity bounded by electric conductors above and below, with the four side walls modelled as magnetic walls where the tangential components of the magnetic field vanish.
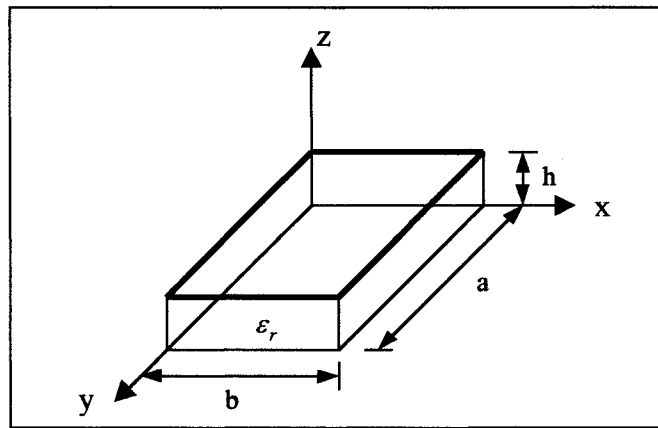
Figure 3.2.2.1: Rectangular microstrip patch geometry

The solution of the field equations in the cavity is obtained by expanding the fields under the patch in terms of the resonant modes[7]. The patch boundary is required to be extended outwards in order to account for the fringing fields so that the effective dimensions are greater than the physical dimensions of the patch. An effective loss tangent which is introduced to account for a conductor loss, a dielectric loss, and, a radiation loss is used in the calculation of input impedance. The resonant frequencies of the antenna are determined by the natural resonant frequencies of the cavity [6].

The cavity model is only accurate for a thin substrate [8] because the high Q resonance of the patch means that the surface current on the patch is not greatly perturbed by details of the feed current. For a microstrip antenna structure with a thin substrate $(h < \lambda_0)$ the dielectric field lines are assumed to be normal to the patch and ground plane so that these is no variation in the z direction within cavity.

Solving the wave equation for the potential in the cavity under the magnetic wall boundary conditions gives the wavenumber components, $k_x = \dfrac{m\pi}{a}$, and, $k_y = \dfrac{n\pi}{b}$, so that

$$k_x^2 + k_y^2 = \left(\frac{m\pi}{a}\right)^2 + \left(\frac{n\pi}{b}\right)^2 = k_{\text{eff}}^2 = \omega^2 \mu_0 \, \varepsilon_0 \, \varepsilon_{\text{eff}} \tag{3.2.2.6}$$

for $m = 1, 2, 3 \ldots\ldots$; $n = 1, 2, 3 \ldots\ldots$

Thus the resonant frequencies for the cavity are given by

$$f_{mn} = \frac{1}{2\pi\sqrt{\mu_0 \, \varepsilon_0 \, \varepsilon_{\text{eff}}}} \sqrt{\left(\frac{m\pi}{a}\right)^2 + \left(\frac{n\pi}{b}\right)^2} \tag{3.2.2.7}$$

Based on the cavity model an equivalent network for the microstrip antenna is shown in figure 3.2.2.2
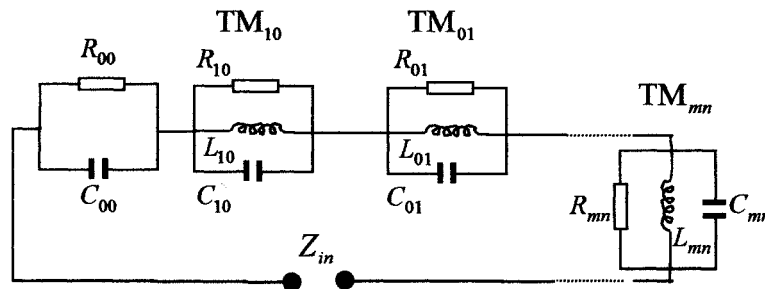
Figure 3.2.2.2: Equivalent network model for microstrip antenna

The rectangular patch is probably the most commonly used microstrip antenna. The electric-field and magnetic-surface-current distributions on the side walls for

24

the TM_{10}, TM_{01} and TM_{20} modes are illustrated in figure 3.2.2.3 For the TM_{10} mode, the magnetic currents along 'b' are constant and in phase while those along 'a' vary sinusoidally and are out of phase. For this reason , the 'b' edge is known as the radiating edge since it contributes predominantly to the radiation. The 'a' edge is known as the non-radiating edge. Similarly, for the TM_{01} mode, the magnetic currents are constant and in phase along 'a' and are out of phase and vary sinusoidally along 'b'. The 'a' edge is thus the radiating edge for the TM_{01} mode.

For circular polarisation design the modes of greatest interest are the TM_{10} and TM_{01} modes [9]. These two modes all have broadside radiation patterns.

(a) TM_{10} Mode

(b) TM_{01} Mode

(c) TM_{20} Mode
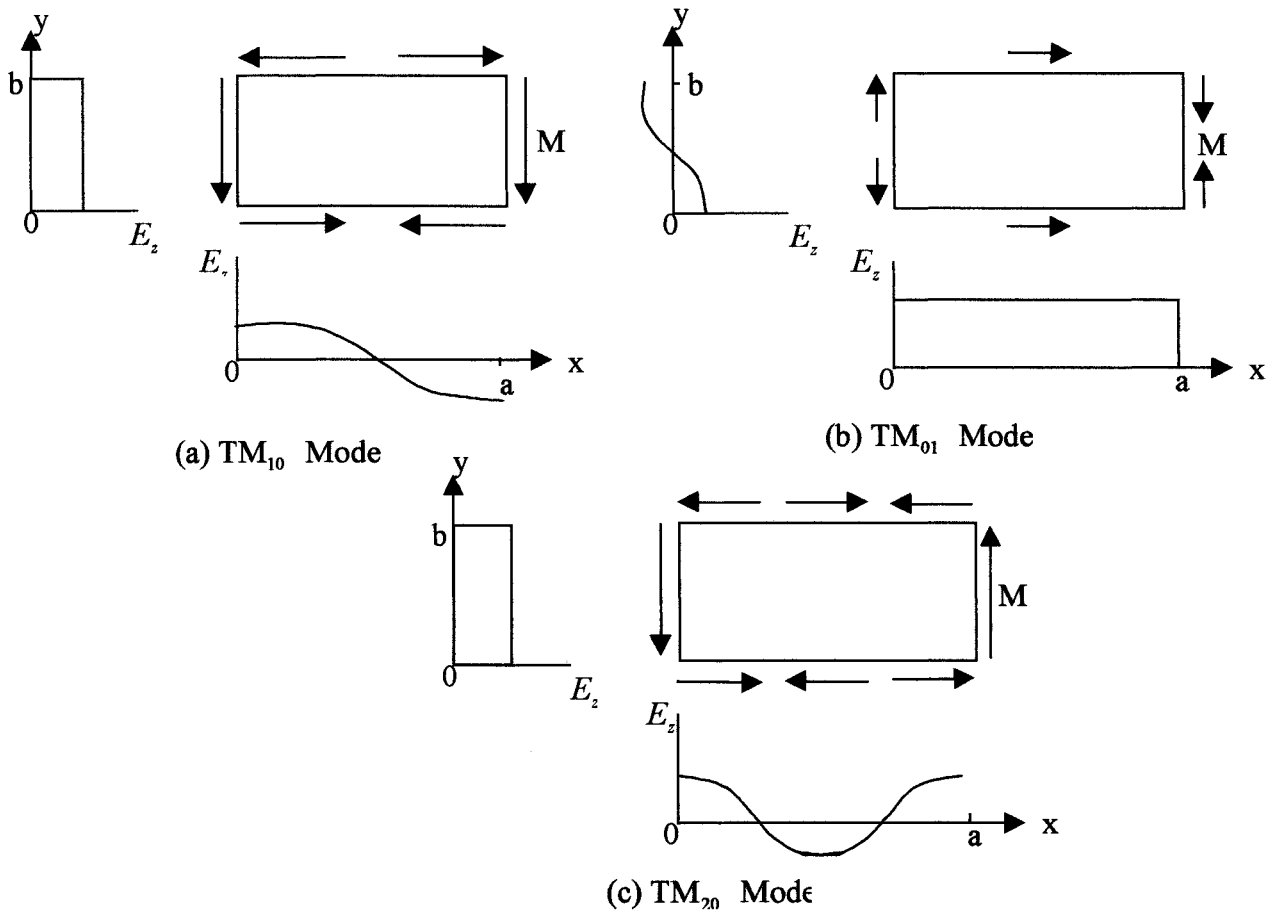
Figure 3.2.2.3: Electric field and magnetic-surface-current distribution in walls for several modes of a rectangular microstrip patch antenna

25

3.2.3 Coplanar Multiport Modelling

Coplanar multiport modelling [9] may be considered as an extension, or, generalisation of the cavity model [8] to antennas of composite geometry. Coplanar analysis is used for thin substrates ($h \ll \lambda$) and is based an relating the voltage at a point on the patch perimeter to the normal current density at another point on the perimeter by means of the Green's function of the patch geometry. For a patch with a known Green's function the input impedance can be obtained directly from the analysis.

For an antenna geometry composed of regular segments having known Green's functions the coplanar analysis is extended to establish multiport perimeter connections between the segments (figure 3.2.3.1). A multiport coplanar matrix circuit analysis [10] can then used to determine the input impedance formula of the composite antenna structure. A full discussion of the analysis and applications is given in chapters 5 and 6.
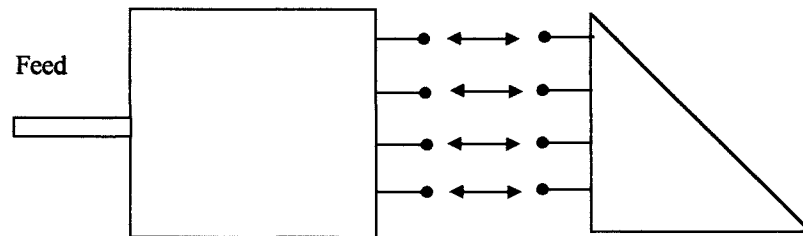
Figure 3.2.3.1: Illustration of multiport segment interconnections

3.2.4 Full Wave Modelling

Full wave modelling assumes an infinite substrate so that no fringe field approximation is employed. Also there is no restriction on the substrate thickness. Both electric and magnetic fields are used in the constitutive Maxwell system of equations. Full wave techniques provide the most accurate solution for the impedance and radiation characteristics [1,9].

Full wave solutions include the effect of dielectric loss, conductors loss, space wave radiation, surface waves, and external coupling. The computational requirements are numerically very intensive and costly.

In full wave analysis Maxwell's equations are solved for the electric current distributions on the conducting elements and once this has been determined all the other parameters of interest can be derived. The currents produce electromagnetic fields which must satisfy certain boundary conditions determined by the antenna structure. The fields must satisfy Maxwell's equations which relate the fields, current sources and charges. Maxwell's equations can be expressed in either differential or integral form. In the differential form the vector wave equations for the electric fields, and, for the magnetic fields within and outside the substrate are expressed in terms of their vector potentials. The vector potential field equations are then solved.

In the integral equation approach the problem is formulated in terms of integral equations in which the unknowns are the surface currents on the metalised conductors. On the

antenna patch, which is assumed to be a perfect electrical conductor, the tangential

electric field is everywhere zero. At the patch the field is due to the incident field from

the feed line, and the field scattered by the patch. These fields are expressed in term of

Green's functions which relate the current sources to the electrical fields.

By mapping the constitutive equations and the boundary conditions onto the Fourier

transform (spectral) domain the problem of finding the Green's function is considerably

simplified. For a regular shape the spectral Green's function is obtained in closed form.

The equations are usually solved for the current distribution by a moment method.

3.3 THE RECTANGULAR AND TRIANGULAR PATCH ANTENNA

The microstrip patch antenna (radiating element) and the feed lines are usually

photoetched on the dielectric substrate. The antenna patch may be square, rectangular,

thin strip(dipole), circular, elliptical, triangular or some other configuration. In the

present study of the deleted corner square patch antenna only the rectangular and

triangular geometries are involved.

3.3.1 An Efficient Expression for the Input Impedance of a Rectangular Microstrip Patch Antenna with a microstrip Offset Feed.

The rectangular patch geometry is the most common form in use today. Characteristics such as input impedance, circular polarisation, dual-frequency operation, frequency agility, broad bandwidth, and feedline flexibility, have been extensively studied [1,6,8,9]. From coplanar analysis applied to a rectangular antenna patch a formula for the input impedance, with offset feed, is obtained. This involves a double infinite series, and, in this section it is shown that the series can be expressed as a single term, together with a single infinite series. Input impedance values, calculated using the new computationally efficient expression are compared with practical results and a simulation based on full-wave analysis.

A rectangular patch antenna having dimensions 'a' and 'b' is shown in figure 3.3.1.1. where, W is the feed width of the microstrip line and T is the offset distance of the feed center from the edge of the antenna.
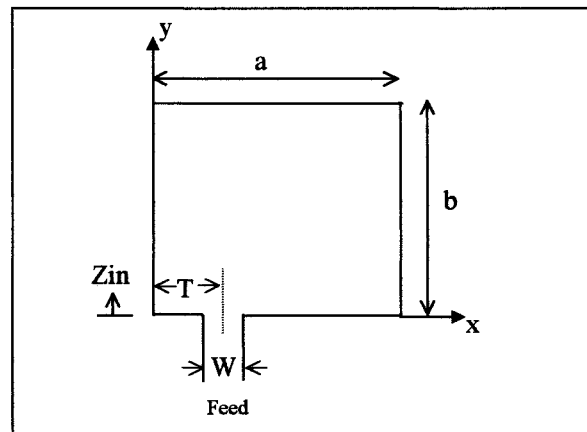
Figure 3.3.1.1: Input impedance of the rectangular patch

The input impedance for a rectangular patch antenna with a single microstrip feed has been derived by Okoshi[10] using the coplanar analysis and involves the evaluation of a double infinite series in terms of the resonant modes m and n. The 'm' and 'n' modes are associated with the 'x' and 'y' dimensions respectively. The Okoshi equation can be put in the following form.

$$Zin = \frac{j4\omega\mu h a^3 b}{W^2 \pi^4} \sum_{m=0}^{\infty} \sum_{n=0}^{\infty} \frac{\varepsilon_m^2 \varepsilon_n^2}{m^2 \left[m^2 b^2 + n^2 a^2 - D^2 \right]} \cos^2\left(\frac{m\pi T}{a} \right) \sin^2\left(\frac{m\pi W}{2a} \right) \quad (3.3.1.1)$$

where, $\varepsilon_m = 1 \, (m = 0)$ $\varepsilon_n = 1 \, (n = 0)$

$\quad\quad\quad = \sqrt{2} \, (m \neq 0)$ $= \sqrt{2} \, (n \neq 0)$

h is the dielectric thickness, $D^2 = k^2 a^2 b^2 / \pi^2$, $k^2 = \omega^2 \mu \varepsilon_o \varepsilon_r (1 - j/Q)$, and,

Q is the total quality loss factor, which includes, copper(Q_c), dielectric(Q_d), radiation(Q_r) and surface wave(Q_{sw}) losses of the structure. The loss factors are connected by the relation

$$\frac{1}{Q} = \frac{1}{Q_c} + \frac{1}{Q_d} + \frac{1}{Q_r} + \frac{1}{Q_{sw}} \quad (3.3.1.2)$$

For thin substrates the losses due to the surface waves are very small and consequently can be neglected[1]. The loss factors are given as follows[1]:

$$Q_c = h\sqrt{\mu_o \pi f_r \sigma_c} \quad (3.3.1.3)$$

where, σ_c is the conductivity of the metal used.

$$Q_d = \frac{1}{\tan \delta} \quad (3.3.1.4)$$

where $\tan \delta$ is the loss tangent of the dielectric.

$$Q_r = \frac{\pi}{4 G Z_o} \quad (3.3.1.5)$$

where, G is the total conductance due to the radiation loss G_R and mutual coupling conductance G_{12} between the radiation slots $\left(G = G_R + G_{12}\right)$ [6]. Z_o is the characteristic impedance of the patch.

The double infinite series in equation (3.3.1.1) can be arranged into the four modal groups, (m = n = 0), (m $\geq$ 1, n = 0), (m = 0, n $\geq$ 1), and, (m $\geq$ 1, n $\geq$ 1) to give,

$$Zin = \frac{j\omega\mu h}{ab}\left[-\frac{1}{k^2} + \frac{8a^4}{\pi^4 W^2}\sum_{m=1}^{\infty}\frac{\left(\cos m\theta_1 \sin m\theta_2\right)^2}{m^2\left[m^2 - A^2\right]} + \frac{2b^2}{\pi^2}\sum_{n=1}^{\infty}\frac{1}{n^2 - B^2}\right.$$

$$\left. + \frac{16a^2b^2}{\pi^4 W^2}\sum_{m=1}^{\infty}\frac{\left(\cos m\theta_1 \sin m\theta_2\right)^2}{m^2}\sum_{n=1}^{\infty}\frac{1}{n^2 + \left(\frac{m^2\pi^2}{a^2} - k^2\right)\frac{b^2}{\pi^2}}\right] \qquad (3.3.1.6)$$

where, $A = ka/\pi$, $B = kb/\pi$, $\theta_1 = \pi T/a$, $\theta_2 = \pi W/2a$.

Equation (3.3.1.6) can then be put in the form

$$Zin = \frac{j\omega\mu h}{ab}\left[-\frac{1}{k^2} + \frac{8a^4}{\pi^4 W^2}Sm + \frac{2b^2}{\pi^2}Sn + \frac{16a^2b^2}{\pi^4 W^2}Smn\right] \qquad (3.3.1.7)$$

where, $Sm = \sum_{m=1}^{\infty}\frac{\left(\cos m\theta_1 \sin m\theta_2\right)^2}{m^2\left[m^2 - A^2\right]}$ $\qquad (3.3.1.8)$

$$Sn = \sum_{n=1}^{\infty}\frac{1}{n^2 - B^2} \qquad (3.3.1.9)$$

and, $Smn = \sum_{m=1}^{\infty}\frac{\left(\cos m\theta_1 \sin m\theta_2\right)^2}{m^2}\sum_{n=1}^{\infty}\frac{1}{n^2 + C^2}$ $\qquad (3.3.1.10)$

where, $C^2 = \frac{b^2}{a^2}\left(m^2 - A^2\right)$

Since, Gradshteyn [11],

31

$$\sum_{n=1}^{\infty} \frac{1}{n^2 + C^2} = \frac{\pi}{2C} \coth \pi C - \frac{a^2}{2b^2 (m^2 - A^2)} \qquad (3.3.1.11)$$

therefore,

$$\frac{16a^2 b^2}{\pi^4 W^2} Smn = \frac{8a^2 b^2}{\pi^3 W^2} \sum_{m=1}^{\infty} \frac{(\cos m\theta_1 \ \sin m\theta_2)^2}{m^2 C} \coth \pi C - \frac{8a^4}{\pi^4 W^2} Sm \qquad (3.3.1.12)$$

which results in the elimination of the Sm infinite series in equation (3.3.1.7).

Substituting from equation (3.3.1.12)into equation (3.3.1.7), then gives

$$Zin = \frac{j\omega \mu}{ab} h \left[-\frac{1}{k^2} + \frac{2b^2}{\pi^2} Sn + \frac{8a^2 b^2}{\pi^3 W^2} \sum_{m=1}^{\infty} \frac{(\cos m\theta_1 \ \sin m\theta_2)^2}{m^2 C} \coth \pi C \right] \qquad (3.3.1.13)$$

Further since, Gradshteyn [11],

$$\sum_{n=1}^{\infty} \frac{1}{n^2 - B^2} = \frac{1}{2B^2} - \frac{\pi}{2B} \cot \pi B \qquad (3.3.1.14)$$

therefore,

$$\frac{2b^2}{\pi^2} Sn = \frac{1}{k^2} - \frac{b}{k} \cot kb \qquad (3.3.1.15)$$

which results in the elimination of the mode $m = 0$, $n = 0$ in equation (3.3.1.13).

Substituting from equation (3.3.1.15) into equation (3.3.1.13), then give a compact equation for Zin

$$Zin = \frac{j\omega \mu h}{a} \left[-\frac{1}{k} \cot kb + \frac{8a^3}{\pi^3 W^2} \sum_{m=1}^{\infty} \frac{(\cos m\theta_1 \ \sin m\theta_2)^2}{m^2 \sqrt{m^2 - A^2}} \coth \pi C \right] \qquad (3.3.1.16)$$

From the above equation (3.3.1.16) numerical evaluation shows that for a centre feed at, $T = a/2$, the first term is dominant and gives the input impedance to four significant figures. Thus the formula

32

$$Z_{in} = \frac{-j\omega\,\mu\,h\cot kb}{ka} \qquad\qquad (3.3.1.17)$$

is a good analytic approximation which can safely be used for practical impedance matching design requirements.

It is also to be observed that for the centre feed position the impedance is virtually independent of the width, W, of the feed line.

In the offset feed positions convergence of Zin to 5, 6 and 8 significant figures is obtained with the upper limit of summation $m = 1$, 4 and 40 respectively.

Equation (3.3.1.16) has been evaluated for a square patch of side, $a = 39.5mm$, with $\varepsilon r = 2.33$ (Duroid 5870), $h = 0.79mm$, $Q = 83$ for the center feed position $T = 19.75mm$ and the resonant frequency, 2.45GHz. The layout of the antenna for the practical experiment to determine the Zin at resonant frequency is illustrated in figure 3.3.1.2.
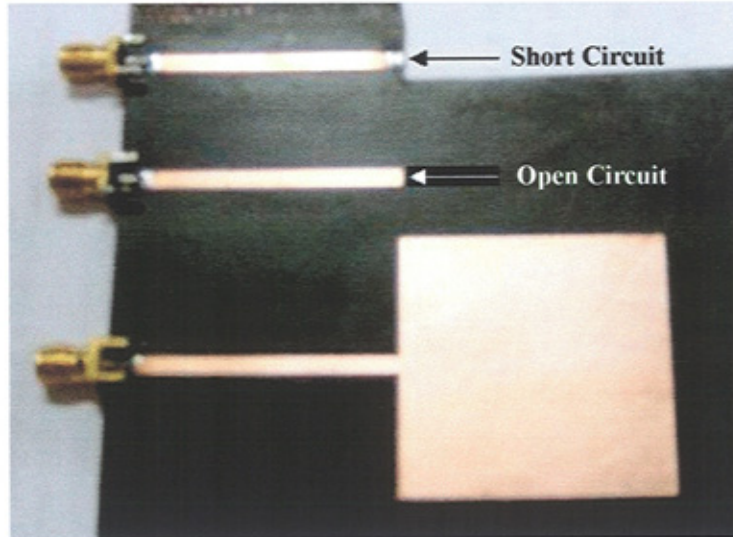
Figure 3.2.1.2: : Experimental offset feed square patch antenna

The results for the variation of input impedance with respect to the center feed position using equation (3.3.1.16), Ensemble™ (full wave analysis software), and, practical measurement, are shown in figure 3.3.1.3(a). Figure 3.3.1.3(b) shows the results for an

33

offset feed position for $T = 11.75mm$. As can be seen in both cases there is a good

agreement between predicted, simulation(Ensemble™) and practical measurement.
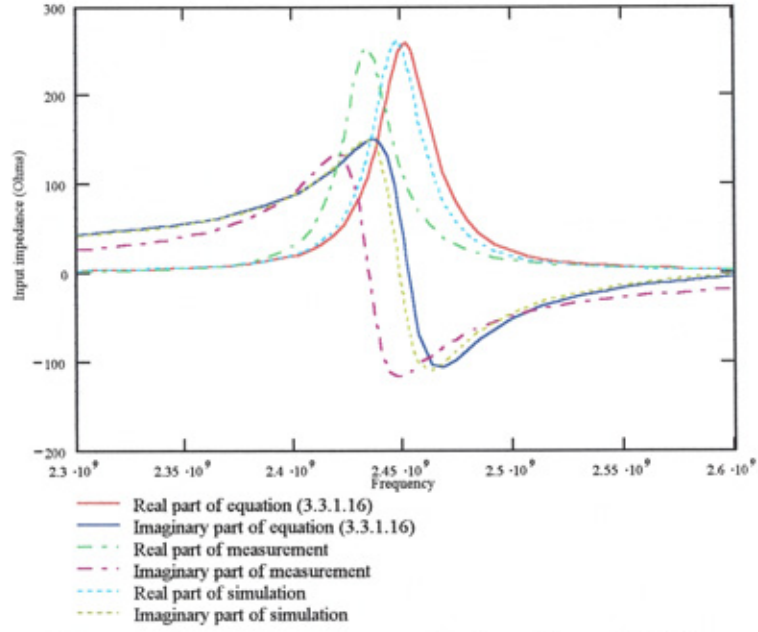
(a) Input impedance of center feed position (19.75mm)
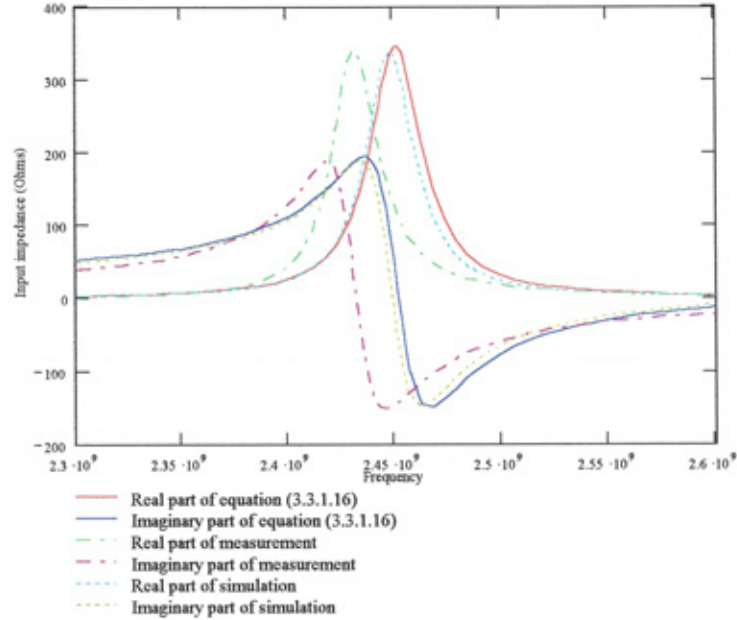
(b) Input impedance of offset feed position (11.75mm)

Figure 3.3.1.3: Input impedance of a 2.45Ghz microstrip square patch antenna fed with a microstrip line along the non-radiating edge of the patch.

34

It was found that the input impedance variation for a sequence of seven rectangular patches is most significant when the rectangle approaches a square (figure 3.3.1.4). This result is relevant to the design of a single feed circular polarized antenna.
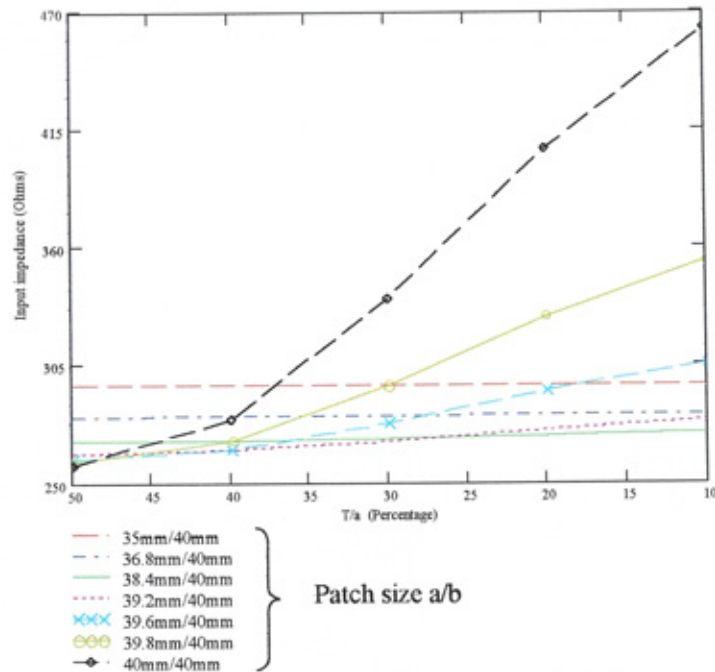
Figure 3.3.1.4 : Input impedance with the different ratio a/b of rectangular patch versus the distance of fed point from the edge of the side

3.3.2 An Efficient Expression for the Input Impedance of a Microstrip Right-angled Isosceles Triangular Patch Antenna.

Several triangular patch shapes are amenable to coplanar analysis. These include the $45^0 - 45^0 - 90^0$, $30^0 - 60^0 - 90^0$, and the $60^0 - 60^0 - 60^0$ triangular patches, for which the necessary Green's functions have been derived by Chada and Gupta[12]. They derive the Green's function by constructing a set of specially selected line sources, the potential from which, is expanded in an infinite series to obtain expansion functions satisfying the associated homogeneous wave equation boundary value problem. These functions are

35

then applied to the nonhomogeneous wave equation to determine the required Green's function expansion coefficients. There have been few investigation on the triangular patch [1].

Using coplanar analysis the following general expression for the input impedance of a single feed microstrip antenna has been derived by Okoshi [10]

$$Zin = \frac{1}{W_s W_{s_0}} \int_{W_s} \int_{W_{s_0}} G(s \,|\, s_0) \ ds \ ds_0 \qquad (3.3.2.1)$$

where, $G(s \,|\, s_0)$ is the Green's function of the patch, and, s, s_0 are running perimeter coordinates. The integrations are taken over the feed to patch interface, and, $W_s, W_{s_0} \ll \lambda$, λ being the wave length in the substrate. Included are the effects of radiation, copper and, dielectric losses [1,14,15].

The above equation is applied to a feed position on the vertical side of the triangle (section 3.3.2.1a) and to a feed position on the hypotenuse (section 3.3.2.1b). in each case the initial numerical results obtained are economised by introducing closed forms of infinite series[11]. These new formulas are verified by comparison with practical results and a simulation based on full wave analysis.

3.3.2.1(a) Patch with feed on vertical side

The geometry with the feed on vertical side is shown in figure 3.3.2.1(a).
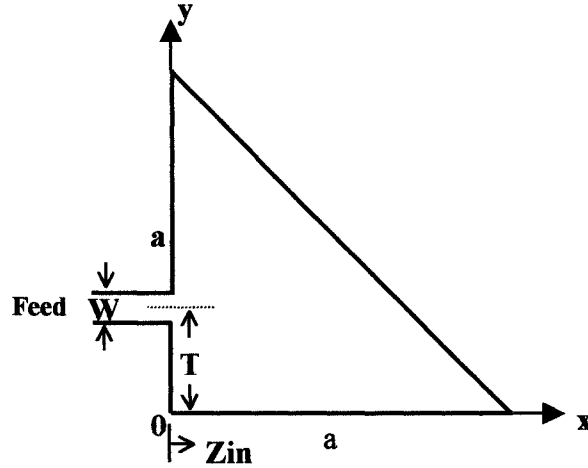
Figure 3.3.2.1(a) : Patch with feed on vertical side

The initial expression for the input impedance involves one constant term, three single infinite series and two double infinite series in terms of the resonant mode contributions (m, n). Introducing closed forms results in the total elimination of two of the three single infinite series while the closed form applied to the remaining single series eliminates the contribution of the $(0, 0)$ mode. Closed forms of the inner summations of each of the two double infinite series reduces each to a single infinite series. These procedures are outlined below.

From Chada and Gupta [12] the Green's function $G(0, y \mid 0, y_0)$ for the triangle can be arranged in the form

$$
\begin{aligned}
G(0, y \mid 0, y_0) \\
= j2\omega h\mu \Biggl\{ &-\frac{1}{k^2 a^2} + \frac{1}{\pi^2}\sum_{m=1}^{\infty}\frac{\left(1 + (-1)^m \cos\frac{m\pi}{a} y\right)\left(1 + (-1)^m \cos\frac{m\pi}{a} y_0\right)}{(m^2 - A^2)} \\
&+ \frac{1}{\pi^2}\sum_{m=1}^{\infty}\sum_{n=1}^{\infty}\frac{\left(\cos\frac{n\pi}{a} y + (-1)^m \cos\frac{m\pi}{a} y\right)\left(\cos\frac{n\pi}{a} y_0 + (-1)^m \cos\frac{m\pi}{a} y_0\right)}{(m^2 + n^2 - A^2)} \Biggr\}
\end{aligned}
\tag{3.3.2.2}
$$

37

where, $A = k\,a/\pi$; h is the dielectric thickness; $k^2 = \omega^2 \mu\, \varepsilon_0 \varepsilon_r (1 - j/Q)$ and, Q is

the total quality loss factor .

From equations (3.3.2.1) and (3.3.2.2), by integration (Appendix 3A)

$$
Zin = \frac{j2\omega\, h\, \mu}{W^2}\left\{ -\frac{W^2}{k^2 a^2} + \frac{W^2}{\pi^2}\sum_{m=1}^{\infty}\frac{1}{m^2 - A^2} + \frac{2aW}{\pi^3}\sum_{m=1}^{\infty}\frac{(-1)^m(\sin m\theta_1 - \sin m\theta_2)}{m(m^2 - A^2)} \right.
$$

$$
+ \frac{a^2}{\pi^4}\sum_{m=1}^{\infty}\frac{(\sin m\theta_1 - \sin m\theta_2)^2}{m^2(m^2 - A^2)} + \frac{2a^2}{\pi^4}\sum_{m=1}^{\infty}\sum_{n=1}^{\infty}\frac{(\sin m\theta_1 - \sin m\theta_2)^2}{m^2(m^2 + n^2 - A^2)}
$$

$$
\left. + \frac{2a^2}{\pi^4}\sum_{m=1}^{\infty}\sum_{n=1}^{\infty}\frac{(-1)^{m+n}(\sin m\theta_1 - \sin m\theta_2)(\sin n\theta_1 - \sin n\theta_2)}{mn\,(m^2 + n^2 - A^2)} \right\}
\qquad (3.3.2.3)
$$

where, $\theta_1 = \dfrac{\pi}{a}\left(T + \dfrac{W}{2}\right)$; $\theta_2 = \dfrac{\pi}{a}\left(T - \dfrac{W}{2}\right)$.

Summing the first of the above double series with respect to the inner summation results in the total elimination of the third single series. Summing the second double infinite series eliminates the second of the above single series. Summing the first of the above single series eliminates the $-W^2/k^2 a^2$ term. The final result of the economisation is the new input impedance formula

$$
Zin = \frac{j\omega\, h\, \mu}{W^2}\left\{ -\frac{W^2}{ka}\cot ka - \frac{W(\sin A\theta_1 - \sin A\theta_2)}{k^2 a \sin A\pi} + \frac{2a^2}{\pi^3}\sum_{m=1}^{\infty}\frac{(\sin m\theta_1 - \sin m\theta_2)^2}{m^2 B}\coth B\pi \right.
$$

$$
\left. + \frac{2a^2}{\pi^3}\sum_{m=1}^{\infty}\frac{(-1)^m(\sin m\theta_1 - \sin m\theta_2)(\sinh B\theta_1 - \sinh B\theta_2)}{m\,(m^2 - A^2)\sinh B\pi} \right\}
\qquad (3.3.2.4)
$$

where, $B = \sqrt{m^2 - A^2}$.

From the above equation (3.3.2.4) numerical evaluation shows that for a centre feed at,

$T = a/2$, the first term is dominant and gives the input impedance to four significant

figures. Thus the formula

$$Z_{in} = \frac{-j\omega \mu h \cot ka}{ka}$$ (3.3.2.5)

is a good analytic approximation which can safely be used for practical impedance

matching design requirements.

For the offset feed position, $T = 24mm$, convergence to 5, 6 and 8 significant figures is

obtained with the upper sum limits $m = 2$, 5 and 24 respectively.

It is also to be observed that for the centre feed position the impedance is virtually

independent of the width, W, of the feed line.

Numerical calculations show for an offset feed position the impedance has a relatively

low value at the right-angled corner but increases rapidly as the offset feed length, T, is

increased.

The resonant frequency of the triangular patch antenna is given by[16]

$$f_0 = \frac{c}{2a\sqrt{\varepsilon_{eff}}}$$ (3.3.2.6)

3.3.2.1(b) Patch with feed on hypotenuse

The geometry with the feed on hypotenuse is shown in figure 3.3.2.1(b).
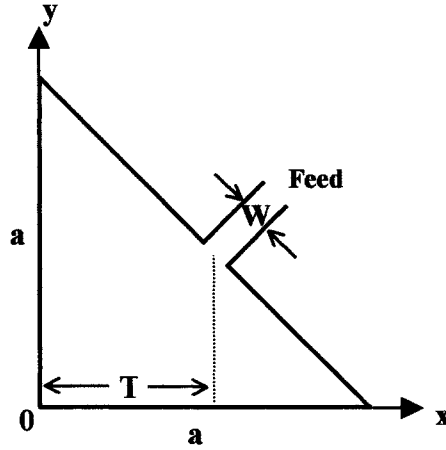
<u>Figure 3.3.2.1(b) : Patch with feed on hypotenuse</u>

The initial expression for the input impedance consists of one constant term, one single infinite series and one double series. The single series reduces to a closed form but the double series cannot be reduced to closed form. Some economisation is obtained by extracting the diagonal modal terms $\left(m \geq 1, n = m \right)$ which take the form of three single infinite series, two of which reduce to closed form. Application of economisation to the third series involves eight single infinite series each one reducing to one of four possible closed forms, which are related to convergence conditions. In term of computationally efficiency it is preferable to directly sum the third series. By symmetry, the remaining double sum reduces to a semi-infinite double series $\left(m \geq 1, n = m + 1 \right)$. These procedures are outlined below.

The Green's function $G(x, a - x \mid x_0, a - x_0)$ can be arranged in the form

$G(x, a - x \mid x_0, a - x_0)$

$$= j2\omega h \mu \left\{ -\frac{1}{k^2 a^2} + \frac{1}{\pi^2} \sum_{m=1}^{\infty} \frac{\left(\cos\frac{m\pi}{a}x + (-1)^m \cos\frac{m\pi}{a}(a-x)\right)\left(\cos\frac{m\pi}{a}x_0 + (-1)^m \cos\frac{m\pi}{a}(a-x_0)\right)}{(m^2 - A^2)} \right.$$

$$+ \frac{1}{\pi^2} \sum_{m=1}^{\infty}\sum_{n=1}^{\infty} \frac{\left(\cos\frac{m\pi}{a}x\cos\frac{n\pi}{a}(a-x) + (-1)^{m+n}\cos\frac{n\pi}{a}x\cos\frac{m\pi}{a}(a-x)\right)}{(m^2 + n^2 - A^2)} \cdot$$

$$\left. \left(\cos\frac{m\pi}{a}x_0\cos\frac{n\pi}{a}(a-x_0) + (-1)^{m+n}\cos\frac{n\pi}{a}x_0\cos\frac{m\pi}{a}(a-x_0)\right) \right\} \qquad (3.3.2.7)$$

From equations (3.3.2.1) and (3.3.2.7), by integration (Appendix 3A)

$$Zin = \frac{j\omega\mu h}{2W^2\pi^2}\left\{ -\frac{W^2\pi^2}{k^2 a^2} + \frac{8a^2}{\pi^4}\sum_{m=1}^{\infty}\frac{\left(\sin m\theta_1 - \sin m\theta_2\right)^2}{m^2(m^2 - A^2)} \right.$$

$$\left. + \frac{2a^2}{\pi^4}\sum_{m=1}^{\infty}\sum_{n=1}^{\infty}\frac{1}{(m^2 + n^2 - A^2)}\left[\frac{\left(\sin(m+n)\theta_1 - \sin(m+n)\theta_2\right)}{(m+n)} + \frac{\left(\sin(m-n)\theta_1 - \sin(m-n)\theta_2\right)}{(m-n)}\right]^2 \right\} \qquad (3.3.2.8)$$

where, $\theta_1 = \frac{\pi}{a}\left(T + \frac{W}{2\sqrt{2}}\right)$; $\theta_2 = \frac{\pi}{a}\left(T - \frac{W}{2\sqrt{2}}\right)$.

In the above formula the single series can be summed to closed form making a contribution to the $-W^2\pi^2/k^2 a^2$ term. The diagonal term $n = m$ from the double sum is extracted and is in the form of three single infinite series, two of which is expressed in closed form. By symmetry the remaining term in the double series are expressed in the form of a semi-infinite double series $(m \geq 1, n = m + 1)$.

41

The final result for the input impedance is given below

$$Zin = \frac{2j\omega\mu h}{W^2}\left\{\frac{W\left(5W - 4\sqrt{2}\pi^2\right)}{2\ k^2 a} + \frac{a^2}{4\pi^2}\sum_{m=1}^{\infty}\frac{\left(\sin 2m\theta_1 - \sin 2m\theta_2\right)^2}{m^2(m^2 - A^2/2)}\right.$$

$$-\ \frac{4\pi^4\left(\cos A\pi - \cos A(\pi - \theta_1 - \theta_2)\cos A(\theta_2 - \theta_1) + 2\sin A(\pi - \theta_1)\sin A\theta_2\right)}{k^3 a \sin ka}$$

$$+\ \frac{\pi^2 W\left(\sin \frac{A}{\sqrt{2}}(\pi - 2\theta_1) - \sin \frac{A}{\sqrt{2}}(\pi - 2\theta_2)\right)}{\sqrt{2}\ k^2\ a \sin ka/\sqrt{2}} - \frac{\pi^2\ W^2\sqrt{2}\ \cot \frac{A}{\sqrt{2}}\ \pi}{4\ k\ a}$$

$$+\frac{4a^2}{\pi^4}\sum_{m=1}^{\infty}\sum_{n=m+1}^{\infty}\left\{\left[\frac{1}{(m^2+n^2-A^2)}\right]\cdot\right.$$

$$\left.\left.\left[\frac{\left(\sin(m+n)\theta_1 - \sin(m+n)\theta_2\right)}{(m+n)} + \frac{\left(\sin(m-n)\theta_1 - \sin(m-n)\theta_2\right)}{(m-n)}\right]^2\right\}\right\} \qquad (3.3.2.9)$$

Using a centre feed only the leading term in equation (3.3.2.9) gives 4 significant figure accuracy. For the offset feed position, $T = 24mm$, convergence to 5, 6 and 8 significant figures is obtained with the upper sum limits $m = 2$, 5 and 35 respectively.

From the above equation (3.3.2.9) numerical evaluations show that, for a feed position on the hypotenuse, the input impedance is a maximum at the ends of the hypotenuse while falling uniformly to near zero at the centre.

Consequently there is a feed location on the hypotenuse giving an input impedance of 50Ω thus allows for simple matching implementation.

42

The impedance expressions (3.3.2.4) and (3.3.2.9) were verified by application to the patch antennas shown in figures 3.3.2.1(a) and 3.3.2.1(b), having a resonant frequency of 2.45GHz, $a = 40mm$, substrate(Duroid 5870) thickness $h = 0.79mm$, $\varepsilon r = 2.33$, $Q = 120$, and, the loss tangent of 0.0012. The layout of the antenna for the practical experiment to determine the Zin at resonant frequency is illustrated in figure 3.3.2.2.
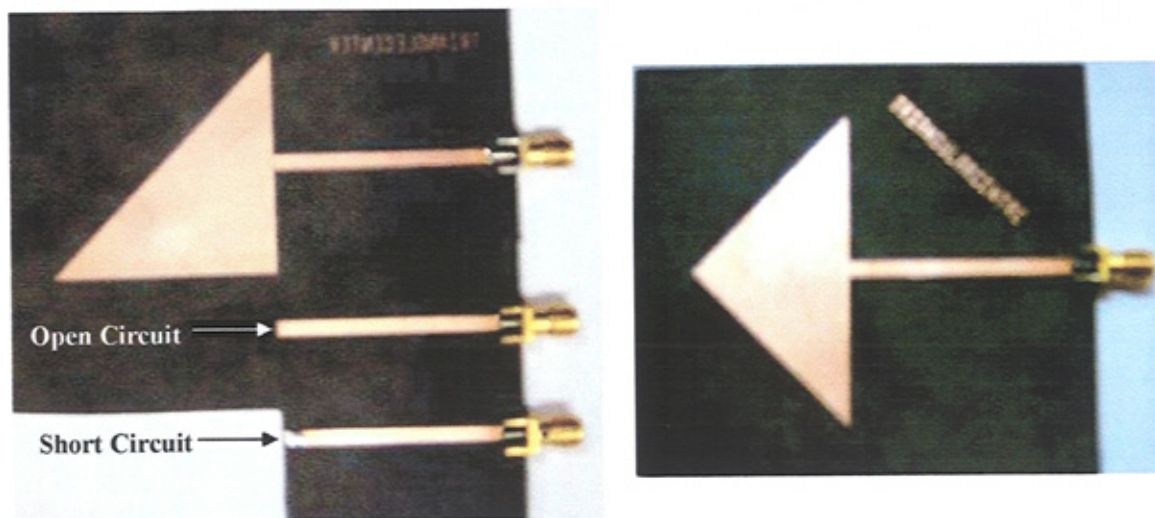
Figure 3.3.2.2: Experimental feed on the vertical and hypotenuse triangle patch antenna

Graphs of the impedance values for two feed positions using the new formulas equation (3.3.2.4) and equation (3.3.2.9), Ensemble™, and, practical measurement, are shown in figures 3.3.2.3(a), 3.3.2.3(b), 3.3.2.4(a) and 3.3.2.4(b).

In all the above cases the graphs show good agreement between the new formulas, practical measurement and Ensemble™ results.
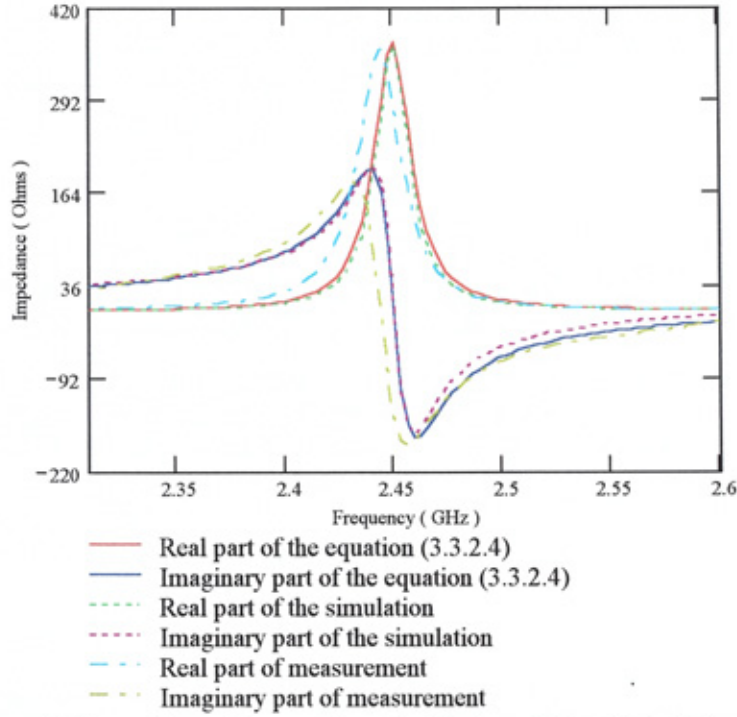
(a) Input impedance of center feed position ($T = 20$mm)
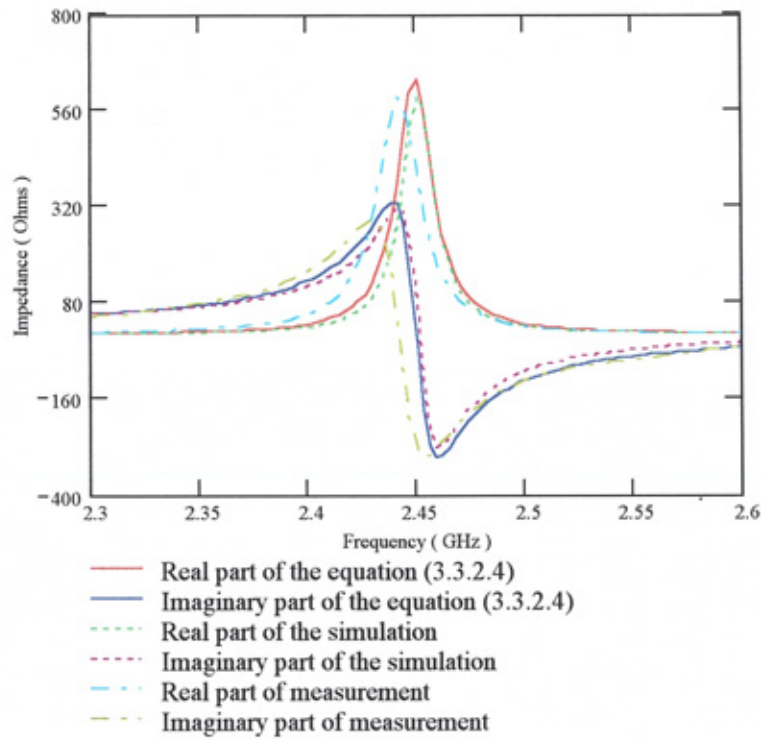
(b) Input impedance of offset feed position ($T = 24$mm)

Figure 3.3.2.3.: Feed on vertical side of isosceles triangular patch antenna.
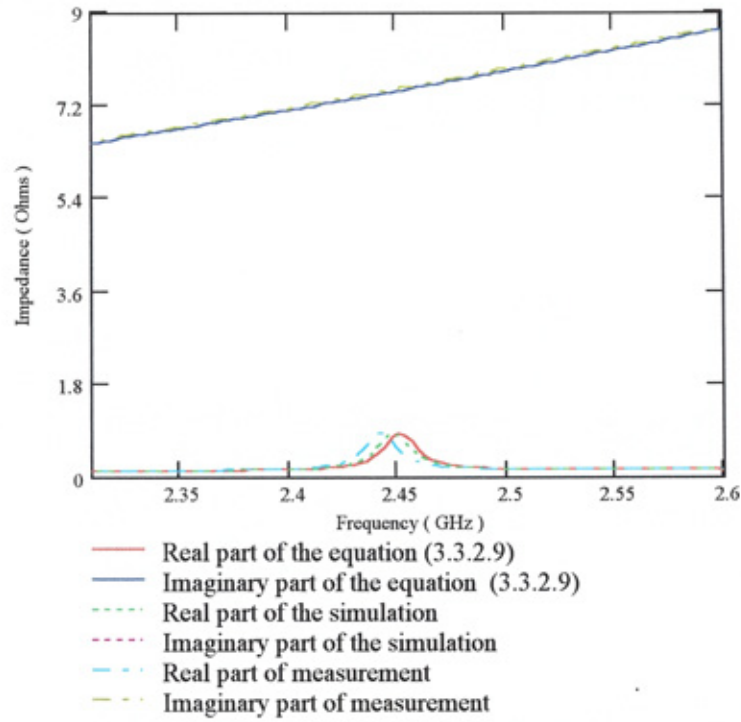
(a) Input impedance of center feed position ($T = 20$mm)
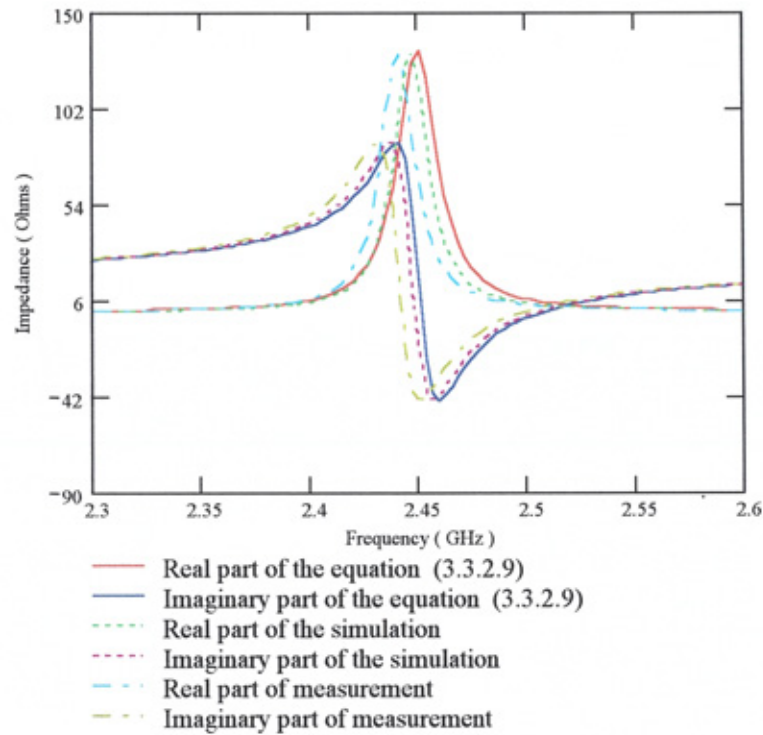
(b) Input impedance of offset feed position ($T = 24$mm)

Figure 3.3.2.4: Feed on the hypotenuse of isosceles triangular patch antenna.

45

3.4 Antenna Feed Structures for Circular Polarisation

A number of methods of achieving circular polarisation in conjunction with microstrip patch antennas have been developed. The two main approaches use either a single feed, or, a dual feed to the antenna.

3.4.1 Linear and Circular Polarisation

Consider a plane wave travelling in a positive z-direction, as shown in Figure 3.4.1(a), with the electric field at all times orientated in the y-direction. This type of wave is termed linearly polarised in the y-direction. As a function of time and position the electric field of such a wave (travelling in the positive z-direction) is given by[17]

$$E_y = E_2 . \sin(\omega t - \beta z) \tag{3.4.1.1}$$

(a) Linear Polarisation   (b) Elliptical Polarisation   (c) Circular Polarisation
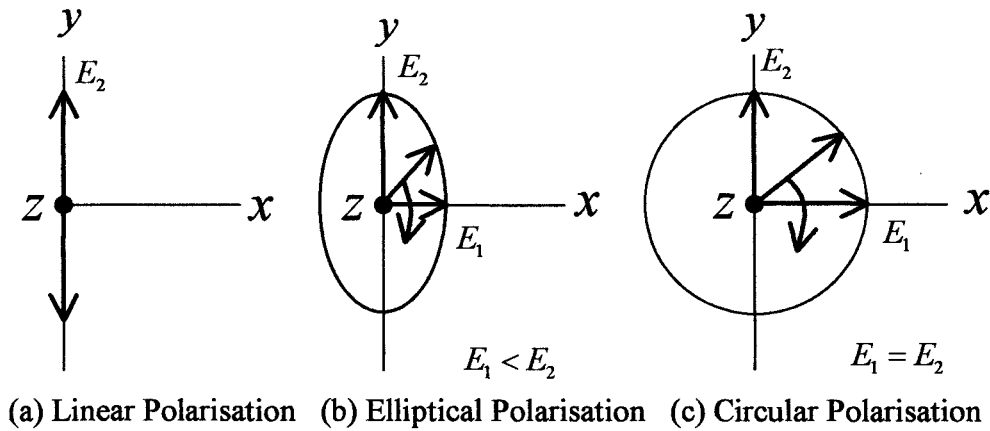
Figure 3.4.1: Various States of Wave Polarisation

In general, the electric field has components in both the x and y-directions, as shown in Figure 3.4.1(b). This type of wave is termed elliptically polarised and may be resolved into two linearly polarised components in the x and y-directions. In this case, for a wave travelling in the positive z-direction, the field components in the x and y-directions are given by equation (3.4.1.2a) and (3.4.1.2b) respectively[17].

46

$$E_x = E_1 \sin(\omega t - \beta z) \tag{3.4.1.2a}$$

$$E_y = E_2 \sin(\omega t - \beta z + \theta) \tag{3.4.1.2b}$$

where, E_1 and E_2 are the amplitude of the fields in the x and y directions respectively; θ is the phase angle by which E_1 leads E_2.

The conditions for circular Polarisation, as shown in Figure 3.4.1(c), are met when the amplitudes of x and y-directed electric field components are equal in magnitude and orthogonal in phase (Ex =Ey and $|\theta|$ =90°). Circular Polarisation is defined as being in one of two states, depending upon the polarity of the phase difference (θ). If θ = -90° this corresponds to left hand circular polarisation (LHCP). while, if θ = +90° this is defined as right hand circularly polarised (RHCP).

3.4.2 Two feed arrangement patch

In a dual feed system the patch element is symmetrical in shape and requires an external polarising feed network in order to generate circular polarisation. The input signals are applied to adjacent edges of the patch and are 90° out of phase and produce circular polarisation. Typical example of two feed arrangements used to produce circular polarisation are shown in figure 3.4.2 [18,19].

a) Incorporating a Reactive Tee Junction   b) Utilising a 3dB Coupler
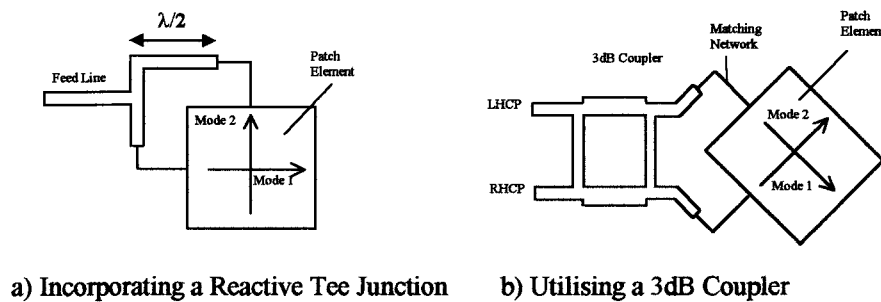
Figure 3.4.2: Dual Feed Circularly Polarised Patch Antennas

3.4.3 Single feed arrangement patch

The single feed is able to excite two electric field modes on the patch, one mode to resonate above and the other mode to resonates below the desired operating frequency. Example of circularly polarised single feed structures are shown in figure 3.4.3 [20].

a)Nearly square   b)Square Patch with Slot   c) Truncated Square Patch
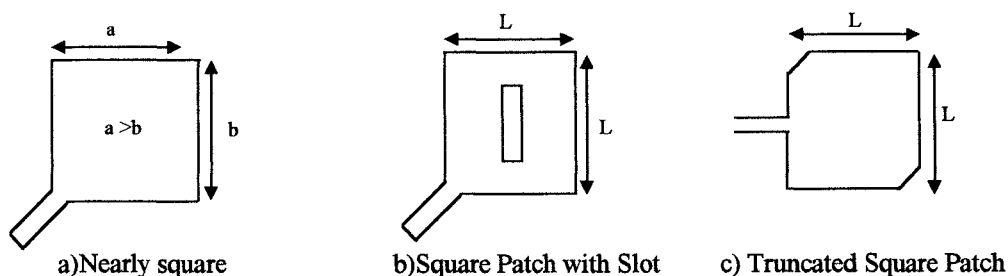
Figure 3.4.3: Single Feed Circularly Polarised Microstrip Patch Antennas

The singly-fed type is especially useful because it requires no external circular polariser such as the 90° hybrid. The wider bandwidth can be archived by using single slot feed but not with the manufacture factor is concerned. The two corner-deleted truncated square patch is preferred because of the lower input impedance in the case of the centre feed and it can be easily match to $50\,\Omega$ by using a single $\lambda/4$ transformer.

Summary

In this chapter various modeling approaches and methods of analysis for the rectangular and triangular microstrip antenna were discussed. New computationally efficient expressions for the input impedance with the offset feed of a rectangular and a triangular patch antenna were derived and applied to obtain impedance-frequency graphs with respect to feed position. Good agreement between the new formulas, practical measurement and Ensemble™ results are obtained. The electric field condition for circular polarisation was described together with possible feed arrangements required to generate circular polarised radiation.

CHAPTER 4

APPLICATION OF PERTURBATION ANALYSIS FOR A TRUNCATED SQUARE PATCH ANTENNA TO PRODUCE CIRCULAR POLARISATION

4.1 Introduction

Haneishi and Yoshida [1] obtained a formula of the perturbation quantities required for a single feed patch antenna with deleted segments in order to produce circular polarisation. Similar analyses are given in [2,3]. In this chapter the perturbation analysis and the equivalent circuit model of Haneishi [1] are employed to determine the proportional amount of perturbation necessary for circular polarisation in respect of a truncated corner square patch antenna.

A variational expression for the eigenvalues of the square patch, correct to first order terms in the variation of electric potential, is derived in section 4.2. Assuming the dominant mode of the perturbed potential is a linear combination of the unperturbed modes, an expression for the perturbed dominant eigenvalue in terms of the dominant unperturbed potential functions, is derived in section 4.3. The result obtained in section 4.3 is then applied to the corner truncated square patch to determine the associated dominant eigenvalues and hence the dominant modal frequencies (section 4.4). In section 4.5 the dominant perturbed orthonormalised eigenfunctions are derived.

In order to use the eigensystem obtained in sections 4.4 and 4.5, to obtain the perturbation condition for circular polarisation, it is necessary to introduce the

equivalent circuit of the antenna model. The circuit, described in section 4.6 is employed to determine the admittances on the antenna due to the dominant x, and y modal voltages, in terms of the modal frequencies obtained in section 4.4. In section 4.7 the voltage amplitude and phase conditions, required for circular polarisation, are then applied, using the results of the previous sections, to obtain the required amount of perturbation.

4.2 Derivation of a Variational Expression for the Eigenvalues of a Square Patch

The coordinate system used in the following analysis is shown in Figure 4.2.1, where 'a' is the length of the side of the square patch.
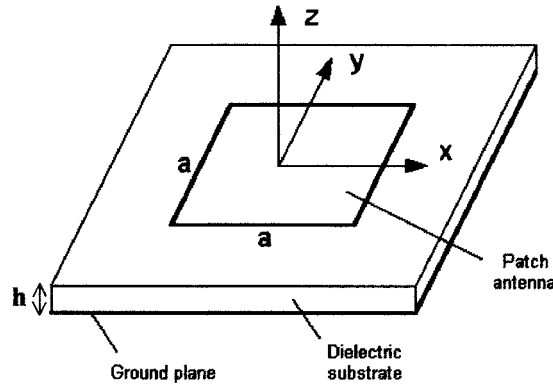
Figure 4.2.1: Coordinate system

In respect of the antenna under consideration the thickness 'h' of the substrate in the 'z' direction is small compared to the wavelength of the fields in the dielectric for frequency at 2.45GHz. Thus field variations in the 'z' direction are neglected and the two dimensional wave equation for the potential, ϕ , within the dielectric is

$$\nabla^2 \phi + k^2 \phi = 0 \qquad , 0 \le z \le h \qquad (4.2.1)$$

In the thin cavity of the patch, magnetic wall boundary conditions are assumed, so that

$$\frac{\partial \phi}{\partial n} = 0 \qquad\qquad\qquad (4.2.2)$$

along the periphery of the patch.

It is shown in Appendix 4A that the dominant normalised eigenfunctions, $(m = 1, n = 0, \text{and}, m = 0, n = 1)$, of the above problem in the x, and y direction are

$$\phi_a = \frac{\sqrt{2}}{a} \sin \frac{\pi}{a} x, \text{ and }, \phi_b = \frac{\sqrt{2}}{a} \sin \frac{\pi}{a} y.$$

Multiplying (4.2.1) by ϕ and integrating over the area S, of the patch, gives

$$\iint_S \phi \, \nabla^2 \phi \, ds = -k^2 \iint_S \phi^2 ds \qquad\qquad (4.2.3)$$

Since (Appendix 4B)

$$\phi \, \nabla^2 \phi = \nabla\left(\phi \, \nabla\phi\right) - \nabla\phi.\nabla\phi \qquad\qquad (4.2.4)$$

the left hand side of equation (4.2.3) can be written as

$$\iint_S \phi \, \nabla^2 \phi \, ds = \iint_S \nabla\left(\phi \, \nabla\phi\right) ds - \iint_S \nabla\phi \,.\nabla\phi \, ds \,. \qquad\qquad (4.2.5)$$

In the first term of the RHS of equation (4.2.5) let

$$\phi \, \nabla\phi = -Q \, \mathbf{i} + P \, \mathbf{j} \qquad\qquad (4.2.6)$$

then,

$$\nabla\left(\phi \, \nabla\phi\right) = \left(\mathbf{i}\frac{\partial}{\partial x} + \mathbf{j}\frac{\partial}{\partial y}\right).\left(-Q \, \mathbf{i} + P \, \mathbf{j}\right)$$

$$= -\frac{\partial Q}{\partial x} + \frac{\partial P}{\partial y} \qquad\qquad (4.2.7)$$

and thus first term an the RHS of (4.2.5) can be written in the form

$$\iint_S \nabla\left(\phi \, \nabla\phi\right) ds = \iint_S \left(-\frac{\partial Q}{\partial P} + \frac{\partial P}{\partial y}\right) ds \qquad\qquad (4.2.8)$$

51

By Green's theorem in the plane relating a surface integral to an equivalent line integral

$$\iint_s \left(-\frac{\partial Q}{\partial x} + \frac{\partial P}{\partial y} \right) = -\oint_l P dx + Q dy$$

$$= -\oint_l (-Q \mathbf{i} + P \mathbf{j}) \cdot \left(\mathbf{i} \frac{\partial y}{\partial l} - \mathbf{j} \frac{\partial x}{\partial l} \right) dl$$

$$= \oint_l \phi \nabla \phi \cdot \left(\mathbf{i} \frac{\partial y}{\partial l} - \mathbf{j} \frac{\partial x}{\partial l} \right) dl \qquad (4.2.9)$$

Further, for any point **r** on the boundary of the patch

$$\mathbf{r} = \mathbf{i} \, x + \mathbf{j} \, y$$

hence,

$$\frac{\partial \mathbf{r}}{\partial l} = \mathbf{i} \frac{\partial x}{\partial l} + \mathbf{j} \frac{\partial y}{\partial l} \qquad (4.2.10)$$

and this is a vector tangential to the boundary.

Then, from (4.2.9) and (4.2.10)

$$\left(\mathbf{i} \frac{\partial y}{\partial l} - \mathbf{j} \frac{\partial x}{\partial l} \right) \cdot \left(\mathbf{i} \frac{\partial x}{\partial l} + \mathbf{j} \frac{\partial y}{\partial l} \right) = \left(\frac{\partial y}{\partial l} \frac{\partial x}{\partial l} - \frac{\partial x}{\partial l} \frac{\partial y}{\partial l} \right) = 0 \qquad (4.2.11)$$

which shows the vector

$$\mathbf{i} \frac{\partial y}{\partial l} - \mathbf{j} \frac{\partial x}{\partial l} = \mathbf{n}$$

in the equation (4.2.9) is normal to the boundary curve 'l' .Therefore in equation

(4.2.9), the term $\nabla \phi \left(\mathbf{i} \frac{\partial y}{\partial l} - \mathbf{j} \frac{\partial x}{\partial l} \right) = \nabla . \mathbf{n}$ is the component of $\nabla \phi$ in the direction

normal to the curve 'l', which by the magnetic boundary wall condition is zero.

Hence equation (4.2.8) becomes

$$\iint_s \nabla (\phi \, \nabla \phi) = 0 \qquad (4.2.12)$$

whence from equation (4.2.5)

$$\iint_S \phi \, \nabla^2 \phi \, ds = -\iint_S (\nabla \phi).(\nabla \phi) \, ds$$

$$= -\iint_S (\nabla \phi)^2 \, ds \qquad (4.2.13)$$

substituting this latter result in equation (4.2.3). Then gives

$$k^2 = \frac{\iint_S (\nabla \phi).(\nabla \phi) ds}{\iint_S \phi^2 ds} \qquad (4.2.14)$$

which is a variational expression for the eigenvalues. That is if ϕ is changed by a small variation to $\phi + \delta\phi$ then k^2 becomes $k^2 + \delta k^2$, and , up to first order terms in $\delta\phi$ and $\nabla\phi$, δk^2 is zero. This is easily seen by writing (4.2.14) as,

$$k^2 \iint_S \phi^2 ds = \iint_S (\nabla \phi)^2 \, ds \qquad (4.2.15)$$

whence,

$$\delta k^2 \iint_S \phi^2 ds + k^2 \iint_S 2\phi \, \delta\phi \, ds = \iint_S 2(\nabla \phi).(\nabla \delta\phi) ds \qquad (4.2.16)$$

so that,

$$\delta k^2 = \frac{2\iint_S \left[(\nabla_T \phi).(\nabla_T \delta\phi) - k^2 \phi \, \delta\phi \right] ds}{\iint_S \phi^2 ds} \qquad (4.2.17)$$

which is zero to the first order variations $\delta\phi$ $\nabla\delta\phi$.

Equation (4.2.14) is the variational expression for the eigenvalues of an unperturbed patch and it is employed in the following section to determine the eigenvalues required for the perturbed patch antenna.

4.3 The Dominant Eigenvalues of a Perturbed Square Patch

In this section the dominant eigenvalues of a perturbed system are obtained in term of the eigenvalues of the corresponding unperturbed system. This result is then applied to obtain the modal resonant frequencies for the truncated square patch antenna in

section 4.4 and the eigenfunctions associated with each of the antennas are then obtained in section 4.5.

Let the dominant eigenfunction and eigenvalue of the perturbed planar circuit be denoted by ϕ' and k'^2, respectively. Considering only the dominant modes required for circular polarisation, ϕ' is taken to be of the form [1, 2],

$$\phi' = P\phi_a + Q\phi_b \qquad (4.3.1)$$

The perturbed eigenvalues, k'^2 (equation 4.2.14), are then given by

$$k'^2 = \frac{\iint\limits_{S+\Delta S} (\nabla\phi').(\nabla\phi')ds}{\iint\limits_{S+\Delta S} \phi'^2 ds} \qquad (4.3.2)$$

where ΔS is the perturbation element.

Substituting (4.3.1) into equation (4.3.2) gives,

$$k'^2 = \frac{\iint\limits_{S+\Delta S} (P\nabla\phi_a + Q\nabla\phi_b) \cdot (P\nabla\phi_a + Q\nabla\phi_b)ds}{\iint\limits_{S+\Delta S} (P\phi_a + Q\phi_b)^2 ds} \qquad (4.3.3)$$

The dominant eigenfunction relates to the smallest eigenvalue so that k'^2 is to be minimised with respect to the parameters P,Q . That is P,Q must satisfy the two conditions

$$\partial k'^2/\partial P = 0 \text{ , and , } \partial k'^2/\partial Q = 0 \qquad (4.3.4)$$

For this purpose it is convenient to write equation (4.3.3) in the form,

$$k'^2 \iint\limits_{S+\Delta S} (P\phi_a + Q\phi_b)^2 ds = \iint\limits_{S+\Delta S} (P\nabla\phi_a + Q\nabla\phi_b).(P\nabla\phi_a + Q\nabla\phi_b) ds \qquad (4.3.5)$$

Differentiating partially with respect to P, gives

$$\frac{\partial k'^2}{\partial P} \iint_{S+\Delta S} (P\phi_a + Q\phi_b)^2 ds + k'^2 \iint_{S+\Delta S} 2(P\phi_a + Q\phi_b)\phi_a ds$$

so the condition, $\partial k'^2/\partial P = 0$ gives

$$k'^2 \iint_{S+\Delta S} \left(P\phi_a^2 + Q\phi_b\phi_a\right) ds = \iint_{S+\Delta S} \left(P\nabla\phi_a.\nabla\phi_a + Q\nabla\phi_b.\nabla\phi_a\right) ds \qquad (4.3.6)$$

Dividing the integration domain $S + \Delta S$ into the two separate domain S and ΔS, equation (4.3.6) can be rewritten as,

$$k'^2 P \iint_S \phi_a^2 ds + k'^2 Q \iint_S \phi_b\phi_a ds + k'^2 P \iint_{\Delta S} \phi_a^2 ds + k'^2 Q \iint_{\Delta S} \phi_b\phi_a ds$$

$$= P \iint_S \nabla\phi_a.\nabla\phi_a ds + Q \iint_S \nabla\phi_b.\nabla\phi_a ds + P \iint_{\Delta S} \nabla\phi_a.\nabla\phi_a ds + Q \iint_{\Delta S} \nabla\phi_b.\nabla\phi_a ds \qquad (4.3.7)$$

Since ϕ_a, ϕ_b have been orthonormalised therefore

$$\iint_S \phi_a\phi_b ds = 0 \qquad \text{if } \phi_a \neq \phi_b$$

$$\iint_S \phi_a\phi_a ds = 1$$

$$\iint_S \nabla_T\phi_a.\nabla_T\phi_b ds = 0 \qquad \text{if } \phi_a \neq \phi_b \qquad (4.3.8)$$

$$\iint_S \nabla_T\phi_a.\nabla_T\phi_a ds = k^2$$

and hence equation (4.3.7) simplifies to

$$k'^2 P + k'^2 P \iint_{\Delta S} \phi_a^2 ds + k'^2 Q \iint_{\Delta S} \phi_b\phi_a ds = Pk^2 + P \iint_{\Delta S} \nabla\phi_a.\nabla\phi_a ds + Q \iint_{\Delta S} \nabla\phi_b.\nabla\phi_a ds \quad (4.3.9)$$

It is convenient to adopt the following notation for the above integrals:

$$\iint_{\Delta S} \phi_a^2 ds = p_1$$

$$\iint_{\Delta S} \phi_a\phi_b ds = p_{12}$$

$$\iint_{\Delta S} (\nabla\phi_a.\nabla\phi_a) ds = q_1 \qquad (4.3.10)$$

$$\iint_{\Delta S} (\nabla\phi_a.\nabla\phi_b) ds = q_{12}$$

Equation (4.3.9) then becomes

$$k^{'2}P + k^{'2}Pp_1 + k^{'2}Qp_{12} = Pk^2 + Pq_1 + Qq_{12} \tag{4.3.11}$$

hence, $P\left[k^{'2} + k^{'2}p_1 - k^2 - q_1\right] + Q\left[k^{'2}p_{12} - q_{12}\right] = 0$ (4.3.12)

being a linear algebraic equation for P and Q.

Similarly from equation (4.3.5), with $\partial k^{'2} / \partial Q = 0$, a second linear algebraic

equation for ' P ' and ' Q ', namely,

$$P\left[q_{12} - k^{'2}p_{12}\right] + Q\left[k^2 + q_2 - k^{'2}\left(1 + p_2\right)\right] = 0 \tag{4.3.13}$$

is obtained, where

$$p_2 = \iint_{\Delta S} \phi_b^2 ds, \text{ and, } q_2 = \iint_{\Delta S} \left(\nabla \phi_b\right)^2 ds$$

Equation (4.3.12) and (4.3.13) are two homogeneous linear algebraic equation

in the unknown constants, P and Q .

For non-trivial solutions for P,Q it is necessary that the determinant of coefficients is

zero . That is

$$\begin{vmatrix} k^2 + q_1 - k^{'2}\left(1 + p_1\right) & q_{12} - k^{'2}p_{12} \\ q_{12} - k^{'2}p_{12} & k^2 + q_2 - k^{'2}\left(1 + p_2\right) \end{vmatrix} = 0 \tag{4.3.14}$$

The solution of which gives the values of dominant values of k^2 for a general

perturbation.

4.4 Dominant Eigenvalues and Modal Frequencies for a Corner Truncated Square Patch

The double integrations (4.3.10) over the deleted triangles, for the evaluation of

$p_1, p_2, q_1, q_2, p_{12}$ and q_{12} , are given in appendix 4C. The values obtained are

$$p_1 = p_2 = 2(\Delta S/S)$$

$$q_1 = q_2 = q_{12} = 0 \qquad\qquad (4.4.1)$$

$$p_{12} = -2(\Delta S/S)$$

The evaluations take place over the triangles $\Delta S1$ as shown in figure 4.4.1.

$\Delta S = d^2$, and, the unperturbed patch area, $S = a^2$.
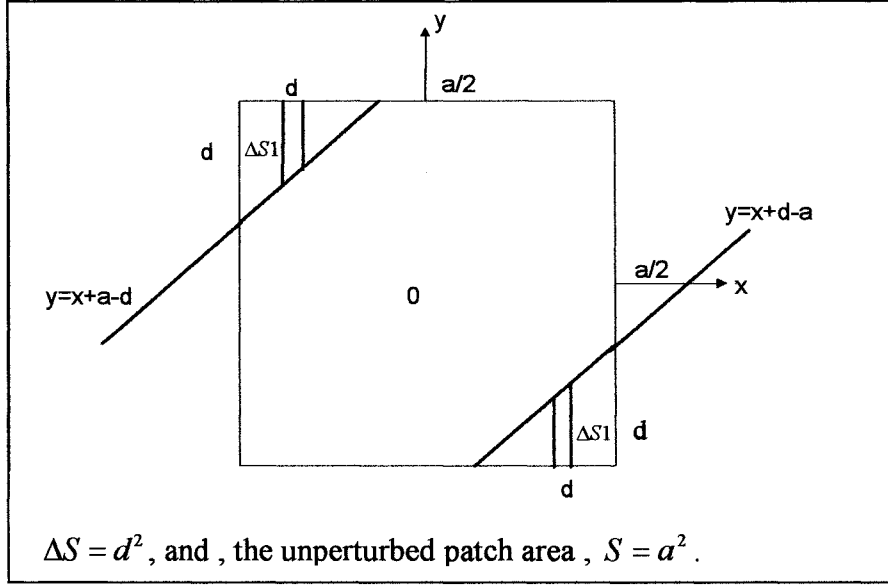
Figure 4.4.1 : The unperturbed square patch antenna

Substituting the results (4.4.1) into equation (4.3.14), gives

$$\begin{vmatrix} k^2 - k'^2\left(1 + \dfrac{2\Delta S}{S}\right) & k'^2 \dfrac{2\Delta S}{S} \\[2mm] k'^2 \dfrac{2\Delta S}{S} & k^2 - k'^2\left(1 + \dfrac{2\Delta S}{S}\right) \end{vmatrix} = 0$$

so that,

$$\left(k^2 - k'^2\left(1 + \frac{4\Delta S}{S}\right)\right)\cdot\left(k^2 - k'^2\right) = 0$$

Therefore,

$$k'^2 = k^2 \quad, \quad \frac{k^2}{\left(1 + \dfrac{4\Delta S}{S}\right)}$$

On using the binomial expansion,

$$k_a^{'2} = k^2 \left(1 - \frac{4\Delta S}{S} \right), \text{ and, } k_b^{'2} = k^2 \qquad (4.4.2)$$

where k is the resonant wave number of the unperturbed structure.

That is, $k = 2\pi/\lambda$, where λ is the modal wavelength which in terms of the modal frequency.

The values of $k_a^{'}$, $k_b^{'}$ are the resonant wave number of the resonant modes produced by perturbed system.

Thus, $k_a^{'} = 2\pi/\lambda_a$, and, $k_b^{'} = 2\pi/\lambda_b$

where λ_a, λ_b are the modal wavelength.

Therefore from equation(4.4.2),

$$f_a = \frac{ck_a^{'}}{2\pi} = \frac{ck}{2\pi} \left(1 - \frac{4\Delta S}{S} \right)^{\frac{1}{2}} \cong \frac{ck}{2\pi} \left(1 - \frac{2\Delta S}{S} \right)$$

and,

$$f_b = \frac{ck_b^{'}}{2\pi} = \frac{ck}{2\pi}$$

Thus, in terms of the unperturbed modal frequency, f_b,

$$f_a = f_b \left(1 - \frac{2\Delta S}{S} \right) \qquad (4.4.3)$$

Two resonant frequencies, f_a, f_b are shown on the impedance-frequency graphs in figure 4.4.2 below
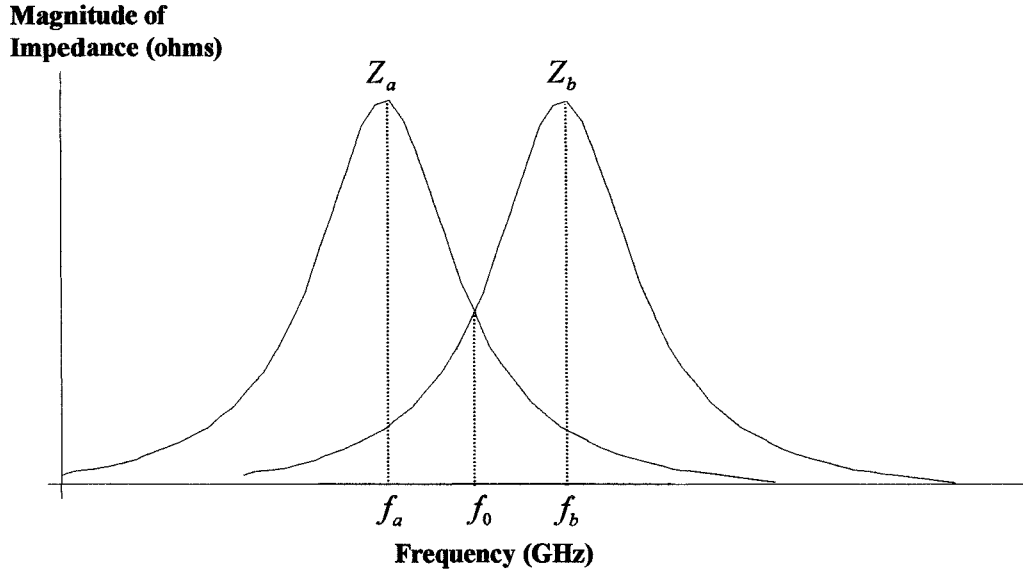
Figure 4.4.2: Two mode resonant frequencies

4.5 The Dominant Orthonormalised Eigenfunctions

The eigenfunction for the perturbed structure corresponding to an eigenvalue $k^{'}$ is

$$\phi^{'} = P\phi_a + Q\phi_b \qquad (4.5.1)$$

Using the first equation for P and Q in system of equation (4.3.14), and, putting

$q_1 = 0$, $q_{12} = 0$, and $p_{12} = -p_1$ from equation (4.4.1), gives

$$P\left(k^2 - k^{'2}(1 + p_1)\right) + Qk^{'2}p_1 = 0 \qquad (4.5.2)$$

There are two cases to consider, one in respect of the eigenpair k_a' , ϕ_a' with

associated values P_a, Q_a, and the, eigenpair k_b' , ϕ_b' and associated values P_b and Q_b.

In the first case, with, $\phi_a' = P_a\phi_a + Q_a\phi_b$, equation (4.5.2) gives,

$$P_a\left(k^2 - k_a'^2(1+p_1)\right) + Q_a k_a'^2 p_1 = 0$$

where ,

$$k_a'^2 = \frac{k^2}{(1+2p_1)}$$

Therefore,

59

$$P_a\left(k^2 - \frac{k^2}{1+2p_1}(1+p_1)\right) + Q_a p_1 \frac{k^2}{1+2p_1} = 0$$

which reduces to,

$$P_a p_1 + Q_a p_1 = 0$$

Therefore,

$$P_a + Q_a = 0 \text{, and, } P_a = -Q_a$$

hence, $\phi'_a = P_a \phi_a + Q_a \phi_b = P_a(\phi_a - \phi_b)$

On squaring and integrating over S , gives

$$\iint_S \phi'^2_a \, dx \, dy = \iint_S \left(\phi'^2_a + \phi^2_b - 2\phi_a\phi_b\right) dx \, dy$$

$$= P_a^2(1 + 1 - 0) = 2P_a^2$$

The orthonormal condition requires, $P_a = 1/\sqrt{2}$

Therefore,

$$\phi'_a = V_0/\sqrt{2}\left(\sin k_a x - \sin k_a y\right) \tag{4.5.3}$$

In the second case, with, $\phi'_b = P_b \phi_a + Q_b \phi_b$, equation (4.5.2) gives,

$$P_b\left(k^2 - k_b'^2(1 + p_1)\right) + Q_b k_b'^2 p_1 = 0$$

where, $k_a'^2 = k^2$

Therefore,

$$-P_b p_1 + Q_b p_1 = 0$$

so that, $P_b - Q_b = 0$, and, $P_b = Q_b$

and the orthonormal condition gives

$$P_b = 1/\sqrt{2}$$

60

hence, $\phi_b' = V_0 / \sqrt{2} \left(\sin k_b x + \sin k_b y \right)$ (4.5.4)

4.6 The Equivalent Circuit Model and Admittances for the Dominant Model Voltages

The equivalent circuit of a single feed circularly polarised patch antenna is shown in figure 4.6.1.1 [1,4] while figure 4.4.2 is the two resonant frequencies of the circuit. The ϕ_a' potential is modelled by a voltage V_a across an $R_a L_a C_a$ resonant circuit and the ϕ_b' potential correspondingly modelled, by a voltage V_b across an $R_b L_b C_b$ resonant circuit. Excitation by the feed is modelled by a voltage V_f which generates both V_a and V_b by means of transformers T_a, T_b connecting the feed voltage to the individual R-L-C resonant circuits. The turns ratios are $N_a : 1$ and $N_b : 1$.

The conditions for circular polarisation are that the feed position must be correctly located and that at resonance, the mode amplitudes are equal $\left(\left| V_a \right| = \left| V_b \right| \right)$, and, the phase difference of the two modes is $\pm \pi / 2$ $\left(\arg(V_a / V_b) = \pi / 2 \right)$. Hence the turns ratios N_a, N_b are also equal in magnitude.

The turns ratio

$$N_a \propto V_a = K \phi_a' = K \left(\sin kx - \sin ky \right)$$

while,

$$N_b \propto V_b = K \phi_b' = K \left(\sin kx + \sin ky \right)$$

where the K is a constant at proportionality.

For N_a, N_b to be of equal magnitude, either

(a) $y = 0$, $-\dfrac{a}{2} \leq x \leq \dfrac{a}{2}$.

(b) $x = 0$, $-\dfrac{a}{2} \leq y \leq \dfrac{a}{2}$.

That is the feed must either be located on the x-axis (case (a)), or , on the y-axis (case(b)) .
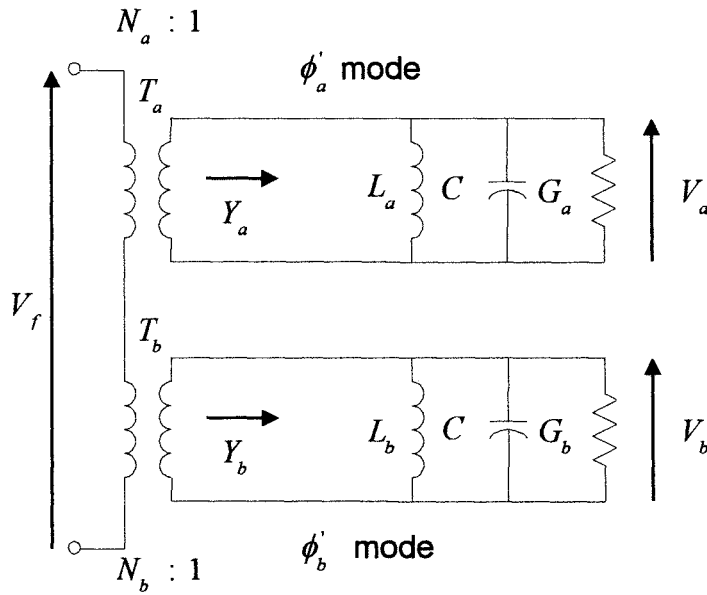
Figure 4.6.1.1: Equivalent circuit of a truncated patch antenna

For this case $G_a = G_b = G$.

For a parallel circuit ,

$$G = wC/Q \tag{4.6.1}$$

The admittances Y_a and Y_b of the RLC circuits are

$$Y_a = G + jwC + \frac{1}{jwL_a} = G + j\left(wC - \frac{1}{wL_a} \right) \tag{4.6.2}$$

and,

$$Y_b = G + jwC + \frac{1}{jwL_b} = G + j\left(wC - \frac{1}{wL_b} \right) \tag{4.6.3}$$

where Q is the unloaded Q-factor

Substituting equation (4.6.1) into equation (4.6.2) and (4.6.3) gives

$$Y_a = 2\pi\, C \left(\frac{f_a}{Q_a} + j\left(f - \frac{f_a^2}{f} \right) \right)$$ (4.6.4)

similarly,

$$Y_b = 2\pi\, C \left(\frac{f_b}{Q_b} + j\left(f - \frac{f_b^2}{f} \right) \right)$$ (4.6.5)

where Q_a and Q_b are the unloaded Q-factors of the ϕ_a' and ϕ_b' modes respectively.

The frequency shift of the two mode ϕ_a' and ϕ_b' is small and it can be assumed that

$$Q_a = Q_b = Q$$

where, Q is the unloaded Q-factor at the design frequency , f_0. Equations 4.6.4 and 4.6.5 are used in the conditions for the circular polarisation in the following section.

4.7 Application of Modal Admittance System to Circular Polarisation Conditions

From the equivalent circuit as shown in figure 4.6.1 , assuming the currents flowing in each R-L-C circuit are equal then the ratio of the voltages V_a, V_b is given by (Appendix 4D)

$$\left| \frac{V_b}{V_a} \right| = \left| \left(\frac{N_b}{N_a} \right) \cdot \left(\frac{Y_a}{Y_b} \right) \right|$$ (4.7.1)

substituting equations 4.6.1 and 4.6.2 into the equation 4.7.1 gives

$$\left| \frac{V_b}{V_a} \right| = \left| \left(\frac{N_b}{N_a} \right) \cdot \frac{\left(\frac{f_a}{Q} + j\left(f - \frac{f_a^2}{f} \right) \right)}{\left(\frac{f_b}{Q} + j\left(f - \frac{f_b^2}{f} \right) \right)} \right|$$ (4.7.2)

The algebraic sign of N_b/N_a is determined by the location of the feed line as discussed above. Thus equation 4.7.2 can now be written as,

$$\frac{V_b}{V_a} = \pm \left(\frac{\dfrac{f_a}{Q} + j\left(f - \dfrac{f_a^2}{f}\right)}{\dfrac{f_b}{Q} + j\left(f - \dfrac{f_b^2}{f}\right)} \right)$$ (4.7.3)

Substituting the modal frequencies,

$$f_a = f_o\left(1 - \frac{2\Delta S}{S}\right) = f_o M$$ (4.7.4)

where, $f_b = f_o$, and, $M = 1 - 2\Delta S/S$ (4.7.5)

into equation 4.7.3 gives

$$\frac{V_b}{V_a} = \pm \left(\frac{\dfrac{f_o M}{Q} + j\left(f - \dfrac{f_o^2 M^2}{f}\right)}{\dfrac{f_o}{Q} + j\left(f - \dfrac{f_o^2}{f}\right)} \right)$$ (4.7.6)

For circular polarisation conditions, requires that

$$\frac{V_b}{V_a} = \pm j$$

where + sign is used for right-hand circular polarisation and the − sign is used for left-hand circular polarisation.

For the magnitude condition as shown in Appendix 4E,

$$\frac{1}{Q^2} - 2 + \frac{(M^2 + 1)}{\alpha^2} = 0$$ (4.7.7)

where,
$$\alpha = f/f_o$$

so,

$$\alpha^2 = (M^2 + 1)\bigg/\left(\frac{1}{Q^2} - 2\right)$$ (4.7.8)

For the phase condition $\pm\pi/2$, requires that

$$\arg V_a - \arg V_b = \arg\left(V_a/V_b\right) = \pm\pi/2$$

Rationalising V_a/V_b , gives (Appendix 4E)

$$\frac{\dfrac{f_o^2}{Q}\left(f-\dfrac{f_o^2 M^2}{f}\right)-\dfrac{f_o M}{Q}\left(f-\dfrac{f_o^2}{f}\right)}{\dfrac{f_o^2 M}{Q^2}+\left(f-\dfrac{f_o^2 M^2}{f}\right)\left(f-\dfrac{f_o^2}{f}\right)}=\tan\left(\pm\frac{\pi}{2}\right)=\pm\infty$$

which requires,

$$\frac{f_o^2 M}{Q^2}+\left(f-\frac{f_o^2 M^2}{f}\right)\left(f-\frac{f_o^2}{f}\right)=0$$

hence,

$$\frac{M}{Q^2}+\alpha^2-M^2-1+\frac{M^2}{\alpha^2}=0 \qquad\qquad (4.7.9)$$

From equations (4.7.8) and (4.7.9) it is shown that (Appendix 4E)

$$Q^2\delta^2=\frac{\left(1-2\delta+\dfrac{3\delta^2}{2}-\dfrac{\delta^3}{2}\right)}{\left(1-\dfrac{\delta}{2}+\dfrac{\delta^2}{4}\right)} \qquad\qquad (4.7.10)$$

where, $\delta = 2\Delta S/S$.

Since in the perturbation analysis $\Delta S/S$ is small compare to unity, therefore equation 4.7.10 gives,

$$\frac{\Delta S}{S}=\frac{1}{2Q} \qquad\qquad (4.7.11)$$

which is the perturbation requirement to produce circular polarisation.

SUMMARY

In this chapter the eigenvalues and eigenfunctions of the dominant field modes for a corner deleted square patch antenna have been derived. The eigensystem has been applied in a perturbation analysis to obtain the corresponding eigenvalues, eigenfunctions and resonant modal frequencies of a square patch with two truncated corners. Using an equivalent circuit model, and, the conditions on the dominant modal voltages for circular polarisation, a formula for the fractional perturbation area in terms of the unloaded Q-factor, has been obtained.

CHAPTER 5

COPLANAR MULTIPORT CIRCUIT ANALYSIS

5.1 Introduction

A microstrip antenna patch is a planar circuit on which the voltage at any point due to a probe feed can be determined in term of the probe feed current density. The voltage satisfies a nonhomogeneous boundary value problem which is solved in section 5.2 using the eigenfunction expansion method which introduces the Green's function of the patch. In section 5.3 it is shown that a perimeter microstrip feed is equivalent to a corresponding probe feed at the same location.

A general formula for the coupling impedance between a perimeter port and a microstrip feed at a second port is obtained in terms of the interport impedance and the Green's function of the patch (section 5.4).

5.2 Patch Voltage for a Probe Feed

An arbitrary shaped patch antenna using a probe feed is shown in figure 5.2.1
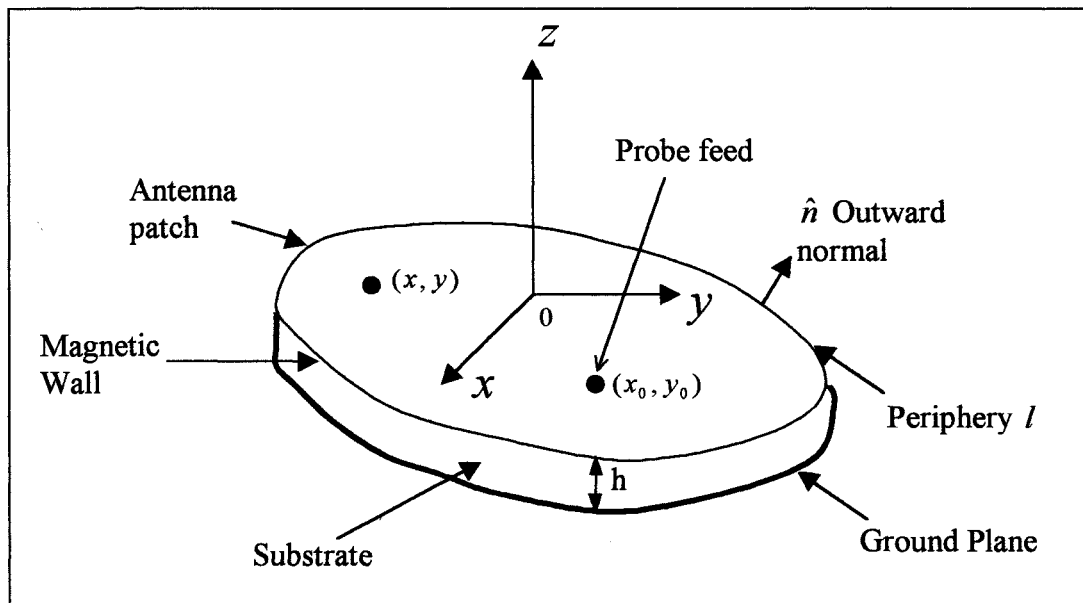
Figure 5.2.1: Antenna structure with probe feed

67

The microstrip antenna structure with the origin of coordinates located on the ground plane is illustrated in figure 5.2.1. In practice the substrate is electrically thin $(h < \lambda_0)$. Therefore, only the z component of electric field, and, the x and y components of the magnetic field, exist in the region bounded by the patch and ground plane. To account for the fringing electric field the geometry of the patch is extended outwards to obtain a model with a magnetic wall, thus making the outward normal voltage gradient on the patch perimeter zero. That is the field structure is based on the "cavity model".

In the above model the voltage, $V = V(x,y)$, at any point on the patch satisfies the two dimensional non-homogenous wave equation [1].

$$\nabla^2 V + k^2 V = -j\omega\mu h J_z \qquad (5.2.1)$$

where, J_z is the current density, at a point (x_o, y_o), of an external feed current injected perpendicular to the patch plane, and, $k = \omega\sqrt{\varepsilon\mu}$ is the free space wave number.

The voltage satisfies the magnetic wall boundary condition,

$$\frac{\partial V}{\partial n} = 0 \qquad (5.2.2)$$

along the patch perimeter.

Equation (5.2.1) , (5.2.2) constitute a non-homogeneous wave equation boundary value problem.

The solution of this problem can be obtained through the solution of the associated homogeneous boundary value problem.

$$\nabla^2 \phi + \lambda^2 \phi = 0 \qquad (5.2.3)$$

$$\frac{\partial \phi}{\partial n} = 0 \qquad (5.2.4)$$

For patch geometries such as rectangles, circles, and, some triangles, the homogeneous problem can be solved analytically as an eigenvalue problem, in which, for each value of $\lambda^2 = \lambda_{m,n}^2$, $m, n \geq 0$, there is a solution $\phi_{m,n}(x, y)$. These are the eigenvalues and eigenfunctions of the boundary value problem and can be derived by the method of separation of variables.

Thus, the voltage modes, $\phi_{m,n}(x, y)$ satisfy the homogeneous wave equation

$$\nabla^2 \phi_{m,n} + \lambda_{m,n}^2 \phi_{m,n} = 0 \tag{5.2.5}$$

The modal fucntions $\phi_{m,n}$ can be scaled to an orthonormalised form, such that

$$\iint_D \phi_{m,n}(x, y)\, \phi_{r,s}(x, y) = \delta_{r,s}^{m,n} \tag{5.2.6}$$

where, D is the domain of the patch, and,

$$\delta_{r,s}^{m,n} = 1 , \qquad \text{both } m = r, \quad \text{and }, n = s \neq 0 \tag{5.2.7}$$

$$= 0 , \qquad \text{otherwise}$$

A solution of the non-homogeneous problem (5.2.1), (5.2.2) can then be obtained, by the eigenfunction expansion method, in the form

$$V(x, y) = \sum_{m=0}^{\infty} \sum_{n=0}^{\infty} \alpha_{m,n}\, \phi_{m,n}(x, y) \tag{5.2.8}$$

where, $\alpha_{m,n}$ are constants obtained as follows.

Substituting the above expression for $V(x, y)$ into the non-homogeneous wave equation (5.2.1), gives

$$\sum_{m=0}^{\infty} \sum_{n=0}^{\infty} \alpha_{m,n} \nabla^2 \phi_{m,n} + k^2 \sum_{m=0}^{\infty} \sum_{n=0}^{\infty} \alpha_{m,n} \phi_{m,n} = -j\omega\mu h J_z \tag{5.2.9}$$

Substituting,

$$\nabla^2 \phi_{m,n} = -\lambda_{m,n}^2 \, \phi_{m,n} \qquad\qquad (5.2.10)$$

from equation (5.2.5), into equation (5.2.9) , gives

$$-\sum_{m=0}^{\infty}\sum_{n=0}^{\infty}\alpha_{m,n} \, \lambda_{m,n}^2 \, \phi_{m,n} + k^2 \sum_{m=0}^{\infty}\sum_{n=0}^{\infty}\alpha_{m,n} \, \phi_{m,n} = -j\omega\,\mu\,h\,J_z$$

or,

$$\sum_{m=0}^{\infty}\sum_{n=0}^{\infty}\alpha_{m,n}\left(k^2 - \lambda_{m,n}^2\right) \, \phi_{m,n} = -j\omega\mu h J_z \qquad\qquad (5.2.11)$$

Multiplying equation (5.2.11), on both sides, by $\phi_{r,s}$ and integrating over the patch

domain, D, gives

$$\iint_{D}\alpha_{m,n}\left(k^2 - \lambda_{m,n}^2\right)\phi_{m,n} \, \phi_{r,s} \, dxdy = -j\omega\mu h\iint_{D} J_z \, \phi_{r,s} \, dxdy \qquad\qquad (5.2.12)$$

Applying the orthonomalisation condition (5.2.6) then gives,

$$\alpha_{m,n}\left(k^2 - \lambda_{m,n}^2\right) = -j\omega\mu h \iint_{D} J_z \, \phi_{m,n} \, dxdy \qquad\qquad (5.2.13)$$

hence,

$$\alpha_{m,n} = \frac{-j\omega\mu h}{\left(k^2 - \lambda_{m,n}^2\right)} \iint_{D} J_z \, \phi_{m,n} \, dxdy \qquad\qquad (5.2.14)$$

which, on substitution into equation (5.2.8) gives the modal expansion solution

$$V(x,y) = -j\omega\mu h \sum_{m=0}^{\infty}\sum_{n=0}^{\infty}\frac{\phi_{m,n}(x,y)}{\left(k^2 - \lambda_{m,n}^2\right)} \iint_{D} J_z(x_o,y_o) \, \phi_{m,n}(x_o,y_o) \, dx_0 \, dy_0 \qquad (5.2.15)$$

where the coordinates x_o, y_o are introduced to distinguish between the function

$\phi_{m,n}(x, y)$ outside the double integration, from the function $\phi_{m,n}(x_o, y_o)$ under the

integration sign.

The above equation (5.2.15) can be written in the form

$$V(x,y) = \iint_D G(x,y \mid x_o, y_o) \, J_z(x_o, y_o) \, dx_o dy_o \qquad (5.2.16)$$

where,

$$G(x,y \mid x_o, y_o) = j\omega\mu h \sum_{m=0}^{\infty} \sum_{n=0}^{\infty} \frac{\phi_{m,n}(x,y)}{\left(\lambda_{m,n}^2 - k^2\right)} \phi_{m,n}(x_o, y_o) \qquad (5.2.17)$$

The function, $G(x,y \mid x_o, y_o)$, is called the Green's function of the patch geometry.

To evaluate equation 5.2.16 it is necessary to obtain an analytical form for the Green's function of each patch geometry. For a rectangular (appendix 4A), or, circular patch, the analytic Green's function can be obtained, in terms of an infinite series, by the method of separation of variables. Schelkunoff S.A [2] gives the result for an equilateral triangle but without a derivation.

Chada and Gupta [3] have derived Green's functions for several triangular geometries by the method of images, using specially selected sets of line sources. The line source potentials are expanded in infinite series to obtain expansion functions satisfying the homogenous boundary value problem. These functions are then used in an infinite series representation of the non-homogenous wave equation which is substituted into the wave equation to determine the unknown expansion coefficients. In this way Green's functions have been obtained for the following triangle geometries.

a) A $30^0 - 60^0$ Right-angle Triangle

b) An Equilateral Triangle

c) An Isosceles Right-angled Triangle

71

It can be seen from inspection that the Green's function for the isosceles right-angled triangle satisfies the homogenous wave equation and the boundary conditions on the perpendicular sides. The boundary condition on the hypotenuse is verified in appendix 5A.

The Green's functions for the above three triangle geometries cannot be obtained by the method of separation of variables. At this time analytic forms of Green's functions for patch geometries other than listed above have not been found.

A generalised mathematical discussion of Green's functions in "Abstract Operator Form", which includes the Helmholtz wave equation, is to be found in Morse & Feszhback [4].

5.3 Microstrip Feed Equivalence to Probe Feed

It is convenient for fabrication and matching to use a microstrip feed line at the perimeter. Consequently it is necessary to show that on the perimeter, the effect of microstrip feed of line density $J_s \left(s_o \right)$ is equivalent to the probe feed of line density $J_z \left(s_o \right)$.

From the Maxwell's equation the magnetic field 'H' in the substrate figure 5.3.2 is

$$\mathbf{H} = - \frac{1}{jw\mu} \nabla \times \mathbf{E} \qquad (5.3.1)$$

The electric field 'E' for the planar structure is

$$\mathbf{E} = \hat{z}\, E_z \left(x, y \right) \qquad (5.3.2)$$

where, E_z is a function of 'x' and 'y' only,

so that,

$$\mathbf{H} = -\frac{1}{jw\mu}\, \nabla \times \hat{\mathbf{z}}\, E_z(x, y)$$

$$= -\frac{1}{jw\mu}\left\{\hat{\mathbf{x}}\,\frac{\partial E_z}{\partial y} - \hat{\mathbf{y}}\,\frac{\partial E_z}{\partial x}\right\}$$

But, since $\dfrac{\partial E_z}{\partial z} = 0$, then the voltage ' v ' between the antenna and the ground plane

is given by

$$v = -E_z h \tag{5.3.3}$$

The equation 5.3.1 for ' $\mathbf{H}$ ' can thus be expressed in the form

$$\mathbf{H} = \frac{1}{jw\mu h}\left\{\hat{\mathbf{x}}\,\frac{\partial v}{\partial y} - \hat{\mathbf{y}}\,\frac{\partial v}{\partial x}\right\} \tag{5.3.4}$$

Using Maxwell's equation for the surface current density $\mathbf{J}_s$ on the antenna patch

$$\mathbf{J}_s = \hat{\mathbf{z}} \times \mathbf{H} \tag{5.3.5}$$

then

$$\mathbf{J}_s = \frac{1}{jw\mu h}\,\hat{\mathbf{z}} \times \left\{\hat{\mathbf{x}}\frac{\partial v}{\partial y} - \hat{\mathbf{y}}\frac{\partial v}{\partial x}\right\}$$

$$= \frac{1}{jw\mu h}\left\{\hat{\mathbf{x}}\frac{\partial v}{\partial x} + \hat{\mathbf{y}}\frac{\partial v}{\partial y}\right\} \tag{5.3.6}$$

In order to apply the magnetic wall boundary condition $\left(\partial V/\partial n = 0\right)$ to the above

expression for the current density vector $\mathbf{J}_s$ it is necessary to convert the Cartesian

form into the form with tangential and normal components (as shown in Appendix

5B) and this results in the following equation

$$\mathbf{J}_s = \frac{1}{jw\mu h}\left\{\frac{\partial v}{\partial s}\,\hat{\mathbf{s}} - \frac{\partial v}{\partial n}\,\hat{\mathbf{n}}\right\} \tag{5.3.7}$$

where $\hat{n}$ is the outward normal.

On a given segment of the perimeter when a uniform current source is applied there is no variation in 'v' over that segment. Thus $(\partial v/\partial s = 0)$, so that equation 5.3.7 reduces to

$$\mathbf{J}_s = -\frac{1}{jw\mu h}\frac{\partial v}{\partial n}\hat{n} \qquad (5.3.8)$$

Further, at all points on the perimeter of the segment where an external source of current is absent, $(\partial v/\partial n = 0)$.

That is a microstrip feed line on the perimeter generates an equivalent feed current normal to the plane of the patch. So that current density $\mathbf{J}_z(x,y)$ applied on the perimeter can be replaced by an equivalent microstrip current density $\mathbf{J}_s(s)$ normal to the perimeter.

For the microstrip feed as shown in figure 5.3.2 the effect of the feed is to produce a $\hat{z}$ directed current $\mathbf{J}_z$ in the dielectric of the same magnitude as the microstrip feed current $\mathbf{J}_s$ at the feed port.
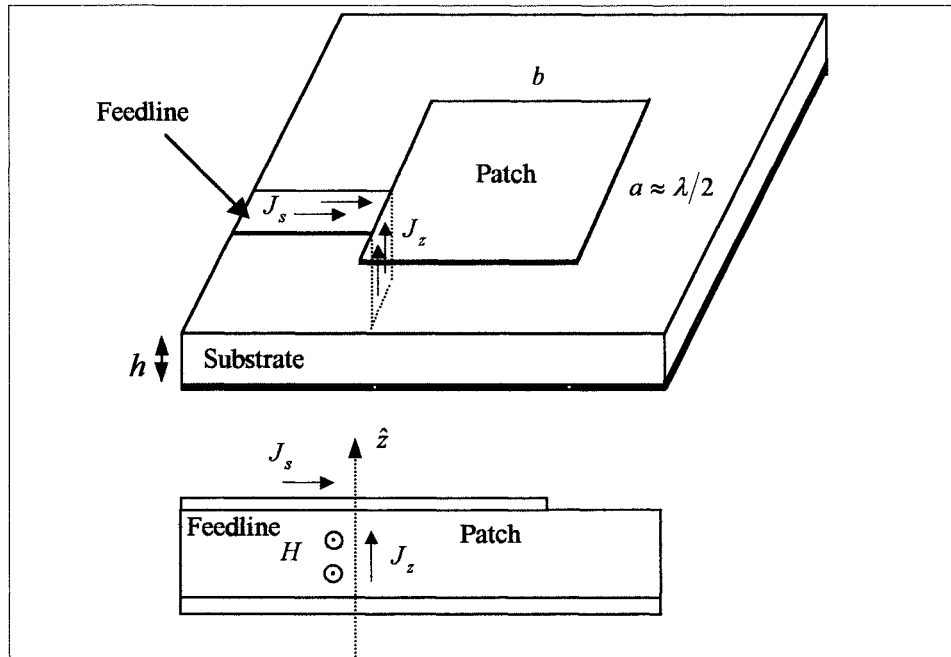
Figure 5.3.2 : Surface current flowing on a microstrip feed line

74

5.4 Formula for Perimeter Port Coupling Impedances

Let $s = s(x, y)$, and, $s_0 = s_0(x_0, y_0)$ be the running coordinates of the i-th, and, j-th perimeter ports respectively, as shown in figure 5.4.1. let the current source, $J_{s_0}(x_0, y_0) = J_{s_0}(s_0)$, be distributed along a length, W_j, of the perimeter. It is recommended by [5] that the width of a port should always be less then $\lambda_g / 20$, where, λ_g is the wave length of the field in the substrate.
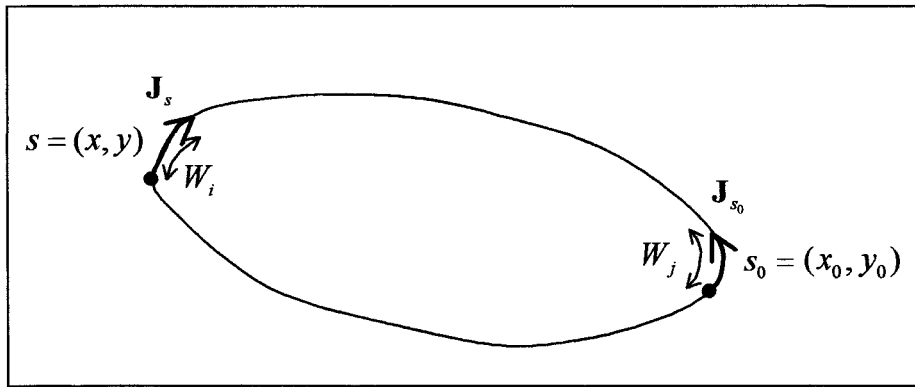
Figure 5.4.1: Microstrip ports with perimeter coordinates

Equation 5.2.16 then takes the form

$$V(s) = \int_{W_j} G(s \mid s_o)\, J_{s_0}(s_o)\, ds_o \tag{5.4.1}$$

A terminal voltage, V_i, on the segment, W_i, is now defined as the average voltage over W_i, so that

$$V_i = \frac{1}{W_i} \int_{W_i} V(s)\, ds \tag{5.4.2}$$

which, on substitution $V(s)$ from equation 5.4.1, gives

$$V_i = \frac{1}{W_i} \int_{W_i} \int_{W_j} G(s \mid s_o)\, J_{s_0}(s_o)\, ds\, ds_o \tag{5.4.3}$$

For a multiport system, $j = 1, 2, 3 \ldots\ldots\ldots$, equation 5.4.3 becomes

$$V_i = \frac{1}{W_i} \sum_j \int\int\limits_{W_i W_j} G(s \mid s_o) \, J_{s_0}(s_o) \, ds \, ds_o \qquad (5.4.4)$$

Let I_j be the average current density over the j-th port, so that

$$I_j = \int\limits_{W_j} \frac{J_{s_0}(s_0) \, ds_0}{W_j} \qquad (5.4.5)$$

then, for sufficiently small port widths, W_j, equation 5.4.4 can be approximated by

$$V_i = \frac{1}{W_i} \sum_j \int\int\limits_{W_i W_j} G(s \mid s_o) \, \frac{I_j}{W_j} \, ds \, ds_o$$

$$= \frac{I_j}{W_i W_j} \sum_j \int\int\limits_{W_i W_j} G(s \mid s_o) \, ds \, ds_o \qquad (5.4.6)$$

The coupling impedance between the i-th, and j-th ports is define as

$$Z_{ij} = \frac{V_i}{I_j} \qquad (5.4.7)$$

Therefore, from equation 5.4.6

$$Z_{ij} = \frac{1}{W_i W_j} \sum_j \int\int\limits_{W_i W_j} G(s \mid s_o) \, ds_o ds \qquad (5.4.8)$$

In particular when there is only a single port $(i = j)$ then the patch input impedance is given by

$$Z_{in} = \frac{1}{W^2} \sum_j \int\int\limits_{W\,W} G(s \mid s_0) \, ds_0 \, ds \qquad (5.4.9)$$

Summary

For a probe feed the voltage at any point in the perimeter has been obtained in term of the Green's function of the patch, and, the current density injected normal to the plane of the patch. It has been shown that the same result is obtained by a corresponding microstrip feed. A formula connecting the voltage at one port on the perimeter to the total normal microstrip current at a second port has been derived and the interport coupling impedance defined.

CHAPTER 6

MULTIPORT SEGMENTATION AND

DESEGMENTATION MODELLING OF COMPOSITE

STRUCTURES

6.1 Introduction

For a patch antenna with a single direct feed whose geometry is either, a rectangle, one of three specific triangles, or a circular sector it is possible to determine the input impedance analytically from planar circuit analysis. This is possible because the Green's functions of the above geometries are known analytically and thus the impedance is determined analytically.

For other geometries, the Green's functions are not available. However in the case that a geometry can be made up of a combination of the above geometries it is possible to determine the input impedance of the combined structure by segmenting the antenna geometry into regular shaped segments for which the Green's function of each individual segment is known.

The physical basis of multiport modelling is illustrated in figure 6.1.1 below
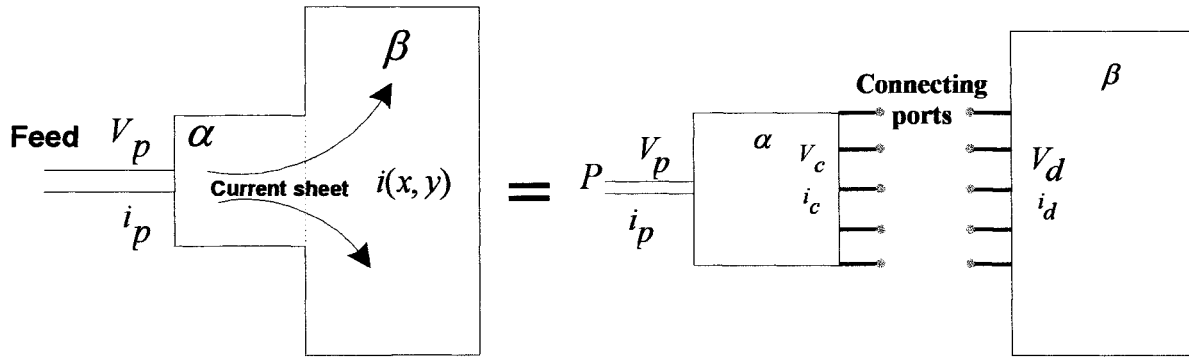
Figure 6.1.1: Current sheet on antenna

where the two regular segments, α and β, of the complete structure are separated but joined by a series of connecting ports. The continuous current sheet distribution across the boundary between the two segments is approximated by the port currents at the connecting ports. This discretization is used in the multiport analysis where the matrix circuit equations conserve the original current distribution on each segment, as this determines the antenna input impedance.

Two methods, segmentation and desegmentation can be used to obtain the multiport modelling structure of the patch antenna. The segmentation method can be applied to planar structures whose segments combine in cascade, or, in a shunt configuration where the segments are attached to a base segment but do not share any common boundary. Separate analyses are required for each of these structures.

The desegmentation method can be applied to planar structures where the deleted segments do not share any common boundary. Published material on the segmentation method is to be found in [1-10], and, for the desegmentation method, [3,4,9,11,12,13].

The segmentation method is applied to a two segment, and, a three segment cascade-type structure in sections 6.2.1 and 6.2.2 respectively, to obtain the input impedance matrix formula. In section 6.3 a new generalised input impedance matrix formula is derived for a shunt-type segmentation structure with any number of attached segments.

The desegmentation analysis for a single deleted segment is given in sections 6.4. A new generalised result for the case of any number of deleted segments is obtained in section 6.5. In section 6.6 a comparison is made between the segmentation method and the desegmentation method as applied to a two corner deleted square patch antenna.

6.2 Multiport Segmentation Modelling for Cascade-type Segmental Structures

Decomposition of a patch geometry into regular shapes is illustrated below in figure 6.2.1
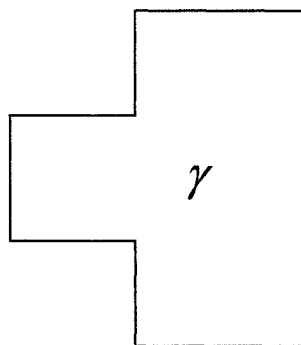
Figure 6.2.1 : The T shape geometry

The above geometry can be segmented as shown in figure 6.2.2
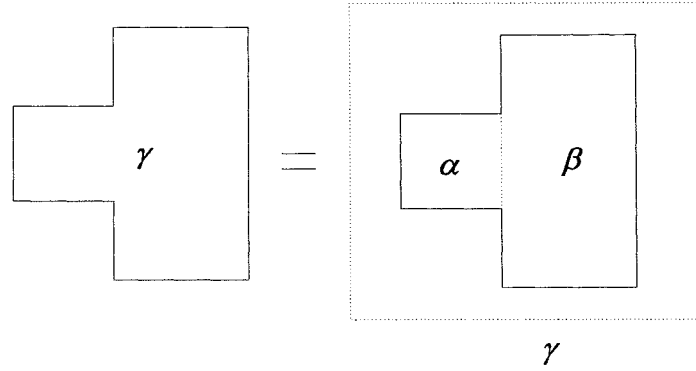
Figure 6.2.2: Segmentation

6.2.1 Input Impedance for a Two Segment Cascade-type Structure

Figure 6.2.1.1 shows the port current and voltage system for two segments.

$\gamma -$ *segment*
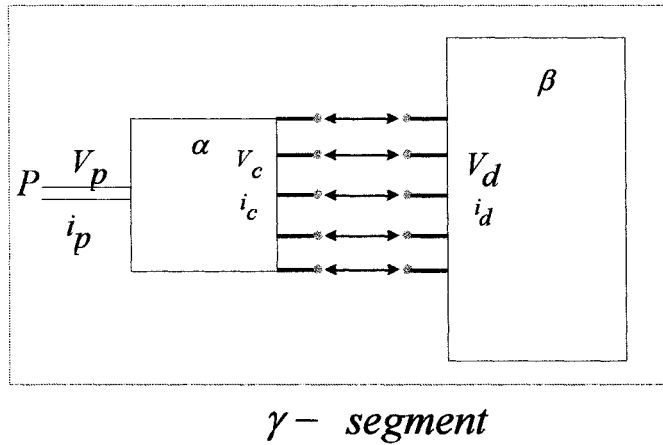
Figure 6.2.1.1 : Connecting port replacement

where, $V_c = (V_{c1}, V_{c2}, \ldots, V_{cN})$, $i_c = (i_{c1}, i_{c2}, \ldots, i_{cN})$, and, similarly for V_d , i_d.

Continuity of current and voltage across the partition interface requires that, $V_c = V_d$, and,

$$i_c = -i_d.$$

The current vectors i_c , i_d and voltages V_c , V_d are related by the following matrix circuit equations

$$V_p = Z_{pp} i_p + Z_{pc} i_c \qquad (6.2.1.1)$$

81

$$V_c = Z_{cp} i_p + Z_{cc} i_c \qquad (6.2.1.2)$$

$$V_d = Z_{dd} i_d \qquad (6.2.1.3)$$

where,

$$Z_{pc} = \begin{pmatrix} Z_{pc1}, & Z_{pc2}, & \ldots\ldots, & Z_{pcN} \end{pmatrix}$$

$$Z_{cp} = Z_{pc}^T$$

$$Z_{cc} = \begin{bmatrix} Z_{cc11} & Z_{cc12} & \cdots\cdots & Z_{cc1N} \\ Z_{cc21} & Z_{cc22} & \cdots\cdots & Z_{cc2N} \\ \vdots & \vdots & \vdots & \vdots \\ Z_{ccN1} & Z_{ccN2} & \cdots\cdots & Z_{ccNN} \end{bmatrix}$$

and similarly for Z_{dd}.

Since $V_c = V_d$, $i_d = -i_c$, the above equations, (6.2.1.1, 6.2.1.2, 6.2.1.3) may be put in the matrix form

$$\begin{bmatrix} V_p \\ V_c \\ V_c \end{bmatrix} = \begin{bmatrix} Z_{pp} & Z_{pc} & 0 \\ Z_{cp} & Z_{cc} & 0 \\ 0 & 0 & Z_{dd} \end{bmatrix} \begin{bmatrix} i_p \\ i_c \\ -i_c \end{bmatrix}$$

$$\qquad (6.2.1.4)$$
$$\qquad (6.2.1.5)$$
$$\qquad (6.2.1.6)$$

Note that Z_{cc}, Z_{dd} are symmetric matrices. The elements in the impedance matrices represent the coupling impedances between each combination of any two of the associated segment ports. From the matrix system of equations 6.2.1.4 to 6.2.1.6, the current i_c is obtained in terms of i_p by equating the matrix equations 6.2.1.5 and 6.2.1.6 to obtain

$$Z_{cp} i_p + Z_{cc} i_c + Z_{dd} i_c = 0$$

whence,

82

$$i_c = \left(Z_{cc} + Z_{dd} \right)^{-1} - Z_{cp} i_p \qquad\qquad (6.2.1.7)$$

Substituting for i_c from equation 6.2.1.7 into equation 6.2.1.4 gives

$$V_p = \left[Z_{pp} - Z_{pc} \left(Z_{cc} + Z_{dd} \right)^{-1} Z_{cp} \right] i_p \qquad\qquad (6.2.1.8)$$

or,

$$V_p = Z_\gamma \, i_p \qquad\qquad (6.2.1.9)$$

whence,

$$Z_\gamma = \left[Z_{pp} - Z_{pc} \left(Z_{cc} + Z_{dd} \right)^{-1} Z_{cp} \right] \qquad\qquad (6.2.1.10)$$

which is the impedance of the overall structure, γ.

Z_{pc} has dimension (N x 1). The matrix, $\left(Z_{cc} + Z_{dd} \right)^{-1} Z_{cp}$ has dimension (N x N) x (N X

1) = N x 1, and, so, $Z_{pc} \left(Z_{cc} + Z_{dd} \right)^{-1} Z_{cp}$ has dimension (1 x N) x (N X 1) = (1 x 1). That

is, the right hand side of equation 6.2.1.10 is a single complex number, namely, the

complex input impedance of the antenna.

6.2.2 Input Impedance for a Three Segment Cascade-type Structure

For the antenna patch geometry shown in figure 6.2.2.1 below
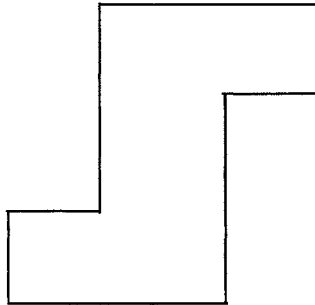
Figure 6.2.2.1: Antenna Patch

the segmentation structure is shown in figure 6.2.2.2 below
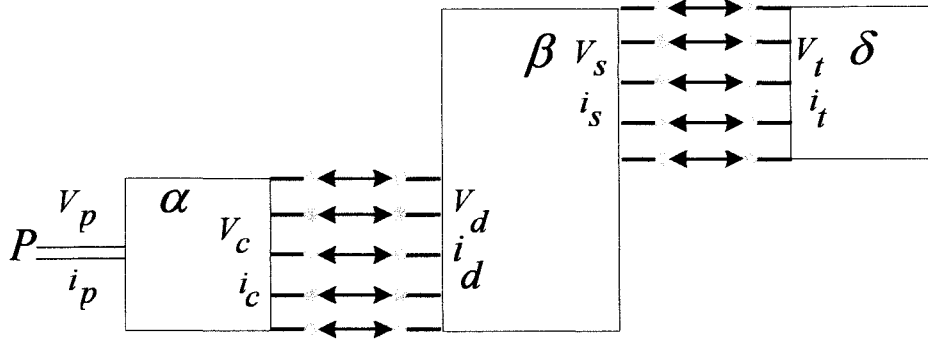
Figure 6.2.2.2: Connecting port replacement.

The matrix circuit equations for the port voltage and currents, shown in figure 6.2.2.2, are:

$$v_p = Z_{pp} i_p + Z_{pc} i_c \qquad (6.2.2.1)$$

$$v_c = Z_{cp} i_p + Z_{cc} i_c \qquad (6.2.2.2)$$

$$v_c = -Z_{dd} i_c + Z_{ds} i_s \qquad (6.2.2.3)$$

$$v_s = -Z_{sd} i_c + Z_{ss} i_s \qquad (6.2.2.4)$$

$$v_s = -Z_{tt} i_s \qquad (6.2.2.5)$$

Equating equation 6.2.2.4 and 6.2.2.5 gives,

$$i_s = (Z_{ss} + Z_{tt})^{-1} Z_{sd} i_c \qquad (6.2.2.6)$$

Equating equation 6.2.2.2 and 6.2.2.3 gives,

$$Z_{cp} i_p + Z_{cc} i_c = -Z_{dd} i_c + Z_{ds} i_s$$

hence from equation 6.2.2.6

$$Z_{cp} i_p = \left[Z_{ds}(Z_{ss} + Z_{tt})^{-1} Z_{sd} - Z_{cc} - Z_{dd} \right] i_c \qquad (6.2.2.7)$$

substitute equation (6.2.2.7) into (6.2.2.1) then gives,

$$Z_{pp\gamma} = \left[Z_{pp\alpha} + Z_{pc\alpha} \left[Z_{ds\beta}(Z_{ss\beta} + Z_{tt\delta})^{-1} Z_{sd\beta} - Z_{cc\alpha} - Z_{dd\beta} \right]^{-1} Z_{cp\alpha} \right] \quad (6.2.2.8)$$

This is a new result.

6.3 Multiport Segmentation for Shunt-type Structures

A Shunt-attached segment type structure is illustrated in figure 6.3.1 below.
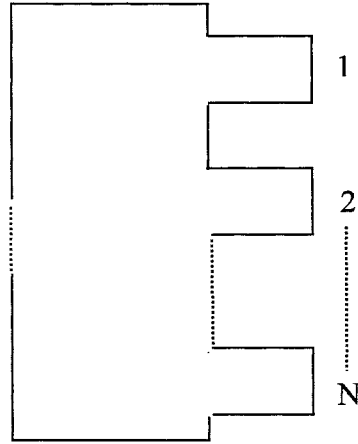
Figure 6.3.1: A shunt-type structure

The segmentation multiport structure is shown in figure 6.3.2 below
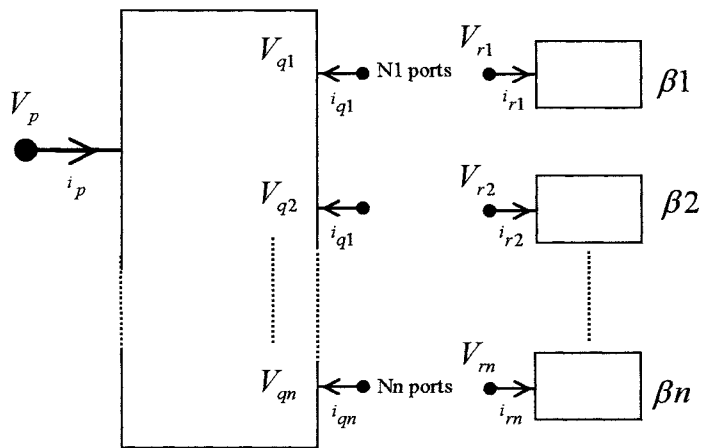
n = number of segments
Nn = number of ports per segment

Figure 6.3.2: Segmentation shunt-type multiport structure

Where each segment β_k has Nk connecting ports, for, $k = 1, n$. The following circuit equations apply to the above segmentation structure.

$$V_p = Z_{pp}i_p + Z_{pq}i_q \quad ; \qquad i_q = \begin{bmatrix} i_{q1}, & i_{q2}, & \dots\dots, & i_{qn} \end{bmatrix}^T \tag{6.3.1}$$

$$V_q = Z_{qp}i_p + Z_{qq}i_q \quad ; \qquad V_q = \begin{bmatrix} V_{q1}, & V_{q2}, & \dots\dots, & V_{qn} \end{bmatrix}^T \tag{6.3.2}$$

where, $Z_{qp} = Z_{pq}^T$

$$V_{ri} = Z_{rri}\, i_{ri} \qquad , \qquad \text{for } i = 1, n \tag{6.3.3}$$

$$V_{ri} = V_{qi} \qquad ; \qquad i_{ri} = -i_{qi} \quad , \qquad \text{for } i = 1, n \tag{6.3.4}$$

From (6.3.3) and (6.3.4):

$$V_{qi} = -Z_{rri}\, i_{qi} \quad , \qquad \text{for } i = 1, n \tag{6.3.5}$$

That is from (6.3.1) and (6.3.2):

$$V_q = - \begin{bmatrix} Z_{rr1} & 0 & 0 & 0 \\ 0 & Z_{rr2} & 0 & 0 \\ 0 & 0 & \searrow & 0 \\ 0 & 0 & 0 & Z_{rrn} \end{bmatrix} i_q \tag{6.3.6}$$

or, $V_q = -Z_{rr}\, i_q \tag{6.3.7}$

where

$$Z_{rr} = \begin{bmatrix} Z_{rr1} & 0 & 0 & 0 \\ 0 & Z_{rr2} & 0 & 0 \\ 0 & 0 & \searrow & 0 \\ 0 & 0 & 0 & Z_{rrn} \end{bmatrix}$$

Each sub-matrix Z_{rrk} has dimension $Nk \times Nk$, and, Z_{rr} has dimension

$\left(N1 + N2 + \dots\dots + Nn \right) \times \left(N1 + N2 + \dots\dots + Nn \right)$.

From (6.3.7) and (6.3.2):

86

$$i_q = -\left(Z_{rr} + Z_{qq}\right)^{-1} Z_{qp} \, i_p \tag{6.3.8}$$

From (6.3.8) and (6.3.1), therefore the input impedance , V_p/i_p , is given by

$$Z_{in} = Z_{pp} - Z_{pq}\left(Z_{qq} + Z_{rr}\right)^{-1} Z_{qp} \tag{6.3.9}$$

This is a new result.

6.4 Multiport Desegmentation Modelling for a Single Deleted Segment Structure

In contrast to a segmentation form of partitioning into segments the desegmentation method *augments* an antenna geometry to achieve a resulting geometry for which the associated Green's function is known. For example the rectangular patch with slot in figure 6.4.1 below,
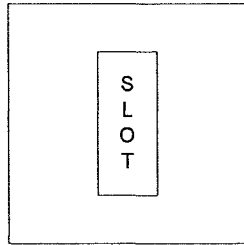
Figure 6.4.1: Slot segment

is augmented by a metalised cover segment over the slot whereby the combination results in a complete rectangle as illustrated below, with labelled segments, in figure 6.4.2.
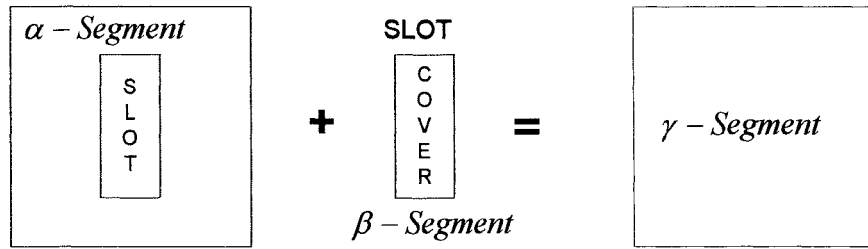
Figure 6.4.2 : Augmentation of slot-segment

Here the α-segment has been augmented with a β-segment to give the γ-segment. The input impedance of the γ-segment is required.

For the purpose of the matrix analysis the multiport structure is displayed as in figure 6.4.3, below. It is convenient to have same number of ports in each of the c, d, and q sets of ports.
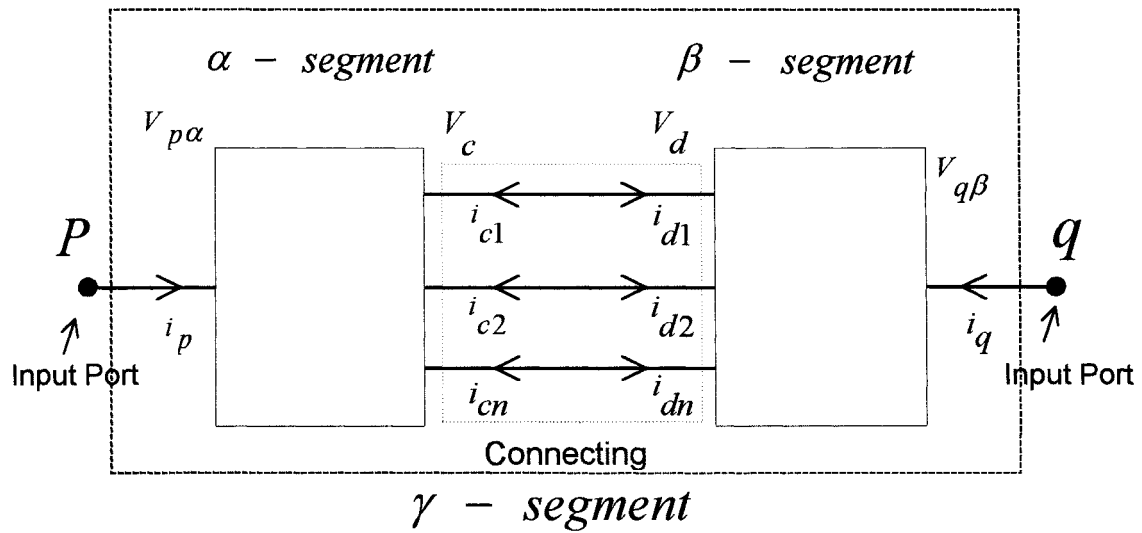
Figure 6.4.3: Multiport desegmentation network

The complete γ-segment is shown below in figure 6.4.4.
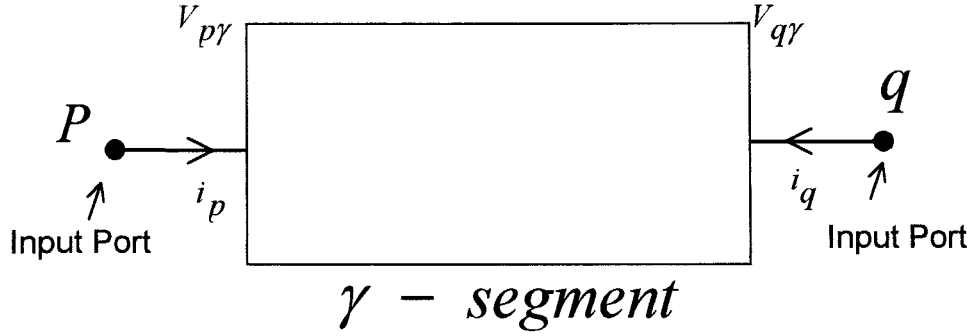
Figure 6.4.4: Complete γ-segment

The segmentation port coupling matrix of the γ-segment is

$$Z_\gamma = \begin{bmatrix} Z_{pp\gamma} & Z_{pq\gamma} \\ Z_{qp\gamma} & Z_{qq\gamma} \end{bmatrix}$$

each matrix element of which can be calculated.

The segmentation port coupling matrix of the β-segment is

$$Z_\beta = \begin{bmatrix} Z_{dd\beta} & Z_{dq\beta} \\ Z_{qd\beta} & Z_{qq\beta} \end{bmatrix}$$

where each matrix element can be calculated.

The segmentation port coupling matrix of the α-segment must be determined by the desegmentation matrix analysis technique, and has the form,

$$Z_\alpha = \begin{bmatrix} Z_{pp\alpha} & Z_{pc\alpha} \\ Z_{cp\alpha} & Z_{cc\alpha} \end{bmatrix}$$

where each element can be obtained in terms of elements of the above two matrices, Z_γ and Z_β. $Z_{pp\alpha}$ is the input impedance as seen at port-p.

A formula for the input impedance, $Z_{pp\alpha}$, is derived in the following analysis and consist of five main steps. For clarity, an overview of the steps used in the solution of the matrix circuit equations is described below.

Procedures in the Matrix Circuit Analysis

The following are used in deriving the matrix input impedance formula:

(a) The voltage-current matrix equations in respect of $V_{p\alpha}, V_{q\beta}, V_c, V_d$ and the interconnecting boundary conditions are set up. This system of matrix equations is formed into a single matrix display.

(b) The matrix formulation obtained in procedure (a) is then partitioned so as to combine the equations in respect of $V_{p\alpha}, V_{q\beta}$ into a form where external port elements are partitioned separately from the interconnecting port elements. The individual partitions are then assigned their individual compact notation and the original matrix system of order 4 reduces to a more convenient system of order 3.

(c) The overall matrix system of order 3 obtained in (b) is then replaced by the equivalent set of 3 individual equations which are then solved for the external port voltage-current matrix relation.

(d) The compact notation introduced in (b) is then used in the matrix equations in (c) to eventually obtain the characteristic impedance Z_γ of the γ-segment in terms of the impedance of the α and β segment.

(e) By equating components of the Z_γ matrix with the expression obtained in (d), the four expressions for $Z_{pp\gamma}, Z_{pq\gamma}, Z_{pq\gamma}$, and $Z_{qq\gamma}$ in terms of the α, β impedance element

are obtained. A back substitution through these equations then gives the required formulas for $Z_{ppa}, Z_{pca}, Z_{cpa}, Z_{cca}$, and, hence the characteristic impedance of the α-segment.

Matrix Circuit Analysis

Step (a)

The basic circuit equations for the α and β-segment are

$$
\begin{aligned}
V_{pa} &= Z_{ppa} i_{pa} + [0] i_{q\beta} + Z_{pc} i_{ca} + [0] i_{dq} \\
V_{q\beta} &= [0] i_{pa} + Z_{qq\beta} i_{q\beta} + [0] i_{ca} + Z_{qd} i_{dq} \\
V_c &= Z_{cp} i_{pa} + [0] i_{q\beta} + Z_{cca} i_{ca} + [0] i_{dq} \\
V_d &= [0] i_{pa} + Z_{dq} i_{q\beta} + [0] i_{ca} + Z_{dd} i_{dq}
\end{aligned}
\tag{6.4.1}
$$

with $V_d = V_c$, and, $i_c + i_d = [0]$ (6.4.2)

which on substituting equation (6.4.2) in (6.4.1) can be written in the matrix form

$$
\begin{bmatrix} V_{pa} \\ V_{q\beta} \\ V_c \\ V_d \end{bmatrix} = \begin{bmatrix} Z_{ppa} & 0 & Z_{pca} & 0 \\ 0 & Z_{qq\beta} & 0 & Z_{qd\beta} \\ Z_{cp} & 0 & Z_{cca} & 0 \\ 0 & Z_{dq} & 0 & Z_{dd\beta} \end{bmatrix} \begin{bmatrix} i_{pa} \\ i_{q\beta} \\ i_c \\ -i_c \end{bmatrix}
\tag{6.4.3}
$$

Step (b)

Grouping of the external coupling matrix terms together, and, grouping the interconnecting coupling matrix terms together is achieved by the following partitioning of the system (6.4.3).

$$\begin{bmatrix} V_{p\alpha} \\ V_{q\beta} \\ \hdashline V_c \\ V_d \end{bmatrix} = \begin{bmatrix} Z_{pp\alpha} & 0 & Z_{pc\alpha} & 0 \\ 0 & Z_{qq\beta} & 0 & Z_{qd\beta} \\ \hdashline Z_{cp} & 0 & Z_{cc\alpha} & 0 \\ 0 & Z_{dq} & 0 & Z_{dd\beta} \end{bmatrix} \begin{bmatrix} i_{p\alpha} \\ i_{q\beta} \\ \hdashline i_c \\ -i_c \end{bmatrix}$$

(6.4.4)

Step (c)

It is convenient to introduce the following compact notation for the above partitioning:

$$Z_{pp} = \begin{bmatrix} Z_{pp\alpha} & 0 \\ 0 & Z_{qq\beta} \end{bmatrix}; \qquad Z_{pc} = \begin{bmatrix} Z_{pc\alpha} \\ 0 \end{bmatrix}; \qquad Z_{qd} = \begin{bmatrix} 0 \\ Z_{qd\beta} \end{bmatrix};$$

$$V_p = \begin{bmatrix} V_{p\alpha} \\ V_{q\beta} \end{bmatrix}; \qquad i_p = \begin{bmatrix} i_{p\alpha} \\ i_{q\beta} \end{bmatrix}$$

and $Z_{cp\alpha} = Z_{pc\alpha}^T$, $Z_{dq} = Z_{qd}^T$

(6.4.5)

With the above notation in place, system (6.4.4) becomes,

$$\begin{bmatrix} V_p \\ V_c \\ V_c \end{bmatrix} = \begin{bmatrix} Z_{pp} & Z_{pc} & Z_{qd} \\ Z_{cp} & Z_{cc\alpha} & 0 \\ Z_{dq} & 0 & Z_{dd} \end{bmatrix} \begin{bmatrix} i_p \\ i_c \\ -i_c \end{bmatrix}$$

(6.4.6)

or,

$$\begin{aligned} V_p &= Z_{pp} i_p + Z_{pc} i_c - Z_{qd} i_c & \text{(i)} \\ V_c &= Z_{cp} i_p + Z_{cc\alpha} i_c & \text{(ii)} \\ V_c &= Z_{dq} i_p - Z_{dd} i_c & \text{(iii)} \end{aligned}$$

(6.4.7)

Equating 6.4.7(ii), (iii) gives

$$i_c = [Z_{cc} + Z_{dd}]^{-1}[Z_{dq} - Z_{cp}] i_p$$

(6.4.8)

Substituting for i_c, in (6.4.7), gives

$$V_p = [Z_{pp} + [Z_{pc} - Z_{qd}][Z_{cc} + Z_{dd}]^{-1}[Z_{dq} - Z_{cp}]] i_p$$

(6.4.9)

92

or, $V_p = Z_\gamma \, i_p$ (6.4.10)

Step (d)

Now, $Z_{pc} - Z_{qd} = \begin{bmatrix} Z_{pc\alpha} \\ 0 \end{bmatrix} - \begin{bmatrix} 0 \\ Z_{qd\beta} \end{bmatrix} = \begin{bmatrix} Z_{pc\alpha} \\ -Z_{qd\beta} \end{bmatrix}$

and, $Z_{dq} - Z_{cp} = \begin{bmatrix} -Z_{cp\alpha} & Z_{dq\beta} \end{bmatrix}$

whence, in (6.4.9)

$$[Z_{pc} - Z_{qd}][Z_{cc} + Z_{dd}]^{-1}[Z_{dq} - Z_{cp}]$$

$$= \begin{bmatrix} -Z_{pc\alpha}[Z_{cc} + Z_{dd}]^{-1}Z_{cp\alpha} & Z_{pc\alpha}[Z_{cc} + Z_{dd}]^{-1}Z_{dq\beta} \\ Z_{qd\beta}[Z_{cc} + Z_{dd}]^{-1}Z_{cp\alpha} & -Z_{qd\beta}[Z_{cc} + Z_{dd}]^{-1}Z_{dq\beta} \end{bmatrix}$$ (6.4.11)

Thus from (6.4.9) and (6.4.11) the impedance matrix of the γ segment is given by

$$Z_\gamma = \begin{bmatrix} Z_{pp\gamma} & Z_{pq\gamma} \\ Z_{qp\gamma} & Z_{qq\gamma} \end{bmatrix}$$

$$= \begin{bmatrix} Z_{pp\alpha} & 0 \\ 0 & Z_{qq\beta} \end{bmatrix} + \begin{bmatrix} -Z_{pc\alpha}[Z_{cc} + Z_{dd}]^{-1}Z_{cp\alpha} & Z_{pc\alpha}[Z_{cc} + Z_{dd}]^{-1}Z_{dq\beta} \\ Z_{qd\beta}[Z_{cc} + Z_{dd}]^{-1}Z_{cp\alpha} & -Z_{qd\beta}[Z_{cc} + Z_{dd}]^{-1}Z_{dq\beta} \end{bmatrix}$$ (6.4.12)

Expressions for $Z_{pp\gamma}, Z_{pq\gamma}, Z_{pq\gamma}$, and $Z_{qq\gamma}$ are obtained form (6.4.11)by equating the

elements on each side of the equation, as in procedure (e)

Step (e)

$$Z_{pp\gamma} = Z_{pp\alpha} - Z_{pc\alpha}[Z_{cc\alpha} + Z_{dd}]^{-1}Z_{cp\alpha} \qquad \text{(i)}$$

$$Z_{pq\gamma} = Z_{pc\alpha}[Z_{cc\alpha} + Z_{dd}]^{-1}Z_{dq\beta} \qquad \text{(ii)}$$

$$Z_{qp\gamma} = Z_{qp\beta}[Z_{cc\alpha} + Z_{dd}]^{-1}Z_{cp\alpha} \qquad \text{(iii)}$$

$$Z_{qq\gamma} = Z_{qq\beta} - Z_{qd\beta}[Z_{cc\alpha} + Z_{dd}]^{-1}Z_{dq\beta} \qquad \text{(iv)}$$

(6.4.13)

93

The element of the characteristic impedance matrix of the α-segment,

$$Z_\alpha = \begin{bmatrix} Z_{pp\alpha} & Z_{pc\alpha} \\ Z_{cp\alpha} & Z_{cc\alpha} \end{bmatrix}$$

(6.4.14)

can now be obtained from equations(6.4.13; I, ii, iii, iv) by back substitution as follows.

From equation (6.4.13; iv):

$$Z_{cc\alpha} = -Z_{dd} + Z_{dq\beta}\left[Z_{qq\beta} - Z_{qq\gamma}\right]^{-1} Z_{qd\beta}$$

(6.4.15)

From equation (6.4.13; iii):

$$Z_{qd\beta}^{-1} Z_{qp\gamma} Z_{cp\alpha}^{-1} = \left[Z_{cc\alpha} + Z_{dd}\right]^{-1}$$

$$= \left[Z_{dq\beta}\left[Z_{qq\beta} - Z_{qq\gamma}\right]^{-1} Z_{qd\beta}\right]^{-1}$$

$$= Z_{qd\beta}^{-1}\left[Z_{qq\beta} - Z_{qq\gamma}\right] Z_{dq\beta}^{-1}$$

therefore $Z_{cp\alpha} = Z_{dq\beta}\left[Z_{qq\beta} - Z_{qq\gamma}\right]^{-1} Z_{qp\gamma}$

(6.4.16)

now, $\quad Z_{pc\alpha} = Z_{cp\alpha}^T$

therefore, $Z_{pc\alpha} = Z_{pq\gamma}\left[Z_{qq\beta} - Z_{qq\gamma}\right]^{-1} Z_{qd\beta}$

(6.4.17)

From equation (6.4.13; i) $Z_{pc\alpha}$ of set (6.4.13):

$$Z_{pp\alpha} = Z_{pp\gamma} + Z_{pc\alpha}\left[Z_{cc\alpha} + Z_{dd\beta}\right]^{-1} Z_{cp\alpha}$$

(6.4.18)

From equation (6.4.15)

$$\left[Z_{cc\alpha} + Z_{dd}\right] = Z_{dq\beta}\left[Z_{qq\beta} - Z_{qq\gamma}\right]^{-1} Z_{qd\beta}$$

therefore,

$$\left[Z_{cc\alpha} + Z_{dd}\right]^{-1} = Z_{qd\beta}^{-1}\left[Z_{qq\beta} - Z_{qq\gamma}\right] Z_{dq\beta}^{-1}$$

(6.4.19)

substituting (6.4.19) into (6.4.18), gives

$$Z_{pp\alpha} = Z_{pp\gamma} + Z_{pc\alpha} Z_{qd\beta}^{-1}\left[Z_{pp\beta} - Z_{qq\gamma}\right] Z_{dq\beta}^{-1} Z_{cp\alpha}$$

(6.4.20)

Substituting for $Z_{pc\alpha}$ from equation (6.4.17) into equation (6.4.20), gives

$$Z_{pp\alpha} = Z_{pp\gamma} + Z_{pq\gamma} \left[Z_{qq\beta} - Z_{qq\gamma} \right]^{-1} Z_{qd\beta} Z_{qd\beta}^{-1} \left[Z_{qq\beta} - Z_{qq\gamma} \right] Z_{dq\beta}^{-1} Z_{cp\alpha}$$

$$= Z_{pp\gamma} + Z_{pq\gamma} \, Z_{dq\beta}^{-1} \, Z_{cp\alpha} \qquad\qquad (6.4.21)$$

Substituting for $Z_{cp\alpha}$ from equation (6.4.16) into equation (6.4.21), gives

$$Z_{pp\alpha} = Z_{pp\gamma} + Z_{pq\gamma} \left[Z_{qq\beta} - Z_{qq\gamma} \right]^{-1} Z_{qp\gamma} \qquad\qquad (6.4.22)$$

$Z_{pp\alpha}$ gives the input impedance of the α-segment.

The above result is for a single deleted segment only. In the following sections 6.5 this result is generalised to structures with multiple deleted segments.

6.5 The Generalised Multiport Desegmentation Modelling for an 'n' Deleted Segment Structure

The previous results obtained for one deleted segment suggests that the methodology employed will apply to the general case of 'n' deleted segments.

The following circuit equation analysis yields the new generalised input impedance formula.

In figure 6.5.1 the α - segment represents the antenna patch geometry which in desegmentation analysis is constructed by deleting the β - segments from γ - segment. The dimension of each deleted segment and the voltages and currents on the connecting ports are also shown in figure 6.5.1.

α - Segment   *β - Segments*   *γ - Segment*
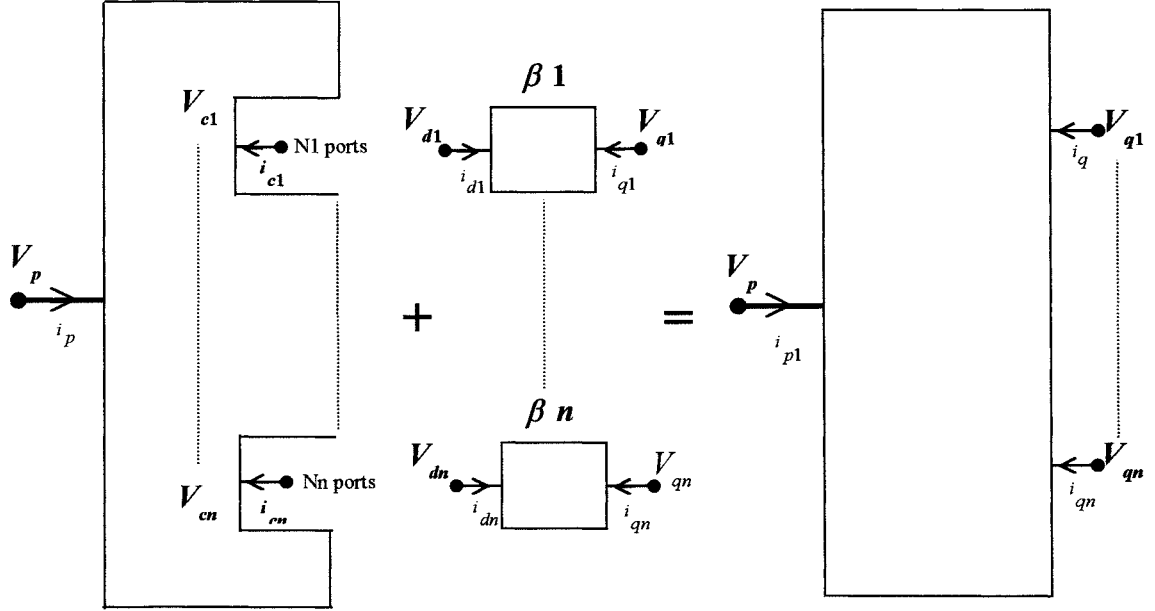
n = number of segments

Nn = number of ports per segment

Figure 6.5.1: n – segment structure with connecting port

For each of the 'n' deleted segments there are Ni connecting ports ($i = 1, 2, ..., Ni$), so that between the α and β structures there are a total of, $M = N1 + N2 + ... + Nn$, connecting ports. On the α - segment the vector connecting port voltage and current systems are,

$$V_{ci} = \begin{bmatrix} V_{ci1}, & V_{ci2}, & ..., & V_{ciNi} \end{bmatrix}^T , \quad i = 1, 2, ..., n$$

$$i_{ci} = \begin{bmatrix} i_{ci1}, & i_{ci2}, & ..., & i_{ciNi} \end{bmatrix}^T , \quad i = 1, 2, ..., n$$

and, similarly, on the β - segments,

$$V_{di} = \begin{bmatrix} V_{di1}, & V_{di2}, & ..., & V_{diNi} \end{bmatrix}^T , \quad i = 1, 2, ..., n$$

$$i_{di} = \begin{bmatrix} i_{di1}, & i_{d12}, & \cdots, & i_{diNi} \end{bmatrix}^T , \qquad i = 1, 2, \ldots, n .$$

Each β_i segment has external ports with voltages, V_{qi} $(i = 1, 2, \ldots, n)$. On the γ - segment the associated external port voltages and currents are V_p , i_p , V_{qi} , i_{qi} ($i = 1$, 2 , $\ldots\ldots$, n).

For the α - structure the voltage – current equations are

$$V_{p\alpha} = Z_{pp\alpha} \, i_p + Z_{pc\alpha} \, i_c \tag{6.5.1}$$

where, the structure of $Z_{pc\alpha} \, i_c$, with dimensions, is

$$Z_{pc\alpha} \, i_c = \begin{bmatrix} \overset{M \times N1}{\overset{\longleftrightarrow}{Z_{pc1\alpha}}} & \overset{M \times N2}{\overset{\longleftrightarrow}{Z_{pc2\alpha}}} & \cdots\cdots & \overset{M \times Nn}{\overset{\longleftrightarrow}{Z_{pcn\alpha}}} \end{bmatrix} \begin{bmatrix} i_{c1} \\ \hline i_{c2} \\ \hline \vdots \\ \hline i_{cn} \end{bmatrix} \begin{matrix} \updownarrow N1 \\ \updownarrow N2 \\ \vdots \\ \updownarrow Nn \end{matrix} \quad M = N1 + N2 + \ldots + Nn \tag{6.5.2}$$

and,

$$i_c = \begin{bmatrix} i_{c1} & \big| & i_{c2} & \big| & \cdots\cdots & \big| & i_{cn} \end{bmatrix}^T \quad ; \quad Z_{pc\alpha} = \begin{bmatrix} Z_{pc1\alpha} & \big| & Z_{pc2\alpha} & \big| & \cdots\cdots & \big| & Z_{pcn\alpha} \end{bmatrix} \tag{6.5.3}$$

The voltage-current circuit equations between the external and connecting ports on the β-segments are

$$\begin{aligned}
V_{q\beta1} &= Z_{qq\beta1} \, i_{q\beta1} + Z_{qd\beta1} \, i_{d\beta1} \\
V_{q\beta2} &= Z_{qq\beta2} \, i_{q\beta2} + Z_{qd\beta2} \, i_{d\beta2} \\
&\vdots \\
V_{q\beta n} &= Z_{qq\beta n} \, i_{q\beta n} + Z_{qd\beta n} \, i_{d\beta n}
\end{aligned} \tag{6.5.4}$$

At this point, for the β-segments, it is important to separate the coupling impedances between the connecting ports themselves, and, the coupling impedances between the external ports themselves. This is shown in the following arrangement of the matrix circuit equations.

$$
\begin{bmatrix} V_{q\beta 1} \\ V_{q\beta 2} \\ \vdots \\ V_{q\beta n} \end{bmatrix} = \begin{bmatrix} Z_{qq\beta 1} & 0 & \cdots & 0 & Z_{qd\beta 1} & 0 & \cdots & 0 \\ 0 & Z_{qq\beta 2} & \cdots & 0 & 0 & Z_{qd\beta 2} & \cdots & 0 \\ 0 & 0 & \searrow & 0 & 0 & 0 & \searrow & 0 \\ 0 & 0 & \cdots & Z_{qq\beta n} & 0 & 0 & \cdots & Z_{qd\beta n} \end{bmatrix} \begin{bmatrix} i_{q\beta 1} \\ i_{q\beta 2} \\ \vdots \\ i_{q\beta n} \\ \cdots \\ i_{d\beta 1} \\ i_{d\beta 2} \\ \vdots \\ i_{d\beta n} \end{bmatrix}
\qquad (6.5.5)
$$

The matrix equation (6.6.5) is now put in the form

$$
V_{q\beta} = \begin{bmatrix} Z_{qq\beta 1} & 0 & \cdots & 0 \\ 0 & Z_{qq\beta 2} & \cdots & 0 \\ 0 & 0 & \searrow & 0 \\ 0 & 0 & \cdots & Z_{qq\beta n} \end{bmatrix} \begin{bmatrix} i_{q\beta 1} \\ i_{q\beta 2} \\ \vdots \\ i_{q\beta n} \end{bmatrix} + \begin{bmatrix} Z_{qd\beta 1} & 0 & \cdots & 0 \\ 0 & Z_{qd\beta 2} & \cdots & 0 \\ 0 & 0 & \searrow & 0 \\ 0 & 0 & \cdots & Z_{qd\beta n} \end{bmatrix} \begin{bmatrix} i_{d\beta 1} \\ i_{d\beta 2} \\ \vdots \\ i_{d\beta n} \end{bmatrix}
\qquad (6.5.6)
$$

where,

$$
V_{q\beta} = \begin{bmatrix} V_{q\beta 1} & V_{q\beta 2} & \cdots & V_{q\beta n} \end{bmatrix}^{\mathrm{T}}
$$

Introducing the following compact notation:

$$
Z_{qq} = \begin{bmatrix} Z_{qq\beta 1} & 0 & \cdots & 0 \\ 0 & Z_{qq\beta 2} & \cdots & 0 \\ 0 & 0 & \searrow & 0 \\ 0 & 0 & \cdots & Z_{qq\beta n} \end{bmatrix} \quad , \quad i_q = \begin{bmatrix} i_{q\beta 1} \\ i_{q\beta 2} \\ \vdots \\ i_{q\beta n} \end{bmatrix}
\qquad (6.5.7)
$$

$$
Z_{qd} = \begin{bmatrix} Z_{qd\beta 1} & 0 & \cdots & 0 \\ 0 & Z_{qd\beta 2} & \cdots & 0 \\ 0 & 0 & \searrow & 0 \\ 0 & 0 & \cdots & Z_{qd\beta n} \end{bmatrix} \quad , \quad i_d = \begin{bmatrix} i_{d\beta 1} \\ i_{d\beta 2} \\ \vdots \\ i_{d\beta n} \end{bmatrix}
\qquad (6.5.8)
$$

the matrix system (6.6.5) can be written as

$$
V_{q\beta} = Z_{qq}\, i_q + Z_{qd}\, i_d
\qquad (6.5.9)
$$

where, $V_{q\beta}$, i_q , i_d , each have dimension N x 1 , and, Z_{qq} , Z_{qd} each have dimension N x N.

Similarly the voltage-current circuit equations between the connecting and external ports on the β - segments are

$$V_{d\beta} = Z_{dd}\, i_d + Z_{dq}\, i_q \qquad (6.5.10)$$

where,

$$V_{d\beta} = \begin{bmatrix} V_{d\beta 1} & V_{d\beta 2} & \cdots & V_{d\beta n} \end{bmatrix}^{\mathrm{T}}$$

$$Z_{dd} = \begin{bmatrix} Z_{dd\beta 1} & 0 & \cdots & 0 \\ 0 & Z_{dd\beta 2} & \cdots & 0 \\ 0 & 0 & \ddots & 0 \\ 0 & 0 & \cdots & Z_{dd\beta n} \end{bmatrix}, \qquad i_d = \begin{bmatrix} i_{d\beta 1} \\ i_{d\beta 2} \\ \vdots \\ i_{d\beta n} \end{bmatrix}$$

$$Z_{dq} = \begin{bmatrix} Z_{dq\beta 1} & 0 & \cdots & 0 \\ 0 & Z_{dq\beta 2} & \cdots & 0 \\ 0 & 0 & \ddots & 0 \\ 0 & 0 & \cdots & Z_{dq\beta n} \end{bmatrix}, \qquad i_q = \begin{bmatrix} i_{qd\beta 1} \\ i_{q\beta 2} \\ \vdots \\ i_{qd\beta n} \end{bmatrix}$$

The α - structure connecting port circuit equations are obtained in the form

$$V_c = Z_{cc}\, i_c + Z_{cp}\, i_p \qquad (6.5.11)$$

where,

$$V_c = \begin{bmatrix} V_{c\alpha 1} & V_{c\alpha 2} & \cdots & V_{c\alpha n} \end{bmatrix}^{\mathrm{T}}$$

$$Z_{cc} = \begin{bmatrix} Z_{cc\alpha 1} & 0 & \cdots & 0 \\ 0 & Z_{cc\alpha 2} & \cdots & 0 \\ 0 & 0 & \ddots & 0 \\ 0 & 0 & \cdots & Z_{cc\alpha n} \end{bmatrix}, \qquad i_c = \begin{bmatrix} i_{c\alpha 1} \\ i_{c\alpha 2} \\ \vdots \\ i_{c\alpha n} \end{bmatrix}$$

$$Z_{cp}\, i_p = \begin{bmatrix} \overset{M \times N1}{\overset{\longleftrightarrow}{Z_{cp1\alpha}}} & \overset{M \times N2}{\overset{\longleftrightarrow}{Z_{cp2\alpha}}} & \cdots & \overset{M \times Nn}{\overset{\longleftrightarrow}{Z_{cpn\alpha}}} \end{bmatrix} \begin{bmatrix} i_p \end{bmatrix}$$
$$\underset{M}{\underleftrightarrow{\hspace{4cm}}}$$

From equation (6.5.1), (6.5.9), (6.5.10), and, (6.5.11) the full circuit equation system is

$$V_{p\alpha} = Z_{pp\alpha}i_p + Z_{pc\alpha}i_c$$

$$V_{q\beta} = Z_{qq\beta}\,i_q + Z_{qd}\,i_d \qquad (6.5.12)$$

$$V_{c\alpha} = Z_{cc\alpha}\,i_c + Z_{cp\alpha}\,i_p$$

$$V_{d\beta} = Z_{dd}\,i_d + Z_{dq}\,i_q$$

The matrix system (6.5.12) can now be presented in the following partitioned form:

$$\begin{bmatrix} V_{p\alpha} \\ V_{q\beta} \\ \hline V_{c\alpha} \\ V_{d\beta} \end{bmatrix} = \begin{bmatrix} Z_{pp\alpha} & 0 & Z_{pc\alpha} & 0 \\ 0 & Z_{qq\beta} & 0 & Z_{qd\beta} \\ \hline Z_{cp\alpha} & 0 & Z_{cc\alpha} & 0 \\ 0 & Z_{dq\beta} & 0 & Z_{dd\beta} \end{bmatrix} \begin{bmatrix} i_{p\alpha} \\ i_{q\beta} \\ i_{c\alpha} \\ i_{d\beta} \end{bmatrix} \qquad (6.5.13)$$

Introducing the following abbreviations

$$V_p = \begin{bmatrix} V_{p\alpha} \\ V_{q\beta} \end{bmatrix}; \qquad Z_{pp} = \begin{bmatrix} Z_{pp\alpha} & 0 \\ 0 & Z_{qq\beta} \end{bmatrix};$$

$$Z_{pc} = \begin{bmatrix} Z_{pc\alpha} \\ 0 \end{bmatrix}; \qquad Z_{qd} = \begin{bmatrix} 0 \\ Z_{qd\beta} \end{bmatrix}; \qquad i_p = \begin{bmatrix} i_{p\alpha} \\ i_{q\beta} \end{bmatrix} \qquad (6.5.14)$$

where,

$$Z_{cp} = Z_{pc}^T; \quad Z_{dq} = Z_{qd}^T$$

and, introducing the interconnection constraints

$$V_{c\alpha} = V_{d\beta}\ , \text{and, } i_{c\alpha} = -i_{d\beta} \qquad (6.5.15)$$

the matrix system (6.5.13) takes the form

$$\begin{bmatrix} V_p \\ V_{c\alpha} \\ V_{c\alpha} \end{bmatrix} = \begin{bmatrix} Z_{pp} & Z_{pc} & Z_{qd} \\ Z_{cp} & Z_{cc} & 0 \\ Z_{dq} & 0 & Z_{dd} \end{bmatrix} \begin{bmatrix} i_p \\ i_{c\alpha} \\ -i_{c\alpha} \end{bmatrix} \qquad (6.5.16)$$

The matrix system (6.5.16) is precisely of the form in the desegmentation analysis [9, 12, 13] and so by the same methodology the solution for the input impedance of the α - segment is given by

$$Z_{pp\alpha} = Z_{pp\gamma} - Z_{pq\gamma}\left[Z_{qq\gamma} - Z_{qq\beta}\right]^{-1} Z_{qp\gamma} \qquad (6.5.17)$$

where,

$$Z_{pq\gamma} = Z_{qp\gamma}^{T} \text{ , and,}$$

$$Z_{qq\beta} = \begin{bmatrix} Z_{qq\beta 1} & & & & \\ & Z_{qq\beta 2} & & & \\ & & \cdot & & \\ & & & \cdot & \\ & & & & Z_{qq\beta n} \end{bmatrix} \qquad (6.5.18)$$

$Z_{pp\alpha}$ in equation (6.5.17) then represents the input impedance.

Equation (6.5.17) is the new "*Generalised Desegmentation Input Impedance Formula*".

101

6.6 The Corner-deleted Square Patch Antenna with Segmental Structures

Segmentation structure
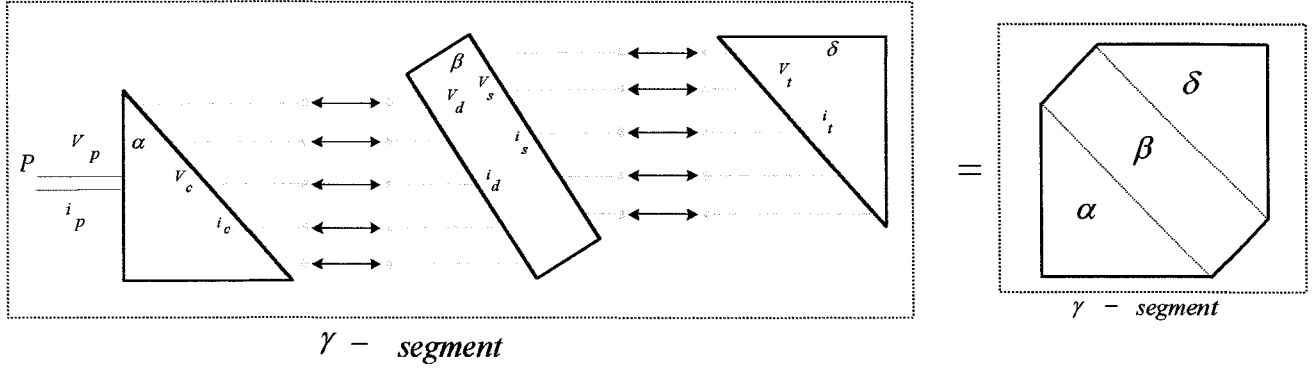
Figure 6.6.1: Segmentation

Desegmentation structure
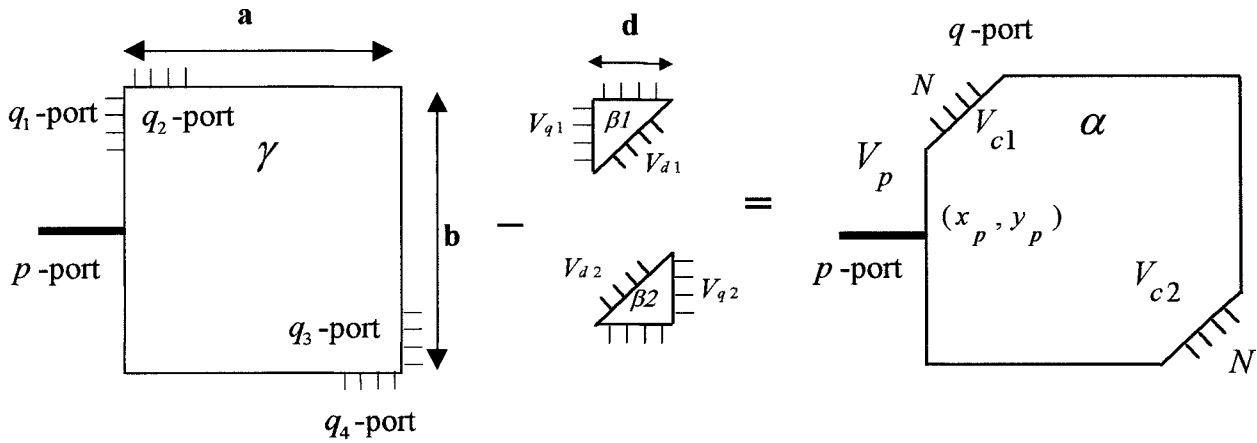
Figure 6.6.2: Desegmentation

From the analyses presented in sections 6.2, 6.3 6.4, 6.5, it is evident that for the deleted-corner structure the desegmentation approach would avoid the calculation of the coupling matrix involving ports on the hypotenuse of the deleted triangles. In the segmentation

approach for this structure there are seven coupling matrices, $Z_{pp\alpha}$, $Z_{pc\alpha}$, $Z_{ds\beta}$, $Z_{ss\beta}$, $Z_{tt\delta}$, $Z_{cc\alpha}$, $Z_{dd\beta}$ to be evaluated.

In contrast in the desegmentation approach there are only four coupling matrices $Z_{pp\gamma}$, $Z_{pq\gamma}$, $Z_{qq\gamma}$, and, $Z_{qq\beta}$ to be evaluated.

The desegmentation method will therefore be used in the computational work to determine the input impedance of this structure. Expressive for the elements of the coupling matrices are derived in the following chapter.

Summary

The basis of multiport modelling in a segmental approach has been described in terms of the conservation of current sheet distributions across the interfaces between segments. A new "Generalised Segmentation input impedance formula" for any number of appended segments in a shunt-type segment structrure has been obtained. A new "Generalised Desegmentation Input Impedance Formula" for any number of deleted segments has been obtained. Matrix input impedance formulas for both segmentation and desegmentation methods have been obtained for computational comparison. In the segmentation approach to the two corner-deleted patch antenna design coupling matrices involving the hypotenuse of the deleted segments are required but are not needed in the desegmentation approach. It has been shown, for the corner deleted antenna design, that the desegmentation method is computationally more efficient.

CHAPTER 7

DERIVATION OF EFFICIENT IMPEDANCE COUPLING EXPRESSIONS BETWEEN PORTS ON A RECTANGULAR PATCH

7.1 Introduction

In this chapter efficient impedance coupling expressions between the perimeter ports on a rectangular patch are obtained using closed form summations of infinite series.

There are three cases to consider (a) two ports on the same side (b) two ports on adjacent sides (c) two ports on opposite sides, as shown in section 7.2, figure 7.2.1. The general form of the infinite series Green's function used in the analysis is expressed in terms of the four modal sets, $(m = 0, n = 0)$, $(m \geq 1, n = 0)$, $(m = 0, n \geq 1)$, $(m \geq 1, n \geq 1)$.

The new impedance coupling expressions for each of the above three cases, (a), (b), and, (c) are derived in sections 7.2.1, 7.2.2, and 7.2.3 respectively. In the derivation, term by term double integration of the Green's function gives, initially, an impedance formula which consist of a single term, two single infinite series, and, one double infinite series. The single infinite series are summed to closed form, while the double infinite series are reduced to a single infinite series.

In case (a) the closed form summations result in the elimination of the constant term and the modal set $m = 0, n \geq 1$. In cases (b) and (c) the closed form summations result in the elimination of the constant term and the modal set $m \geq 1, n = 0$.

The infinite series closed form summation formulas used are given in Gradshtyn [1] apart from the formula used in equation (7.2.2.5) which was derived (Appendix7A).

The initial formulas, obtained by integration of the Green's function, require the evaluation of $M^2 + 2M + 1$ terms, where M is the upper summation limit for numerical convergence. By comparison the economised expressions obtained by using closed forms of infinite series require $M + 1$ terms in respect of the formulas in sections 7.2.1, and, 7.2.3. The formulas in sections 7.2.2 require $M + 2$ terms.

Numerical trials using the new expressions have shown that in all the cases considered only one term of the series is required to give convergence to three significant figures. In the worst case convergence to five significant figures requires at most 4 terms of the series, and, for convergence to seven significant figures 10 terms at most are required.

The result of a test application, for each of the three configurations considered, are given in section 7.3, and, are found to be in good agreement with Ensemble™.

In the following analysis the detail involved in the double integrations, and, the series summations, are omitted, but are outlined in appendices.

7.2 Computational Analysis

The three port configurations in this section are shown in figure 7.2.1.
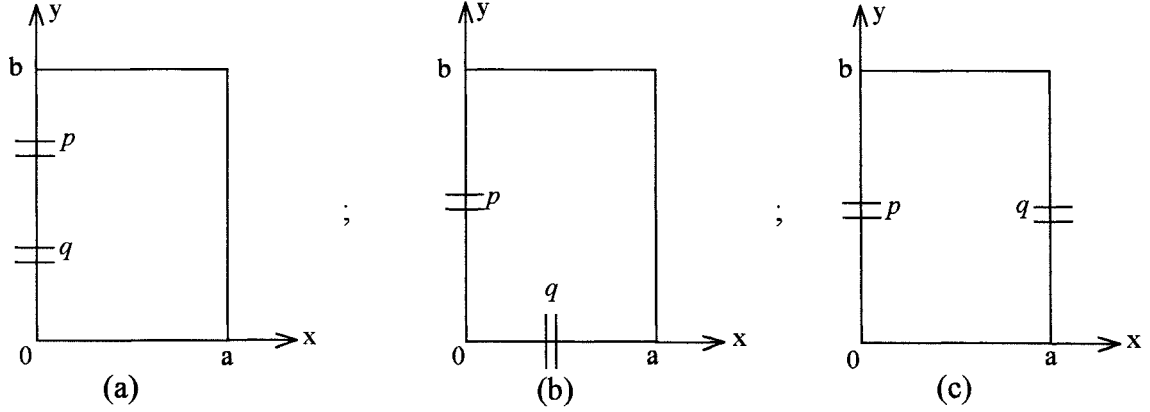
For the rectangular patch, $0 \le x \le a$, $0 \le y \le b$ the Green's function [2] must first be arranged in the following form:

$$G(x_p, y_p \mid x_q, y_q) = \frac{j\omega\mu h}{ab}\left[-\frac{1}{k^2} + \frac{2a^2}{\pi^2}\sum_{m=1}^{\infty}\frac{\cos\frac{m\pi}{b}x_p \cos\frac{m\pi}{b}x_q}{m^2 - A^2} + \frac{2b^2}{\pi^2}\sum_{n=1}^{\infty}\frac{\cos\frac{n\pi}{b}y_p \cos\frac{n\pi}{b}y_q}{n^2 - B^2}\right.$$

$$\left. + \frac{4}{\pi^2}\sum_{m=1}^{\infty}\sum_{n=1}^{\infty}\frac{\cos\frac{m\pi}{b}x_p \cos\frac{m\pi}{b}x_q \cos\frac{n\pi}{b}y_p \cos\frac{n\pi}{b}y_q}{\frac{m^2}{a^2} + \frac{n^2}{b^2} - \frac{k^2}{\pi^2}}\right] \qquad (7.2.1)$$

where the two ports, p and q are located at (x_p, y_p), and, (x_q, y_q); $A = ak/\pi$,

$B = bk/\pi$; h is the dielectric thickness; $k^2 = \omega^2\mu\varepsilon_0\varepsilon_r(1 - j/Q)$ and, Q is the total

quality loss factor, which includes, copper(Q_c), dielectric(Q_d), radiation(Q_r) and

surface wave(Q_{sw}) losses of the structure [3]. The loss factors are connected by the

relation $1/Q = 1/Q_d + 1/Q_c + 1/Q_r + 1/Q_{sw}$. For thin substrates the losses due to the surface

waves are very small and consequently can be neglected[3]. The ports p, q have widths W_p, W_q respectively.

In the following sections coupling impedance formulas are derived for each of the three cases.

7.2.1 Two Ports on the Same Side

The two ports p, q have centers $(0, y_p), (0, y_q)$.

The Green's function becomes

$$G(0, y_p \mid 0, y_q) = \frac{j\omega \mu h}{ab} \left[-\frac{1}{k^2} + \frac{2a^2}{\pi^2} \sum_{m=1}^{\infty} \frac{1}{m^2 - A^2} + \frac{2b^2}{\pi^2} \sum_{n=1}^{\infty} \frac{\cos\frac{n\pi}{b} y_p \cos\frac{n\pi}{b} y_q}{n^2 - B^2} \right.$$

$$\left. + \frac{4}{\pi^2} \sum_{m=1}^{\infty} \sum_{n=1}^{\infty} \frac{\cos\frac{n\pi}{b} y_p \cos\frac{n\pi}{b} y_q}{\frac{m^2}{a^2} + \frac{n^2}{b^2} - \frac{k^2}{\pi^2}} \right] \qquad (7.2.1.1)$$

The coupling impedance between these ports is [2]

$$Z_{pq} = \frac{1}{W_p W_q} \int_{W_p} \int_{W_q} G(0, y_p \mid 0, y_q) \, dy_p \, dy_q \qquad (7.2.1.2)$$

From equation (7.2.1.2), by integration (Appendix 7A)

$$Z_{pq} = \frac{j\omega \mu h}{ab W_p W_q} \left[\frac{-W_p W_q}{k^2} + \frac{2a^2 W_p W_q}{\pi^2} Sm_1 + \frac{2b^2}{\pi^4} Sn_2 + \frac{4a^2 b^2}{\pi^4} Smn_3 \right] \qquad (7.2.1.3)$$

where, using the closed form summations,

$$Sm_1 = \sum_{m=1}^{\infty} \frac{1}{m^2 - A^2}$$

$$= \frac{\pi^2}{2a^2 k^2} - \frac{\pi^2}{2ak} \cot ka \qquad (7.2.1.4)$$

$$Sn_2 = \sum_{n=1}^{\infty} \frac{F_1(n:\theta_1,\theta_2,\theta_3,\theta_4)}{n^2(n^2-B^2)} \qquad (7.2.1.5)$$

$$Smn_3 = \sum_{n=1}^{\infty} \frac{F_1(n:\theta_1,\theta_2,\theta_3,\theta_4)}{n^2} \sum_{m=1}^{\infty} \frac{1}{m^2+D^2}$$

$$= \frac{\pi}{2} \sum_{n=1}^{\infty} \frac{F_1(n:\theta_1,\theta_2,\theta_3,\theta_4)}{n^2 D} \coth D\pi - \frac{b^2}{2a^2} \sum_{n=1}^{\infty} \frac{F_1(n:\theta_1,\theta_2,\theta_3,\theta_4)}{n^2 \ (n^2-B^2)}$$

$$= \frac{\pi}{2} \sum_{n=1}^{\infty} \frac{F_1(n:\theta_1,\theta_2,\theta_3,\theta_4)}{n^2 D} \coth D\pi - \frac{b^2}{2a^2} Sn_2 \qquad (7.2.1.6)$$

where, $A = ak/\pi$, $B = bk/\pi$, $D^2 = (n^2-B^2) \ a^2/b^2$,

$$F_1(n \ : \ \theta_1,\theta_2,\theta_3,\theta_4) = (\sin n\theta_1 - \sin n\theta_2)(\sin n\theta_3 - \sin n\theta_4),$$

$$\theta_1 = \frac{\pi}{b}\left(y_p - \frac{W_p}{2}\right), \ \theta_2 = \frac{\pi}{b}\left(y_p + \frac{W_p}{2}\right), \theta_3 = \frac{\pi}{b}\left(y_q - \frac{W_q}{2}\right) \text{,and,} \ \theta_4 = \frac{\pi}{b}\left(y_q + \frac{W_q}{2}\right).$$

Using equations (7.2.1.4) and (7.2.1.6) in equation (7.2.1.3) eliminates both of the terms

$W_p W_q/k^2$ and Sn_1, to give the coupling impedance

$$Z_{pq} = \frac{j\omega\,\mu\,h}{ab}\left[\frac{-a}{k}\cot ka + \frac{2a^2b^2}{W_p W_q \pi^3} \sum_{n=1}^{\infty} \frac{(\sin n\theta_1 - \sin n\theta_2)(\sin n\theta_3 - \sin n\theta_4)}{n^2 D} \coth D\pi\right] \qquad (7.2.1.7)$$

7.2.2 Two Ports on Adjacent Sides

The two ports p, q have centers $(0,y_p),(x_q,0)$.

The Green's function becomes

$$G(0, y_p \mid x_q, 0) = \frac{j\omega \mu h}{ab}\left[-\frac{1}{k^2} + \frac{2a^2}{\pi^2}\sum_{m=1}^{\infty}\frac{\cos\dfrac{m\pi}{a}x_q}{m^2 - A^2} + \frac{2b^2}{\pi^2}\sum_{n=1}^{\infty}\frac{\cos\dfrac{n\pi}{b}y_p}{n^2 - B^2} \right.$$

$$\left. + \frac{4}{\pi^2}\sum_{m=1}^{\infty}\sum_{n=1}^{\infty}\frac{\cos\dfrac{m\pi}{a}x_q \cos\dfrac{n\pi}{b}y_p}{\dfrac{m^2}{a^2} + \dfrac{n^2}{b^2} - \dfrac{k^2}{\pi^2}} \right] \tag{7.2.2.1}$$

The coupling impedance between these ports is [2]

$$Z_{pq} = \frac{1}{W_p W_q}\int_{W_p}\int_{W_q} G(0, y_p \mid x_q, 0)\, dy_p\, dx_q \tag{7.2.2.2}$$

From equation (7.2.2.2), by integration (Appendix 7A)

$$Z_{pq} = \frac{j\omega \mu h}{abW_p W_q}\left[\frac{W_p W_q}{k^2} - \frac{2a^3 W_p}{\pi^3}Sm_1 - \frac{2b^3 W_q}{\pi^3}Sn_2 - \frac{4ab^3}{\pi^4}Smn_3 \right] \tag{7.2.2.3}$$

where,

$$Sm_1 = \sum_{m=1}^{\infty}\frac{(\sin m\theta_1 - \sin m\theta_2)}{m\,(m^2 - A^2)} \tag{7.2.2.4}$$

$$Sn_2 = \sum_{n=1}^{\infty}\frac{(\sin n\,\theta_3 - \sin n\,\theta_4)}{n(n^2 - B^2)}$$

$$= \frac{\pi^3 W_p}{2k^2 b^3} + \frac{\pi^3\left[\sin B(\pi - \theta_3) - \sin B(\pi - \theta_4)\right]}{2k^2 b^2 \sin B\pi} \tag{7.2.2.5}$$

Smn_3

$$= \sum_{m=1}^{\infty}\frac{(\sin m\theta_1 - \sin m\theta_2)}{m}\sum_{n=1}^{\infty}\frac{(\sin n\theta_3 - \sin n\theta_4)}{n\,(n^2 + C^2)}$$

$$= -\frac{\pi a^2 w_p}{2b^3}\sum_{m=1}^{\infty}\frac{(\sin m\theta_1 - \sin m\theta_2)}{m(m^2 + A^2)} + \frac{\pi a^2}{2b^2}\sum_{m=1}^{\infty}\frac{(\sin m\theta_1 - \sin m\theta_2)\left(\sinh C(\pi - \theta_4) - \sinh C(\pi - \theta_3)\right)}{m(m^2 - A^2)\sinh C\pi}$$

$$= \frac{-\pi a^2 W_p}{2b^3}Sm_1 + \frac{\pi a^2}{2b^2}\sum_{m=1}^{\infty}\frac{(\ \sin m\theta_1 - \sin m\theta_2\ )\left[\sinh C(\pi - \theta_4) - \sinh C(\pi - \theta_3)\right]}{m(m^2 - A^2)\sinh C\pi} \tag{7.2.2.6}$$

where, $C^2 = (m^2 - A^2) \; b^2/a^2$;

$$\theta_1 = \frac{\pi}{a}\left(x_q + \frac{W_q}{2}\right), \theta_2 = \frac{\pi}{a}\left(x_q - \frac{W_q}{2}\right), \theta_3 = \frac{\pi}{b}\left(y_p + \frac{W_p}{2}\right), \text{and}, \; \theta_4 = \frac{\pi}{b}\left(y_p - \frac{W_p}{2}\right).$$

Using equations (7.2.2.5) and (7.2.2.6) in equation (7.2.2.3) eliminates both of the terms

$W_p W_q/k^2$ and Sm_1, to give the coupling impedance

$$Z_{pq} = \frac{j\omega \, \mu \, h}{W_p W_q}\left[\frac{W_q \left[\sin B(\pi - \theta_4) - \sin B(\pi - \theta_3)\right]}{ak^2 \sin kb} \right.$$

$$\left. + \frac{2a^2}{\pi^3}\sum_{m=1}^{\infty}\frac{(\sin m\theta_1 - \sin m\theta_2)\left[\sinh C \; (\pi - \theta_4) - \sinh C \; (\pi - \theta_3)\right]}{m(m^2 - A^2)\sinh C \, \pi} \right] \tag{7.2.2.7}$$

7.2.3 Two Ports on Opposite Sides

The two ports p, q have centers $(0, y_p), (a, y_q)$.

The Green's function becomes

$$G(0, y_p \mid a, y_q) = \frac{j\omega \, \mu \, h}{ab}\left[-\frac{1}{k^2} + \frac{2a^2}{\pi^2}\sum_{m=1}^{\infty}\frac{(-1)^m}{m^2 - A^2} + \frac{2b^2}{\pi^2}\sum_{n=1}^{\infty}\frac{\cos\dfrac{n\pi}{b}y_p \cos\dfrac{n\pi}{b}y_q}{n^2 - B^2} \right.$$

$$\left. + \frac{4}{\pi^2}\sum_{m=1}^{\infty}\sum_{n=1}^{\infty}\frac{(-1)^m \cos\dfrac{n\pi}{b}y_p \cos\dfrac{n\pi}{b}y_q}{\dfrac{m^2}{a^2} + \dfrac{n^2}{b^2} - \dfrac{k^2}{\pi^2}} \right] \tag{7.2.3.1}$$

The coupling impedance between these ports is [2]

$$Z_{pq} = \frac{1}{W_p W_q}\int_{W_p}\int_{W_q} G(0, y_p \mid a, y_q)\, dy_p\, dx_q \tag{7.2.3.2}$$

From equation (7.2.3.2), by integration (Appendix 7A)

110

$$Z_{pq} = \frac{j\omega\mu\,h}{a\,b}\left[\frac{W_p W_q}{k^2} - \frac{2a^2 W_p W_q}{\pi^2}Sm_1 - \frac{2b^4}{\pi^4}Sn_2 - \frac{4a^2 b^2}{\pi^4}Smn_3\right] \qquad (7.2.3.3)$$

where,

$$Sm_1 = \sum_{m=1}^{\infty}\frac{(-1)^m}{m^2 - A^2}$$

$$= \frac{1}{2A^2} - \frac{\pi}{2A\,\sin\,A\pi} \qquad (7.2.3.4)$$

$$Sn_2 = \sum_{n=1}^{\infty}\frac{F_1(n:\theta_1,\theta_2,\theta_3,\theta_4)}{n^2(n^2 - B^2)} \qquad (7.2.3.5)$$

$$Smn_3 = \sum_{n=1}^{\infty}\frac{F_1(n:\theta_1,\theta_2,\theta_3,\theta_4)}{n^2}\sum_{m=1}^{\infty}\frac{(-1)^m}{m^2 + D^2}$$

$$= \frac{\pi}{2}\sum_{n=1}^{\infty}\frac{F_1(n:\theta_1,\theta_2,\theta_3,\theta_4)}{D\sinh D\pi} - \frac{b^2}{2a^2}\sum_{n=1}^{\infty}\frac{F_1(n:\theta_1,\theta_2,\theta_3,\theta_4)}{n^2(n^2-B^2)}$$

$$= \frac{\pi}{2}\sum_{n=1}^{\infty}\frac{F_1(n:\theta_1,\theta_2,\theta_3,\theta_4)}{D\sinh D\pi} - \frac{b^2}{2a^2}Sn_2 \qquad (7.2.3.6)$$

where, $F_1(n:\theta_1,\theta_2,\theta_3,\theta_4)$, θ_1, θ_2, θ_3, θ_4 are as defined in case (a).

Using equations (7.2.3.4) and (7.2.3.6) in equation (7.2.3.3) eliminates both of the terms $W_p W_q/k^2$ and Sn_2, to give the coupling impedance

$$Z_{pq} = \frac{j\omega\,\mu\,h}{bW_p W_q}\left[\frac{W_p W_q}{k\,\sin\,ka} - \frac{2ab^2}{\pi^3}\sum_{n=1}^{\infty}\frac{(\sin n\theta_1 - \sin n\theta_2)(\sin n\theta_3 - \sin n\theta_4)}{D\,\sinh\,D\pi}\right] \qquad (7.2.3.7)$$

7.3 Test Applications

The new expressions for the coupling impedances were tested on a square patch of side $a = 40mm$ at a frequency of 2.45GHz on a substrate(Duroid 5870) where $\varepsilon r = 2.33$, thickness $h = 0.79mm$, and, a loss tangent of 0.0012.

A square patch was chosen since, for ports on the same side, this geometry produces a variation of coupling impedance depending on the separation between the two ports in contrast to the rectangular patch case when the coupling impedance is essentially independent of the separation. The quality factor of 87 was used which takes into account copper, dielectric and radiation losses.

Results for two different separations between the paired ports were obtained for each of the three cases and compared with those predicted by a full wave analysis software (Ensemble™). These result s are shown in the graphs in figures 7.3.1,7.3.2 and 7.3.3.

As can be seen in figure 7.3.1(a) and 7.3.1(b) for case (a), the coupling impedances decrease with separation of the two ports. Figure 7.3.2(a) and 7.3.2(b) show the comparison of results for case (b) as expected, the mutual impedance increase as the two ports are brought closer together. Finally figure 7.3.3(a) and 7.3.3(b) shows the results for case (c). For all three cases there is an excellent agreement between the results obtained from the new efficient computational expressions with that predicted by the Ensemble™.
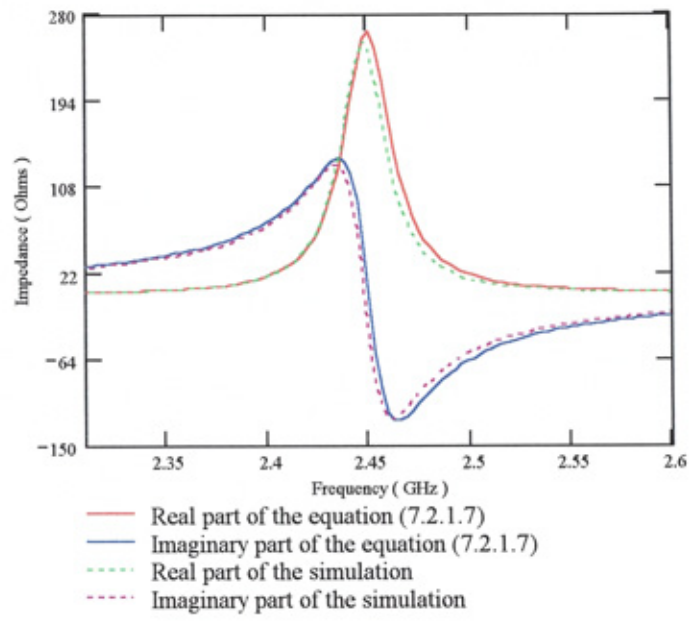
(a) Coupling impedances for $y_p = 18mm$ and $y_q = 22mm$
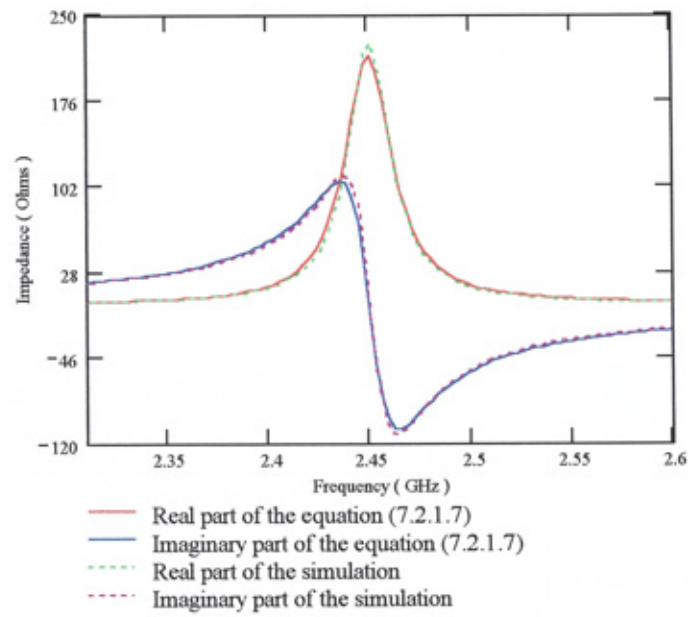
(b) Coupling impedances for $y_p = 14mm$ and $y_q = 26mm$

Figure 7.3.1: Coupling impedances of two ports located on the same edge at $(0, y_p)$,

$(0, y_q)$.
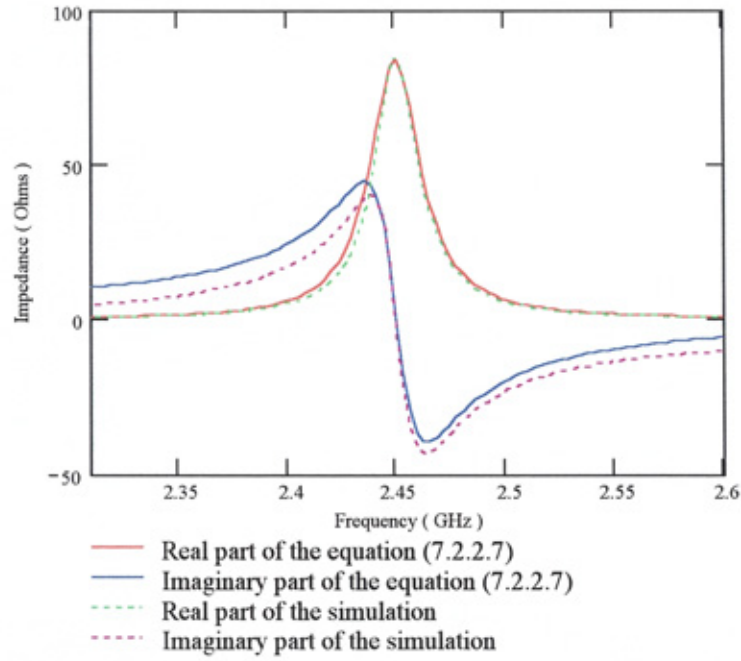
(a) Coupling impedances for $y_p = x_q = 18mm$
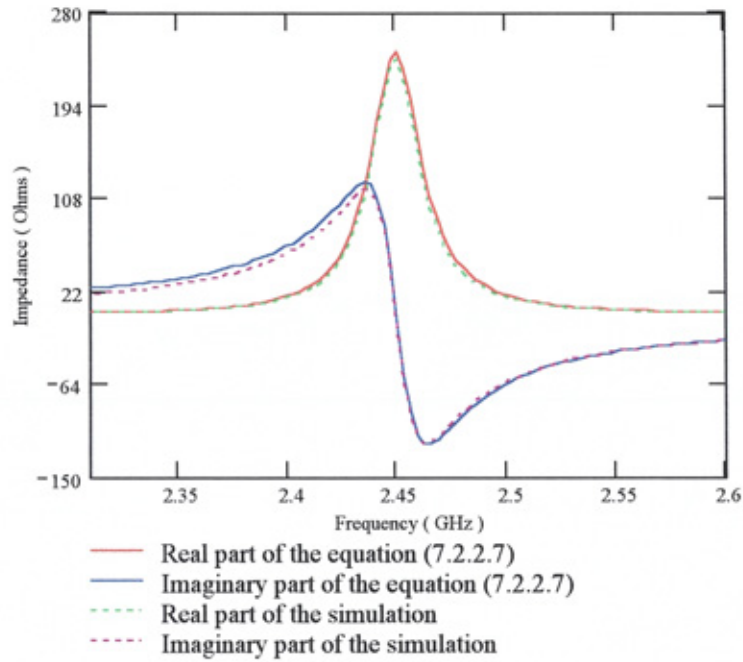

(b) Coupling impedances for $y_p = x_q = 14mm$

Figure 7.3.2: Coupling impedances of two ports located on adjacent edges at $(0, y_p)$, $(x_q, 0)$.
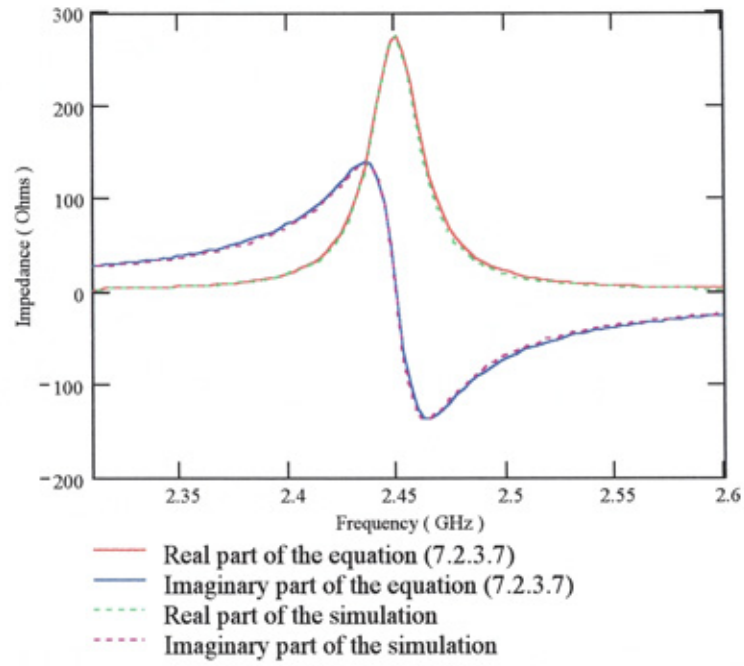
(a) Coupling impedances for $y_p = 18mm$ and $y_q = 22mm$
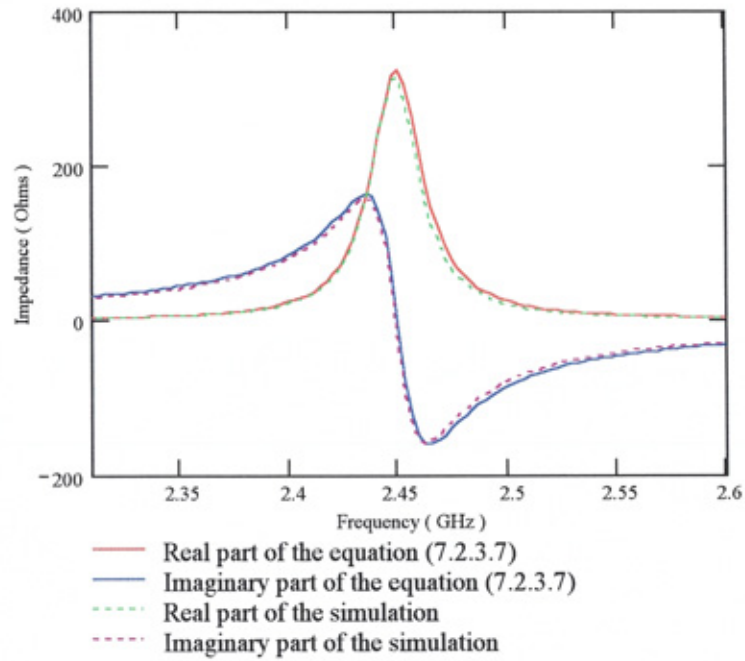
(b) Coupling impedances for $y_p = 14mm$ $y_q = 26mm$

Figure 7.3.3: Coupling impedances of two ports located on opposite edges at $(0, y_p)$, (a, y_q).

7.4 Summary

In this chapter efficient computational expressions for each of the three possible rectangular patch coupling impedance configurations, has been obtained. The number of terms in the series formulas for a required accuracy is given. A test application using Ensemble™ showed good agreement.

CHAPTER 8

DERIVATION OF EFFICIENT IMPEDANCE COUPLING EXPRESSIONS BETWEEN PORTS ON A RIGHT-ANGLED ISOSCELES TRIANGULAR PATCH

8.1 Introduction

In this chapter efficient impedance coupling expressions between the perimeter ports on a right angled isosceles triangle patch are obtained using closed form summations of infinite series. There are four cases to consider (a) two ports on a vertical side, (b) two ports on adjacent vertical horizontal sides, (c) one port on a vertical side, and, one port on the hypotenuse, and (d) two ports on the hypotenuse, as shown in section 8.2, figure 8.2.1. The general form of the Green's function used in the analysis is given in this section, and, is expressed in terms of the four modal sets, $(m = 0, n = 0)$, $(m \geq 1, n = 0)$, $(m \geq 1, n \geq 1)$.

The new impedance coupling expressions for each of the above four cases (a), (b), (c), and, (d) are derived in sections 8.2.1, 8.2.2, 8.2.3, and, 8.2.4 respectively. In the derivation, term by term double integration of the Green's function produces, initially, an impedance formula which consists of a constant term, and, several single and double infinite series.

The single infinite series are summed to a closed form and for the coupling ports not on the hypotenuse the double series reduces to a single infinite series. The reduction of the double series results in the constant term and the modal set which $m = 0, n \geq 1$, to be eliminated in each of the cases (a) and (b).

For coupling ports involving the hypotenuse the double infinite series cannot be reduced to a single infinite series. However, the double series can be economised by extracting the diagonal terms which can be summed to closed form. The remaining terms, by symmetry, can then be expressed in the form of semi-infinite double series for which $m \geq 1$, $n \geq m + 1$.

The infinite series closed form summation formulas used are either given, or, have been derived from results in Gradshtyn[1]. Derived expressions (Appendix 8A) are used in equations (8.2.1.4), (8.2.1.8), (8.2.2.6), (8.2.3.4), (8.2.3.5), (8.2.3.7), (8.2.4.6), and, (8.2.4.7).

The initial expressions obtained by integration of the Green's function require the evaluation of $M^2 + M + 1$ terms, where M is the upper summation limit for numerical convergence. By comparison the economised expressions obtained by using closed forms of infinite series require $2(M + 1)$ terms in respect of the formulas in sections 8.2.1, and, 8.2.2. The formulas in sections 8.2.3, and, 8.2.4 require $(M^2 + M + 8)/2$ terms.

Numerical trials show that in the worst case, for convergence to seven significant figures

an upper summation index of 9, at most, is required. The results of a test application, for each of the four configurations considered, are given in section 8.3, and, are found to be in good agreement with Ensemble™. In the following analysis the details involved in the double integrations, and, the series summations, are omitted, but are outlined in Appendices 8A.

8.2 Computational Analysis

The four p and q port configurations in this section are shown in figure 8.2.1 below.
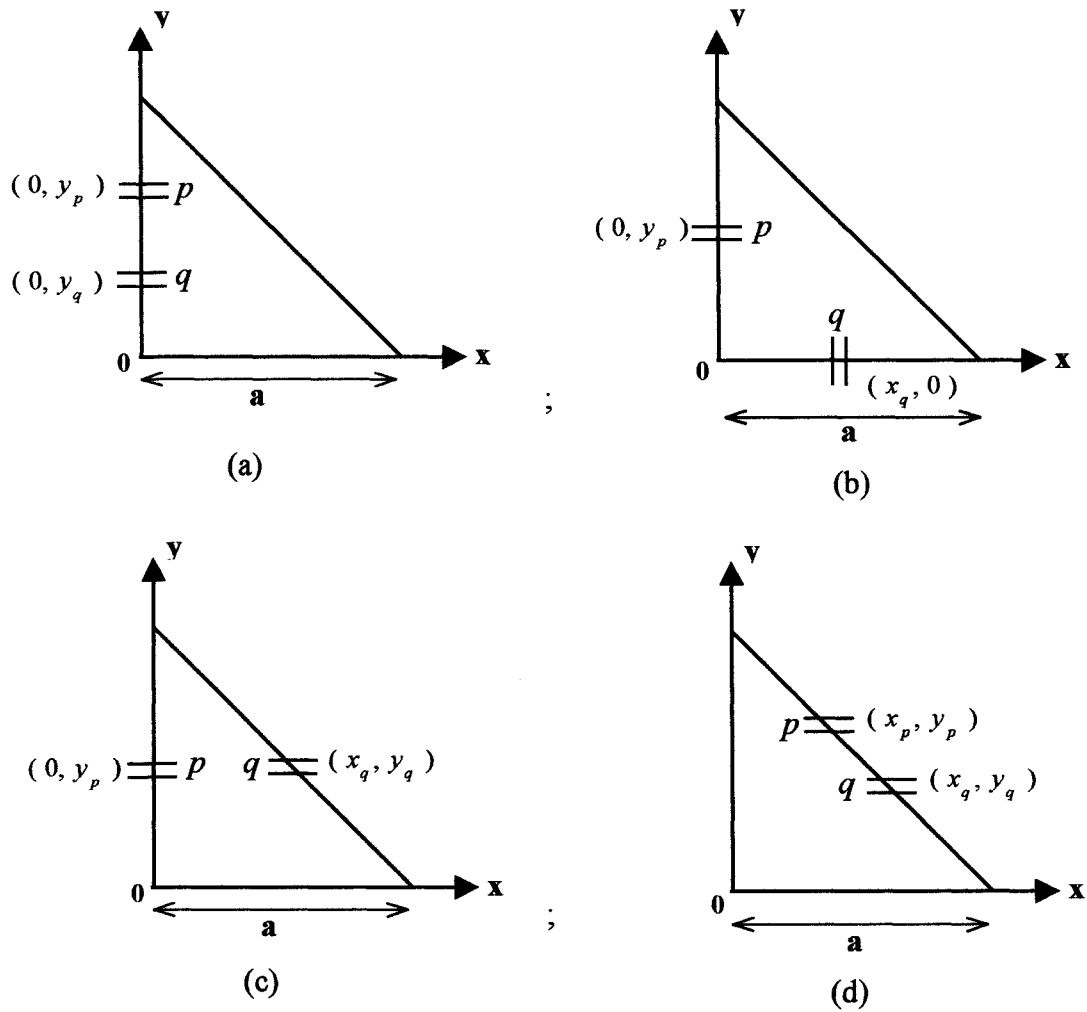
Figure 8.2.1: Four port configurations

The Green's function for an isosceles right angled triangle is given by [2]

$$G(x_p, y_p \mid x_q, y_q) = \frac{j\omega\mu h}{2} \sum_{-\infty}^{\infty}\sum_{-\infty}^{\infty} \frac{T_{mn}(x_p, y_p)\,T_{mn}(x_q, y_q)}{(m^2 + n^2)\pi^2 - a^2 k^2} \tag{8.2.1}$$

where $T_{mn}(x, y) = \cos\dfrac{m\pi}{a} x \cos\dfrac{n\pi}{a} y + (-1)^{m+n}\cos\dfrac{n\pi}{a} x \cos\dfrac{m\pi}{a} y$ (8.2.2)

and a is the length of a perpendicular side, and, h is the dielectric thickness;

$k^2 = \omega^2\mu\,\varepsilon_0\varepsilon_r(1 - j/Q)$, and, Q is the total quality loss factor [3].

The above expression for the Green's function must first be arranged in the following form

$$G(x_p, y_p \mid x_q, y_q) = \frac{j2\omega\mu h}{\pi^2}\left\{ -\frac{\pi^2}{a^2 k^2} + \sum_{m=1}^{\infty}\frac{T_{m0}(x_p, y_p)\,T_{m0}(x_q, y_q)}{m^2 - A^2} + \sum_{m=1}^{\infty}\sum_{n=1}^{\infty}\frac{T_{mn}(x_p, y_p)\,T_{mn}(x_q, y_q)}{m^2 + n^2 - A^2}\right\} \tag{8.2.3}$$

where $A = ak/\pi$.

The ports p, q have widths W_p, W_q respectively. In the following analysis coupling

impedance formulas are derived for each of the four cases.

8.2.1 Two Ports on the Same Vertical Side.

The two ports p, q have centers $(0, y_p), (0, y_q)$.

The Green's function becomes

$$G(0, y_q \mid 0, y_q) = \frac{j2\omega\mu h}{\pi^2}\left\{ -\frac{\pi^2}{a^2 k^2} + \sum_{m=1}^{\infty}\frac{\left(1 + (-1)^m\cos\dfrac{m\pi}{a} y_p\right)\left(1 + (-1)^m\cos\dfrac{m\pi}{a} y_q\right)}{(m^2 - A^2)}\right.$$

$$\left. + \sum_{m=1}^{\infty}\sum_{n=1}^{\infty}\frac{\left(\cos\dfrac{n\pi}{a} y_p + (-1)^{m+n}\cos\dfrac{m\pi}{a} y_p\right)\left(\cos\dfrac{n\pi}{a} y_q + (-1)^{m+n}\cos\dfrac{m\pi}{a} y_q\right)}{(m^2 + n^2 - A^2)}\right\} \tag{8.2.1.1}$$

The coupling impedance between these ports is [4]

$$Z_{pq} = \frac{1}{W_p W_q} \int_{W_p} \int_{W_q} G(0, y_p \mid 0, y_q)\, dy_p\, dy_q \qquad (8.2.1.2)$$

where, the integrations are over the intervals $\left(y_p - \dfrac{W_p}{2}, y_p + \dfrac{W_p}{2} \right)$, and,

$$\left(y_q - \frac{W_q}{2}, y_q + \frac{W_q}{2} \right).$$

From equations (8.2.1.1) and (8.2.1.2), by integration (Appendix 8A)

$$Z_{pq} = \frac{j2\omega \mu h}{W_p W_q} \left\{ -\frac{W_p W_q}{k^2 a^2} + \frac{1}{\pi^2} Sm_1 + \frac{aW_q}{\pi^3} Sm_2 + \frac{a^2}{\pi^4} Sm_3 + \frac{2a^2}{\pi^4}\left[Smn_4 + Smn_5 \right] \right\} \qquad (8.2.1.3)$$

where,

$$Sm_1 = \sum_{m=1}^{\infty} \frac{W_p W_q}{m^2 - A^2} + \frac{(-1)^m a W_p (\sin m\theta_3 - \sin m\theta_4)}{m\pi(m^2 - A^2)}$$

$$= \frac{W_p W_q \pi^2}{k^2 a^2} - \frac{W_p W_q \pi \cot \pi A}{2A} + \frac{\pi^2 W_p (\sin A\theta_4 - \sin A\theta_3)}{ak^2 \sin A\pi} \qquad (8.2.1.4)$$

$$Sm_2 = \sum_{m=1}^{\infty} \frac{(-1)^m \left(\sin m\theta_1 - \sin m\theta_2 \right)}{m^2 (m^2 - A^2)} \qquad (8.2.1.5)$$

$$Sm_3 = \sum_{m=1}^{\infty} \frac{F_1(m : \theta_1, \theta_2, \theta_3, \theta_4)}{m^2 (m^2 - A^2)} \qquad (8.2.1.6)$$

$$Smn_4 = \sum_{m=1}^{\infty} \sum_{n=1}^{\infty} \frac{F_1(m : \theta_1, \theta_2, \theta_3, \theta_4)}{m^2 (m^2 + n^2 - A^2)}$$

$$= \frac{\pi}{2} \sum_{m=1}^{\infty} \frac{F_1(m : \theta_1, \theta_2, \theta_3, \theta_4) \coth \pi B}{m^2 B} - \frac{1}{2} \sum_{m=1}^{\infty} \frac{F_1(m : \theta_1, \theta_2, \theta_3, \theta_4)}{m^2 (m^2 - A^2)}$$

$$= \frac{\pi}{2} \sum_{m=1}^{\infty} \frac{F_1(m : \theta_1, \theta_2, \theta_3, \theta_4) \coth \pi B}{m^2 B} - \frac{1}{2} Sm_3 \qquad (8.2.1.7)$$

121

$$Smn_5 = \sum_{m=1}^{\infty}\sum_{n=1}^{\infty} \frac{(-1)^{m+n} F_2(m,n:\theta_1,\theta_2,\theta_3,\theta_4)}{mn(m^2+n^2-A^2)}$$

$$= \frac{\pi}{2}\sum_{m=1}^{\infty} \frac{(-1)^m(\sin m\theta_1 - \sin m\theta_2)(\sinh B\theta_3 - \sinh B\theta_4)}{m(m^2-A^2)\sinh B\pi} - \frac{W_q\pi}{2a}\sum_{m=1}^{\infty}\frac{(-1)^m\left(\sin m\theta_1 - \sin m\theta_2\right)}{m^2(m^2-A^2)}$$

$$= \frac{\pi}{2}\sum_{m=1}^{\infty}\frac{(-1)^m(\sin m\theta_1 - \sin m\theta_2)(\sinh B\theta_3 - \sinh B\theta_4)}{m(m^2-A^2)\sinh B\pi} - \frac{W_q\pi}{2a}Sm_2 \qquad (8.2.1.8)$$

where, $B^2 = m^2 - A^2$, $F_1(m:\theta_1,\theta_2,\theta_3,\theta_4) = (\sin m\theta_1 - \sin m\theta_2)(\sin m\theta_3 - \sin m\theta_4)$,

$F_2(m,n:\theta_1,\theta_2,\theta_3,\theta_4) = (\sin m\theta_1 - \sin m\theta_2)(\sin n\theta_3 - \sin n\theta_4)$, and,

$$\theta_1 = \frac{\pi}{a}\left(y_p + \frac{W_p}{2}\right); \theta_2 = \frac{\pi}{a}\left(y_p - \frac{W_p}{2}\right); \theta_3 = \frac{\pi}{a}\left(y_q + \frac{W_q}{2}\right); \quad \theta_4 = \frac{\pi}{a}\left(y_q - \frac{W_q}{2}\right).$$

Using equations (8.2.1.4), (8.2.1.7) and (8.2.1.8) in equation (8.2.1.3) eliminates in turn the three terms $W_pW_q/k^2 a^2$, Sm_3 and Sm_2, to give the economised form of the coupling impedance

$$Z_{pq} = \frac{j\omega\mu h}{W_pW_q}\left\{-\frac{W_pW_q}{ka}\cot\pi A + \frac{W_p(\sin A\theta_4 - \sin A\theta_3)}{k^2a\sin ka} + \frac{2a^2}{\pi^3}\sum_{m=1}^{\infty}\frac{(\sin m\theta_1 - \sin m\theta_2)(\sin m\theta_3 - \sin m\theta_4)\coth \pi B}{m^2 B}\right.$$

$$\left. + \frac{2a^2}{\pi^3}\sum_{m=1}^{\infty}\frac{(-1)^m(\sin m\theta_1 - \sin m\theta_2)(\sinh B\theta_3 - \sinh B\theta_4)}{mB^2\sinh \pi B}\right\} \qquad (8.2.1.9)$$

8.2.2 Two Ports on Adjacent Vertical-horizontal Sides

The two ports p, q have centers $(0, y_p), (x_q, 0)$.

The Green's function becomes

$$G(0, y_p \mid x_q, 0) = \frac{j2\omega\mu h}{\pi^2} \left\{ -\frac{\pi^2}{a^2 k^2} + \sum_{m=1}^{\infty} \frac{\left(1 + (-1)^m \cos\dfrac{m\pi}{a} y_p\right)\left((-1)^m + \cos\dfrac{m\pi}{a} x_q\right)}{(m^2 - A^2)} \right.$$

$$\left. + \sum_{m=1}^{\infty}\sum_{n=1}^{\infty} \frac{\left(\cos\dfrac{n\pi}{a} y_p + (-1)^{m+n} \cos\dfrac{n\pi}{a} y_p\right)\left(\cos\dfrac{n\pi}{a} x_q + (-1)^{m+n} \cos\dfrac{n\pi}{a} x_q\right)}{(m^2 + n^2 - A^2)} \right\} \quad (8.2.2.1)$$

The coupling impedance between these ports is given by

$$Z_{pq} = \frac{1}{W_p W_q} \int_{W_p} \int_{W_q} G(0, y_p \mid x_q, 0)\, dy_p\, dx_q \qquad (8.2.2.2)$$

where the integrations are over the intervals $\left(y_p - \dfrac{W_p}{2}, y_p + \dfrac{W_p}{2} \right)$, and,

$$\left(x_q + \frac{W_q}{2}, x_q - \frac{W_q}{2} \right).$$

From equation (8.2.2.1) and (8.2.2.2), by integration (Appendix 8A)

$$Z_{pq} = -\frac{2j\omega\mu h}{W_p W_q} \left[-\frac{W_p W_q}{k^2 a^2} - \frac{W_p W_q}{\pi^2} Sm_1 - \frac{aW_q}{\pi^3} Sm_2 - \frac{aW_p}{\pi^3} Sm_3 - \frac{a^2}{\pi^4} Sm_4 - \frac{2a^2}{\pi^4} Smn_5 \right.$$

$$\left. - \frac{2a^2}{\pi^4} Smn_6 \right] \qquad (8.2.2.3)$$

where, $\quad Sm_1 = \sum_{m=1}^{\infty} \dfrac{(-1)^m}{m^2 - A^2}$

$$= \frac{\pi^2}{2a^2 k^2} - \frac{\pi}{2A \sin A\pi} \qquad (8.2.2.4)$$

$$Sm_2 = \sum_{m=1}^{\infty} \frac{(\sin m\theta_1 - \sin m\theta_2)}{m(m^2 - A^2)} \qquad (8.2.2.5)$$

$$Sm_3 = \sum_{m=1}^{\infty} \frac{(\sin m\theta_3 - \sin m\theta_4)}{m \ (m^2 - A^2)}$$

$$= \frac{W_q \pi^3}{2k^2 a^3} + \frac{\pi^2 \left(\sin A(\pi - \theta_3) - \sin A(\pi - \theta_4)\right)}{2k^2 a^2 \sin ka} \qquad (8.2.2.6)$$

$$Sm_4 = \sum_{m=1}^{\infty} \frac{(-1)^m F_1\left(m : \theta_1, \theta_2, \theta_3, \theta_4\right)}{m^2 (m^2 - A^2)} \qquad (8.2.2.7)$$

$$Smn_5 = \sum_{m=1}^{\infty} \sum_{n=1}^{\infty} \frac{F_2(m,n : \theta_1, \theta_2, \theta_3, \theta_4)}{m \ n(m^2 + n^2 - A^2)}$$

$$= -\frac{\pi}{2} \sum_{m=1}^{\infty} \frac{(\sin m\theta_1 - \sin m\theta_2)\left[\sinh B(\pi - \theta_3) - \sinh B(\pi - \theta_4)\right]}{m \ (m^2 - A^2) \sinh B\pi} - \frac{\pi^2}{2a^2} \sum_{m=1}^{\infty} \frac{(\sin m\theta_1 - \sin m\theta_2)}{m(m^2 - A^2)}$$

$$= -\frac{\pi}{2} \sum_{m=1}^{\infty} \frac{(\sin m\theta_1 - \sin m\theta_2)\left[\sinh B(\pi - \theta_3) - \sinh B(\pi - \theta_4)\right]}{m(m^2 - A^2) \sinh B\pi} - \frac{\pi^2}{2a^2} Sm_2 \qquad (8.2.2.8)$$

$$Smn_6 = \sum_{m=1}^{\infty} \sum_{n=1}^{\infty} \frac{(-1)^{m+n} F_1(m : \theta_1, \theta_2, \theta_3, \theta_4)}{m^2 (m^2 + n^2 - A^2)}$$

$$= -\frac{1}{2} \sum_{m=1}^{\infty} \frac{(-1)^m F_1(m : \theta_1, \theta_2, \theta_3, \theta_4)}{m^2 B \sinh \pi B} + \frac{\pi^2}{2a^2} \sum_{m=1}^{\infty} \frac{(-1)^m F_1(m : \theta_1, \theta_2, \theta_3, \theta_4)}{m^2 (m^2 - A^2)}$$

$$= -\frac{1}{2} \sum_{m=1}^{\infty} \frac{(-1)^m F_1(m : \theta_1, \theta_2, \theta_3, \theta_4)}{m^2 B \sinh \pi B} + \frac{\pi^2}{2a^2} Sm_4 \qquad (8.2.2.9)$$

where, $F_1(m : \theta_1, \theta_2, \theta_3, \theta_4)$ and $F_2(m,n : \theta_1, \theta_2, \theta_3, \theta_4)$ are defined as in case(a), and,

$$\theta_1 = \frac{\pi}{a}\left(y_p + \frac{W_p}{2}\right); \quad \theta_2 = \frac{\pi}{a}\left(y_p - \frac{W_p}{2}\right); \quad \theta_3 = \frac{\pi}{a}\left(x_q + \frac{W_q}{2}\right); \quad \theta_3 = \frac{\pi}{a}\left(x_q - \frac{W_q}{2}\right).$$

Using equations (8.2.2.4), (8.2.2.6), (8.2.2.8) and (8.2.2.9) in equation (8.2.2.3) eliminates the terms $W_p W_q / k^2 a^2$, Sm_2 and Sm_4, to give the coupling impedance

$$Z_{pq} = \frac{j\omega\,\mu\,h}{W_p W_q}\left[\frac{W_p W_q}{ka\sin ka} - \frac{W_p\left(\sin A(\pi - \theta 3) - \sin A(\pi - \theta 3)\right)}{k^2 a\sin ka} - \frac{2a^2}{\pi^3}\sum_{m=1}^{\infty}\frac{(-1)^m F_1(m\,:\,\theta_1,\theta_2,\theta_3,\theta_4)}{m^2 B\sinh \pi B}\right.$$

$$\left. + \frac{2a^2}{\pi^3}\sum_{m=1}^{\infty}\frac{(\sin m\theta_1 - \sin m\theta_2)\left[\sinh B(\pi - \theta_3) - \sinh B(\pi - \theta_4)\right]}{mB^2\sinh B\pi}\right] \qquad (8.2.2.10)$$

8.2.3. One Port on a Perpendicular Side and One Port on the Hypotenuse

The two ports p, q have centers $(0, y_p), (x_q, a - x_q)$.

The Green's function becomes

$$G(0, y_p \mid x_q, a - x_q) = \frac{j2\omega\mu h}{\pi^2}\left\{\frac{-\pi^2}{a^2 k^2} + \sum_{m=1}^{\infty}\frac{\left(1 + (-1)^m\cos\frac{m\pi}{a}y_p\right)\left(\cos\frac{m\pi}{a}x_q + (-1)^m\cos\frac{m\pi}{a}(a - x_q)\right)}{(m^2 - A^2)}\right.$$

$$\left. + \sum_{n=1}^{\infty}\sum_{m=1}^{\infty}\frac{\left(\cos\frac{n\pi}{a}y_p + (-1)^{m+n}\cos\frac{m\pi}{a}y_p\right)\left(\cos\frac{n\pi}{a}x_q\cos\frac{n\pi}{a}(a - x_q) + (-1)^{m+n}\cos\frac{m\pi}{a}x_q\cos\frac{m\pi}{a}(a - x_q)\right)}{(m^2 + n^2 - A^2)}\right\} (8.2.3.1)$$

The coupling impedance between these ports is given by

$$Z_{pq} = \frac{\sqrt{2}}{W_p W_q}\int_{W_p}\int_{W_q} G(0, y_p \mid x_q, a - x_q)\, dy_p\, dx_q \qquad (8.2.3.2)$$

where the integrations are over the intervals $\left(y_p - \dfrac{W_p}{2}, y_p + \dfrac{W_p}{2}\right)$, and,

$$\left(x_q + \frac{W_q}{2\sqrt{2}}, x_q - \frac{W_q}{2\sqrt{2}}\right).$$

From equation (8.2.3.1) and (8.2.3.2), by integration (Appendix 8A)

$$Z_{pq} = \frac{j2}{W_p W_q}\,\omega\,\mu\,h\left[-\frac{W_p W_q}{k^2 a^2} + \frac{2\sqrt{2}\,a W_p}{\pi^3}Sm_1 + \frac{2\sqrt{2}\,a^2}{\pi^4}Sm_2 + \frac{\sqrt{2}\,a^2}{2\pi^4}Sm_3\right.$$

$$\left. + \frac{aW_q}{\pi^3}Sm_4 + \frac{4\sqrt{2}\,a^2}{\pi^4}Smn_5\right] \qquad (8.2.3.3)$$

where,

$$Sm_1 = \sum_{m=1}^{\infty}\frac{(\sin m\theta_3 - \sin m\theta_4)}{m\ (m^2 - A^2)}$$

$$= \frac{W_q \pi^3}{2\sqrt{2}\ k^2 a^3} + \frac{\pi^2}{2k^2 a^2 \sin ka}\left[\sin A(\pi - \theta_3) - \sin A(\pi - \theta_4)\right] \qquad (8.2.3.4)$$

$$Sm_2 = \sum_{m=1}^{\infty}\frac{(-1)^m F_1(m:\theta_1,\theta_2,\theta_3,\theta_4)}{m^2\ (m^2 - A^2)}$$

$$= \frac{W_p W_q \pi^4}{2\sqrt{2}\ k^2 a^4} + \frac{\pi^4(\sin A\theta_1 - \sin A\vartheta_2)(\sin A\theta_3 - \sin A\vartheta_4)}{k^3 a^3 \sin ka} \qquad (8.2.3.5)$$

$$Sm_3 = \sum_{m=1}^{\infty}\frac{(-1)^m(\sin m\theta_1 - \sin m\theta_2)(\sin m2\theta_3 - \sin m2\theta_4)}{m^2\ (m^2 - A^2/2)} \qquad (8.2.3.6)$$

$$Sm_4 = \sum_{m=1}^{\infty}\frac{(-1)^m(\sin m\theta_1 - \sin m\theta_2)}{m^2\ (m^2 - A^2/2)}$$

$$= \frac{W_p \pi^3}{k^2 a^3} - \frac{\pi^3\left(\sin\frac{A}{\sqrt{2}}\theta_1 - \sin\frac{A}{\sqrt{2}}\theta_2\right)}{k^2 a^2 \sin\frac{ka}{\sqrt{2}}} \qquad (8.2.3.7)$$

$$Smn_5 = \sum_{n=1}^{\infty}\sum_{m=n+1}^{\infty}\frac{(-1)^m(\sin m\theta_1 - \sin m\theta_2)}{m\ (m^2 + n^2 - A^2)}\left[\frac{\sin(m+n)\theta_3 - \sin(m+n)\theta_4}{m+n}\right.$$

$$\left. + \frac{\sin(m-n)\theta_3 - \sin(m-n)\theta_4}{m-n}\right] \qquad (8.2.3.8)$$

where, $F_1(m:\theta_1,\theta_2,\theta_3,\theta_4)$ is defined as in section 8.2.1,

$$\theta_1 = \frac{\pi}{a}\left(y_p + \frac{W_p}{2}\right); \quad \theta_2 = \frac{\pi}{a}\left(y_p - \frac{W_p}{2}\right); \quad \theta_3 = \frac{\pi}{a}\left(x_q + \frac{W_q}{2\sqrt{2}}\right); \quad \theta_3 = \frac{\pi}{a}\left(x_q - \frac{W_q}{2\sqrt{2}}\right).$$

Using equations (8.2.3.4), (8.2.3.5) and (8.2.3.7) in equation (8.2.3.3) eliminates the term $W_p W_q / k^2 a^2$ to give the coupling impedance

$$Z_{pq} = -\frac{j2\omega\mu h}{W_p W_q}\left[\frac{2W_p W_q}{k^2 a} + \frac{\sqrt{2}\ W_p\left(\sin A(\pi-\theta_3) - \sin A(\pi-\theta_4)\right)}{k^2 a \pi \sin ka} - \frac{\sqrt{2}\left(\sin A\theta_1 - \sin A\theta_2\right)\left(\sin A\theta_3 - \sin A\theta_4\right)}{k^3 a \sin ka}\right.$$

$$-\frac{W_q\left(\sin\frac{A}{\sqrt{2}}\theta_1 - \sin\frac{A}{\sqrt{2}}\theta_2\right)}{k^2 a \sin\frac{ka}{\sqrt{2}}} + \frac{a^2\sqrt{2}}{2\pi^4}\sum_{m=1}^{\infty}\frac{(-1)^m(\sin m\theta_1 - \sin m\theta_2)(\sin m2\theta_3 - \sin m2\theta_4)}{m^2\ (m^2 - A^2/2)}$$

$$+\frac{2\sqrt{2}\ a^2}{\pi^4}\sum_{n=1}^{\infty}\sum_{m=n+1}^{\infty}\frac{(-1)^m(\sin m\theta_1 - \sin m\theta_2)}{m\ (m^2 + n^2 - A^2)}\left[\frac{\sin(m+n)\theta_3 - \sin(m+n)\theta_4}{m+n}\right.$$

$$\left.\left. + \frac{\sin(m-n)\theta_3 - \sin(m-n)\theta_4}{m-n}\right]\right] \qquad (8.2.3.9)$$

8.2.4 Two Ports on the Hypotenuse

The two ports p, q have centers $(x_p, a - x_p), (x_p, a - x_p)$.

The Green's function becomes

$$G(x_p, a - x_p \mid x_q, a - x_q)$$

$$= \frac{j2\omega\mu h}{\pi^2}\left\{ -\pi^2 \left[\frac{-\pi^2}{k^2 a^2} + \sum_{m=1}^{\infty} \frac{\left(\cos\frac{m\pi}{a}x_p + (-1)^m \cos\frac{m\pi}{a}(a - x_q) \right)\left(\cos\frac{m\pi}{a}x_q + (-1)^m \cos\frac{m\pi}{a}(a - x_q) \right)}{(m^2 - A^2)} \right. \right.$$

$$+ \sum_{m=1}^{\infty}\sum_{n=1}^{\infty} \left[\frac{\left(\cos\frac{m\pi}{a}x_p \cos\frac{n\pi}{a}(a - x_p) + (-1)^{m+n}\cos\frac{n\pi}{a}x_p \cos\frac{m\pi}{a}(a - x_p) \right)}{(m^2 + n^2 - A^2)} \right.$$

$$\left.\left. \left[\cos\frac{m\pi}{a}x_q \cos\frac{n\pi}{a}(a - x_q) + (-1)^{m+n}\cos\frac{n\pi}{a}x_q \cos\frac{m\pi}{a}(a - x_q) \right] \right] \right\} \quad (8.2.4.1)$$

The coupling impedance between these ports is given by

$$Z_{pq} = \frac{2}{W_p W_q}\int_{W_p}\int_{W_q} G(x_p, a - x_p \mid x_q, a - x_q)\, dx_p\, dx_q \qquad (8.2.4.2)$$

where the integrations are over the intervals $\left(x_p + \dfrac{W_p}{2\sqrt{2}}, y_p - \dfrac{W_p}{2\sqrt{2}} \right)$, and,

$$\left(y_q + \frac{W_q}{2\sqrt{2}}, y_q - \frac{W_q}{2\sqrt{2}} \right).$$

From equation (8.2.4.1) and (8.2.4.2), by integration (Appendix 8A)

$$Z_{pq} = \frac{j2\,\omega\,\mu\,h}{W_p W_q}\left[-\frac{W_p W_q}{k^2 a^2} + \frac{8}{\pi^4}\frac{a^2}{}Sm_1 + \frac{a^2}{4\pi^4}Sm_2 + \frac{a^2 W_p}{2\sqrt{2}\pi^4}Sm_3 + \frac{a^2 W_q}{2\sqrt{2}\pi^4}Sm_4 + \frac{a^2 W_p W_q}{2\pi^4}Sm_5 \right.$$

$$\left. + \frac{4a^2}{\pi^4}Smn_6 \right] \qquad (8.2.4.3)$$

where,

$$Sm_1 = \sum_{m=1}^{\infty}\frac{F_1(m:\theta_1,\theta_2,\theta_3,\theta_4)}{m^2(m^2 - A^2)}$$

$$= \frac{\pi^4 W_p W_q}{2k^2 a^4} + \frac{\pi^4\left(\sin A(\pi - \theta_1) - \sin A(\pi - \theta_2) \right)\left(\sin A\theta_3 - \sin A\theta_4 \right)}{k^3 a^3 \sin ka} \qquad (8.2.4.4)$$

128

$$Sm_2 = \sum_{m=1}^{\infty} \frac{(\sin m2\theta_1 - \sin m2\theta_2)(\sin m2\theta_3 - \sin m2\theta_4)}{m^2 \ (m^2 - A^2/2)} \tag{8.2.4.5}$$

$$Sm_3 = \sum_{m=1}^{\infty} \frac{(\sin m2\theta_3 - \sin m2\theta_4)}{m \ (m^2 - A^2/2)}$$

$$= \frac{\pi^3 W_q}{\sqrt{2} \ k^2 a^3} + \frac{\pi^3 \left(\sin \dfrac{A}{\sqrt{2}} \ (\pi - 2\theta_3) - \sin \dfrac{A}{\sqrt{2}} \ (\pi - 2\theta_4) \right)}{k^2 a^2 \ \sin ka/\sqrt{2}} \tag{8.2.4.6}$$

$$Sm_4 = \sum_{m=1}^{\infty} \frac{(\sin m2\theta_1 - \sin m2\theta_2)}{m \ (m^2 - A^2/2)}$$

$$= \frac{\pi^3 W_q}{\sqrt{2} \ k^2 a^3} + \frac{\pi^3 \left(\sin \dfrac{A}{\sqrt{2}} \ (\pi - 2\theta_1) - \sin \dfrac{A}{\sqrt{2}} \ (\pi - 2\theta_2) \right)}{k^2 a^2 \ \sin ka/\sqrt{2}} \tag{8.2.4.7}$$

$$Sm_5 = \sum_{m=1}^{\infty} \frac{1}{(m^2 - A^2/2)}$$

$$= \frac{\pi^2}{k^2 a^2} - \frac{\sqrt{2} \ \pi \ \cot ka/\sqrt{2}}{2ka} \tag{8.2.4.8}$$

$$Smn_6 = \sum_{n=1}^{\infty} \sum_{m=n+1}^{\infty} \left[\frac{\left(\sin(m+n)\theta_1 - \sin(m+n)\theta_2 \right)}{(m^2 + n^2) \ (m^2 + n^2 - A^2)} + \frac{\left(\sin(m-n)\theta_1 - \sin(m-n)\theta_2 \right)}{(m^2 - n^2) \ (m^2 + n^2 - A^2)} \right] \ .$$

$$\left[\frac{\left(\sin(m+n)\theta_3 - \sin(m+n)\theta_4 \right)}{(m^2 + n^2)} + \frac{\left(\sin(m-n)\theta_3 - \sin(m-n)\theta_4 \right)}{(m^2 - n^2)} \right] \tag{8.2.4.9}$$

where, $F_1(m \ : \ \theta_1, \theta_2, \theta_3, \theta_4)$ is defined as in Section 8.2.1 , $\theta_1 = \dfrac{\pi}{a} \left(x_p - \dfrac{W_p}{2\sqrt{2}} \right)$,

$\theta_2 = \dfrac{\pi}{a} \left(x_p + \dfrac{W_p}{2\sqrt{2}} \right)$, $\theta_3 = \dfrac{\pi}{a} \left(x_q - \dfrac{W_q}{2\sqrt{2}} \right)$, $\theta_4 = \dfrac{\pi}{a} \left(x_q - \dfrac{W_q}{2\sqrt{2}} \right)$.

129

Using equations (8.2.4.4), (8.2.4.6), (8.2.4.7) and (8.2.4.8) in equation (8.2.4.3) eliminates the term $W_p W_q / k^2 a^2$ to give

$$Z_{pq} = -\frac{j2\omega\mu h}{W_p W_q}\left[\frac{W_p W_q}{k^2 d^2} + \frac{W_p W_q}{4\pi k^2 a} + \frac{W_q^2}{4\pi^2 ka} + \frac{W_p W_q}{2\pi^2 k^2} + \frac{4\big(\sin A(\pi-\theta_1) - \sin A(\pi-\theta_2)\big)\big(\sin A\theta_3 - \sin A\theta_4\big)}{k^3 a \sin ka}\right.$$

$$+ \frac{W_p\left(\sin\frac{A}{\sqrt{2}}(\pi - 2\theta_3) - \sin\frac{A}{\sqrt{2}}(\pi - 2\theta_4)\right)}{2\sqrt{2}\pi\ k^2 \sin ka/\sqrt{2}} + \frac{W_q\left(\sin\frac{A}{\sqrt{2}}(\pi - 2\theta_1) - \sin\frac{A}{\sqrt{2}}(\pi - 2\theta_2)\right)}{2\sqrt{2}\pi\ k^2 \sin ka/\sqrt{2}}$$

$$+ \frac{a^2}{4\pi^4} \sum_{m=1}^{\infty} \frac{(\sin m2\theta_1 - \sin m2\theta_2)(\sin m2\theta_3 - \sin m2\theta_4)}{m^2\ (m^2 - A^2/2)}$$

$$+ \frac{4a^2}{\pi^4} \sum_{n=1}^{\infty}\sum_{m=n+1}^{\infty}\left[\frac{\big(\sin(m+n)\theta_1 - \sin(m+n)\theta_2\big)}{(m^2+n^2)(m^2+n^2-A^2)} + \frac{\big(\sin(m-n)\theta_1 - \sin(m-n)\theta_2\big)}{(m^2-n^2)(m^2+n^2-A^2)}\right]\left[\frac{\big(\sin(m+n)\theta_3 - \sin(m+n)\theta_4\big)}{(m^2+n^2)}\right.$$

$$\left.\left. + \frac{\big(\sin(m-n)\theta_3 - \sin(m-n)\theta_4\big)}{(m^2-n^2)}\right]\right] \quad (8.2.4.10)$$

8.3 Test Application

The new coupling impedance expressions (8.2.1.9), (8.2.2.10), (8.2.3.9) and (8.2.4.10) were used in the test application to the patch antennas shown in figure 8.2.1, with a resonant frequency of 2.45GHz, $a = 40mm$, $W = 0.067mm$, substrate (Duroid 5870) $h = 0.79mm$, $\varepsilon r = 2.33$, and, a loss tangent of 0.0012.

Results for two different separations between the two ports were obtained for the four cases and compared with those predicted by a full wave analysis software (Ensemble™). These result s are shown in graphs 8.3.1, 8.3.2, 8.3.3 and 8.3.4.

As can be seen in figure 8.3.1(a) and 8.3.1(b) for ports on the y-axis, the coupling impedances decrease with separation of the two ports. Figure 8.3.2(a) and 8.3.2(b) show the comparison of results for coupling between the ports on x and y-axes ,and, as expected the impedances decrease due to the natural low impedance at the right angle corner of the triangular patch. Figure 8.3.3(a) and 8.3.3(b) shows the results for coupling ports between the y-axis and the hypotenuse, the impedances increase with the very high impedance at the right hand corner of the triangular patch. Finally figure 8.3.4(a) and 8.3.4(b) shows the results for coupling ports on the hypotenuse. In all four cases there is an excellent agreement between the results obtained from the new economised computational expressions with that predicted by the Ensemble™.

8.4 Summary

In this chapter an efficient computational expressions for each of the four possible right-angled isosceles triangular patch coupling impedance configurations has been obtained. The number of terms in the series for a required accuracy is given. Good agreement between results using the new expressions and Ensemble™ is obtained in each of the test applications.
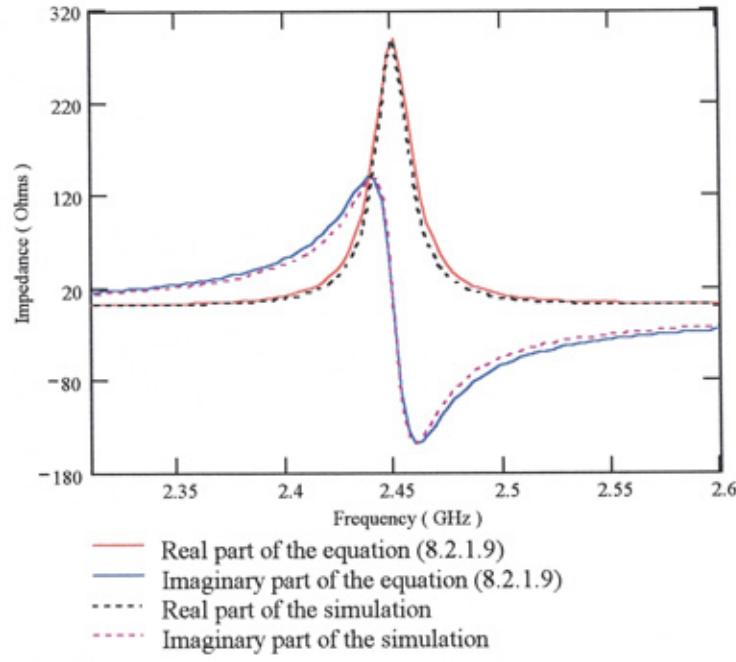
(a) Coupling impedances for $y_p = 18mm$ and $y_q = 22mm$
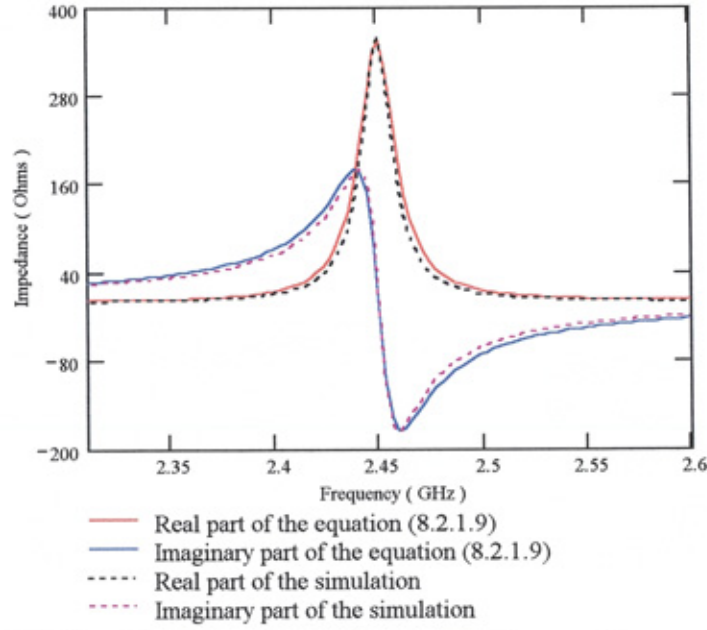
(b) Coupling impedances for $y_p = 14mm$ and $y_q = 26mm$

Figure 8.3.1: Coupling impedances of two ports located on the same edge at $(0, y_p)$,

$(0, y_q)$.
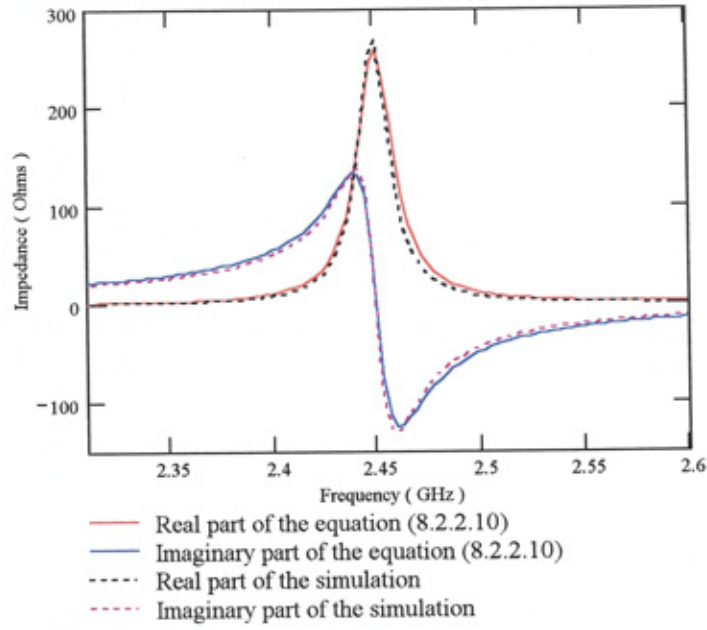
(a) Coupling impedances for $y_p = x_q = 18mm$
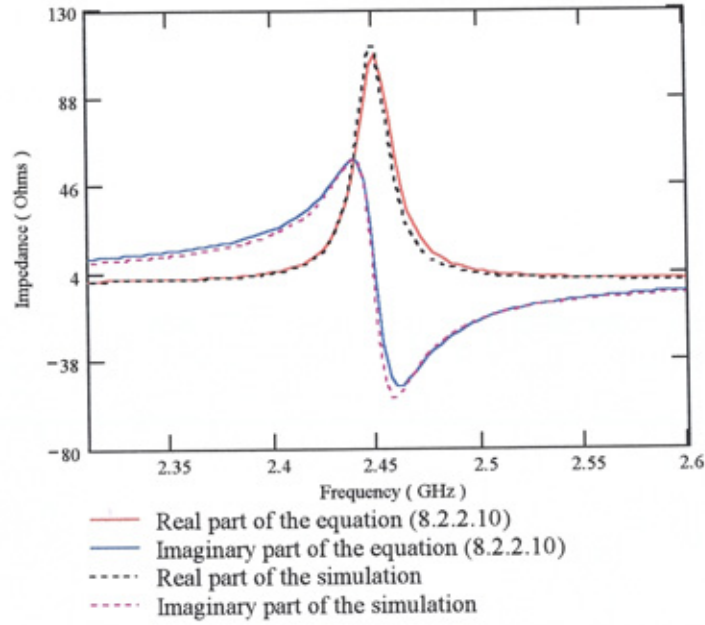
(b) Coupling impedances for $y_p = x_q = 14mm$

Figure 8.3.2: Coupling impedances of two ports located on adjacent edges at $(0, y_p)$,

$(x_q, 0)$.
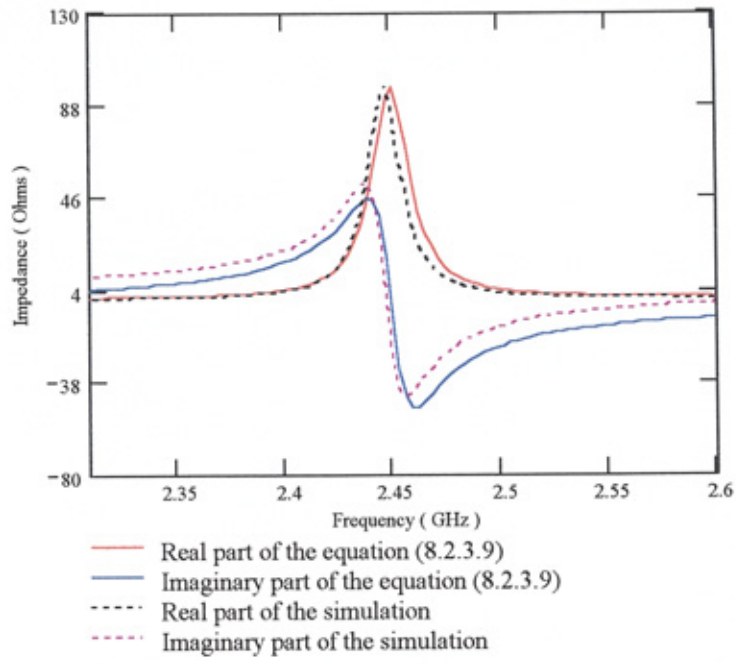
(a) Coupling impedances for $y_p = x_q = 18mm$
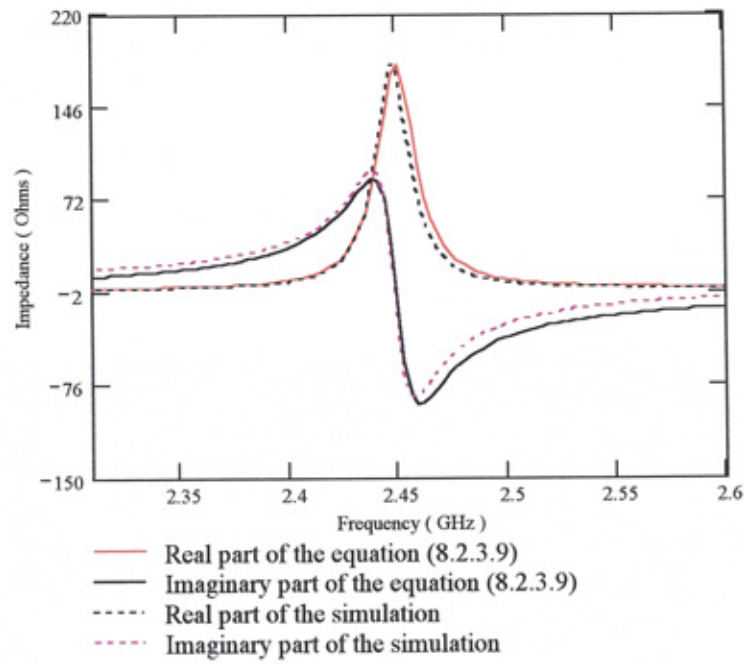
(b) Coupling impedances for $y_p = x_q = 14mm$

Figure 8.3.3: Coupling impedances of one port on perpendicular edge and one port on the

hypotenuse at $(0, y_p), (x_q, 0)$.
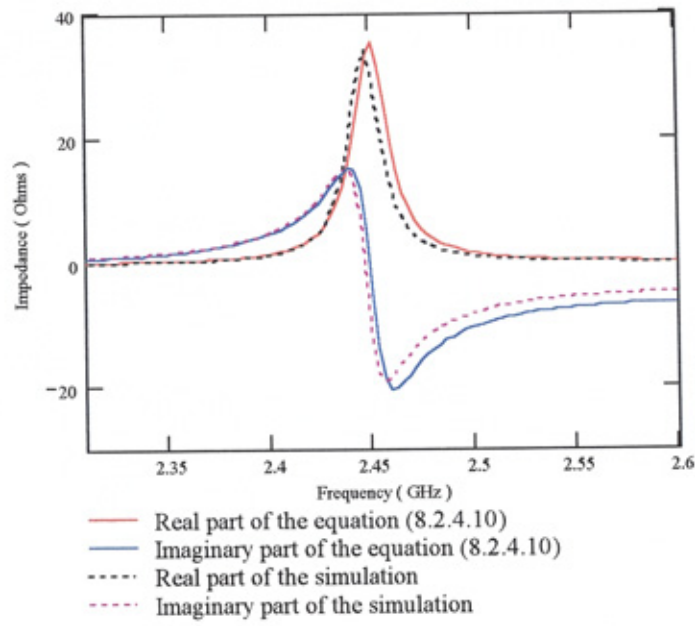
(a) Coupling impedances for $x_p = 18mm$ and $x_q = 22mm$
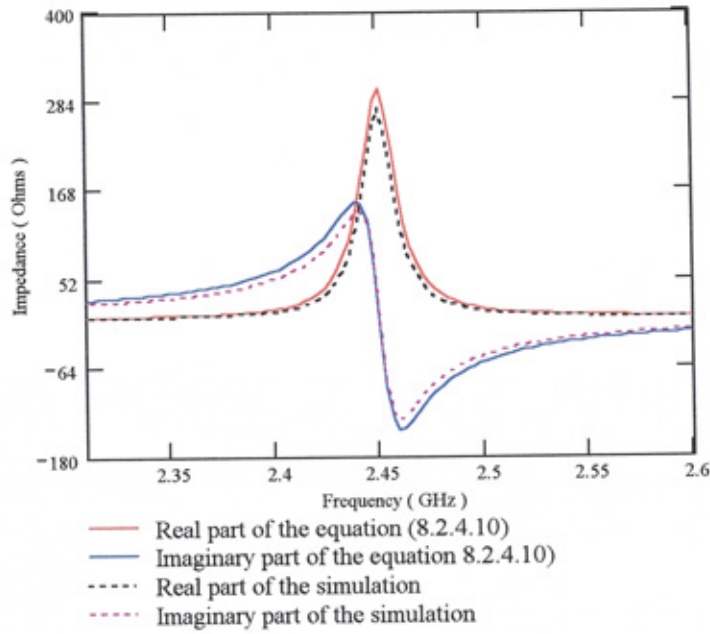
(b) Coupling impedances for $x_p = 14mm$ and $x_q = 26mm$

Figure 8.3.4: Coupling impedances of two ports on the hypotenuse at $(x_p, 0), (x_q, 0)$.

CHAPTER 9

THE CORNER-DELETED-SQUARE MICROSTRIP

ANTENNA DESIGN IMPLEMENTATION

9.1 Introduction

A design procedure for the design of a centre-fed two corner-deleted truncated circular polarised patch antenna is presented. The circular polarisation results from perturbing a square antenna geometry, and, the amount of perturbation is obtained by an application of perturbation analysis (Chapter4). To calculate the input impedance of the antenna the desegmentation method is used (Chapter 6). In this method connecting ports are introduced between the segments and a multiport coplanar analysis applied to obtain the overall characteristic of the combined structure (Chapter 5). The analysis employs interport coupling impedance formulas which are derived using the Green's functions for a square, and, a right angled isosceles triangle path geometry.

New computationally efficient expressions for the interconnecting port impedances on a rectangle, and, on a right angled isosceles triangle shaped antenna patch, have been obtained (Chapter 7 and 8).

In this chapter the computational steps, required to determine the antenna size and input impedance are given in section 9.2. The detailed structural properties of the impedance

coupling matrices together with the new computationally efficient formulas for the elements of each matrix are given in section 9.3.

The design geometry and input impedance for an antenna with an operational radiating frequency, f_0 of 2.45GHz is calculated and the results presented in section 9.4. The impedance of the matching network is discussed in section 9.5.

All the results from the above work show close agreement with full-wave software simulation and practical results.

9.2 Design Procedure Implementation

A procedure for the evaluation of the antenna input impedance using the Desegmentation technique and the application of this technique to the two deleted corner truncated patch antenna is presented as below.

1. Assign numerical values to the constants

   $$f_0, h, W, T, \sigma_c, N, N1, M1.$$

   where, f_0 is Operation frequency (2.45 GHz)

   h is Thickness of substrate

   W is Width of the feed line

   T is Offset feed line position

   σ_c is Conductivity of the copper 5.7×10^7 s/M

   N is Number of ports

   $N1$ is Upper summation limit of infinite series

   $M1$ is Upper summation limit of infinite series

2. Evaluate unloaded Q -factor, Q, from formula(3.3.1.2.2),

$$\frac{1}{Q} = \frac{1}{Q_c} + \frac{1}{Q_d} + \frac{1}{Q_r}$$

(9.2.1)

3. In the perturbation analysis for circular polarisation the electric field is separated into orthogonal modes of equal amplitude and with a phase difference of 90^0 [2]. The radiated fields excited by these two modes are perpendicular to each other and 90^0 out of phase. The typical impedance amplitude and phase diagrams are shown in figure 9.2.1.
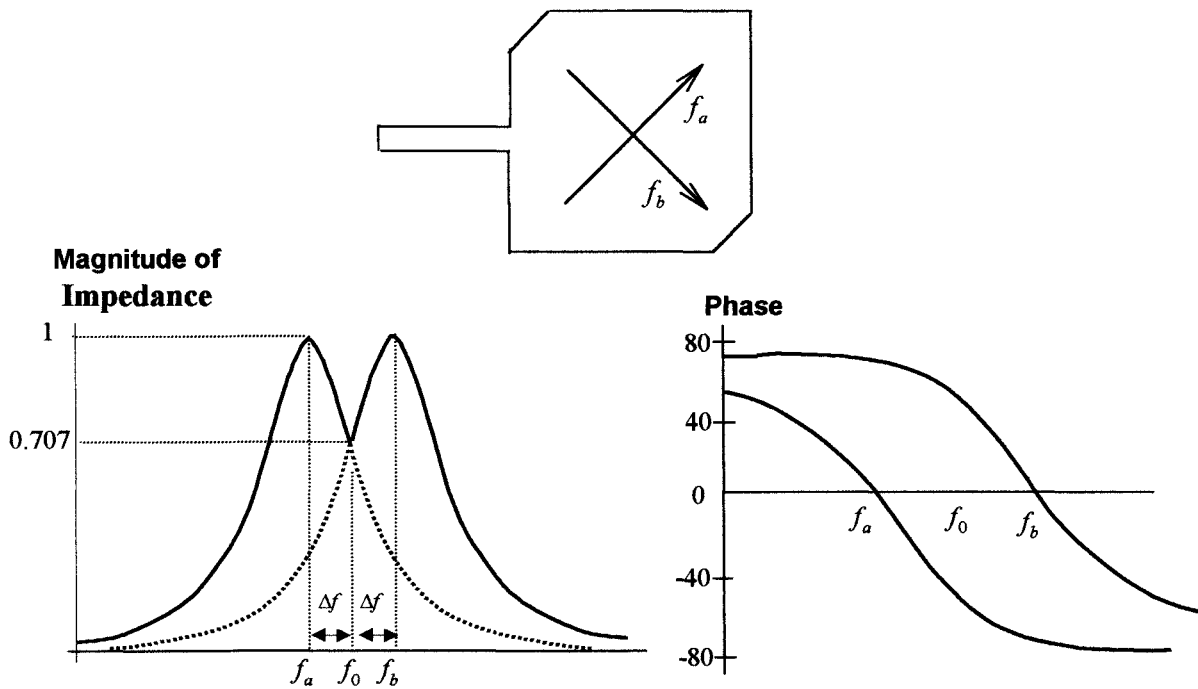

Figure 9.2.1: Amplitude and phase diagrams for a single fed circularly polarised microstrip antenna

138

The circular polarisation condition, for a centre feed, is characterised in the above impedance and phase curves. The design estimates the required offset frequency Δf (figure1), the unperturbed dimension 'a' of the antenna, and, the perturbation area ΔS obtained from perturbation analysis. Graphs of the individual mode impedances against frequency are obtained.

The required offset frequency Δf for each mode is related to the pre-assigned (detuned) resonant frequency, f_0, and, the unloaded Q-factor Q by

$$\Delta f = \frac{f_0}{2Q}$$

(9.2.2)

4. The lower and higher mode frequencies f_a and f_b are given by

$$f_a = f_0 - \Delta f$$

(9.2.3)

$$f_b = f_0 + \Delta f$$

(9.2.4)

5. The resonant frequency of the square patch is given by [7]

$$f_r = \frac{c}{2a\sqrt{\varepsilon_{eff}}}$$

(9.2.5)

where,

a = Length of the unperturbed patch incorporates the fringe field extension

c = Velocity of light

ε_{eff} = Effective dielectric constant of the substrate

6. From the perturbation analysis the higher mode resonant frequency is the resonant frequency before the perturbation. Therefore , the value of 'a' is determined by taking $f_r = f_b$.

The perturbation analysis results give the following relation [3]

$$\frac{\Delta S}{S} = \frac{1}{2Q} \tag{9.2.6}$$

where, ΔS is the total area of the deleted segments and S is the area of the

unperturbed patch

The dimension of the unperturbed square patch with fringe field extensions is then calculated and the dimension of a deleted triangle is obtained from the perturbation analysis, where the value of 'a' incorporates the fringe field extension.

7. Evaluate the desegmentation impedance coupling matrices

$$Z_{pp\gamma}, \quad Z_{pq\gamma}, \quad Z_{pp\gamma}, \quad Z_{qq\beta}$$

8. Generate the $Z_{pp\gamma}$ -frequency curve from the formula (6.6.17)

$$Z_{pp\alpha} = Z_{pp\gamma} - Z_{pq\gamma}\left[Z_{qq\gamma} - Z_{qq\beta}\right]^{-1} Z_{qp\gamma} \tag{9.2.6}$$

where,

$$Z_{pq\gamma} = Z_{qp\gamma}^T .$$

9. The fabrication dimension of 'a' then obtained by subtracting the fringe extension. This completes the design computation.

9.3 Evaluation of Coupling matrices for Input Impedance

The desegmentation configuration of the square patch antenna with two deleted corners, and, a centre feed, is shown in figure 9.3.1.
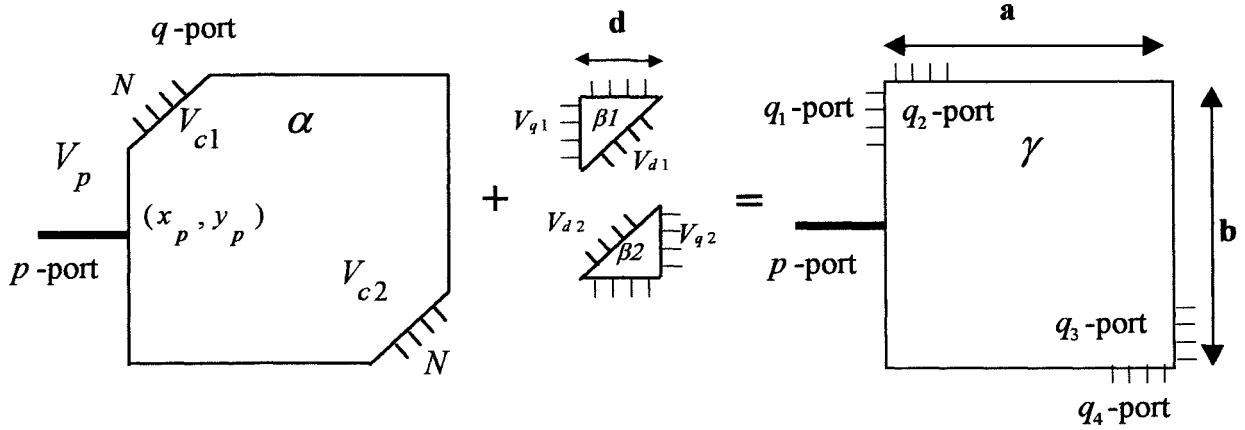
Figure 9.3.1: Microstrip fed antenna and desegmentation method

In this section the general structure and properties of the segmental coupling matrices $Z_{pp\gamma}$, $Z_{pq\gamma}$, $Z_{qq\gamma}$, and, $Z_{qq\beta}$ used in the input impedance formula are described. Using the impedance coupling matrices of each of the segments shown in figure 9.3.1, the microstrip input impedance of the antenna is given by the matrix formula

$$Z_{in} = Z_{pp\gamma} - Z_{pq\gamma} \left[Z_{qq\gamma} - Z_{qq\beta} \right]^{-1} Z_{qp\gamma}$$ (9.3.1)

where,

$$Z_{pq\gamma} = Z_{qp\gamma}^{T}$$

and, N is the number of the ports on each of the q_1, q_2, q_3, and, q_4 section of q-ports as shown in figure 9.3.1.

The number $Z_{pp\gamma}$ represents the interaction of the input feed port with itself, that is, port 'p' to port 'p', and is given by

141

$$Z_{pp\gamma} = \frac{j\omega\mu h}{a^2}\left[\frac{-a}{k}\cot ka + \frac{2a^4}{W_p W_q \pi^3}\sum_{n=1}^{\infty}\frac{(\sin n\theta_1 - \sin n\theta_2)\ (\sin n\theta_3 - \sin n\theta_4)}{n^2 D}\coth D\pi\right] \qquad (9.3.2)$$

where, $A = ka/\pi$, $k^2 = \omega^2\mu\ \varepsilon_0\varepsilon_r(1 - j/Q)$, $D^2 = (n^2 - A^2)$, $\theta_1 = \dfrac{\pi}{a}\left(y_p - \dfrac{W_p}{2}\right)$,

$\theta_2 = \dfrac{\pi}{a}\left(y_p + \dfrac{W_p}{2}\right)$, $\theta_3 = \dfrac{\pi}{a}\left(y_q - \dfrac{W_q}{2}\right)$,and, $\theta_4 = \dfrac{\pi}{a}\left(y_q + \dfrac{W_q}{2}\right)$.

where (y_p, y_q) is the feed location coordinate.

The impedance coupling matrices $Z_{pq\gamma}$, and, $Z_{qp\gamma}$ represent the interactions between the

feed port 'p' and the interconnecting q-ports, and vice-versa. $Z_{pq\gamma}$ is a vector of order

$4N$.

The coupling matrix $Z_{pq\gamma}$ connects the single input p-port with the interconnecting q-

ports, and has the following structure:

$$Z_{pq\gamma} = \begin{bmatrix} Z_{pq_1\gamma}, & Z_{pq_2\gamma}, & Z_{pq_3\gamma}, & Z_{pq_4\gamma} \end{bmatrix} \qquad (9.3.3)$$

where each of the above sub-matrices is a vector of order N, and, the expressions for the

elements in each of the four matrices are given below.

$$Z_{pq_1\gamma}^{(i)} = \frac{j\omega\mu h}{a^2}\left[\frac{-a}{k}\cot ka + \frac{2a^4}{W_p W_q \pi^3}\sum_{n=1}^{\infty}\frac{(\sin n\theta_1 - \sin n\theta_2)\ (\sin n\theta_3 - \sin n\theta_4)}{n^2 D}\coth D\pi\right] \qquad (9.3.4)$$

where, $A = ka/\pi$, $D^2 = (n^2 - A^2)$, $\theta_1 = \dfrac{\pi}{a}\left(y_p - \dfrac{W_p}{2}\right)$, $\theta_2 = \dfrac{\pi}{a}\left(y_p + \dfrac{W_p}{2}\right)$,

$\theta_3 = \dfrac{\pi}{a}\left(y_{qi} - \dfrac{W_q}{2}\right)$, $\theta_4 = \dfrac{\pi}{a}\left(y_{qi} + \dfrac{W_q}{2}\right)$, for $i = 1, N$.

The N elements of the submatrix $Z_{pq_2\gamma}$ are given by

$$Z_{pq_2\gamma}^{(i)} = \frac{j\omega\,\mu\,h}{W_p W_q}\left[\frac{W_q\;[\;\sin B(\pi-\theta_4)-\sin B(\pi-\theta_3)]}{ak^2\sin ka}\right.$$

$$\left. + \frac{2a^2}{\pi^3}\sum_{m=1}^{\infty}\frac{(\sin m\theta_1-\sin m\theta_2)[\sinh C\;(\pi-\theta_4)-\sinh C\;(\pi-\theta_3)]}{m\,(m^2-A^2)\sinh C\,\pi}\right] \quad (9.3.5)$$

where, $A = ka/\pi$, $C^2 = (m^2-A^2)$; $\theta_1 = \dfrac{\pi}{a}\left(x_{qi}+\dfrac{W_q}{2}\right)$, $\theta_2 = \dfrac{\pi}{a}\left(x_{qi}-\dfrac{W_q}{2}\right)$,

$\theta_3 = \dfrac{\pi}{a}\left(y_p+\dfrac{W_p}{2}\right)$, $\theta_4 = \dfrac{\pi}{a}\left(y_p-\dfrac{W_p}{2}\right)$, for $i = N+1, 2N$.

The N elements of the submatrix $Z_{pq_3\gamma}$ are given by

$$Z_{pq_3\gamma}^{(i)} = \frac{j\omega\,\mu\,h}{aW_p W_q}\left[\frac{W_p W_q}{k\sin ka}-\frac{2a^3}{\pi^3}\sum_{n=1}^{\infty}\frac{(\sin n\theta_1-\sin n\theta_2)\;(\sin n\theta_3-\sin n\theta_4)}{D\sinh D\pi}\right] \quad (9.3.6)$$

where, A, D, θ_1, θ_2, θ_3, θ_4 are same as defined in equation (9.3.4) ,and, for $i = 2N+1, 3N$.

The N elements of the submatrix $Z_{pq_4\gamma}$ are given by

$$Z_{pq_4\gamma}^{(i)} = \frac{j\omega\,\mu\,h}{W_p W_q}\left[\frac{W_q\;[\;\sin B(\pi-\theta_4)-\sin B(\pi-\theta_3)]}{ak^2\sin ka}\right.$$

$$\left. + \frac{2a^2}{\pi^3}\sum_{m=1}^{\infty}\frac{(\sin m\theta_1-\sin m\theta_2)[\sinh C\;(\pi-\theta_4)-\sinh C\;(\pi-\theta_3)]}{m\,(m^2-A^2)\sinh C\,\pi}\right] \quad (9.3.7)$$

where, A, C, θ_1, θ_2, θ_3, θ_4 are same as defined in equation (9.3.5) and $i = 3N+1, 4N$.

The symmetric coupling matrix $Z_{qq\gamma}$, of dimension $4N$ x $4N$, represents the interactions between each individual interconnection port on the γ-segment and has the form

$$Z_{qq\gamma} = \begin{bmatrix} Z_{q_1 q_1 \gamma} & Z_{q_1 q_2 \gamma} & Z_{q_1 q_3 \gamma} & Z_{q_1 q_4 \gamma} \\ \cdot & Z_{q_1 q_1 \gamma} & Z_{q_1 q_4 \gamma} & Z_{q_1 q_3 \gamma} \\ \cdot & \cdot & Z_{q_1 q_1 \gamma} & Z_{q_1 q_2 \gamma} \\ \cdot & \cdot & \cdot & Z_{q_1 q_1 \gamma} \end{bmatrix} \qquad (9.3.8)$$

and contains four distinct submatrices out of a total of sixteen sub-matrices. The dimension of each submatrix is N x N.

Formulas for the elements in each of the four distinct matrices, $Z_{q_1 q_1 \gamma}$, $Z_{q_1 q_2 \gamma}$, $Z_{q_1 q_3 \gamma}$, $Z_{q_1 q_4 \gamma}$, are given below.

The N^2 elements of the submatrix $Z_{q_1 q_1 \gamma}$ are given by

$$Z_{q_1 q_1 \gamma}^{(i,j)} = \frac{j\omega \, \mu \, h}{a^2}\left[\frac{-a}{k}\cot ka + \frac{2a^4}{W_p W_q \pi^3} \sum_{n=1}^{\infty} \frac{(\sin n\theta_1 - \sin n\theta_2)}{n^2 D} \frac{(\sin n\theta_3 - \sin n\theta_4)}{n^2 D} \coth D\pi \right] \quad (9.3.9)$$

where, $A = ka/\pi$, $D^2 = (n^2 - A^2)$, $\theta_1 = \frac{\pi}{a}\left(y_{q_i} - \frac{W_p}{2}\right)$, $\theta_2 = \frac{\pi}{a}\left(y_{q_i} + \frac{W_p}{2}\right)$,

$\theta_3 = \frac{\pi}{a}\left(y_{q_j} - \frac{W_q}{2}\right)$, $\theta_4 = \frac{\pi}{a}\left(y_{q_j} + \frac{W_q}{2}\right)$, for $i = 1, N$ and, $j = 1, N$.

The N^2 elements of the submatrix $Z_{q_1 q_2 \gamma}$ are given by

$$Z_{q_1 q_2 \gamma}^{(i,j)} = \frac{j\omega \mu h}{W_p W_q}\left[\frac{W_q\left[\sin B(\pi - \theta_4) - \sin B(\pi - \theta_3)\right]}{ak^2 \sin ka} \right.$$

$$\left. + \frac{2a^2}{\pi^3} \sum_{m=1}^{\infty} \frac{(\sin m\theta_1 - \sin m\theta_2)\left[\sinh C\ (\pi - \theta_4) - \sinh C\ (\pi - \theta_3)\right]}{m\ (m^2 - A^2)\sinh C\ \pi} \right] \quad (9.3.10)$$

where, $A = ka/\pi$, $C^2 = (m^2 - A^2)$; $\theta_1 = \dfrac{\pi}{a}\left(x_{q_2 j} + \dfrac{W_q}{2}\right)$, $\theta_2 = \dfrac{\pi}{a}\left(x_{q_2 j} - \dfrac{W_q}{2}\right)$

, $\theta_3 = \dfrac{\pi}{a}\left(y_{q_1 i} + \dfrac{W_p}{2}\right)$, $\theta_4 = \dfrac{\pi}{a}\left(y_{q_1 i} - \dfrac{W_p}{2}\right)$, $i = 1, N$ and $j = N + 1, 2N$.

The N^2 elements of the submatrix $Z_{q_1 q_3 \gamma}$ are given by

$$Z_{q_1 q_3 \gamma}^{(i,j)} = \frac{j\omega\,\mu\,h}{aW_p W_q}\left[\frac{W_p W_q}{k\sin ka} - \frac{2a^3}{\pi^3}\sum_{n=1}^{\infty}\frac{(\sin n\theta_1 - \sin n\theta_2)\,(\sin n\theta_3 - \sin n\theta_4)}{D\sinh D\pi}\right] \qquad (9.3.11)$$

where, $A = bk/\pi$, $D^2 = (n^2 - A^2)$, $\theta_1 = \dfrac{\pi}{a}\left(y_{q_1 i} - \dfrac{W_p}{2}\right)$, $\theta_2 = \dfrac{\pi}{a}\left(y_{q_1 i} + \dfrac{W_p}{2}\right)$,

$\theta_3 = \dfrac{\pi}{a}\left(y_{q_3 j} - \dfrac{W_q}{2}\right)$, $\theta_4 = \dfrac{\pi}{a}\left(y_{q_3 j} + \dfrac{W_q}{2}\right)$, for $i = 1, N$ and $j = 2N + 1, 3N$.

The N^2 elements of the submatrix $Z_{q_1 q_4 \gamma}$ are given by

$$Z_{q_1 q_4 \gamma}^{(i,j)} = \frac{j\omega\,\mu h}{W_p W_q}\left[\frac{W_q\left[\sin B(\pi - \theta_4) - \sin B(\pi - \theta_3)\right]}{ak^2\sin ka}\right.$$

$$\left. + \frac{2a^2}{\pi^3}\sum_{m=1}^{\infty}\frac{(\sin m\theta_1 - \sin m\theta_2)\left[\sinh C\,(\pi - \theta_4) - \sinh C\,(\pi - \theta_3)\right]}{m\,(m^2 - A^2)\sinh C\,\pi}\right] \qquad (9.3.12)$$

where, $A = ka/\pi$, $C^2 = (m^2 - A^2)$; $\theta_1 = \dfrac{\pi}{a}\left(x_{q_4 j} + \dfrac{W_q}{2}\right)$, $\theta_2 = \dfrac{\pi}{a}\left(x_{q_4 j} - \dfrac{W_q}{2}\right)$

, $\theta_3 = \dfrac{\pi}{a}\left(y_{q_1 i} + \dfrac{W_p}{2}\right)$, $\theta_4 = \dfrac{\pi}{a}\left(y_{q_1 i} - \dfrac{W_p}{2}\right)$, for $i = 1, N$ and $j = 3N + 1, 4N$.

145

The coupling matrix $Z_{qq\beta}$, of dimension $4N \times 4N$, represents the interactions between each individual interconnecting port on the two β-segments. Since the values of the impedance coupling elements are independent of the coordinates system, and, the two β-segments have the same geometry.

$$Z_{qq\beta} = \begin{bmatrix} Z_{qq\beta 1} & 0 \\ 0 & Z_{qq\beta 1} \end{bmatrix} \tag{9.3.13}$$

The dimension of $Z_{qq\beta}$ and the null sub-matrix is $2N \times 2N$.

The sub-matrix $Z_{qq\beta 1}$ has the form

$$Z_{qq\beta 1} = \begin{bmatrix} Z_{q_1 q_1 \beta 1} & Z_{q_1 q_2 \beta 1} \\ Z^T_{q_1 q_2 \beta 1} & Z_{q_1 q_1 \beta 1} \end{bmatrix} \tag{9.3.14}$$

where each sub-matrix is of order $N \times N$.

Expressions for the elements in the matrices $Z_{q_1 q_1 \beta}$ and $Z_{q_1 q_2 \beta}$ are given below:

The N^2 elements of the submatrix $Z_{q_1 q_1 \beta}$ are given by

$$Z_{qq\beta}^{(i,j)} = \frac{j\omega\mu h}{W_p W_q} \left\{ \frac{W_p W_q}{kd} \cot \pi A + \frac{W_p(\sin A\theta_4 - \sin A\theta_3)}{k^2 d\sin kd} + \frac{2d^2}{\pi^3} \sum_{m=1}^{\infty} \frac{(\sin m\theta_1 - \sin m\theta_2)(\sin m\theta_3 - \sin m\theta_4)\coth \pi B}{m^2 B} \right.$$

$$\left. + \frac{2d^2}{\pi^3} \sum_{m=1}^{\infty} \frac{(-1)^m (\sin m\theta_1 - \sin m\theta_2)(\sinh B\theta_3 - \sinh B\theta_4)}{mB^2 \sinh \pi B} \right\} \tag{9.3.15}$$

where, $A = kd/\pi$, $B^2 = m^2 - A^2$, $\theta_1 = \frac{\pi}{d}\left(y_{q_i} + \frac{W_p}{2}\right)$; $\theta_2 = \frac{\pi}{d}\left(y_{q_i} - \frac{W_p}{2}\right)$;

$\theta_3 = \frac{\pi}{d}\left(y_{q_j} + \frac{W_q}{2}\right)$; $\theta_4 = \frac{\pi}{d}\left(y_{q_j} - \frac{W_q}{2}\right)$, for $i = 1, N$ and $j = 1, N$.

The N^2 elements of the submatrix $Z_{q_1q_2\beta}$ are given by

$$Z^{(i,j)}_{q_1q_2\beta} = \frac{j\omega}{W_pW_q}\frac{\mu}{h}\left[\frac{W_pW_q}{kd\sin kd} - \frac{W_p\left(\sin A(\pi-\theta 3)-\sin A(\pi-\theta 3)\right)}{k^2d\sin kd} - \frac{2d^2}{\pi^3}\sum_{m=1}^{\infty}\frac{(-1)^m F_1(m:\theta_1,\theta_2,\theta_3,\theta_4)}{m^2 B\sinh\pi B}\right.$$

$$\left. + \frac{2d^2}{\pi^3}\sum_{m=1}^{\infty}\frac{(\sin m\theta_1 - \sin m\theta_2)\left[\sinh B(\pi-\theta_3)-\sinh B(\pi-\theta_4)\right]}{mB^2\sinh B\pi}\right] \qquad (9.3.16)$$

where, $A = kd/\pi$, $B^2 = m^2 - A^2$, $\theta_1 = \dfrac{\pi}{d}\left(y_{q_1i}+\dfrac{W_p}{2}\right)$; $\theta_2 = \dfrac{\pi}{d}\left(y_{q_1i}-\dfrac{W_p}{2}\right)$;

$\theta_3 = \dfrac{\pi}{d}\left(x_{q_2j}+\dfrac{W_q}{2}\right)$; $\theta_3 = \dfrac{\pi}{d}\left(x_{q_2j}-\dfrac{W_q}{2}\right)$, for $i = 1, N$ and $j = N+1, 2N$.

The Mathcad program listing for the impedance evaluation is given in Appendix 9A.

9.4 Computational and Experiment Results of Input impedance

The procedure in section 9.2 has been used to obtain the computational results for a single feed two corner-deleted square patch antenna with, $a = 40mm$, $d = 4.402mm$ $W = 0.0067mm$, $\varepsilon r = 2.33$ (Duroid 5870), and, the resonant frequency $f_0 = 2.45GHz$. For this particular structure, it was found that 15 of the q-ports, and, using an upper summation limit $m = 10$, in the infinite series expressions, gives good results. The layout of the antenna for the practical experiment to determine the Zin at resonant frequency is is illustrated in figure 9.4.1.
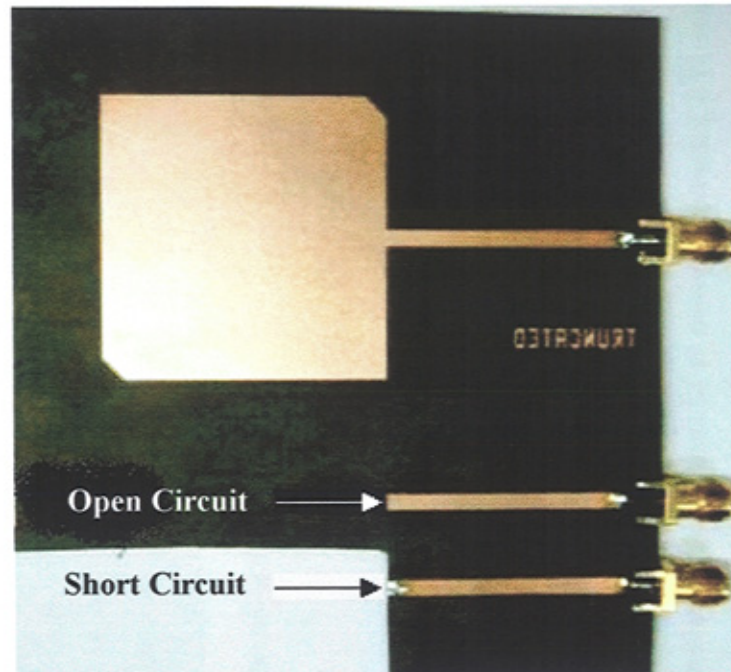
Figure 9.4.1: Experimental two corner-deleted circular polarised patch antenna

Figures 9.4.2 and 9.4.3 show the results obtained from the above calculation, from practical measurement, and, from Ensemble™. The circular polarisation condition in this designed antenna has been verified by practical measurements (figure 9.4.4 and 9.4.5), and, axial ratio is measured as a function of frequency and the angle (Theta). Taking into account the approximations in the theory and fabrication errors the above results are in good agreement.
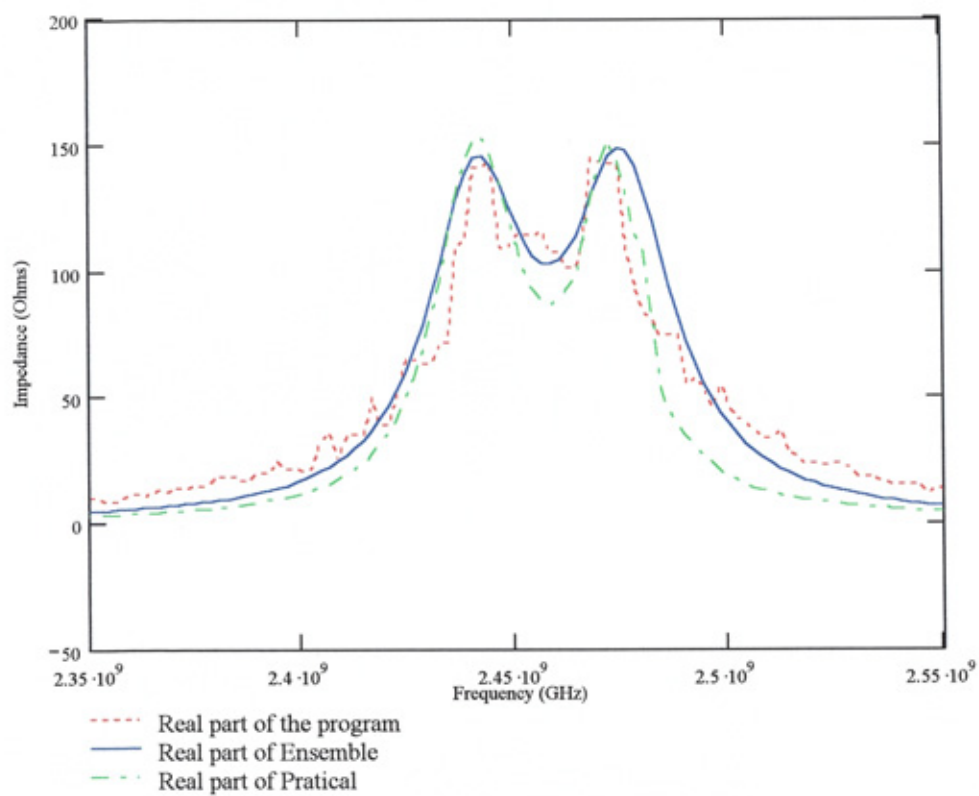
Figure 9.4.2: Real part of the input impedance
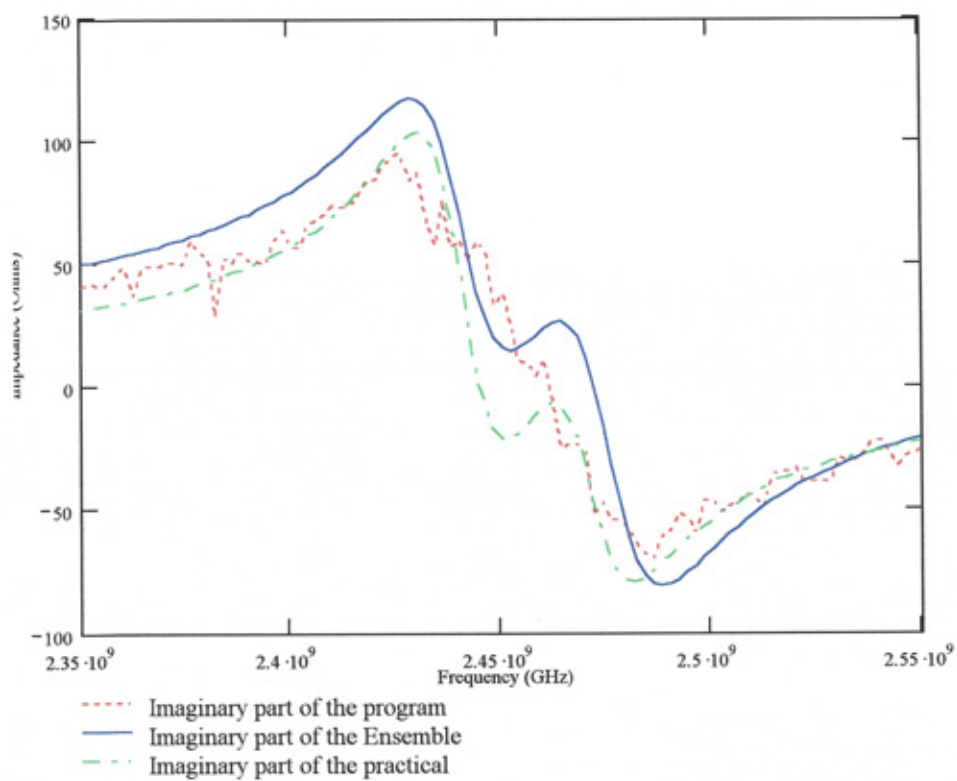
Figure 9.4.3: Imaginary part of the input

149
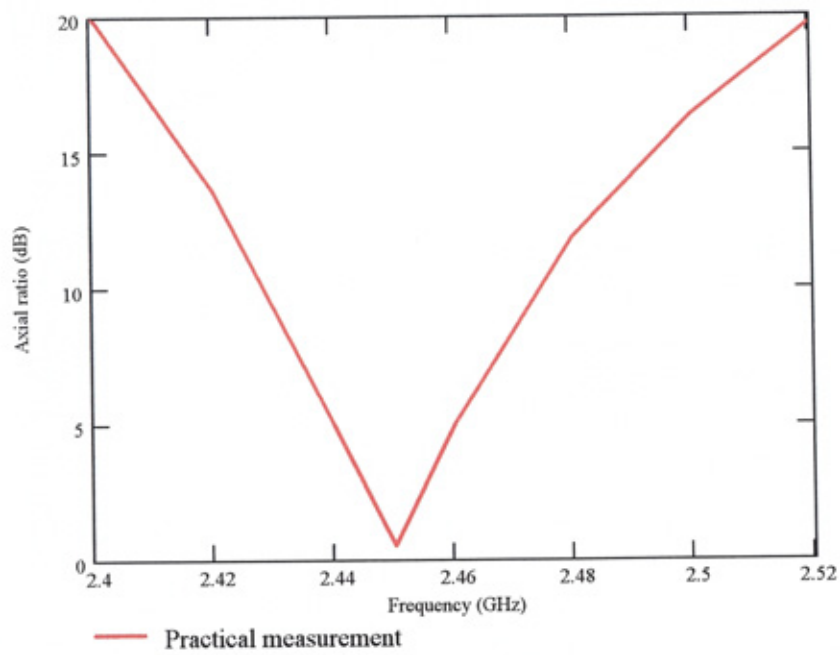
Figure 9.4.4: Axial ratio in dB versus frequency
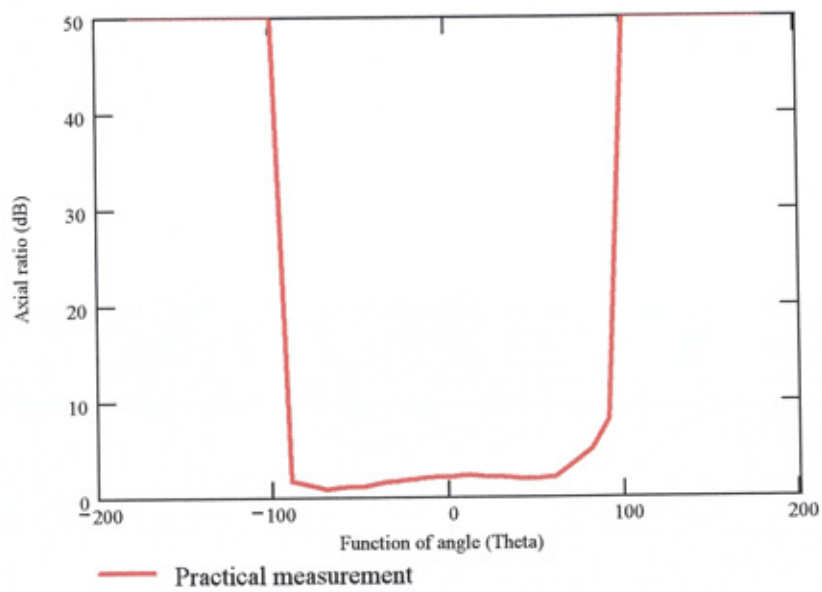
Figure 9.4.4: Axial ratio in dB as a function of angle (Theta)

9.5 Matching Network for a Single Feed Two Corner-deleted Circular Polarised Patch Antenna

The fabricated antenna with its matching network is shown in Figure 9.5.1. The figure shows the antenna with the external matching network consisting of the 50Ω standard input port and the quarter-wavelength matching impedance transformer, (90^0). The input impedance of the two corner-deleted patch was designed and discussed in section 9.4, $Z_{incp} = 103\ \Omega$.
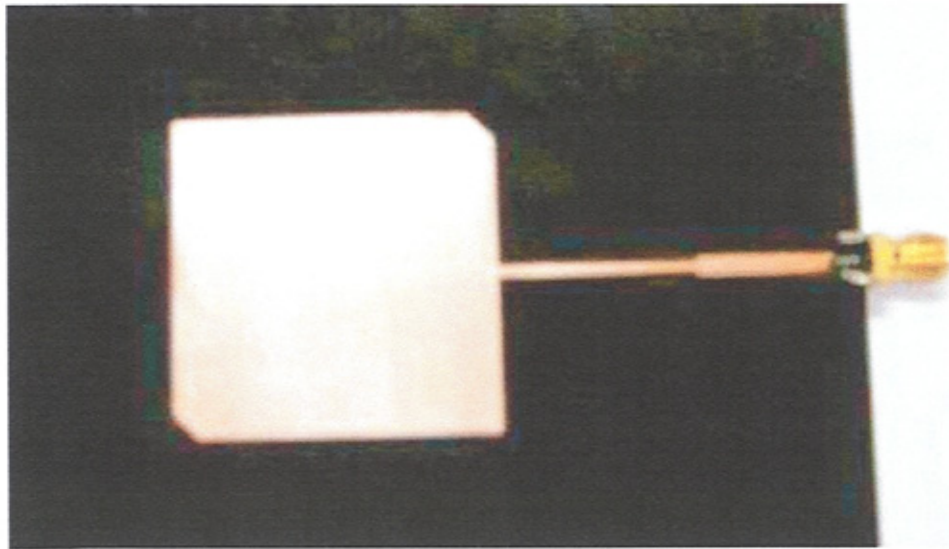
Figure 9.5.1: Matched two corner-deleted circular polarised patch antenna

This unit has been used to obtain measurements of the return loss and gain. Figure 9.5.2 and figure 9.5.3 show the return loss and gain as a function of frequency and angle. The results clearly show that the operation of the antenna is highly satisfactory.
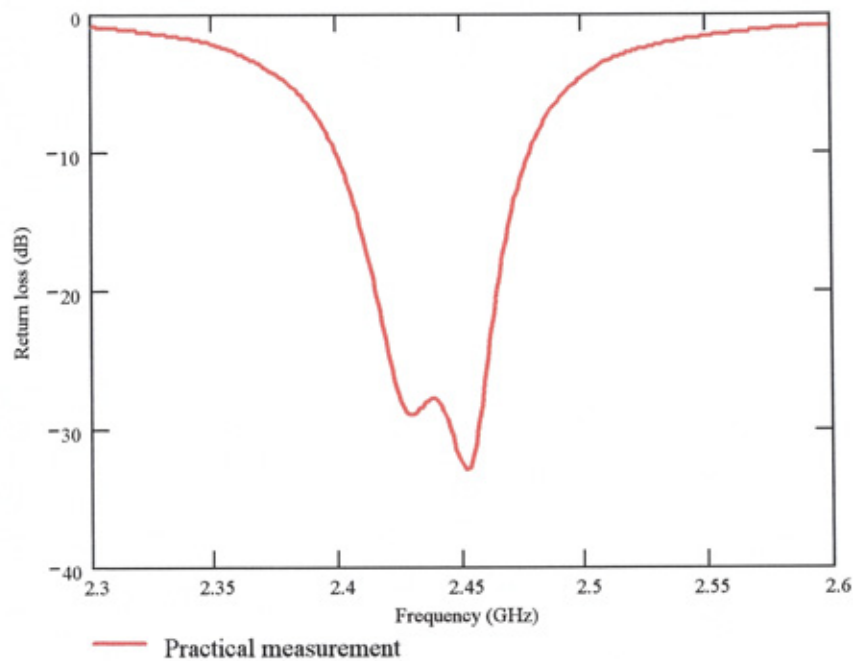
Figure 9.5.2: Return loss (dB)
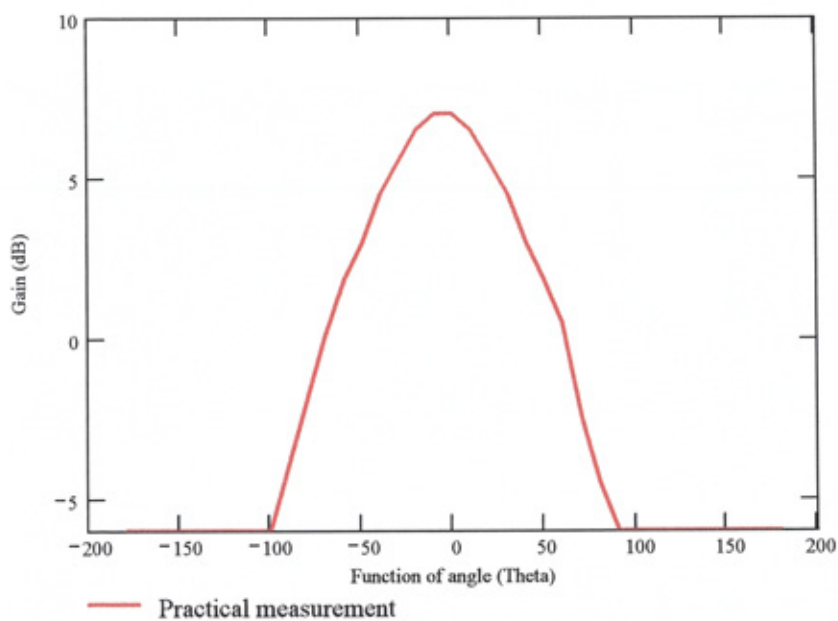
Figure 9.5.3: Gain (dB) as a function of angle (Theta)

Summary

A design procedure for the corner-deleted microstrip antenna together with a complete description of its computer implementation has been presented. Numerical tests show that, the run time using the initially derived formulas would be of the order of several hours but with the new efficient expressions (Chapter 7 and 8) only half an hour is needed. Taking into account the approximations in the theory and fabrication errors all the results obtained are in good agreement. Practical results for the axial ratio, return loss and gain indicate a good operational performance for the antenna.

153

CHAPTER 10

SUMMARY OF THE RESEARCH CARRIED OUT AND FUTHER WORK

10.1 Summary and Conclusions

In this thesis the results have been presented of the research that has been carried out in an investigation of the segmentation and desegmentation approaches to evaluate the input impedance of a composite geometry microstrip antenna. Results from this investigation have been applied in the design of a circular polarised microstrip antenna. The research implements a design procedure for a single feed two corner-deleted circularly polarised microstrip antenna.

Chapter 2

The basis of the short-range prototype microwave system developed for automatic debiting application in the vehicle tolling and car park access have been discussed. The operation of a microwave system to be used in traffic applications is described. Block diagrams showing the communications operation between the RSU and OBU have been presented. The circuits diagram of the wake-up tag has been described. A table which illustrates the possibilities with different remote identification technologies has been tabulated.

Chapter 3

The various modelling approaches and methods of analysis for the microstrip antenna were discussed. The coplanar coupling port impedance properties of the rectangular and triangular microstrip patch antenna have been presented. A new computationally

efficient expressions for the input impedance, with the offset feed, of a rectangular and a triangular patch antenna were derived and applied to obtain impedance-frequency graphs with respect to the feed position. Good agreement between the new formulas, practical measurement and Ensemble™ results are obtained. The electric field condition for circular polarisation was described together with possible feed arrangements required to generate circular polarised radiation.

Chapter 4

The eigenvalues and eigenfunctions of the dominant field modes for a square patch antenna have been derived. They have been used in a perturbation analysis to obtain the corresponding eigenvalues, eigenfunctions and resonant modal frequencies of a perturbed square patch with two truncated corners. Using an equivalent circuit model, and, the conditions on the dominant modal voltages for circular polarisation, a formula for the fractional perturbation area in terms of the unloaded Q-factor, has been obtained.

Chapter 5

Using coplanar multiport circuit analysis a general formula for the interport coupling impedance between two perimeter ports has been derived in terms of the Green's function of the patch geometry. Coalescence of the two ports then gives an input impedance formula.

Chapter 6

The basis of multiport modelling in a segmental approach has been described in terms of the conservation of current sheet distributions across the interfaces between

segments. Input impedance matrix formulas for two and three cascade-segments in the segmentation method have obtained. For the shunt-segment structure a new generalised input impedance matrix formula has been obtained for a number of deleted shunt-segment elements. In the desegmentation method a new generalised impedance matrix formula has been obtained for any number of deleted segments. Comparison between the segmentation method and the desegmentation shows that the latter is computationally more efficient when applied to the two corner-deleted square patch antenna.

Chapter 7

Efficient computational expressions for the elements of the interport coupling impedance matrices in respect of the three possible rectangular patch coupling impedances configurations, has been obtained. The number of terms in the series expressions for a required accuracy is given. A test application using Ensemble™ showed good agreement.

Chapter 8

Efficient computational expressions for the elements of the interport coupling impedance matrices in respect of the four possible right-angled isosceles triangular patch coupling impedance configurations, has been obtained. The number of terms in the series expressions for a required accuracy is given. Good agreement between results using the new expressions and Ensemble™ is obtained in each of the test applications.

A design procedure for the corner-deleted microstrip antenna together with a complete description of its computer implementation has been presented. The program run time to produce the frequency-impedance graphs is of the order half an hour. It may then be inferred from our computational analysis (Chapter 7,8) that the run time using the initial derived formulas would be of the order of several hours. Taking into account the approximations in the theory and fabrication errors all the results obtained are in god agreement. Practical results for the axial ratio, return loss and gain indicate a good operational performance for the antenna.

10.2 Suggestions and further work

The new generalisation of the desegmentation matrix impedance expression to any number of deleted segments, together with the collection of all possible coupling impedance economised expressions, opens the way to calculate the input impedances for the following complex practical antenna structures.

1. Using the program in section 9.2, a two-corner-deleted patch antenna with the offset feed can be investigated. To retain the circular polarisation condition, the small adjustment might be needed to enlarge the amount of the perturbation (chapter 2). This would be very useful since then the manufacturing tolerances could be relaxed.

2. A novel circular polarisation (CP) design of a single-feed microstrip antenna with truncated corners and central slot (figure 10.2.1) has been described by [1]. Experimental results show that this proposed design has a reduced antenna size as

compared to the patch antenna without the central slot. Also the required size of the truncated corners for CP operation is larger for the slot design than for the design without a slot, so that the fabrication tolerance is relaxed for the slot design.

The input impedance of the new proposed design can be found using the desegmentation method. The two deleted triangles and the slot of proposed design will be treated as three deleted segments.
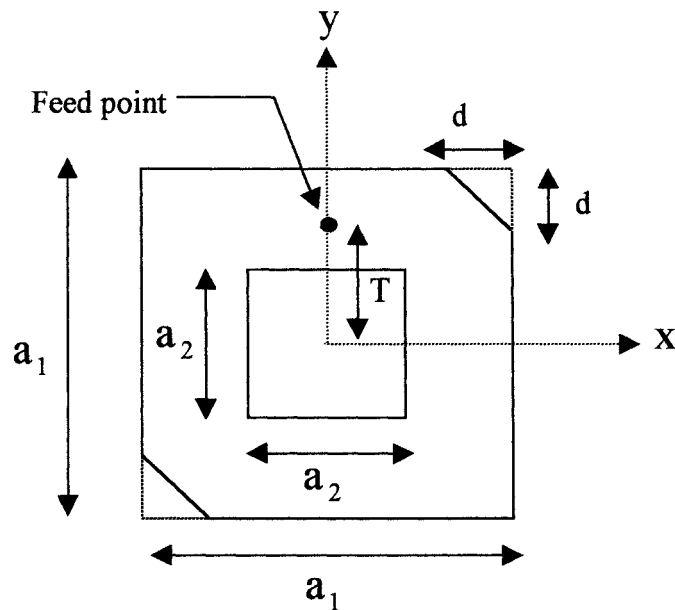

Figure 10.2.1: Square ring microstrip antenna with truncated corners

3. The Green's function has been obtained for another two triangular [2], namely a) a $30^0 - 60^0$ right angled triangle and b) an equilateral triangle. The same technique can be applied as in chapter 8 in order to obtain efficient computational expressions for each of the possible triangular patch coupling impedances configurations.
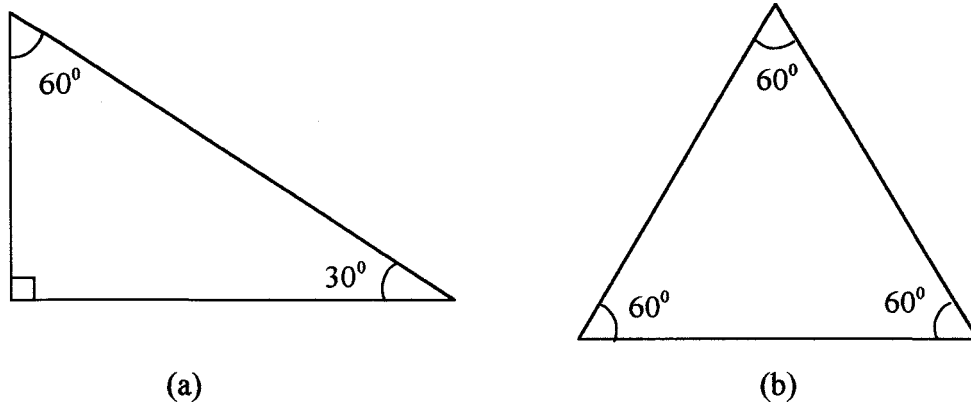
Figure 10.2.2: A right angled triangle and an equilateral triangle

4. In respect of a rectangular microstrip antenna it has been reported [3] that the feed location for circular polarisation is not restricted to central locations and a formula for the locus of possible feed locations has been derived. It is thought that the methodology used in this paper may be transported to a corresponding study in respect of the corner deleted square patch antenna.

5. The computer run time for more than three deleted segments would be considerable. A significant reduction could be achieved by cable coupling of several PC units to evaluate separately the individual impedance coupling matrices (i.e. multi-parallel processing).

6. The triangle in figure 10.2.3 with an offset location may be found to give circular polarisation.
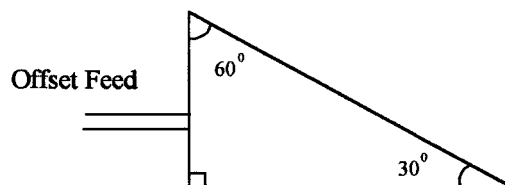
Figure 10.2.3: Triangle patch with offset position

7. In the present study the segmentation method addresses those segment partitions which have a cascade type of interconnecting port structure as illustrated in an antenna, of current practical interest [4], shown below.
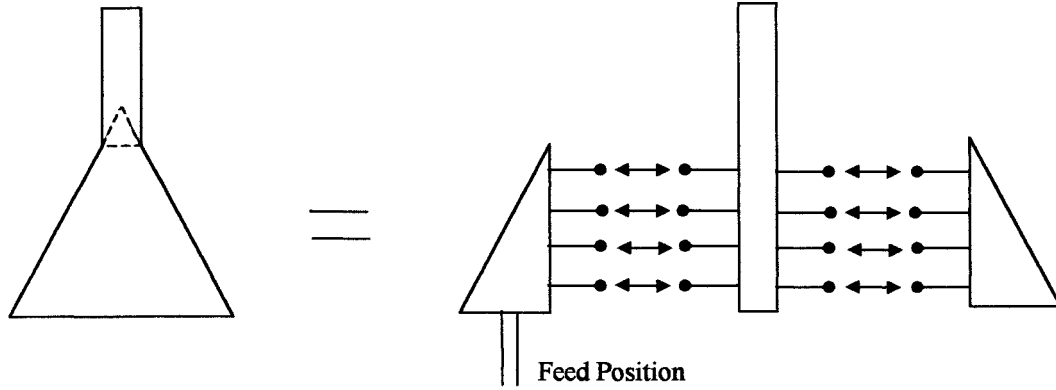
Figure 10.2.4: Cascade type of interconnecting port structure

The input impedance of the above configuration can be calculated using the result in equation 6.3.8 (Chapter 6).

On the other hand, when, in the above illustration (figure 10.2.4), the feed position is located on the rectangular segment the interconnecting port structure is of a shunt type, as shown below.
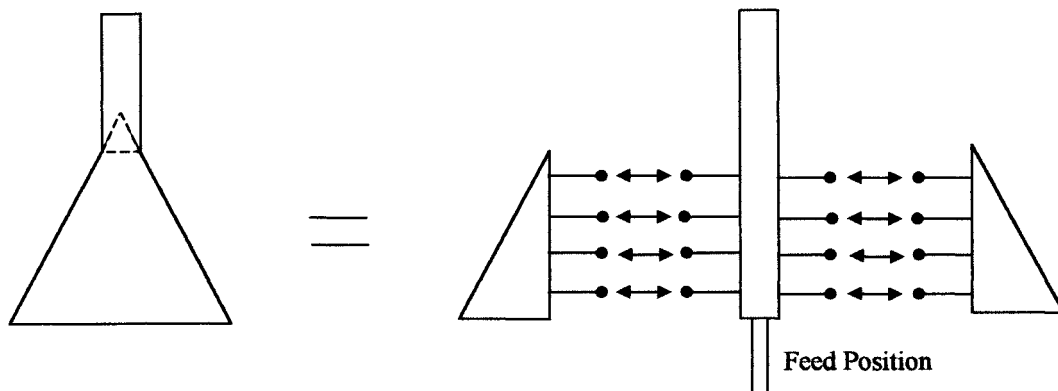
Figure 10.2.5: Shunt type of interconnecting port structure

The matrix impedance formula 6.3.9 (chapter 6) is then required for this case.

In respect of the desegmentation method the present study addresses a partitioning scheme in which each deleted segment is not itself of composite form. This would however arise in the present case.

8. The desegmentation method would be applied to the deleted circular patch as in figure 10.2.6.
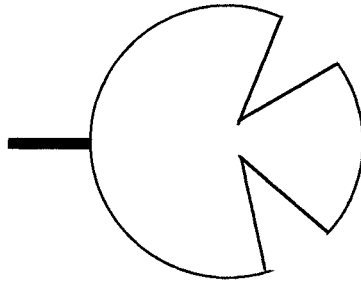
Figure 10.2.6: The deleted circular patch

REFERENCES

Chapter 1

[1] "The transport bill: Part III road charging and workplace parking",
http://www.parliament.uk/commons/lib/research/rp99/rp99-104.pdf, 2000.

[2] P. Harrop,: "Smart labels analyst", http://www.idtechex.com/Journal1/issue1.doc,
2001.

[3] T.K.Chan, "Development of a Two-Way Microwave Communications Systems
for Traffic Applications," PhD Thesis, University of Northumbria, 1994.

[4] P.Lowes, "Radio antennas on glass," PhD Thesis, University of Northumbria, 1995.

[5] B.W.Lim, "Design and modelling of a corner fed circularly polarised patch antenna,"
PhD Thesis, University of Northumbria, Sept. 1996.

[6] T.Vlasits, "Modelling and application of a cross-aperture coupled single feed
circularly polarised patch antenna," PhD Thesis, University of Northumbria, 1997.

[7] M. Haneishi, and S. Yoshida, :"A design Method of Circularly Polarised Rectangular
Microstrip Antenna By One-Point Feed", Electronics and Communications Japan. Vol.
64-B. No. 4. 1981.

Chapter 3

[1] R. Garg, P. Bhartia, I. Bahl, and A. Ittipiboon,:"Microstrip antenna design handbook",
MA: Artech House, 2000.

[2] R.E.Munson, "Conformal microstrip antennas and microstrip phased arrays.", IEEE Transactions on antennas and propagation, Jan 1974, 22, p.74-78.

[3] A.Van de Capelle, "Transmission line model for rectangular microstrip antennas", Handbook of microstrip antenna, chapter 10, Peter peregrinus Ltd, ISBN 0 86341 150 9, 1989.

[4] H.Pues, and V.D.Capelle, "A simple accurate formula for the radiation conductance of a rectangular microstrip antenna", Proceedings of IEEE conference on antennas and propagation, Los Angeles, USA, pp.23-26, June 1981.

[5] E.Lier, "Improved formulas for input impedance of coax-fed microstrip patch antennas", IEE Proc. Microwave, Antennas and Propagation, Vol.129, No.4, pp.161-164, 1982.

[6] C. A. Balanis, :"Antenna theory analysis and design", John Wiley & Sons, Inc., 1996.

[7]A.G.Derneryd, and A.G.Lind, "Cavity model of the rectangular microstrip antenna" Proceeding of workshop on printed circuit antenna technology, New Maxico State, 17-19 Oct 1979.

[8] K. F. Lee, and, W. Chen, :"Advances in microstrip and printed antennas", John Wiley & Sons, Inc., 1997.

[9] J.R.James, and P.S.Hall, "Handbook of mircostrip antennas", Vols. 1 and 2, peter peregrinus, London, UK, 1989.

[10] T.Okoshi, "Planar circuits for microwave and lightwaves", Springer-Verlag, 1985.

[11] I.S.Gradshteyn, and, I.M.Ryzhik, "Table of Integrals, series, and Product", New York: Academic Press, 1994.

[12] Chada, R., and Gupta, K.C.:"Green's function for triangular segments in planar microwave circuits", IEEE Trans. Microwave Theory and techniques, 1980, Vol. MTT-28, No.10, pp1139-1143.

[13] S.A.Schelkunoff, "Electromagnetic Waves", Van Nostrand, New York 1943.

[14] Keuster, E.F., and Chang, D.C.:"A geometrical theory for the resonant frequencies and Q factors of some triangular microstrip patch antennas", IEEE Trans. Antennas Propagation, 1983, Vol.AP-31, No.1, pp.27-34.

[15] Dahele J.S., and Lee, K.F.:"Experimental study of the triangular microstrip antenna", IEEE Ap/S Int. Symp. Dig., 1984, pp.283-286.

[16] A.K. Sharma,: "Spectral domian analysis of microstrip resonant structures", PhD thesis, Indian institute of technology, 1979.

[17] Kraus and Carver,: "Electromagnetics", 3rd edition, Mc Graw-Hill int. BK.Co. 1984.

[18] T.K.Chan, "Development of a Two-Way Microwave Communications Systems for Traffic Applications," PhD Thesis, University of Northumbria, 1994.

[19] B.Aljibouri, E.G.Lim, H.Evans and A.Sambell, "Multiobjective genetic algorithm approach for a dual-feed circular polarised patch antenna design", Electronics Letters, 8th Jun 2000, Vol.36, No.12, pp.1005-1006.

[20] B.W.Lim, "Design and modelling of a corner fed circularly polarised patch antenna," PhD Thesis, University of Northumbria, Sept. 1996.

Chapter 4

[1] M. Haneishi, and S. Yoshida, :"A design Method of Circularly Polarised Rectangular Microstrip Antenna By One-Point Feed", Electronics and Communications Japan. Vol. 64-B. No. 4. 1981.

[2] J. P. Shu,: "Application of degenerate mode of microwave planar circuits to band-pass filter and discriminator", Rept. Microwave group. I.E.C.E. MW71-53. Sept 1971.

[3] J. R. James, and P.S. Hall,: "Handbook of Microstrip antennas", Peter Peregrinus Ltd. 1989.

Chapter 5

[1] R. Garg, P. Bhartia, I. Bahl, and A. Ittipiboon,:"Microstrip antenna design handbook", MA: Artech House, 2000.

[2] S.A.Schelkunoff, "Electromagnetic Waves", Van Nostrand, New York 1943.

[3] Chada, R., and Gupta, K.C.:"Green's function for triangular segments in planar microwave circuits", IEEE Trans. Microwave Theory and techniques, 1980, Vol. MTT-28, No.10, pp1139-1143.

[4]P.M.Morse, H.Feshbach, "Method of theoretical physics, part 1, McGraw-hill, New york, 1953.

[5] V. Palanisamy, and R. Garg,: "Anajysis of circularly polarised square ring and crossed-strip microstrip antennas", IEEE Trans. on antennas and prop. Vol.AP-34. No.11. Nov 1986.

Chapter 6

[1] T. Okoshi, and T. Takeuchi,: "Analysis of planar circuits by segmentation method", Electronic and comms. In Japan. Vol. 58-B. No. 8. 1975

[2] T. Okoshi, Y. Uehara, and T. Takeuchi,: "The segmentation method-an approach to the analysis of microwave planar circuits", IEEE Trans. on microwave theory and tech. Oct 1976.

[3] K. C. Gupta, R. Garg, and R. Chadha,: "Computer-aided design of microwave circuits", Artech House USA. 1981.

[4] K. C. Gupta, and P. C. Sharma,: "Segmentation and Desegmentation techniques for the analysis of planar microstrip antennas", Antennas Prop. Soc. Int. Symp. Digest. 1981.

[5] R. Chadha, and K. C. Gupta,: "Segmentation method using impedance matrices for analysis of planar microwave circuits", IEEE Trans. on microwave theory and tech. Vol. MTT-29. No.1. Jan 1981.

[6] T.Okoshi,: "Planar circuits for microwave and lightwaves", Springer-Verlag, 1985.

[7] V. Palanisamy, and R. Garg,: "Analysis of arbitrarily shaped microstrip patch antennas using segmentation technique and cavity model", IEEE Trans. on antennas and prop. Vol. AP-34, No. 10, Oct 1986.

[8] V. Palanisamy, and R. Garg,: "Analysis of circularly polarised square ring and crossed-strip microstrip antennas", IEEE Trans. on antennas and prop. Vol. AP-34, No. 11, Nov 1986.

[9] James, J.R., and Hall, P.S.:"Handbook of microstrip antennas", Peter Pergrinus Ltd. London, 1989.

[10] K. C. Gupta, and A. Benalla,: "Multiport network modeling approach for CAD of microstrip patches", Electromagnetic. Vol. 9, Pt. 4, 1989.

[11] P. C. Sharma, and K. C. Gupta,: "Desegmentation method for analysis of two-dimensional microwave circuits", IEEE Trans. on Microwave theory and tech. Vol. MTT-29, No. 10, Oct 1981.

[12] P. C. Sharma, and K. C. Gupta,: "Analysis and optimised design of single feed circularly polarised microstrip antennas", IEEE Trans. on antenna and prop. Vol.AP-31, No. 6, Nov 1983.

[13] W.S. Chen, C.H. Wu, and K.L. Wong,: "Square ring microstrip antenna with a cross strip for compact circular polarisation operation", IEEE Antennas and Propagation, Vol.47, pp. 1566 –1567. 1999.

Chapter 7

[1] I.S.Gradshteyn, and, I.M.Ryzhik, "Table of Integrals, series, and Product", New York: Academic Press, 1994.

[2] T.Okoshi, "Planar circuits for microwave and lightwaves", Springer-Verlag, 1985.

[3] J.R.James, and P.S.Hall, "Handbook of mircostrip antennas", Vols. 1 and 2, peter peregrinus, London, UK, 1989.

Chapter 8

[1] Gradshteyn, I.S., and, Ryzhik, I.M.:"Table of Integrals, series, and Product", New York: Academic Press, 1994.

[2] Chada, R., and Gupta, K.C.:"Green's function for triangular segments in planar microwave circuits", IEEE Trans. Microwave Theory and techniques, Oct 1980, Vol. MTT-28, No.10, Pp1139-1143.

[3] Bahl, I.J. and Bhartis, P.:"Microstrip antennas", MA: Artech House, 1980.

[4] Okoshi, T.:"Planar circuits for microwave and lightwaves", Springer-Verlag, 1985.

Chapter 9

[1] James, J.R., and Hall, P.S.:"Handbook of mircostrip antennas", Vols. 1 and 2, Peter Peregrinus, London, UK, 1989.

[2] K. R. Carver, and J. W. Mink,: "Microstrip antenna technology", IEEE Trans. On Antenna and prop. Vol. AP-29. No. 1. Jan 1981.

Chapter 10

[1] W.S, Chen, C.K, Wu, and K.L, Wong, : "Single feed square-ring microstrip antenna with truncated corners for compact circular polarisation operation", IEE Electronics Letters, 1998, Vol:34(11), pp. 1045-1047.

[2] R. Chada, and K.C, Gupta, :"Green's function for triangular segments in planar microwave circuits", IEEE Trans. Microwave Theory and techniques, Vol. MTT-28, No.10, Pp1139-1143, Oct 1980.

[3] M.I. Aksun, S.U. Chuang, and, Y.L. Lo, :"On Slot-coupled microstrip antennas and their applications to CP operation – theory and experiment", IEEE Trans. On Antennas and Propagation, Vol. 38, No.8, Pp1224-1230, 1990.

[4] J.L. Lu, and K.L. wong,: "Single-feed circularly polarised equilateral-triangular microstrip antenna with a tuning stub", IEEE Trans. On Antennas and Propagation, Vol. 48, No.12, Pp.1869-1872, 2000.

APPENDIX 3A

Input impedance formulas for a right-angled isosceles triangle

3A.1 Closed Form Summation Formulas

The following summation formulas, which are used in obtaining the input impedance expressions, are based on the series tables in Gradshtyn [11].

1. $\displaystyle\sum_{m=1}^{\infty} \frac{1}{m^2 - A^2} = \frac{\pi}{2A}\left[\frac{1}{\pi A} - \cot A\pi\right]$

2. $\displaystyle\sum_{m=1}^{\infty} \frac{1}{m^2 + A^2} = \frac{\pi}{2A}\coth A\pi - \frac{1}{2A^2}$

3. $\displaystyle\sum_{m=1}^{\infty} \frac{(-1)^m}{m^2 - A^2} = \frac{1}{2A^2} - \frac{\pi}{2A\sin A\pi}$

4. $\displaystyle\sum_{m=1}^{\infty} \frac{\cos m\theta}{m^2 - A^2} = \frac{1}{2A^2} - \frac{\pi\cos A(\pi - \theta)}{2A\sin A\pi}$; $0 \le \theta \le 2\pi$

5. $\displaystyle\sum_{m=1}^{\infty} \frac{\sin m\theta}{m(m^2 - A^2)} = \frac{\theta - \pi}{2A^2} + \frac{\pi\sin A(\pi - \theta)}{2A^2\sin A\pi}$; $0 \le \theta \le 2\pi$

6. $\displaystyle\sum_{m=1}^{\infty} \frac{(-1)^m\cos m\theta}{m^2 + A^2} = \frac{\pi\cosh A\theta}{2A\sinh A\pi} - \frac{1}{2A^2}$; $-\pi \le \theta \le \pi$

7. $\displaystyle\sum_{m=1}^{\infty} \frac{(-1)^m\sin m\theta}{m(m^2 + A^2)} = \frac{\pi\sinh A\theta}{2A^2\sinh A\pi} - \frac{\theta}{2A^2}$; $-\pi \le \theta \le \pi$

Formulas 1, 2, 3, 4, and, 6 are given directly in the Gradshtyn tables.

Formulas 5, 7 are obtained, respectively, from formulas 4, 6 by integration.

The new formula (5) and (7) above are derived in Appendix 7A and 8A.

3A.2 Patch with Feed on Vertical Side

A: Integrations

$$Z_{in} = 2\frac{j\omega\mu h}{W^2}\left\{-\frac{1}{a^2k^2}\left[\int_l^u 1 dy\right]^2 + \frac{1}{\pi^2}\sum_{m=1}^{\infty}\frac{1}{m^2 - A^2}\left[\int_l^u\left(1 + (-1)^m\cos m\frac{\pi}{a}y\right)dy\right]^2\right.$$

$$\left. + \frac{1}{\pi^2}\sum_{m=1}^{\infty}\sum_{n=1}^{\infty}\frac{1}{m^2 + n^2 - A^2}\left[\int_l^u\left(\cos n\frac{\pi}{a}y + (-1)^{m+n}\cos m\frac{\pi}{a}y\right)dy\right]^2\right\} \quad (3A.2.1)$$

where, $\quad u = T + \dfrac{W}{2}, \quad l = T - \dfrac{W}{2}$

Integration for FIRST TERM

$$I_1 = \left[\int_l^u 1 dy\right]^2 = W^2 \quad\quad (3A.2.2)$$

Integration for SECOND TERM

$$I_2 = \left[\int_l^u\left(1 + (-1)^m\cos m\frac{\pi}{a}y\right)dy\right]^2$$

$$= \left[W + \frac{(-1)^m a}{m\pi}(\sin m\theta_1 - \sin m\theta_2)\right]^2$$

$$= W^2 + \frac{2(-1)^m Wa}{m\pi}fm_1 + \frac{a^2}{m^2\pi^2}(fm_2)^2 \quad\quad (3A.2.3)$$

where, $\theta_1 = \dfrac{\pi u}{a}, \quad \theta_2 = \dfrac{\pi l}{a}, \quad fm_1 = \sin m\theta_1 - \sin m\theta_2$.

Integration for THIRD TERM

$$I_3 = \left[\int_l^u\left(\cos n\frac{\pi}{a}y + (-1)^{m+n}\cos m\frac{\pi}{a}y\right)dy\right]^2$$

$$= \left[\frac{a}{n\pi}f_1(n) + \frac{(-1)^{m+n}a}{m\pi}f_1(m)\right]^2$$

$$= \frac{2a^2}{m^2\pi^2}(fm_1)^2 + \frac{2(-1)^{m+n}a^2}{mn\pi^2}fm_1\,fn_1 \quad\quad (3A.2.4)$$

B: Summation

$$Z_{in} = \frac{j2\omega h\mu}{W^2}\left[-\frac{W^2}{k^2a^2} + \frac{W^2}{\pi^2}Sm_1 + \frac{2aW}{\pi^3}Sm_2 + \frac{a^2}{\pi^4}Sm_3 + \frac{2a^2}{\pi^4}Sm_4 + \frac{2a^2}{\pi^4}Smn_5\right] \quad (3A.2.5)$$

where,

$$Sm_1 = \sum_{m=1}^{\infty}\frac{1}{m^2 - A^2}$$

$$= \frac{\pi^2}{2k^2a^2} - \frac{\pi^2}{2ka}\cot ka \quad (3A.2.6)$$

$$Sm_2 = \sum_{m=1}^{\infty}\frac{(-1)^m(\sin m\theta_1 - \sin m\theta_2)}{m(m^2 - A^2)}$$

$$= \frac{\pi^3 W}{2k^2a^3} - \frac{\pi^3}{2k^2a^2}\frac{(\sin A\theta_1 - \sin A\theta_2)}{\sin ka} \quad (3A.2.7)$$

$$Sm_3 = \sum_{m=1}^{\infty}\frac{(\sin m\theta_1 - \sin m\theta_2)^2}{m^2(m^2 - A^2)} \quad (3A.2.8)$$

$$Sm_4 = \sum_{m=1}^{\infty}\sum_{n=1}^{\infty}\frac{(\sin m\theta_1 - \sin m\theta_2)^2}{m^2(m^2 + n - A^2)}$$

$$= \frac{\pi}{2}\sum_{m=1}^{\infty}\frac{(\sin m\theta_1 - \sin m\theta_2)^2}{m^2 B}\coth B\pi - \frac{1}{2}S_3(m) \quad (3A.2.9)$$

$$Smn_5 = \sum_{m=1}^{\infty}\sum_{n=1}^{\infty}\frac{(-1)^{m+n}(\sin m\theta_1 - \sin m\theta_2)(\sin n\theta_1 - \sin n\theta_2)}{mn(m^2 + n^2 - A^2)}$$

$$= \frac{\pi}{2}\sum_{m=1}^{\infty}\frac{(-1)^m(\sin m\theta_1 - \sin m\theta_2)(\sinh B\theta_1 - \sinh B\theta_2)}{m(m^2 - A^2)\sinh B\pi} - \frac{W\pi}{2a}S_2(m) \quad (3A.2.10)$$

where, $B = \sqrt{m^2 - A^2}$.

Using equations (3A.2.6), (3A.2.7), (3A.2.9) and (3A.2.10) in equation (3A.2.5), eliminates the Sm_3 term, to give

$$Z = \frac{j2\omega\ h\ \mu}{W^2}\left[-\frac{W^2}{2k^2a^2} - \frac{W^2}{2ka}\cot ka + \frac{Wa}{\pi^3}Sm_2 + \frac{a^2}{\pi^3}\sum_{m=1}^{\infty}\frac{(\sin m\theta_1 - \sin m\theta_2)}{m^2 B}\coth B\pi\right.$$

$$\left. + \frac{a^2}{\pi^3}\sum_{m=1}^{\infty}\frac{(-1)^m(\sin m\theta_1 - \sin m\theta_2)(\sinh B\theta_1 - \sinh B\theta_2)}{m(m^2 - A^2)\sinh B\pi}\right] \quad (3A.2.11)$$

171

Substituting for Sm_2, from equation (3A.2.7) into equation (3A.2.11) , eliminate the $W^2/2a^2k^2$ term, to give

$$Z = \frac{j\omega h \mu}{W^2}\left[-\frac{W^2}{ka}\cot ka - \frac{W(\sin A\theta_1 - \sin A\theta_2)}{k^2 a \sin A\pi} + \frac{2a^2}{\pi^3}\sum_{m=1}^{\infty}\frac{(\sin m\theta_1 - \sin m\theta_2)^2}{m^2 B}\coth B\pi\right.$$

$$\left.+ \frac{2a^2}{\pi^3}\sum_{m=1}^{\infty}\frac{(-1)^m(\sin m\theta_1 - \sin m\theta_2)(\sinh B\theta_1 - \sinh B\theta_2)}{m\,(m^2 - A^2)\sinh B\pi}\right] \qquad (3A.2.12)$$

3A.3 Patch with Feed on Hypotenuse

A: Integrations

$$Z_{in} = \frac{2j\omega\mu h}{W^2\pi^2}\left\{\frac{\pi^2}{a^2k^2}\left[\int_l^u 1\sqrt{2}\,dx\right]^2 + \sum_{m=1}^{\infty}\frac{1}{m^2 - A^2}\left[\int_l^u \cos m\frac{\pi}{a}x + (-1)^m\cos m\frac{\pi}{a}(a-x)\sqrt{2}\,dx\right]^2\right.$$

$$\left.+\sum_{m=1}^{\infty}\sum_{n=1}^{\infty}\frac{1}{m^2+n^2-A^2}\left[\int_l^u\left(\cos m\frac{\pi}{a}x\cos n\frac{\pi}{a}(a-x)+(-1)^{m+n}\cos n\frac{\pi}{a}x\cos m\frac{\pi}{a}(a-x)\right)\sqrt{2}dx\right]^2\right\}(3A.3.1)$$

where, $u = T + \dfrac{W}{2\sqrt{2}}$, $l = T - \dfrac{W}{2\sqrt{2}}$

Integration for FIRST TERM

$$I_1 = \left[\int_l^u 1\sqrt{2}\,dx\right]^2 = W^2 \qquad (3A.3.2)$$

Integration for SECOND TERM

$$I_2 = \left[\int_l^u \cos m\frac{\pi}{a}x + (-1)^m\cos m\frac{\pi}{a}(a-x)\sqrt{2}\,dx\right]^2$$

$$= \frac{8a^2}{m^2\pi^2}(\sin m\theta_1 - \sin m\theta_2)^2 = \frac{8a^2}{m^2\pi^2}(fm_1)^2 \qquad (3A.3.3)$$

Where, $\theta_1 = \dfrac{\pi u}{a}$, $\theta_2 = \dfrac{\pi l}{a}$, $fm_1 = \sin m\theta_1 - \sin m\theta_2$,

Integration for THIRD TERM

$$\left[\int_l^u \left(\cos m\frac{\pi}{a}x\cos n\frac{\pi}{a}(a-x)+(-1)^{m+n}\cos n\frac{\pi}{a}x\cos m\frac{\pi}{a}(a-x)\right)\sqrt{2}dx\right]^2$$

$$=\left[(-1)^n 2\int_l^u \left(\cos\frac{m\pi}{a}x\cos\frac{n\pi}{a}x\right)\sqrt{2}dx\right]^2$$

$$=\frac{2a^2}{\pi^2}\left[\frac{\sin(m+n)\theta_1-\sin(m+n)\theta_2}{m+n}+\frac{\sin(m-n)\theta_1-\sin(m-n)\theta_2}{m-n}\right]^2 \qquad (3A.3.4)$$

B: Summations

From the integrations, therefore,

$$Z_{in}=\frac{2j\omega\mu h}{W^2}\left\{-\frac{W^2\pi^2}{k^2a^2}+\frac{8}{\pi^4}\frac{a^2}{}Sm_1+\frac{a^2}{4\pi^2}Sm_2+\frac{aW}{\pi\sqrt{2}}Sm_3+\frac{W^2}{2}Sm_4+\frac{2a^2}{\pi^4}Smn_5\right\}(3A.3.5)$$

where,

$$Sm_1=\sum_{m=1}^{\infty}\frac{(\sin m\theta_1-\sin m\theta_2)^2}{m^2(m^2-A^2)}$$

$$=\sum_{m=1}^{\infty}\frac{1}{m^2(m^2-A^2)}-\sum_{m=1}^{\infty}\frac{\cos m2\theta_1}{2m^2(m^2-A^2)}-\sum_{m=1}^{\infty}\frac{\cos m2\theta_2}{2m^2(m^2-A^2)}-\sum_{m=1}^{\infty}\frac{\cos m(\theta_1-\theta_2)}{m^2(m^2-A^2)}+\sum_{m=1}^{\infty}\frac{\cos m(\theta_1+\theta_2)}{m^2(m^2-A^2)}$$

therefore the expression for $S_1(m)$ simplifies to

$$Sm_1=-\frac{4\pi^2W}{2\sqrt{2}\,k^2a^3}+\frac{2\pi^2W^2}{k^2a^2}$$

$$+\frac{4\pi^2}{k^3a\sin ka}\left[-\cos A\pi+\cos A(\pi-\theta_1-\theta_2)\cos A(\theta_2-\theta_1)-2\sin A(\pi-\theta_1)\sin A\theta_2\right](3A.3.6)$$

$$Sm_2=\sum_{m=1}^{\infty}\frac{(\sin m2\theta_1-\sin m2\theta_2)^2}{m^2(m^2-A^2/2)} \qquad (3A.3.7)$$

$$Sm_3=\sum_{m=1}^{\infty}\frac{\sin m2\theta_1-\sin m2\theta_2}{m(m^2-A^2/2)}$$

$$=\frac{W^2\pi^2}{k^2a^2}+\frac{W\pi^2}{\sqrt{2}\,k^2a\sin A\pi/\sqrt{2}}\left(\sin\frac{A}{\sqrt{2}}(\pi-2\theta_1)-\sin\frac{A}{\sqrt{2}}(\pi-2\theta_2)\right) \qquad (3A.3.8)$$

$$Sm_4 = \sum_{m=1}^{\infty} \frac{1}{\left(m^2 - A^2/2\right)}$$

$$= \frac{W^2 \pi^2}{2k^2 a^2} - \frac{W^2 \pi^2 \sqrt{2}}{4ka} \cot \frac{A\pi}{\sqrt{2}} \tag{3A.3.9}$$

$$Smn_5 = \sum_{n=1}^{\infty} \sum_{m=n+1}^{\infty} \frac{1}{(m^2 + n^2 - A^2)} \left[\frac{\left(\sin(m+n)\theta_1 - \sin(m+n)\theta_2\right)}{(m+n)} + \frac{\left(\sin(m-n)\theta_1 - \sin(m-n)\theta_2\right)}{(m-n)} \right]^2 \tag{3A.3.10}$$

Using equations (3A.5.6), (3A.3.8), and (3A.3.9) in equation (3A.3.5)eliminates the term $W_p W_q / k^2 \ a^2$ to give

$$Z_{in} = \frac{2j\omega\mu h}{W^2} \left\{ \frac{W\left(5W - 4\sqrt{2}\pi^2\right)}{2k^2 a} + \frac{a^2}{4\pi^2} \sum_{m=1}^{\infty} \frac{\left(\sin 2m\theta_1 - \sin 2m\theta_2\right)^2}{m^2 (m^2 - A^2/2)} \right.$$

$$- \frac{4\pi^4 \left(\cos A\pi - \cos A\left(\pi - \theta_1 - \theta_2\right)\cos A\left(\theta_2 - \theta_1\right) + 2\sin A(\pi - \theta_1)\sin A\theta_2\right)}{k^3 a \sin ka}$$

$$+ \frac{\pi^2 W \left(\sin \frac{A}{\sqrt{2}}(\pi - 2\theta_1) - \sin \frac{A}{\sqrt{2}}(\pi - 2\theta_2)\right)}{\sqrt{2} \ k^2 a \sin ka/\sqrt{2}} - \frac{\pi^2 W^2 \sqrt{2} \cot \frac{A}{\sqrt{2}} \pi}{4 \ k \ a}$$

$$+ \frac{4a^2}{\pi^4} \sum_{n=1}^{\infty} \sum_{m=n+1}^{\infty} \frac{1}{(m^2 + n^2 - A^2)} \left[\frac{\left(\sin(m+n)\theta_1 - \sin(m+n)\theta_2\right)}{(m+n)} + \frac{\left(\sin(m-n)\theta_1 - \sin(m-n)\theta_2\right)}{(m-n)} \right]^2 \right\} \tag{3A.3.10}$$

174

APPENDIX 4A

Eigensystem and Green's Function for a Rectangle Patch Geometry
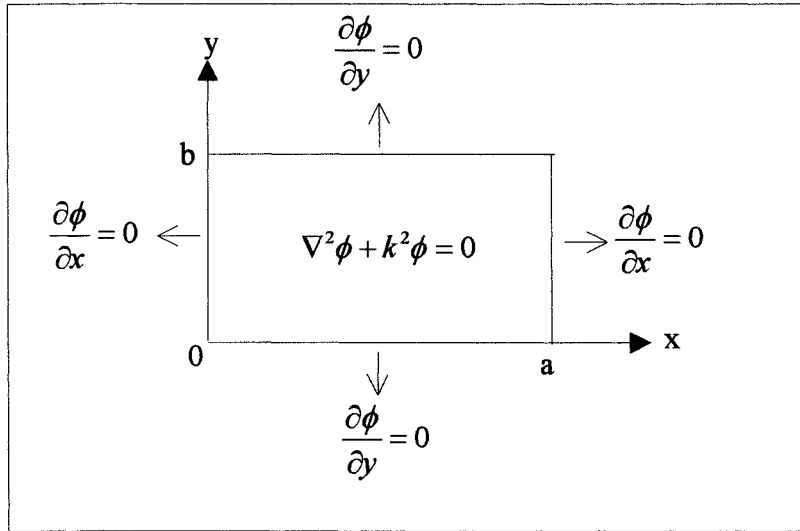
Figure 4A.1: Boundary Value Problem

The boundary value problem consist of the equation

$$\nabla^2\phi + \lambda^2\phi = 0 \tag{4A.1}$$

where, $\phi = \phi(x,y)$, and, the boundary conditions

$$\frac{\partial\phi}{\partial x}(0,y) = 0 \quad , \quad \frac{\partial\phi}{\partial x}(a,y) = 0 \quad , \quad 0 \le y \le b \tag{4A.2}$$

$$\frac{\partial\phi}{\partial y}(x,o) = 0 \quad , \quad \frac{\partial\phi}{\partial y}(x,b) = 0 \quad , \quad 0 \le x \le a \tag{4A.3}$$

let, $\phi(x,y) = X(x)Y(y)$ \hfill (4A.4)

then, the boundary conditions (4A.2) require

$$X'(0) = X'(a) = 0 \tag{4A.5}$$

175

and, $Y'(0) = Y'(b) = 0$ (4A.6)

substituting, $\phi = X\,Y$, from (4A.4) into equation (4A.1) gives

$$X'' + \lambda^2 X = 0$$ (4A.7)

and, $Y'' + p^2 Y = 0$ (4A.8)

where, $p^2 = \lambda^2 - \gamma^2$ (4A.9)

and γ is the constant of separation.

From equation (4A.4)

$$X(x) = A\cos\lambda x + B\sin\lambda x$$ (4A.10)

Applying the boundary condition (4A.5), to (4A.10), gives, $B = 0$, and,

$$\lambda = \frac{m\pi}{a}$$ (4A.11)

Similarly, from equation (4A.8)

$$Y''(y) = C\cos px + D\sin px$$ (4A.12)

Applying the boundary condition (4A.8), to (4A.12), gives, $D = 0$, and,

$$p = \frac{n\pi}{b}$$ (4A.13)

Therefore, the eigenfunctions, $\phi_{m,n}(x, y)$ are

$$\phi_{m,n}(x, y) = k_{m,n} \cos\frac{m\pi}{a}x \cos\frac{n\pi}{b}y \quad , \quad m, n = 0, 1, 2 \ldots\ldots$$ (4A.14)

for constant, $k_{m,n}$.

The eigenvalues are therefore,

$$\lambda^2 = \frac{m^2\pi^2}{a^2} + \frac{n^2\pi^2}{b^2} \quad , \quad m, n = 0, 1, 2 \ldots\ldots$$ (4A.15)

176

Normalised Eigenfunctions

The normalisation condition

$$\int_0^a \int_0^b \phi_{m,n}^2(x,y)\, dx\, dy = 1 \tag{4A.16}$$

gives, $\quad k_{m,n} = \varepsilon_m \varepsilon_n \tag{4A.17}$

where, $\quad \varepsilon_0 = 1$

$$\varepsilon_m = \sqrt{2}, \quad m \geq 1 \tag{4A.18}$$

Thus, the normalised eigensystem is

$$\phi_{m,n}(x,y) = \varepsilon_m \, \varepsilon_n \, \cos\frac{m\pi}{a} x \, \cos\frac{n\pi}{b} y, \quad m,n = 0,1,2\ldots\ldots \tag{4A.19}$$

and, $\quad \lambda_{m,n}^2 = \dfrac{m^2\pi^2}{a^2} + \dfrac{n^2\pi^2}{b^2} \quad, \quad m,n = 0,1,2\ldots\ldots \tag{4A.20}$

Green's function

For the non-homogenous wave equation

$$\nabla^2 V + k^2 V = -j\omega\,\mu h J_z \tag{4A.21}$$

the Green's function is (see 5.2.17)

$$G(x,y\,|\,x_0,y_0) = \frac{-j\omega\,\mu h}{ab} \sum_{m=0}^{\infty} \sum_{n=0}^{\infty} \frac{\varepsilon_m^2 \varepsilon_n^2}{\left(k^2 - \lambda^2\right)} \phi(x,y)\,\phi_{m,n}(x_0,y_0) \tag{4A.22}$$

That is ,

$$G(x,y\,|\,x_0,y_0) = \frac{j\omega\mu h}{ab} \sum_{m=0}^{\infty} \sum_{n=0}^{\infty} \frac{\varepsilon_m^2\varepsilon_n^2}{\left(\dfrac{m^2\pi^2}{a^2} + \dfrac{n^2\pi^2}{b^2} - k^2\right)} \cos\frac{m\pi}{a}x\cos\frac{n\pi}{b}y\cos\frac{m\pi}{a}x_0\cos\frac{n\pi}{b}y_0 \tag{4A.23}$$

for $m,n = 0,1,2,\ldots\ldots$.

APPENDIX 4B

To Prove

$$div\left(u\ \mathbf{v}\right) = \nabla u.\mathbf{v} + u\ div\ \mathbf{v}$$

Where, $u = u(x, y)$, $\mathbf{v} = \mathbf{v}(x,y) = \mathbf{i}\ v_1 + \mathbf{j}\ v_2$,

Proof

$$div\left(u\ \mathbf{v}\right) = \left(\mathbf{i}\ \frac{\partial}{\partial x} + \mathbf{j}\ \frac{\partial}{\partial y}\right).\left(u\ \mathbf{v}\right)$$

$$= \left(\mathbf{i}\ \frac{\partial}{\partial x} + \mathbf{j}\ \frac{\partial}{\partial y}\right).\left[\ u\left(\mathbf{i}\ v_1 + \mathbf{j}\ v_2\right)\right]$$

$$= \frac{\partial}{\partial x}\left(uv_1\right) + \frac{\partial}{\partial y}\left(uv_2\right)$$

$$= u\left(\frac{\partial v_1}{\partial x} + \frac{\partial v_2}{\partial y}\right) + \left(\frac{\partial u}{\partial x}\ v_1 + \frac{\partial u}{\partial y}\ v_2\right)$$

$$= u\left(\mathbf{i}\ \frac{\partial}{\partial x} + \mathbf{j}\ \frac{\partial}{\partial y}\right).\left(\mathbf{i}\ v_1 + \mathbf{j}\ v_2\right) + \left(\mathbf{i}\ \frac{\partial u}{\partial x} + \mathbf{j}\ \frac{\partial u}{\partial y}\right).\left(\mathbf{i}\ v_1 + \mathbf{j}\ v_2\right)$$

$$= u\left(\mathbf{i}\ \frac{\partial}{\partial x} + \mathbf{j}\ \frac{\partial}{\partial y}\right).\mathbf{v} + \left(\mathbf{i}\ \frac{\partial u}{\partial x} + \mathbf{j}\ \frac{\partial u}{\partial y}\right).\mathbf{v}$$

$$= u\nabla\mathbf{v} + \nabla u.\mathbf{v}$$

Further let $u = \phi$, and, $\mathbf{v} = \nabla\phi$, then,

$$div\ \phi\ \nabla\phi = \phi\ \nabla.\nabla\phi + \nabla\phi.\nabla\phi$$

that is

$$\nabla\left(\phi\ \nabla\phi\right) = \phi\ \nabla^2\phi + \nabla\phi\ .\nabla\phi$$

where,

$$\nabla^2\phi = \nabla.\nabla\phi$$

as required for equation (4.2.4) of chapter 4.

APPENDIX 4C

Evaluation of $p_1, p_2, q_1, q_2, p_{12}, q_{12}$ to terms of order d^2.

The required expressions are as follows :

$$p_1 = \iint_{\Delta S} \phi_a^2 ds \quad ; p_2 = \iint_{\Delta S} \phi_b^2 ds \quad ; \iint_{\Delta S} \phi_a \phi_b ds = p_{12}$$

$$q_1 = \iint_{\Delta S} \left(\nabla_T \phi_a . \nabla_T \phi_a \right) ds \quad ; q_2 = \iint_{\Delta S} \left(\nabla_T \phi_b . \nabla_T \phi_b \right) ds ; \quad q_{12} = \iint_{\Delta S} \left(\nabla_T \phi_a . \nabla_T \phi_b \right) ds$$

where , $\phi_a = \dfrac{\sqrt{2}}{a} \sin kx$, $\phi_b = \dfrac{\sqrt{2}}{a} \sin ky$, $k = \dfrac{\pi}{a}$, $\Delta S = \Delta S_1 + \Delta S_2$, and ,

$$\nabla = i \frac{\partial}{\partial x} + j \frac{\partial}{\partial y} \ .$$

The evaluations take place over the triangles ΔS_1 and ΔS_2 as shown below,
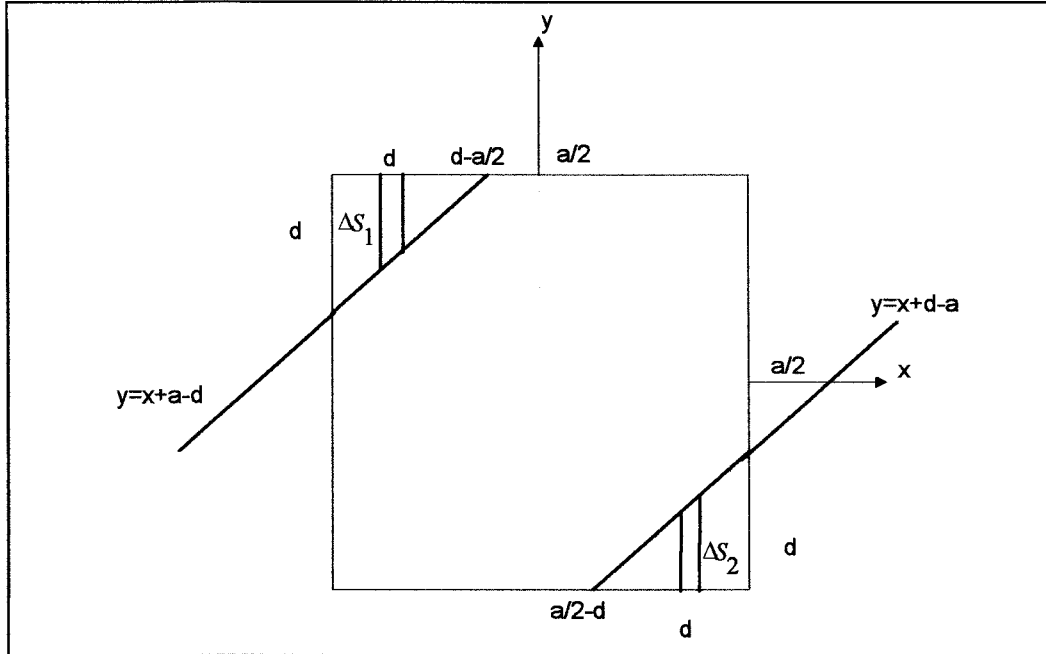
Figure 4C.1 . The unperturbed square patch antenna

Here, $\Delta S = d^2$, and , the unperturbed patch area , $S = a^2$.

All double integrals over ΔS_1 are of the form

$$\int\limits_{x=-\frac{a}{2}}^{x=d-\frac{a}{2}} \int\limits_{y=x+a-d}^{y=\frac{a}{2}} (\text{function})\ dxdy$$

All double integrals over ΔS_2 are of the form

$$\int\limits_{x=\frac{a}{2}-d}^{x=\frac{a}{2}} \int\limits_{y=x+d-a}^{y=-\frac{a}{2}} (\text{function})\ dxdy$$

Evaluation of p_1

$$p_1 = \iint\limits_{\Delta S_1} \phi_a^2 ds + \iint\limits_{\Delta S_2} \phi_a^2 ds$$

Since the integrand is everywhere positive, therefore,

$$p_1 = 2\iint\limits_{\Delta S_1} \phi_a^2 ds$$

$$= \frac{4}{a^2} \int\limits_{-\frac{a}{2}}^{d-\frac{a}{2}} \int\limits_{x+a-d}^{\frac{a}{2}} \sin^2 kx\ dxdy$$

$$= \frac{4}{a^2} \int\limits_{-\frac{a}{2}}^{d-\frac{a}{2}} \sin^2 kx \left\{ \int\limits_{x+a-d}^{\frac{a}{2}} 1.dy \right\} dx$$

$$= \frac{4}{a^2} \int\limits_{-\frac{a}{2}}^{d-\frac{a}{2}} \sin^2 kx \left(d - \tfrac{a}{2} - x\right)\ dx$$

$$= \frac{2}{a^2} \int\limits_{-\frac{a}{2}}^{d-\frac{a}{2}} \left(d - \tfrac{a}{2} - x\right)\left(1 - \cos 2kx\right)\ dx$$

$$= \frac{2}{a^2}\left\{ \left[\left(d - \frac{a}{2} - x\right)\left(x - \frac{\sin 2kx}{2k}\right)\right]_{-\frac{a}{2}}^{d-\frac{a}{2}} + \int\limits_{-\frac{a}{2}}^{d-\frac{a}{2}} \left(x - \frac{\sin 2kx}{2k}\right)\ dx \right\}$$

$$= \frac{2}{a^2}\left\{ \frac{d\,a}{2} - \frac{d\sin ka}{2k} + \left[\frac{x^2}{2} + \frac{\cos 2kx}{4k^2}\right]_{-\frac{a}{2}}^{d-\frac{a}{2}} \right\}$$

$$= \frac{2}{a^2}\left\{\frac{d\,a}{2} - \frac{d\sin ka}{2k} + \frac{d(d-a)}{2} + \frac{1}{4k^2}\left(\cos k(2d-a) - \cos ka\right)\right\}$$

$$= \frac{1}{a^2}\left\{d^2 - \frac{d}{k}\sin ka + \frac{1}{2k^2}\left(\cos 2kd\cos ka + \sin 2kd\sin ka - \cos ka\right)\right\}$$

With $k = \dfrac{\pi}{2}$, $\sin ka = 0$, $\cos ka = -1$, so, that,

$$p_1 = \frac{1}{a}\left\{d^2 + \frac{1}{2k^2}(-\cos 2kd + 1)\right\}$$

For small 'd', $\cos 2kd \approx 1 - 4k^2 d^2/2 = 1 - 2k^2 d^2$

To terms of order d^2, p_1 has the value

$$p_1 = \frac{1}{a^2}\left\{d^2 + \frac{1}{2k^2}\left(1 - 1 + 2k^2 d^2\right)\right\}$$

$$= 2\frac{d^2}{a^2} = 2\frac{\Delta S}{S}$$

Evaluation of p_2

By symmetry $p_2 = p_1$

Evaluation of q_1

$$\nabla\phi_a = \left(\mathbf{i}\,\frac{\partial}{\partial x} + \mathbf{j}\,\frac{\partial}{\partial y}\right)\frac{\sqrt{2}}{a}\sin kx$$

$$= \mathbf{i}\sqrt{2}\,\frac{k}{a}\cos kx$$

Therefore,

$$\nabla\phi_a.\nabla\phi_a = \frac{2k^2}{a^2}\cos^2 kx$$

$$= \frac{2k^2}{a^2}\left(1 - \sin^2 kx\right)$$

181

so that, by symmetry

$$q_1 = \frac{4}{a^2} \iint_{\Delta S_1} k^2 \left(1 - \sin^2 kx\right) ds$$

$$= \frac{4k^2}{a^2} \frac{d^2}{2} - \frac{4k^2}{a^2} \iint_{\Delta S_1} \sin^2 kx \, ds$$

$$= \frac{2k^2 d^2}{a^2} - k^2 p_1$$

$$= \frac{2k^2 d^2}{a^2} - \frac{k^2 2d^2}{a^2}$$

$$= 0$$

Evaluation of q_2

By symmetry $q_2 = q_1 = 0$

Evaluation of p_{12}

$$p_{12} = \iint_{\Delta S} \phi_a \phi_b ds$$

$$= \frac{2}{a^2} \iint_{\Delta S = \Delta S_1 + \Delta S_2} \sin kx \sin ky \, ds$$

By symmetry

$$p_{12} = \frac{4}{a^2} \iint_{\Delta S_1} \sin kx \sin ky \, ds$$

$$= \frac{4}{a^2} \int_{-\frac{a}{2}}^{d-\frac{a}{2}} \sin kx \left\{ \int_{x+a-d}^{\frac{a}{2}} \sin ky \, dy \right\} dx$$

$$= \frac{4}{a^2} \int_{-\frac{a}{2}}^{d-\frac{a}{2}} \sin kx \left[-\frac{\cos ky}{k} \right]_{x+a-d}^{\frac{a}{2}} dx$$

$$= -\frac{4}{ka^2} \int_{-\frac{a}{2}}^{d-\frac{a}{2}} \sin kx \left\{ \cos \frac{ka}{2} - \cos k(x+a-d) \right\} dx$$

Since, $k = \pi/a, \cos ka/2 = 0$,
so that,

182

$$p_{12} = \frac{4}{ka^2} \int_{-\frac{a}{2}}^{d-\frac{a}{2}} \sin kx \cos k(x+a-d) \; dx$$

$$= \frac{2}{ka^2} \int_{-\frac{a}{2}}^{d-\frac{a}{2}} \left\{ \sin k(2x+a-d) + \sin k(d-a) \right\} \; dx$$

$$= \frac{2}{ka^2} \left[-\frac{\cos k(2x+a-d)}{2k} + x \sin k(d-a) \right]_{-\frac{a}{2}}^{d-\frac{a}{2}}$$

$$= \frac{2}{ka^2} \left[-\frac{1}{2k} \left\{ \cos kd - \cos kd \right\} + d \sin k(d-a) \right]$$

$$= \frac{2d}{ka^2} \left(\sin kd \cos ka - \cos kd \sin ka \right)$$

$$= \frac{2d}{ka^2} \left(-\sin kd \right)$$

$$= \frac{2c}{ka^2} (kd)$$

to terms in d^2.

Therefore,

$$p_{12} = -\frac{2d^2}{a^2}$$

$$= -\frac{2 \Delta S}{S}$$

Evaluation of q_{12}

$$\nabla \phi_a = \left(\mathbf{i} \frac{\partial}{\partial x} + \mathbf{j} \frac{\partial}{\partial y} \right) \frac{\sqrt{2}}{a} \sin kx$$

$$= \mathbf{i}\sqrt{2} \; \frac{k}{a} \cos kx$$

183

$$\nabla \phi_b = \left(\mathbf{i} \frac{\partial}{\partial x} + \mathbf{j} \frac{\partial}{\partial y} \right) \frac{\sqrt{2}}{a} \sin ky$$

$$= \mathbf{j}\sqrt{2} \ \frac{k}{a} \cos ky$$

Therefore,

$$\nabla \phi_a . \nabla \phi_b = \mathbf{i}\sqrt{2} \ \frac{k}{a} \cos kx \ . \ \mathbf{j}\sqrt{2} \ \frac{k}{a} \cos ky$$

$$= 0$$

so that,

$$q_{12} = \iint_{\Delta s} \nabla \phi_a . \nabla \phi_b ds$$

$$= \iint_{\Delta s} 0 \ ds$$

$$= 0$$

APPENDIX 4D

Ratio of the voltages V_a , V_b

The figure 4.6.1.1 can be redrawn as below :
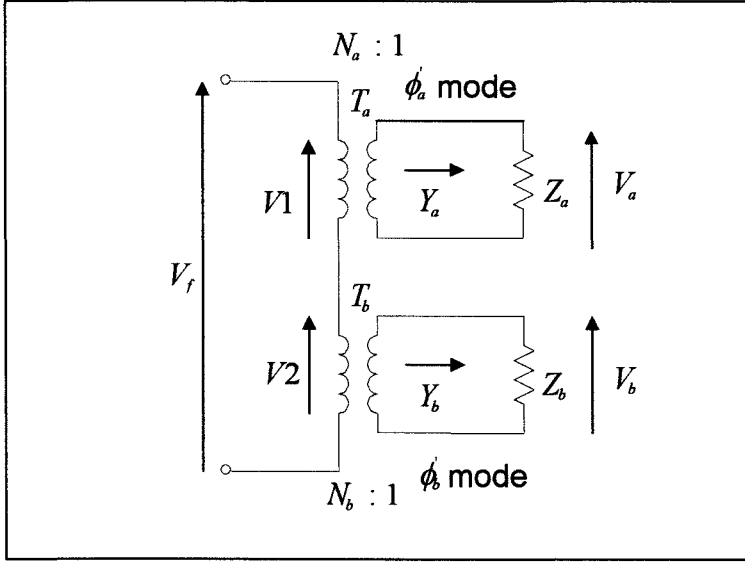
Figure 4D.1 Equivalent circuit

For step down transformer ,

$$\frac{V1}{V_a} = N_a \quad , \text{and}, \qquad \frac{V2}{V_b} = N_b$$

therefore,

$$\frac{V_b}{V_a} = \left(\frac{N_a}{N_b}\right) \cdot \left(\frac{V2}{V1}\right) \qquad (4D.1)$$

and

$$V1 = I \cdot Z_a' \qquad (4D.2)$$

$$V2 = I \cdot Z_b' \qquad (4D.3)$$

Where

185

$$Z_a^{'} = N_a^2 \cdot Z_a \qquad \text{and} \qquad Z_b^{'} = N_b^2 \cdot Z_b$$

Substituting equation 4D.2 and 4D.3 into equation 4D.1 gives,

$$\frac{V_b}{V_a} = \left(\frac{N_a}{N_b} \right) \cdot \left(\frac{I \cdot N_b^2 \cdot Z_b}{I \cdot N_a^2 \cdot Z_a} \right)$$

therefore,

$$\frac{V_b}{V_a} = \left(\frac{N_b \cdot Y_a}{N_a \cdot Y_b} \right) \qquad\qquad\qquad (4D.4)$$

where ,

$$Y_a = Z_a \qquad \text{and} \qquad Y_b = Z_b$$

and this is the result required for equation (4.7.1) of chapter 4.

APPENDIX 4E

Magnitude and Phase Relationship for Circular Polarisation

For the mode amplitudes to be equal requires

$$\left| V_a \right|^2 = \left| V_b^{\ 2} \right|$$

so that equation 4.7.6 can put into the form,

$$\left(\frac{f_o M}{Q} \right)^2 + \left(f - \frac{f_o^2 M}{f} \right)^2 = \left(\frac{f_o}{Q} \right)^2 + \left(f - \frac{f_o^2}{f} \right)^2$$

$$\frac{f_o^2 M}{Q^2} + f^2 - 2f_o^2 M^2 + \frac{f_o^4 M^4}{f^2} = \frac{f_o^2}{Q^2} + f^2 - 2f_o^2 + \frac{f_o^4}{f^2}$$

$$\frac{f_o^2}{Q^2}\left(M^2 - 1\right) - 2f_o^2\left(M^2 - 1\right) + \frac{f_o^4}{f^2}\left(M^4 - 1\right) = 0$$

$$\frac{f_o^2}{Q^2}\left(M^2 - 1\right) - 2f_o^2\left(M^2 - 1\right) + \frac{f_o^4}{f^2}\left(M^2 - 1\right)\left(M^2 + 1\right) = 0$$

$$\frac{f_o^2}{Q^2} - 2f_o^2 + \frac{f_o^4}{f^2}\left(M^2 + 1\right) = 0$$

$$\frac{1}{Q^2} - 2 + \frac{f_o^2}{f^2}\left(M^2 + 1\right) = 0$$

$$\frac{1}{Q^2} - 2 + \frac{\left(M^2 + 1\right)}{\alpha^2} = 0 \tag{4E.1}$$

where,

$$\alpha = f / f_o$$

so,

187

$$\alpha^2 = \left(M^2 + 1\right) \bigg/ \left(\frac{1}{Q^2} - 2\right)$$

For the mode phase difference to be $\pm \pi/2$, requires that

$$\arg V_a - \arg V_b = \arg\left(V_a/V_b\right) = \pm \pi/2$$

Rationalising V_a/V_b equation 4.7.6 can put into the form,

$$\frac{V_b}{V_a} = \frac{\left(\dfrac{f_o M}{Q} + j\left(f - \dfrac{f_o^2 M^2}{f}\right)\right)\left(\dfrac{f_o}{Q} - j\left(f - \dfrac{f_o^2}{f}\right)\right)}{\left(\dfrac{f_o}{Q} + j\left(f - \dfrac{f_o^2}{f}\right)\right)\left(\dfrac{f_o}{Q} - j\left(f - \dfrac{f_o^2}{f}\right)\right)}$$

$$\frac{V_b}{V_a} = \frac{\dfrac{f_o^2 M}{Q^2} + \left(f - \dfrac{f_o^2 M^2}{f}\right)\left(f - \dfrac{f_o^2}{f}\right) + j\left(\dfrac{f_o^2}{Q}\left(f - \dfrac{f_o^2 M^2}{f}\right) - \dfrac{f_o M}{Q}\left(f - \dfrac{f_o^2}{f}\right)\right)}{\dfrac{f_o^2}{Q^2} + \left(f - \dfrac{f_o^2}{f}\right)^2}$$

Then,

$$\arg\left\{\frac{V_b}{V_a}\right\} = \tan^{-1}\left\{\frac{\dfrac{f_o^2}{Q}\left(f - \dfrac{f_o^2 M^2}{f}\right) - \dfrac{f_o M}{Q}\left(f - \dfrac{f_o^2}{f}\right)}{\dfrac{f_o^2 M}{Q^2} + \left(f - \dfrac{f_o^2 M^2}{f}\right)\left(f - \dfrac{f_o^2}{f}\right)}\right\}$$

That is,

$$\frac{\dfrac{f_o^2}{Q}\left(f - \dfrac{f_o^2 M^2}{f}\right) - \dfrac{f_o M}{Q}\left(f - \dfrac{f_o^2}{f}\right)}{\dfrac{f_o^2 M}{Q^2} + \left(f - \dfrac{f_o^2 M^2}{f}\right)\left(f - \dfrac{f_o^2}{f}\right)} = \tan\left(\pm\frac{\pi}{2}\right) = \pm\infty$$

which requires,

$$\frac{f_o^2 M}{Q^2} + \left(f - \frac{f_o^2 M^2}{f}\right)\left(f - \frac{f_o^2}{f}\right) = 0$$

Thus

$$\frac{f_o^2 M}{Q^2} + f^2 - f_o^2 M^2 - f_o^2 + \frac{f_o^2 M^2}{f^2} = 0$$

$$\frac{M}{Q^2} + \frac{f^2}{f_o^2} - M^2 - 1 + \frac{f_o^2 M^2}{f^2} = 0$$

$$\frac{M}{Q^2} + \alpha^2 - M^2 - 1 + \frac{M^2}{\alpha^2} = 0 \qquad\qquad (4E.3)$$

Eliminating α^2 between equations 4E.2 and 4E.3, gives

$$\frac{M}{Q^2} + \frac{(M^2 + 1)Q^2}{(2Q^2 - 1)} - (M^2 + 1) + \frac{M^2(2Q^2 - 1)}{(M^2 + 1)Q^2} = 0$$

$$\frac{(M^2 + 1)Q^2}{(2Q^2 - 1)} - (M^2 + 1) + \frac{M}{Q^2}\left[1 + \frac{M(2Q^2 - 1)}{(M^2 + 1)}\right] = 0$$

$$(M^2 + 1)\left[\frac{Q^2 - 2Q^2 + 1}{(2Q^2 - 1)}\right] + \frac{M}{Q^2}\left[1 + \frac{M(2Q^2 - 1)}{(M^2 + 1)}\right] = 0$$

$$\frac{(M^2 + 1)(Q^2 - 1)Q^2}{(2Q^2 - 1)} = M\left[1 + \frac{M(2Q^2 - 1)}{(M^2 + 1)}\right] = 0 \qquad (4E.4)$$

In application it can be assumed that Q is much greater than '1' (about 70) so that

assume $2Q^2 - 1 \approx 2Q^2$ and $Q^2 - 1 \approx Q^2$, equation 4E.4 gives

$$Q^2(M^2 + 1) = 2M + \frac{4Q^2 M^2}{(M^2 + 1)}$$

$$Q^2\left[(M^2 + 1)^2 - 4M^2\right] = 2M(M^2 + 1)$$

$$Q^2(M^2 + 1)^2(M^2 - 1)^2 = 2M(M^2 + 1) \qquad\qquad (4E.5)$$

Let $M = 1 - 2\Delta S/S = 1 - \delta$, equation 4E.5 gives,

$$Q^2\left(4 - 2\delta + \delta^2\right)\delta^2 = 2\left(1 - \delta\right)\left(\delta^2 - 2\delta + 2\right)$$

$$Q^2\delta^2 = \frac{\left(2 - 4\delta + 3\delta^2 - \delta^3\right)}{\left(2 - \delta + \dfrac{\delta^2}{2}\right)}$$

$$Q^2\delta^2 = \frac{\left(1 - 2\delta + \dfrac{3\delta^2}{2} - \dfrac{\delta^3}{2}\right)}{\left(1 - \dfrac{\delta}{2} + \dfrac{\delta^2}{4}\right)} \qquad\qquad (4E.6)$$

and this is the result required for equation (4.7.11) of chapter 4.

APPENDIX 5A:

Verification of the Normal Zero Boundary Condition for the

Green's Function on An Isosceles Triangle

The Green's function for the triangle in fig.5A.1 below
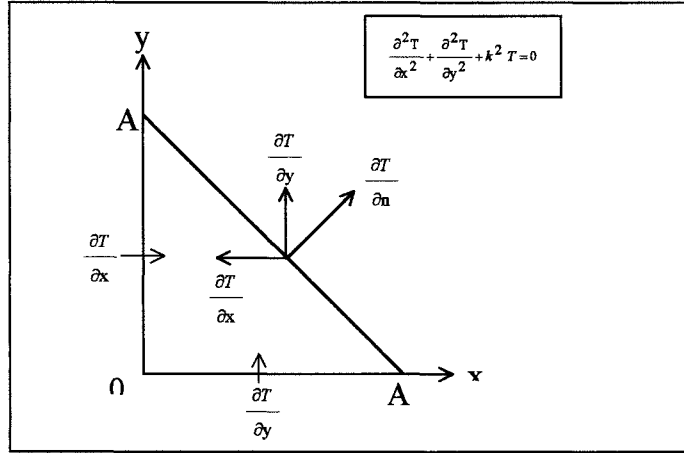
Figure 5A.1: The zero normal boundary condition

given by Gupta[3] is of the form

$$G(x, y) = \sum_{m=-\infty}^{+\infty} \sum_{n=-\infty}^{+\infty} F(m, n ; x_o, y_o) T(x, y) \tag{5A.1}$$

where, $T_{m,n}(x, y) = \cos \dfrac{m\pi}{A} x \cos \dfrac{n\pi}{A} y + (-1)^{m+n} \cos \dfrac{n\pi}{A} x \cos \dfrac{m\pi}{A} y$ \hfill (5A.2)

The zero normal boundary condition can be verified by showing that

$\partial T/\partial x$, $\partial T/\partial y$, and, $\partial T/\partial n$ are zero along the respective boundaries.

Let $\pi/A = k$, then

$$T_{m,n} = \cos mkx \cos nky + (-1)^{m+n} \cos nkx \cos mky \tag{5A.3}$$

191

$$\frac{\partial T}{\partial x} = -k\left[m \sin mkx \cos nky + (-1)^{m+n} n \sin nkx \cos mky\right] \qquad (5A.4)$$

On the ' y ' axis , $x = 0$, so that $\partial T/\partial x$ vanishes on this axis.

$$\frac{\partial T}{\partial y} = -k\left[n \cos mkx \sin nky + (-1)^{m+n} m \cos nkx \sin mky\right] \qquad (5A.5)$$

On the ' x ' axis, $y = 0$, so that $\partial T/\partial y$ vanishes on this axis.

On the hypotenuse the normal $\partial T/\partial n$ can be resolved into perpendicular component, so that,

$$\frac{\partial T}{\partial n} = \cos \frac{\pi}{4} \frac{\partial T}{\partial y} + \cos \frac{\pi}{4} \frac{\partial T}{\partial x} = \left(\frac{\partial T}{\partial x} + \frac{\partial T}{\partial y}\right) \frac{1}{\sqrt{2}} \qquad (5A.6)$$

On the hypotenuse, $y = A - x$, so that

$$\cos nky = \cos nk(A - x) = \cos(n\pi - nkx) = (-1)^n \cos nkx \qquad (5A.7)$$

and, $\cos mky = (-1)^m \cos mkx \qquad (5A.8)$

and, $\sin nky = \sin nk(A - x) = \sin(n\pi - nkx) = -(-1)^n \sin nkx \qquad (5A.9)$

and, $\sin mky = -(-1)^m \sin mkx \qquad (5A.10)$

Substituting (5A.7), (5A.8) into (5A.4), gives

$$\frac{\partial T}{\partial x} = -k(-1)^n\left[m \sin mkx \cos nkx + n \sin nkx \cos mkx\right] \qquad (5A.11)$$

Substituting (5A.9), (5A.10) into (5A.5), gives

$$\frac{\partial T}{\partial y} = -k(-1)^n\left[n \cos mkx \sin nkx + m \cos nkx \sin mkx\right] \qquad (5A.12)$$

Thus from (5A.11) and (5A.12)

$$\frac{\partial T}{\partial n} = \left(\frac{\partial T}{\partial x} + \frac{\partial T}{\partial y}\right) \frac{1}{\sqrt{2}} = 0 \qquad (5A.13)$$

The normal zero boundary condition on the hypotenuse.

APPENDIX 5B

Vector Transformation Between the Rectangular Cartesian and Tangential / Normal Coodinate System

The rectangular form of the current density is given by

$$\mathbf{J}_s = \frac{1}{jw\mu h}\left\{\hat{\mathbf{x}}\,\frac{\partial v}{\partial x} + \hat{\mathbf{y}}\,\frac{\partial v}{\partial y}\right\}$$
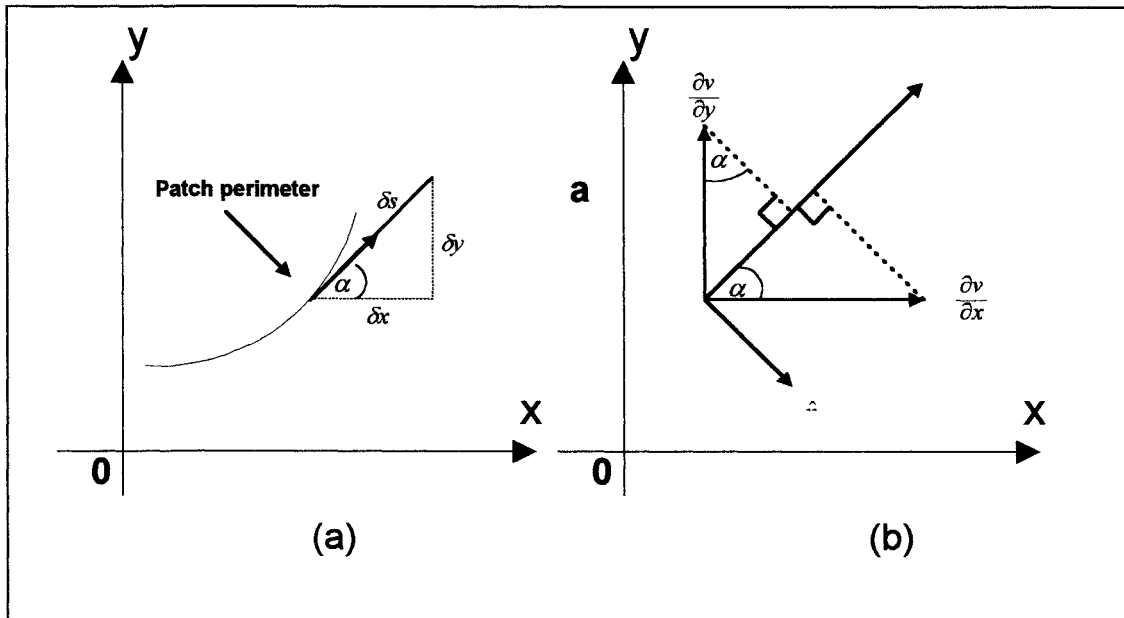

Figure 5B.1 : Cartesian and tangential system

From figure 5B.1a and 5B.1b :

The component of $\dfrac{\partial v}{\partial x}$ in the $\hat{\mathbf{s}}$ direction is $\dfrac{\partial v}{\partial x}\cos\alpha$.

The component of $\dfrac{\partial v}{\partial y}$ in the $\hat{\mathbf{s}}$ direction is $\dfrac{\partial v}{\partial y}\sin\alpha$.

The total component of $\mathbf{J}_s$ in the $\hat{s}$ direction is therefore

$$\mathbf{J}_s = \frac{1}{jw\mu h} \left\{ \frac{\partial v}{\partial x} \cos \alpha + \frac{\partial v}{\partial y} \sin \alpha \right\} \qquad (5B.1)$$

since,

$$\delta v = \frac{\partial v}{\partial x} \delta x + \frac{\partial v}{\partial y} \delta y$$

therefore,

$$\frac{dv}{ds} = \frac{\partial v}{\partial x} \frac{dx}{ds} + \frac{\partial v}{\partial y} \frac{dy}{ds}$$

$$= \frac{\partial v}{\partial x} \cos \alpha + \frac{\partial v}{\partial y} \sin \alpha \qquad (5B.2)$$

thus, from (5B.1) and (5B.2) :

$$\frac{1}{jw\mu h} \left\{ \frac{dv}{ds} \right\} = \text{total component in the } \hat{s} \text{ direction.}$$
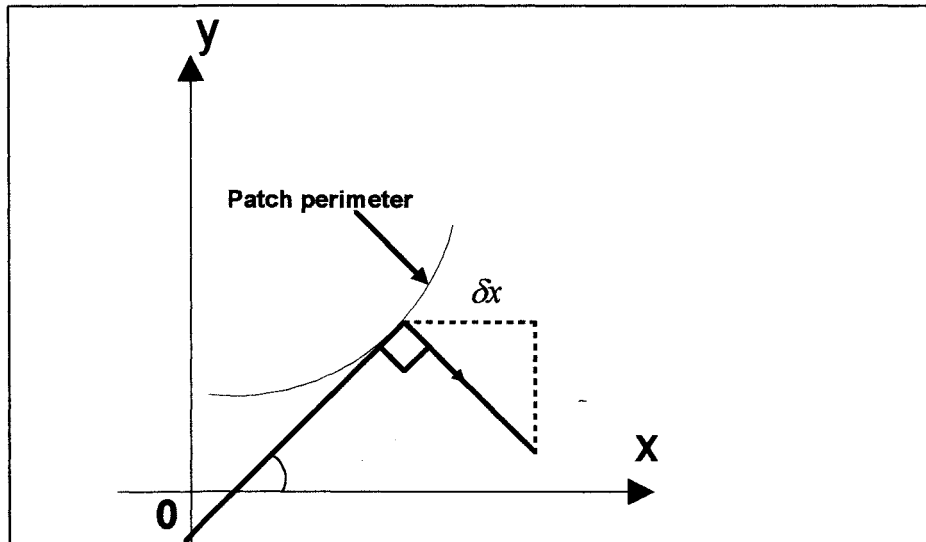
Figure 5B.2 : Cartesian and tangential system

From figure 5B.1b and 5B.2 :

The component of $\dfrac{\partial v}{\partial x}$ in the $\hat{n}$ direction is $\dfrac{\partial v}{\partial x} \sin \alpha$.

The component of $\dfrac{\partial v}{\partial y}$ in the $\hat{n}$ direction is $-\dfrac{\partial v}{\partial y} \cos \alpha$.

The total component of $\mathbf{J}_s$ in the $\hat{n}$ direction is therefore

$$\mathbf{J}_s = \frac{1}{jw\mu h} \left\{ \frac{\partial v}{\partial x} \cos \alpha - \frac{\partial v}{\partial y} \sin \alpha \right\} \qquad (5B.3)$$

since,

$$\frac{dv}{ds} = \frac{\partial v}{\partial x} \frac{dx}{dn} + \frac{\partial v}{\partial y} \frac{dy}{dn}$$

$$= \frac{\partial v}{\partial x} \cos \alpha - \frac{\partial v}{\partial y} \sin \alpha \qquad (5B.4)$$

therefore from (5B.3) and (5B.4) the total component of $\mathbf{J}_s$ in the n direction is

$$\frac{1}{jw\mu h} \left\{ \frac{dv}{dn} \right\}$$

Thus $\mathbf{J}_s$ can be written in the form

$$\mathbf{J}_s = \frac{1}{jw\mu h} \left\{ \frac{\partial v}{\partial s} \hat{s} + \frac{\partial v}{\partial n} \hat{n} \right\} \qquad (5B.5)$$

where $\hat{n}$ is the outward normal.

APPENDIX 7A:

Coupling Impedance Formulas for a Rectangle

7A.1 Closed form summation formulas

The following summation formulas, which are used in obtaining the input impedance expressions, are based on the series tables in Gradshteyn [1].

1. $$\sum_{m=1}^{\infty} \frac{1}{m^2 - A^2} = \frac{1}{2A^2} - \frac{\pi}{2A} \cot A\pi$$

2. $$\sum_{m=1}^{\infty} \frac{(-1)^m}{m^2 - A^2} = \frac{1}{2A^2} - \frac{\pi \cos 2A\pi}{2A \sin A\pi} \qquad ; \quad \pi \le \theta \le 3\pi$$

3. $$\sum_{m=1}^{\infty} \frac{1}{m^2 + A^2} = \frac{\pi}{2A} \coth A\pi - \frac{1}{2A^2}$$

4. $$\sum_{m=1}^{\infty} \frac{(-1)^m}{m^2 + A^2} = \frac{-1}{2A^2} - \frac{\pi}{2A \sinh A\pi}$$

5. $$\sum_{m=1}^{\infty} \frac{\sin m\theta}{m(m^2 + A^2)} = \frac{(\pi - \theta)}{2A^2} - \frac{\pi \sinh A(\pi - \theta)}{2A^2 \sinh A\pi}$$

6. $$\sum_{m=1}^{\infty} \frac{\cos m\theta}{m^2 - A^2} = \frac{1}{2A^2} - \frac{\pi \cos A(\pi - \theta)}{2A \sin A\pi} \qquad ; \quad 0 \le \theta \le 2\pi$$

7. $$\sum_{m=1}^{\infty} \frac{\sin m\theta}{m(m^2 - A^2)} = \frac{\theta - \pi}{2A^2} + \frac{\pi \sin A(\pi - \theta)}{2A^2 \sin A\pi} \qquad ; \quad 0 \le \theta \le 2\pi$$

8. $$\sum_{m=1}^{\infty} \frac{\sin m\theta}{m(m^2 - A^2)} = \frac{\theta}{2A^2} - \frac{\pi \sin 3A\pi}{2A^2 \sin A\pi} - \frac{\pi \sin A(3\pi - \theta)}{2A^2 \sin A\pi} \qquad ; \quad 2\pi \le \theta \le 4\pi$$

The first six formulas in the above list are given directly in the Gradshteyn tables. Formula number seven is obtained from formula six by integration which improves convergence by one order. However, in order to meet the convergence interval required in the impedance calculations it was, in addition, necessary to replace, θ, by, $\theta - 2\pi$.

The new formula (7) above is obtained as follows:

Using formula (6)

$$\sum_{m=1}^{\infty} \frac{\cos m\theta}{m^2 - A^2} = \frac{1}{2A^2} - \frac{\pi}{2} \frac{\cos A(\pi - \theta)}{A \sin A\pi}$$

and integrating, gives

$$\sum_{m=1}^{\infty} \frac{\sin m\theta}{m(m^2 - A^2)} = \frac{\theta}{2A^2} + \frac{\pi}{2} \frac{\sin A(\pi - \theta)}{A^2 \sin A\pi} + C$$

when $\theta = 0$,

$$C = -\frac{\pi}{2A^2}$$

and therefore the new formula (7) is obtained:

$$\sum \frac{\sin m\theta}{m(m^2 - A^2)} = \frac{\theta - \pi}{2A^2} + \frac{\pi \sin A(\pi - \theta)}{2A^2 \sin A\pi} \qquad ; \quad 0 \le \theta \le 2\pi$$

7A.2 Case (a): Ports at centres $(0, y_p)$, $(0, y_q)$.

A: Integrations

$$Z_{pq} = \frac{j\omega\mu h}{abW_pW_q} \int_l^u \int_L^U \left\{ \frac{-1}{k^2} + \frac{2a^2}{\pi^2} \sum_{m=1}^{\infty} \frac{1}{m^2 - A^2} + \frac{2b^2}{\pi^2} \sum_{n=1}^{\infty} \frac{\cos\frac{n\pi}{b}y_p \cos\frac{n\pi}{b}y_q}{n^2 - B^2} \right.$$

$$\left. + \sum_{m=1}^{\infty}\sum_{n=1}^{\infty} \frac{\cos\frac{n\pi}{b}y_p \cos\frac{n\pi}{b}y_q}{\frac{m^2\pi^2}{a^2} + \frac{n^2\pi^2}{b^2} - k^2} \right\} dy_p\, dy_q \qquad (7A.2.1)$$

where, $U = y_p + \dfrac{W_p}{2}$, $L = y_p - \dfrac{W_p}{2}$, $u = y_q + \dfrac{W_q}{2}$, $l = y_q - \dfrac{W_q}{2}$, $A = \dfrac{ka}{\pi}$, $B = \dfrac{kb}{\pi}$.

Integration for FIRST TWO TERMS

$$I_1 = \int_l^u \int_L^U 1 \; dy_p\, dy_q = W_pW_q \qquad (7A.2.2)$$

Integration for THIRD TERM

$$I_2 = \int_l^u \int_L^U \cos\frac{n\pi}{b}y_p \cos\frac{n\pi}{b}y_q \; dy_p\, dy_q$$

$$= \frac{b^2}{n^2\pi^2} F_1(n : \theta_1, \theta_2, \theta_3, \theta_4) \qquad (7A.2.3)$$

197

where, $F_1(n : \theta_1, \theta_2, \theta_3, \theta_4) = (\sin n\theta_1 - \sin n\theta_2)(\sin n\theta_3 - \sin n\theta_4)$, $\theta_1 = \dfrac{\pi U}{b}$, $\theta_2 = \dfrac{\pi L}{b}$,

$\theta_3 = \dfrac{\pi u}{b}$, $\theta_4 = \dfrac{\pi l}{b}$.

B: Summations

From the equation (7A.2.1), therefore,

$$Z_{pq} = \frac{j\omega \, \mu \, h}{a\, b\, W_p W_q}\left[\frac{-W_p W_q}{k^2} + \frac{2a^2 W_p W_q}{\pi^2}Sm_1 + \frac{2b^2}{\pi^4}Sn_2 + \frac{4a^2 b^2}{\pi^4}Sn_3\right] \qquad (7A.2.4)$$

where,

$$Sm_1 = \sum_{m=1}^{\infty}\frac{1}{m^2 - A^2}$$

$$= \frac{\pi^2}{2a^2 k^2} - \frac{\pi^2}{2ak}\cot ka \qquad (7A.2.5)$$

$$Sn_2 = \sum_{n=1}^{\infty}\frac{F_1(n : \theta_1, \theta_2, \theta_3, \theta_4)}{n^2(n^2 - B^2)} \qquad (7A.2.6)$$

$$Smn_3 = \sum_{n=1}^{\infty}\frac{F_1(n : \theta_1, \theta_2, \theta_3, \theta_4)}{n^2}\sum_{m=1}^{\infty}\frac{1}{m^2 + D^2}$$

$$= \frac{\pi}{2}\sum_{n=1}^{\infty}\frac{F_1(n : \theta_1, \theta_2, \theta_3, \theta_4)}{n^2 D}\coth D\pi - \frac{b^2}{2a^2}\sum_{n=1}^{\infty}\frac{F_1(n : \theta_1, \theta_2, \theta_3, \theta_4)}{n^2(n^2 - B^2)}$$

$$= \frac{\pi}{2}\sum_{n=1}^{\infty}\frac{F_1(n : \theta_1, \theta_2, \theta_3, \theta_4)}{n^2 D}\coth D\pi - \frac{b^2}{2a^2}Sn_2 \qquad (7A.2.7)$$

where, $D^2 = (n^2 - B^2)\, a^2/b^2$,

Using equations (7A.2.5) and (7A.2.7) in equation (7A.2.4) eliminates both of the terms $W_p W_q/k^2$ and Sn_1, to give

$$Z_{pq} = \frac{j\omega \, \mu \, h}{ab}\left[\frac{-a}{k}\cot ka + \frac{2a^2 b^2}{W_p W_q \pi^3}\sum_{n=1}^{\infty}\frac{(\sin n\theta_1 - \sin n\theta_2)(\sin n\theta_3 - \sin n\theta_4)}{n^2 D}\coth D\pi\right] \qquad (7A.2.8)$$

7A.3 Case (b): Ports at centres $(0, y_p)$, $(x_q, 0)$

A : Integrations

$$Z_{pq} = \frac{jw\mu h}{abW_p W_q} \int_u^l \int_L^U \left\{ -\frac{1}{k^2} + \frac{2a^2}{\pi^2} \sum_{m=1}^{\infty} \frac{\cos\dfrac{m\pi}{a}x_q}{m^2 - A^2} + \frac{2b^2}{\pi^2} \sum_{n=1}^{\infty} \frac{\cos\dfrac{n\pi}{b}y_p}{n^2 - B^2} \right.$$

$$\left. + 4\sum_{m=1}^{\infty}\sum_{n=1}^{\infty} \frac{\cos\dfrac{m\pi}{a}x_q \cos\dfrac{n\pi}{b}y_p}{\dfrac{m^2\pi^2}{a^2} + \dfrac{n^2\pi^2}{b^2} - k^2} \right\} dy_p dx_q \qquad (7A.3.1)$$

where, $U = y_p + \dfrac{W_p}{2}$, $L = y_p - \dfrac{W_p}{2}$, $u = x_q + \dfrac{W_q}{2}$, $l = x_q - \dfrac{W_q}{2}$

The integration limits take into account the current circuit direction.

Integration for FIRST TERM

$$I_1 = \int_l^u \int_L^U -1 \cdot dy_p dx_q = -W_p W_q \qquad (7A.3.2)$$

Integration for SECOND TERM

$$I_2 = \int_l^u \int_L^U -1 \cdot \cos\frac{m\pi}{a} dy_p dx_q = W_p \int_L^U \cos\frac{m\pi}{a}x_q dx_q = -\frac{W_p}{m\pi}a\left(\sin m\theta_1 - \sin m\theta_2\right) \qquad (7A.3.3)$$

where, $\theta_1 = \dfrac{\pi u}{a}$, $\theta_2 = \dfrac{\pi l}{a}$

Integration for THIRD TERM

Similar to "SECOND TERM": $I_3 = -\dfrac{W_q b}{n\pi}\left(\sin n\theta_3 - \sin n\theta_4\right) \qquad (7A.3.4)$

where, $\theta_3 = \dfrac{\pi U}{b}$, $\theta_4 = \dfrac{\pi L}{b}$

Integration for FOURTH TERM

$$I_4 = \int_l^u \int_L^U -\cos\frac{m\pi}{a}x_q \cos\frac{n\pi}{a}y_p dy_p dx_q = -\frac{W_p a\left(\sin m\theta_1 - \sin m\theta_2\right)\left(\sin n\theta_3 - \sin n\theta_4\right)}{mn\pi^2} \qquad (7A.3.5)$$

B: Summations

From the equation (7A.3.1), therefore,

$$Z_{pq} = \frac{j\omega\,\mu\,h}{a\,bW_pW_q}\left[\frac{W_pW_q}{k^2} - \frac{2a^3W_p}{\pi^3}Sm_1 - \frac{2b^3W_q}{\pi^3}Sn_2 - \frac{4ab^3}{\pi^4}Smn_3\right] \tag{7A.3.6}$$

where,

$$Sm_1 = \sum_{m=1}^{\infty}\frac{(\sin m\theta_1 - \sin m\theta_2)}{m\ (m^2 - A^2)} \tag{7A.3.7}$$

$$Sn_2 = \sum_{n=1}^{\infty}\frac{(\sin n\theta_3 - \sin n\,\theta_4)}{n(n^2 - B^2)}$$

$$= \frac{\pi^3 W_p}{2k^2b^3} + \frac{\pi^3\left[\sin B(\pi - \theta_3) - \sin B(\pi - \theta_4)\right]}{2k^2b^2\,\sin B\pi} \tag{7A.3.8}$$

Smn_3

$$= \sum_{m=1}^{\infty}\frac{(\sin m\theta_1 - \sin m\theta_2)}{m}\sum_{n=1}^{\infty}\frac{(\sin n\theta_3 - \sin n\theta_4)}{n\ (n^2 + C^2)}$$

$$= -\frac{\pi a^2 W_p}{2b^3}\sum_{n=1}^{\infty}\frac{\left(\sin n\theta_3 - \sin n\theta_4\right)}{m\left(m^2 + A^2\right)} + \frac{\pi a^2}{2b^2}\sum_{m=1}^{\infty}\frac{\left(\sin m\theta_1 - \sin m\theta_2\right)\left(\sinh C\left(\pi - \theta_4\right) - \sinh C\left(\pi - \theta_3\right)\right)}{m\left(m^2 - A^2\right)\sinh C\pi}$$

$$= \frac{-\pi a^2 W_p}{2b^3}S_1(m) + \frac{\pi a^2}{2b^2}\sum_{m=1}^{\infty}\frac{(\ \sin m\theta_1 - \sin m\theta_2\ )\ \left[\ \sinh C(\pi - \theta_4) - \sinh C(\pi - \theta_3)\right]}{m(m^2 - A^2)\sinh C\pi} \tag{7A.3.9}$$

where,

$$C^2 = (m^2 - A^2)\ b^2/a^2\ ;\ \ \theta_1 = \frac{\pi}{a}\left(x_q + \frac{W_q}{2}\right), \theta_2 = \frac{\pi}{a}\left(y_q - \frac{W_q}{2}\right), \theta_3 = \frac{\pi}{a}\left(x_p - \frac{W_p}{2}\right),\ \text{and,}$$

$$\theta_4 = \frac{\pi}{a}\left(y_p + \frac{W_p}{2}\right).$$

Using equations (7A.3.8) and (7A.3.9) in equation (7A.3.6) eliminates both of the terms W_pW_q/k^2 and Sm_1, to give

$$Z_{pq} = \frac{j\omega\,\mu\,h}{W_pW_q}\left[\frac{W_q\left[\sin B(\pi - \theta_4) - \sin B(\pi - \theta_3)\right]}{ak^2\,\sin kb}\right.$$

$$\left.+ \frac{2a^2}{\pi^3}\sum_{m=1}^{\infty}\frac{(\sin m\theta_1 - \sin m\theta_2)\left[\sinh C\ (\pi - \theta_4) - \sinh C\ (\pi - \theta_3)\right]}{m(m^2 - A^2)\sinh C\ \pi}\right] \tag{7A.3.10}$$

7A.4 Case (c): Ports at centres $(0, y_p)$, (a, y_q)

A : Integrations

$$Z_{pq} = \frac{jw\mu h}{abW_pW_q} \int_u^l \int_L^U \left\{ -\frac{1}{k^2} + \frac{2a^2}{\pi^2} \sum_{m=1}^{\infty} \frac{(-1)^m}{m^2 - A^2} + \frac{2b^2}{\pi^2} \sum_{n=1}^{\infty} \frac{\cos\dfrac{n\pi}{b}y_p \cos\dfrac{n\pi}{b}y_q}{n^2 - B^2} \right.$$

$$\left. +4\sum_{m=1}^{\infty}\sum_{n=1}^{\infty} \frac{(-1)^m \cos\dfrac{n\pi}{a}y_p \cos\dfrac{n\pi}{b}y_q}{\dfrac{m^2\pi^2}{a^2} + \dfrac{n^2\pi^2}{b^2} - k^2} \right\} dy_p dy_q \qquad (7A.4.1)$$

where, $U = y_p - \dfrac{W_p}{2}$, $L = y_p + \dfrac{W_p}{2}$, $u = y_q - \dfrac{W_q}{2}$, $l = y_q + \dfrac{W_q}{2}$

The integration limits take into account the current circuit direction.

Integration for FIRST and SECOND TERMS

$$I_1 = \int_l^u \int_L^U -1 \cdot dy_p dy_q = -W_p W_q \qquad (7A.4.2)$$

Integration for THIRD and FOURTH TERMS

$$I_2 = \int_l^u \int_L^U -\cos\frac{n\pi}{b}y_p \cos\frac{n\pi}{b}y_q dy_p dy_q = -\frac{b^2}{n^2\pi^2}F_1(n:\theta_1,\theta_2,\theta_3,\theta_4) \qquad (7A.4.3)$$

where, $\theta_1 = \dfrac{\pi L}{b}$, $\theta_2 = \dfrac{\pi U}{b}$, $\theta_3 = \dfrac{\pi l}{b}$, $\theta_4 = \dfrac{\pi u}{b}$, and,

$$F_1(n:\theta_1,\theta_2,\theta_3,\theta_4) = (\sin n\theta_1 - \sin n\theta_2)(\sin n\theta_3 - \sin n\theta_4)$$

B: Summations

From the equation, therefore,

$$Z_{pq} = \frac{j\omega \mu h}{ab}\left[\frac{W_pW_q}{k^2} - \frac{2a^2W_pW_q}{\pi^2}Sm_1 - \frac{2b^4}{\pi^4}Sn_2 - \frac{4a^2b^2}{\pi^4}Smn_3 \right] \qquad (7A.4.4)$$

where,

$$Sm_1 = \sum_{m=1}^{\infty} \frac{(-1)^m}{m^2 - A^2}$$

$$= \frac{1}{2A^2} - \frac{\pi}{2A \sin A\pi} \qquad (7A.4.5)$$

$$Sn_2 = \sum_{n=1}^{\infty} \frac{F_1(n:\theta_1,\theta_2,\theta_3,\theta_4)}{n^2(n^2 - B^2)} \qquad (7A.4.6)$$

$$Smn_3 = \sum_{n=1}^{\infty} \frac{F_1(n:\theta_1,\theta_2,\theta_3,\theta_4)}{n^2} \sum_{m=1}^{\infty} \frac{(-1)^m}{m^2 + D^2}$$

$$= \frac{\pi}{2} \sum_{n=1}^{\infty} \frac{F_1(n:\theta_1,\theta_2,\theta_3,\theta_4)}{D \sinh D\pi} - \frac{b^2}{2a^2} \sum_{n=1}^{\infty} \frac{F_1(n:\theta_1,\theta_2,\theta_3,\theta_4)}{n^2(n^2 - B^2)}$$

$$= \frac{\pi}{2} \sum_{n=1}^{\infty} \frac{F_1(n:\theta_1,\theta_2,\theta_3,\theta_4)}{D \sinh D\pi} - \frac{b^2}{2a^2} Sn_2 \qquad (7A.4.7)$$

where, $F_1(n : \theta_1,\theta_2,\theta_3,\theta_4)$, θ_1, θ_2, θ_3, θ_4 are as defined in section A.

Using equations (7A.4.5)and (7A.4.7)in equation (7A.4.4)eliminates both of the terms W_pW_q/k^2 and Sn_2, to give

$$Z_{pq} = \frac{j\omega\,\mu\,h}{bW_pW_q} \left[\frac{W_pW_q}{k\sin ka} - \frac{2ab^2}{\pi^3} \sum_{n=1}^{\infty} \frac{(\sin n\theta_1 - \sin n\theta_2)(\sin n\theta_3 - \sin n\theta_4)}{D \sinh D\pi} \right] \qquad (7A.4.8)$$

APPENDIX 8A:

Coupling impedance formulas for a right-angled Isosceles Triangle

8A.1 Closed form summation formulas

The following summation formulas, which are used in obtaining the input impedance expressions, are based on the series tables in Gradshteyn [5].

1. $\displaystyle\sum_{m=1}^{\infty}\frac{1}{m^2-A^2}=\frac{\pi}{2A}\left[\frac{1}{\pi A}-\cot A\pi\right]$

2. $\displaystyle\sum_{m=1}^{\infty}\frac{1}{m^2+A^2}=\frac{\pi}{2A}\coth A\pi-\frac{1}{2A^2}$

3. $\displaystyle\sum_{m=1}^{\infty}\frac{(-1)^m}{m^2-A^2}=\frac{1}{2A^2}-\frac{\pi}{2A\sin A\pi}$

4. $\displaystyle\sum_{m=1}^{\infty}\frac{\cos m\theta}{m^2-A^2}=\frac{1}{2A^2}-\frac{\pi\cos A(\pi-\theta)}{2A\sin A\pi}$; $0\le\theta\le2\pi$

5. $\displaystyle\sum_{m=1}^{\infty}\frac{\sin m\theta}{m(m^2-A^2)}=\frac{\theta-\pi}{2A^2}+\frac{\pi\sin A(\pi-\theta)}{2A^2\sin A\pi}$; $0\le\theta\le2\pi$

6. $\displaystyle\sum_{m=1}^{\infty}\frac{(-1)^m\cos m\theta}{m^2-A^2}=\frac{1}{2A^2}-\frac{\pi\cos A(2\pi-\theta)}{2A\sin A\pi}$; $\pi\le\theta\le3\pi$

7. $\displaystyle\sum_{m=1}^{\infty}\frac{(-1)^m\sin m\theta}{m(m^2-A^2)}=\frac{\theta}{2A^2}-\frac{\pi\sin A\theta}{2A^2\sin A\pi}$; $\pi\le\theta\le3\pi$

8. $\displaystyle\sum_{m=1}^{\infty}\frac{(-1)^m\cos m\theta}{m^2+A^2}=\frac{\pi\cosh A\theta}{2A\sinh A\pi}-\frac{1}{2A^2}$; $-\pi\le\theta\le\pi$

9. $\displaystyle\sum_{m=1}^{\infty}\frac{(-1)^m\sin m\theta}{m(m^2+A^2)}=\frac{\pi\sinh A\theta}{2A^2\sinh A\pi}-\frac{\theta}{2A^2}$; $-\pi\le\theta\le\pi$

Formulas 1, 2, 3, 4, 6 and, 8 are given directly in the Gradshteyn tables.

Formulas 5, 7, 9 are obtained, respectively, from formulas 4, 6, 8, by integration.

The new formula (5) above has been derived in Appendix 7A.

The new formula (7) above is obtained as follows:

Using formula (6)

$$\sum_{m=1}^{\infty} \frac{(-1)^m \cos m\theta}{m^2 - A^2} = \frac{1}{2A^2} - \frac{\pi \cos A\theta}{2A \sin A\pi}$$

and integrating, gives

$$\sum_{m=1}^{\infty} \frac{(-1)^m \sin m\theta}{m(m^2 - A^2)} = \frac{\theta}{2A^2} - \frac{\pi \sin A\theta}{2A^2 \sin A\pi} + C$$

when, $\theta = 0$

$$C = 0$$

and therefore the new formula (7) is obtained:

$$\sum_{m=1}^{\infty} \frac{(-1)^m \sin m\theta}{m(m^2 - A^2)} = \frac{\theta}{2A^2} - \frac{\pi \sin A\theta}{2A^2 \sin A\pi} \qquad ; \pi \le \theta \le 3\pi$$

In a similar way the new formula (9) is obtained.

A8.2 Case (a) : Ports at Centres $(0, y_p)$, $(0, y_q)$

A : Integrations

$$Z_{pq} = 2 \frac{j\omega\mu h}{W_p W_q} \int_l^u \int_L^U \left\{ -\frac{1}{a^2 k^2} + \frac{1}{\pi^2} \sum_{m=1}^{\infty} \frac{\left[1 + (-1)^m \cos m \frac{\pi}{a} y_p \right]\left[1 + (-1)^m \cos m \frac{\pi}{a} y_q \right]}{m^2 - A^2} \right.$$

$$\left. + \frac{1}{A^2} \sum_{m=1}^{\infty} \sum_{n=1}^{\infty} \frac{\left[\cos n \frac{\pi}{a} y_p + (-1)^{m+n} \cos m \frac{\pi}{a} y_p \right]\left[\cos n \frac{\pi}{a} y_q + (-1)^{m+n} \cos m \frac{\pi}{a} y_q \right]}{m^2 + n^2 - A^2} \right\} dy_p dy_q \qquad (8A.2.1)$$

where, $U = y_p + \dfrac{W_p}{2}$, $L = y_p - \dfrac{W_p}{2}$, $u = y_q + \dfrac{W_q}{2}$, $l = y_q - \dfrac{W_q}{2}$

Integration for FIRST TERM

$$I_1 = \int_l^u \int_L^U 1 \cdot dy_p dy_q = W_p W_q \qquad (8A.2.2)$$

Integration for SECOND TERM

$$I_2 = \int_{l}^{u}\int_{L}^{U}\left[1+(-1)^m\cos\frac{m\pi}{a}y_p\right]\left[1+(-1)^m\cos\frac{m\pi}{a}y_q\right]dy_p dy_q$$

$$=\left[W_p+\frac{(-1)^m a}{m\pi}(\sin m\theta_1 - \sin m\theta_2)\right]\left[W_q+\frac{(-1)^m a}{m\pi}(\sin m\theta_3 - \sin m\theta_4)\right]$$

$$=W_p W_q+\frac{(-1)^m W_q a}{m\pi}fm_1+\frac{(-1)^m W_p a}{m\pi}fm_2+\frac{a^2}{m^2\pi^2}fm_1\,fm_2 \qquad (8A.2.3)$$

Where, $\theta_1 = \dfrac{\pi U}{a}$, $\theta_2 = \dfrac{\pi L}{a}$, $\theta_3 = \dfrac{\pi l}{a}$, $\theta_4 = \dfrac{\pi u}{a}$, $fm_1 = \sin m\theta_1 - \sin m\theta_2$, $fm_2 = \sin m\theta_3 - \sin m\theta_4$

Integration for THIRD TERM

$$I_3 = \int_{l}^{u}\int_{L}^{U}\left[\cos\frac{n\pi}{a}y_p+(-1)^{m+n}\cos\frac{m\pi}{a}y_p\right]\left[\cos\frac{n\pi}{a}y_q+(-1)^{m+n}\cos\frac{m\pi}{a}y_q\right]dy_p dy_q$$

$$=\left[\frac{a}{n\pi}fn_1+\frac{(-1)^{m+n}a}{m\pi}fm_1\right]\left[\frac{a}{n\pi}fn_2+\frac{(-1)^{m+n}a}{m\pi}fm_2\right]$$

When the four terms arising from the above product are introduced into the double sum (8A.2.1) it is found, by symmetry that duplicated occurs and only the following two terms are required.

$$I_3 = \frac{2a^2}{m^2\pi^2}fm_1\,fm_2+\frac{2(-1)^{m+n}a^2}{mn\pi^2}fm_1\,fn_2 \qquad (8A.2.4)$$

B: Summations

From the integrations, therefore,

$$Z_{pq} = \frac{j2\omega\mu h}{W_p W_q}\left\{-\frac{W_p W_q}{k^2 a^2}+\frac{1}{\pi^2}Sm_1+\frac{aW_q}{\pi^3}Sm_2+\frac{a^2}{\pi^4}Sm_3+\frac{2a^2}{\pi^4}[Smn_4+Smn_5]\right\} \qquad (8A.2.5)$$

where,

$$Sm_1 = \sum_{m=1}^{\infty}\frac{W_p W_q}{m^2-A^2}+\frac{aW_p}{\pi}\frac{(-1)^m(\sin m\theta_3 - \sin m\theta_4)}{m\,(m^2-A^2)}$$

$$=\frac{W_p W_q\,\pi^2}{k^2 a^2}-\frac{W_p W_q\,\pi\cot\pi A}{2A}+\frac{\pi^2 W_p(\sin A\theta_4 - \sin A\theta_3)}{ak^2\sin A\pi} \qquad (8A.2.6)$$

$$Sm_2 = \sum_{m=1}^{\infty}\frac{(-1)^m(\sin m\theta_1 - \sin m\theta_2)}{m^2(m^2-A^2)} \qquad (8A.2.7)$$

$$Sm_3 = \sum_{m=1}^{\infty} \frac{F_1(m:\theta_1,\theta_2,\theta_3,\theta_4)}{m^2(m^2-A^2)}$$

(8A.2.8)

$$Smn_4 = \sum_{m=1}^{\infty}\sum_{n=1}^{\infty} \frac{F_1(m:\theta_1,\theta_2,\theta_3,\theta_4)}{m^2(m^2+n^2-A^2)}$$

$$= \sum_{m=1}^{\infty} \frac{F(m:\theta_1,\theta_2,\theta_3,\theta_4)}{m^2(m^2+n^2-A^2)} \sum_{n=1}^{\infty} \frac{1}{n^2+B^2}$$

where, $B^2 = m^2 - A^2$.

Therefore,

$$Smn_4 = \sum_{m=1}^{\infty} \frac{F_1(m:\theta_1,\theta_2,\theta_3,\theta_4)}{m^2} \left\{ \frac{\pi}{2B}\coth B\pi - \frac{1}{2B^2} \right\}$$

$$= \frac{\pi}{2}\sum_{m=1}^{\infty} \frac{F_1(m:\theta_1,\theta_2,\theta_3,\theta_4)\coth \pi B}{m^2 B} - \frac{1}{2}\sum_{m=1}^{\infty} \frac{F_1(m:\theta_1,\theta_2,\theta_3,\theta_4)}{m^2(m^2-A^2)}$$

$$= \frac{\pi}{2}\sum_{m=1}^{\infty} \frac{F_1(m:\theta_1,\theta_2,\theta_3,\theta_4)\coth \pi B}{m^2 B} - \frac{1}{2}S_3(m)$$

(8A.2.9)

$$Smn_5 = \sum_{m=1}^{\infty}\sum_{n=1}^{\infty} \frac{(-1)^{m+n}F_2(m,n:\theta_1,\theta_2,\theta_3,\theta_4)}{mn(m^2+n^2-A^2)}$$

$$= \sum_{m=1}^{\infty} \frac{(-1)^m(\sin m\theta_1 - \sin m\theta_2)}{m} \sum_{n=1}^{\infty} \frac{(-1)^n(\sin n\theta_3 - \sin n\theta_4)}{n(n^2+B^2)}$$

$$= \sum_{m=1}^{\infty} \frac{(-1)^m(\sin m\theta_1 - \sin m\theta_2)}{m} \left\{ \frac{1}{2A^2}\left(\frac{\pi(\sinh B\theta_3 - \sinh B\theta_4)}{\sinh B\pi} - \theta_3 + \theta_4 \right) \right\}$$

$$= \frac{\pi}{2}\sum_{m=1}^{\infty} \frac{(-1)^m(\sin m\theta_1 - \sin m\theta_2)(\sinh B\theta_3 - \sinh B\theta_4)}{m(m^2-A^2)\sinh B\pi} - \frac{W_q\pi}{2a}\sum_{m=1}^{\infty} \frac{(-1)^m(\sin m\theta_1 - \sin m\theta_2)}{m^2(m^2-A^2)}$$

$$= \frac{\pi}{2}\sum_{m=1}^{\infty} \frac{(-1)^m(\sin m\theta_1 - \sin m\theta_2)(\sinh B\theta_3 - \sinh B\theta_4)}{m(m^2-A^2)\sinh B\pi} - \frac{W_q\pi}{2a}S_2(m) \quad (8A.2.10)$$

where, $F_1(m:\theta_1,\theta_2,\theta_3,\theta_4) = (\sin m\theta_1 - \sin m\theta_2)(\sin m\theta_3 - \sin m\theta_4)$,

$F_2(m,n:\theta_1,\theta_2,\theta_3,\theta_4) = (\sin m\theta_1 - \sin m\theta_2)(\sin n\theta_3 - \sin n\theta_4)$, and,

$$\theta_1 = \frac{\pi}{a}\left(y_p + \frac{W_p}{2}\right); \theta_2 = \frac{\pi}{a}\left(y_p - \frac{W_p}{2}\right); \theta_3 = \frac{\pi}{a}\left(y_q + \frac{W_q}{2}\right); \theta_4 = \frac{\pi}{a}\left(y_q - \frac{W_q}{2}\right).$$

Using equations (8A.2.6), (8A.2.9)and (8A.2.10)in equation (8A.2.5) eliminates in turn the three terms $W_pW_q/k^2 a^2$, $S_3(m)$ and $S_2(m)$, to give the economised form

$$Z_{pq} = \frac{j\omega\mu h}{W_p W_q} \left\{ -\frac{W_p W_q}{ka} \cot \pi A + \frac{W_p (\sin A\theta_4 - \sin A\theta_3)}{k^2 a \sin ka} + \frac{2a^2}{\pi^3} \sum_{m=1}^{\infty} \frac{(\sin m\theta_1 - \sin m\theta_2)(\sin m\theta_3 - \sin m\theta_4) \coth \pi B}{m^2 B} \right.$$

$$\left. + \frac{2a^2}{\pi^3} \sum_{m=1}^{\infty} \frac{(-1)^m (\sin m\theta_1 - \sin m\theta_2)(\sinh B\theta_3 - \sinh B\theta_4)}{mB^2 \sinh \pi B} \right\} \qquad (8A.2.11)$$

A8.3 Case (b) : Ports at Centres $\left(0, y_p\right)$, $\left(x_q, 0\right)$

A : Integrations

$$Z_{pq} = 2\frac{j\omega\mu h}{W_p W_q \pi^2} \int_u^U \int_L^U \left\{ -\frac{\pi^2}{a^2 k^2} + \sum_{m=1}^{\infty} \frac{\left[1 + (-1)^m \cos \frac{m\pi}{a} y_p\right]\left[(-1)^m \cos \frac{m\pi}{a} x_q\right]}{m^2 - A^2} \right.$$

$$\left. + \sum_{m=1}^{\infty} \sum_{n=1}^{\infty} \frac{\left[\cos \frac{n\pi}{a} y_p + (-1)^{m+n} \cos \frac{m\pi}{a} y_p\right]\left[\cos \frac{m\pi}{a} x_q + (-1)^{m+n} \cos \frac{n\pi}{a} x_q\right]}{m^2 + n^2 - A^2} \right\} dy_p dx_q \qquad (8A.3.1)$$

where, $U = y_p + \frac{W_p}{2}$, $L = y_p - \frac{W_p}{2}$, $u = x_q + \frac{W_q}{2}$, $l = x_q - \frac{W_q}{2}$

Integration for FIRST TERM

$$I_1 = \int_l^u \int_L^U -1 \cdot dy_p dx_q = -W_p W_q \qquad (8A.3.2)$$

Integration for SECOND TERM

$$I_2 = \int_l^u \int_L^U -\left[1 + (-1)^{m+n} \cos \frac{m\pi}{a} y_p\right]\left[(-1)^m \cos \frac{m\pi}{a} x_q\right] dy_p dx_q$$

$$= \left[-W_p - \frac{(-1)^m a}{m\pi}(\sin m\theta_1 - \sin m\theta_2)\right]\left[(-1)^m W_q + \frac{a}{m\pi}(\sin m\theta_3 - \sin m\theta_4)\right]$$

$$= -\left[(-1)^m W_p W_q + \frac{W_q a}{m\pi} fm_1 + \frac{W_p a}{m\pi} fm_2 + \frac{(-1)^m a^2}{m^2 \pi^2} fm_1 fm_2\right] \qquad (8A.3.3)$$

where, $\theta_1 = \frac{\pi U}{a}$, $\theta_2 = \frac{\pi L}{a}$, $\theta_3 = \frac{\pi u}{a}$, $\theta_4 = \frac{\pi l}{a}$, $fm_1 = \sin m\theta_1 - \sin m\theta_2$,

$$fm_2 = \sin m\theta_3 - \sin m\theta_4.$$

Integration for THIRD TERM

$$I_3 = \int_u^l \int_L^U -\left[\cos\frac{n\pi}{a}y_p + (-1)^{m+n}\cos\frac{m\pi}{a}y_p\right]\left[\cos\frac{m\pi}{a}x_q + (-1)^{m+n}\cos\frac{n\pi}{a}x_q\right]dy_p dx_q$$

$$= \left[-\frac{a}{n\pi}fn_1 + \frac{(-1)^{m+n}a}{m\pi}fm_1\right]\left[\frac{a}{m\pi}fm_2 + \frac{(-1)^{m+n}a}{n\pi}fn_2\right]$$

$$= -\frac{a^2}{mn\pi^2}fn_1 fm_2 - \frac{(-1)^{m+n}a^2}{m^2\pi^2}fm_1 fm_2 - \frac{(-1)^{m+n}a^2}{n^2\pi^2}fn_1 fn_2 - \frac{a^2}{mn\pi^2}fm_1 fn_2$$

When the four terms arising from the above product are introduced into the double sum (8A.3.1) it is found, by symmetry that duplication occurs and only the following two terms are required.

$$I_3 = -\frac{2a^2}{mn\pi^2}fn_1 fm_2 - \frac{(-1)^{m+n}2a^2}{m^2\pi^2}fm_1 fm_2 \qquad (8A.3.4)$$

B: Summations

From the integrations, therefore,

$$Z_{pq} = -\frac{2j\omega\mu h}{W_p W_q}\left[-\frac{W_p W_q}{k^2 a^2} - \frac{W_p W_q}{\pi^2}Sm_1 - \frac{aW_q}{\pi^3}Sm_2 - \frac{aW_p}{\pi^3}Sm_3 - \frac{a^2}{\pi^4}Sm_4 - \frac{2a^2}{\pi^4}Smn_5\right.$$

$$\left.-\frac{2a^2}{\pi^4}Smn_6\right] \qquad (8A.3.5)$$

where,

$$Sm_1 = \sum_{m=1}^{\infty}\frac{(-1)^m}{m^2 - A^2}$$

$$= \frac{\pi^2}{2a^2 k^2} - \frac{\pi}{2A\sin A\pi} \qquad (8A.3.6)$$

$$Sm_2 = \sum_{m=1}^{\infty}\frac{(\sin m\theta_1 - \sin m\theta_2)}{m\ (m^2 - A^2)} \qquad (8A.3.7)$$

$$Sm_3 = \sum_{m=1}^{\infty}\frac{(\sin m\theta_3 - \sin m\theta_4)}{m\ (m^2 - A^2)}$$

$$= \frac{W_q \pi^3}{2k^2 a^3} + \frac{\pi^2\big(\sin A(\pi - \theta_3) - \sin A(\pi - \theta_4)\big)}{2k^2 a^2 \sin ka} \qquad (8A.3.8)$$

208

$$Sm_4 = \sum_{m=1}^{\infty} \frac{(-1)^m F_1(m:\theta_1,\theta_2,\theta_3,\theta_4)}{m^2(m^2-A^2)}$$

(8A.3.9)

$$Smn_5 = \sum_{m=1}^{\infty}\sum_{n=1}^{\infty} \frac{F_2(m,n:\theta_1,\theta_2,\theta_3,\theta_4)}{mn(m^2+n^2-A^2)}$$

$$= \sum_{m=1}^{\infty} \frac{(\sin m\theta_1 - \sin m\theta_2)}{m} \sum_{n=1}^{\infty} \frac{(-1)^n(\sin n\theta_3 - \sin n\theta_4)}{n(n^2+B^2)}$$

$$= \sum_{m=1}^{\infty} \frac{(\sin m\theta_1 - \sin m\theta_2)}{m} \left\{ \frac{\pi \sinh B\theta_3}{2B^2 \sinh B\pi} - \frac{\theta_3}{2B^2} - \frac{\pi \sinh B\theta_4}{2B^2 \sinh B\pi} + \frac{\theta_4}{2B^2} \right\}$$

$$= -\frac{\pi}{2}\sum_{m=1}^{\infty} \frac{(\sin m\theta_1 - \sin m\theta_2)\left[\sinh B\ (\pi-\theta_3)-\sinh B\ (\pi-\theta_4)\right]}{m\ (m^2-A^2)\sinh B\pi} - \frac{\pi^2}{2a^2}\sum_{m=1}^{\infty} \frac{(\sin m\theta_1 - \sin m\theta_2)}{m\ (m^2-A^2)}$$

$$= -\frac{\pi}{2}\sum_{m=1}^{\infty} \frac{(\sin m\ \theta_1 - \sin m\ \theta_2)\left[\sinh B\ (\pi-\theta_3)-\sinh B\ (\pi-\theta_4)\right]}{m\ (m^2-A^2)\sinh B\pi} - \frac{\pi^2}{2\ a^2}Sm_2$$

(8A.3.10)

$$Smn_6 = \sum_{m=1}^{\infty}\sum_{n=1}^{\infty} \frac{(-1)^{m+n} F_1(m:\theta_1,\theta_2,\theta_3,\theta_4)}{m^2(m^2+n^2-A^2)}$$

$$= \sum_{m=1}^{\infty} \frac{(-1)^m F_1(m:\theta_1,\theta_2,\theta_3,\theta_4)}{m^2} + \sum_{n=1}^{\infty} \frac{(-1)^n}{n^2+B^2}$$

$$= \sum_{m=1}^{\infty} \frac{(-1)^m F_1(m:\theta_1,\theta_2,\theta_3,\theta_4)}{m^2} \left\{ \frac{\pi}{2B\sinh B\pi} - \frac{1}{2B^2} \right\}$$

$$= -\frac{1}{2}\sum_{m=1}^{\infty} \frac{(-1)^m F_1(m:\theta_1,\theta_2,\theta_3,\theta_4)}{m^2\ B\sinh \pi B} + \frac{\pi^2}{2a^2}\sum_{m=1}^{\infty} \frac{(-1)^m F_1(m:\theta_1,\theta_2,\theta_3,\theta_4)}{m^2(m^2-A^2)}$$

$$= -\frac{1}{2}\sum_{m=1}^{\infty} \frac{(-1)^m F_1(m:\theta_1,\theta_2,\theta_3,\theta_4)}{m^2\ B\sinh \pi B} + \frac{\pi^2}{2a^2}Sm_4$$

(8A.3.11)

where, $F_1(m:\theta_1,\theta_2,\theta_3,\theta_4)$ and $F_2(m,n:\theta_1,\theta_2,\theta_3,\theta_4)$ are defined as in case(A), and,

$$\theta_1 = \frac{\pi}{a}\left(y_p+\frac{W_p}{2}\right); \quad \theta_2 = \frac{\pi}{a}\left(y_p-\frac{W_p}{2}\right); \quad \theta_3 = \frac{\pi}{a}\left(x_q+\frac{W_q}{2}\right); \quad \theta_3 = \frac{\pi}{a}\left(x_q-\frac{W_q}{2}\right).$$

Using equations (8A.3.6), (8A.3.8), (8A.3.10)and (8A.3.11) in equation (8A.3.5) eliminates the terms $W_pW_q/k^2\ a^2$, Sm_2 and Sm_4, to give

$$Z_{pq} = \frac{j\omega\mu h}{W_p W_q}\left[\frac{W_p W_q}{ka\sin ka} - \frac{W_p(\sin A(\pi - \theta 3) - \sin A(\pi - \theta 3))}{k^2 a \sin ka} - \frac{2a^2}{\pi^3}\sum_{m=1}^{\infty}\frac{(-1)^m F_1(m:\theta_1,\theta_2,\theta_3,\theta_4)}{m^2 B \sinh\pi B}\right.$$

$$\left. + \frac{2a^2}{\pi^3}\sum_{m=1}^{\infty}\frac{(\sin m\theta_1 - \sin m\theta_2)[\sinh B(\pi - \theta_3) - \sinh B(\pi - \theta_4)]}{mB^2 \sinh B\pi}\right] \qquad (8A.3.12)$$

A8.4 Case (c) : Ports at Centres $(0, y_p)$, $(x_q, a - x_q)$

A : Integrations

$$Z_{pq} = \frac{2\sqrt{2} j\omega\mu h}{W_p W_q \pi^2}\int_l^u\int_L^U\left\{-\frac{\pi^2}{a^2 k^2} + \sum_{m=1}^{\infty}\frac{\left[1+(-1)^m\cos\frac{m\pi}{a}y_p\right]\left[\cos\frac{m\pi}{a}x_q + (-1)^m\cos\frac{m\pi}{a}x_q\right]}{m^2 - A^2}\right.$$

$$+ \sum_{m=1}^{\infty}\sum_{n=1}^{\infty}\left[\cos\frac{n\pi}{a}y_p + (-1)^{m+n}\cos\frac{m\pi}{a}y_p\right] \times$$

$$\left. \frac{\left[\cos\frac{m\pi}{a}x_q\cos\frac{n\pi}{a}(a-x_q) + (-1)^{m+n}\cos\frac{n\pi}{a}x_q\cos\frac{m\pi}{a}(a-x_q)\right]}{m^2 + n^2 - A^2}\right\}dy_p dx_q \quad (8A.4.1)$$

where, $U = y_p + \dfrac{W_p}{2}$, $L = y_p - \dfrac{W_p}{2}$, $u = x_q + \dfrac{W_q}{2\sqrt{2}}$, $l = x_q - \dfrac{W_q}{2\sqrt{2}}$

Integration for FIRST TERM

$$I_1 = \int_l^u\int_L^U 1 \cdot dy_p dx_q = \frac{W_p W_q}{\sqrt{2}} \qquad (8A.4.2)$$

Integration for SECOND TERM

$$I_2 = \int_l^u\int_L^U\left[1+(-1)^m\cos\frac{m\pi}{a}y_p\right]\left[\cos\frac{m\pi}{a}x_q + (-1)^m\cos\frac{m\pi}{a}(a-x_q)\right]dy_p dx_q$$

$$= \left[W_p + \frac{(-1)^m a}{m\pi}(\sin m\theta_1 - \sin m\theta_2)\right]\left[\frac{a}{m\pi}(\sin m\theta_3 - \sin m\theta_4) + (-1)^m\frac{a}{m\pi}[\sin m(\pi-\theta_3) - \sin m(\pi-\theta_4)]\right]$$

$$= \frac{W_p 2a}{m\pi}fm_2 + (-1)^m\frac{2a^2}{m^2\pi^2}fm_1 fm_2 \qquad (8A.4.3)$$

Where, $\theta_1 = \dfrac{\pi U}{a}$, $\theta_2 = \dfrac{\pi L}{a}$, $\theta_3 = \dfrac{\pi u}{a}$, $\theta_4 = \dfrac{\pi l}{a}$, $fm_1 = \sin m\theta_1 - \sin m\theta_2$,

$fm_2 = \sin m\theta_3 - \sin m\theta_4$.

<u>Integration for THIRD TERM</u>

$$I_3 = \int\limits_u^l \int\limits_L^U \left[\cos n\frac{\pi}{a} y_p + (-1)^{m+n} \cos m\frac{\pi}{a} y_p \right] \text{ x}$$

$$\left[\cos\frac{m\pi}{a} x_q \cos\frac{n\pi}{a}(a - x_q) + (-1)^{m+n} \cos\frac{n\pi}{a} x_q \cos\frac{m\pi}{a}(a - x_q) \right] dy_p dx_q$$

$$= \left[\frac{a}{n\pi} fm_1 + \frac{(-1)^{m+n} a}{m\pi} fm_1 \right] \text{ x}$$

$$\left[\frac{(-1)^n a}{(m+n)\pi}\left[\sin(m+n)\theta_3 - \sin(m+n)\theta_4 \right] + \frac{(-1)^n a}{(m-n)\pi}\left[\sin(m-n)\theta_3 - \sin(m-n)\theta_4 \right] \right] \quad (8A.4.4)$$

B: Summations

From the integrations, therefore,

$$Z_{pq} = \frac{j2\omega\mu h}{W_p W_q}\left[-\frac{W_p W_q}{k^2 a^2} + \frac{2\sqrt{2} a W_p}{\pi^3} Sm_1 + \frac{2\sqrt{2} a^2}{\pi^4} Sm_2 + \frac{\sqrt{2} a^2}{2\pi^4} Sm_3 \right.$$

$$\left. + \frac{a W_q}{\pi^3} Sm_4 + \frac{4\sqrt{2} a^2}{\pi^4} Smn_5 \right] \qquad (8A.4.5)$$

where,

$$Sm_1 = \sum_{m=1}^{\infty} \frac{(\sin m\theta_3 - \sin m\theta_4)}{m \ (m^2 - A^2)}$$

$$= \frac{W_q \pi^3}{2\sqrt{2} \ k^2 a^3} + \frac{\pi^2}{2k^2 a^2 \sin ka} \left[\sin A(\pi - \theta_3) - \sin A(\pi - \theta_4) \right] \qquad (8A.4.6)$$

$$Sm_2 = \sum_{m=1}^{\infty} \frac{(-1)^m F_1(m : \theta_1, \theta_2, \theta_3, \theta_4)}{m^2 \ (m^2 - A^2)}$$

$$= \sum_{m=1}^{\infty} \frac{(-1)^m (\sin m\theta_1 - \sin m\theta_2)(\sin m\theta_3 - \sin m\theta_4)}{m^2 \ (m^2 - A^2)}$$

$$= \sum_{m=1}^{\infty} \frac{(-1)^m (\sin m\theta_1 \sin m\theta_3 - \sin m\theta_2 \sin m\theta_3 - \sin m\theta_1 \sin m\theta_4 + \sin m\theta_2 \sin m\theta_4)}{m^2 \ (m^2 - A^2)}$$

$$= \frac{1}{2} \sum_{m=1}^{\infty} \frac{(-1)^m \left[\displaystyle\sum_{i=1,4,6,7} \cos m\alpha_i - \sum_{i=2,3,5,8} \cos m\alpha_i \right]}{m^2 \ (m^2 - A^2)}$$

where, $\alpha_1 = \theta_1 - \theta_3$, $\quad \alpha_2 = \theta_1 + \theta_3$, $\quad \alpha_3 = \theta_2 - \theta_3$, $\quad \alpha_4 = \theta_2 + \theta_3$, $\quad \alpha_5 = \theta_1 - \theta_4$, $\quad \alpha_6 = \theta_1 + \theta_4$,

$\alpha_7 = \theta_2 - \theta_4 \quad \alpha_8 = \theta_2 + \theta_4$.

Therefore,

$$Sm_2 = \frac{1}{2} \sum_{m=1}^{\infty} \left\{ \sum_{i=1,4,6,7} \frac{(-1)^m \cos m\alpha_i}{m^2 (m^2 - A^2)} - \sum_{i=2,3,5,8} \frac{(-1)^m \cos m\alpha_i}{m^2 (m^2 - A^2)} \right\}$$

$$= \frac{1}{2} \left\{ \frac{1}{2A^2} \left[-\frac{\alpha_1^2}{2} - \frac{\pi \cos A\alpha_1}{A \sin A\pi} + \frac{\pi^2}{6} + \frac{1}{A^2} \right] \pm \left(\begin{array}{l} \text{Duplicate terms in } \alpha_2, \alpha_3, \ldots \ldots \alpha_8 \\ \text{a total of 32 terms.} \end{array} \right) \right\}$$

From the extensive algebraic detail it is found that 16 of the 32 terms cancel along with the terms $\pi^2/6$, and, $1/A^2$. Hence,

$$Sm_2 = \frac{1}{2} \left\{ \frac{1}{2A^2} \left[-\frac{\alpha_1^2}{2} - \frac{\pi \cos A\alpha_1}{A \sin A\pi} \right] \pm \left(\begin{array}{l} \text{Duplicate terms in } \alpha_2, \alpha_3, \ldots \ldots \alpha_8 \\ \text{a total of 16 terms.} \end{array} \right) \right\}$$

Further,

$$\sum_{i=1,4,6,7} \alpha_i^2 - \sum_{i=2,3,5,8} \alpha_i^2 = 4(\theta_1 - \theta_2)(\theta_3 - \theta_4) = \frac{4\pi^2 W_p W_q}{a^2 \sqrt{2}}$$

and,

$$\sum_{i=1,4,6,7} \cos A\alpha_i - \sum_{i=2,3,5,8} \cos A\alpha_i = 2(\sin A\theta_1 - \sin A\theta_2)(\sin A\theta_3 - \sin A\theta_4)$$

therefore the expression for Sm_2 simplifies to

$$Sm_2 = \frac{W_p W_q \pi^4}{2\sqrt{2} k^2 a^4} + \frac{\pi^4 (\sin A\theta_1 - \sin A\theta_2)(\sin A\theta_3 - \sin A\theta_4)}{k^3 a^3 \sin ka} \qquad (8A.4.7)$$

$$Sm_3 = \sum_{m=1}^{\infty} \frac{(-1)^m (\sin m\theta_1 - \sin m\theta_2)(\sin m2\theta_3 - \sin m2\theta_4)}{m^2 \ (m^2 - A^2/2)} \qquad (8A.4.8)$$

$$Sm_4 = \sum_{m=1}^{\infty} \frac{(-1)^m (\sin m\theta_1 - \sin m\theta_2)}{m^2 \ (m^2 - A^2/2)}$$

$$= \frac{W_p \pi^3}{k^2 a^3} - \frac{\pi^3 \left(\sin \frac{A}{\sqrt{2}} \theta_1 - \sin \frac{A}{\sqrt{2}} \theta_2 \right)}{k^2 a^2 \sin \frac{ka}{\sqrt{2}}} \qquad (8A.4.9)$$

$$Smn_5 = \sum_{n=1}^{\infty} \sum_{m=n+1}^{\infty} \frac{(-1)^m (\sin m\theta_1 - \sin m\theta_2)}{m \ (m^2 + n^2 - A^2)} \left[\frac{\sin(m+n)\theta_3 - \sin(m+n)\theta_4}{m+n} \right.$$

$$\left. + \frac{\sin(m-n)\theta_3 - \sin(m-n)\theta_4}{m-n} \right] (8A.4.10)$$

where, $F_1(m : \theta_1, \theta_2, \theta_3, \theta_4)$ is defined as in section A8.2,

$$\theta_1 = \frac{\pi}{a} \left(y_p + \frac{W_p}{2} \right); \quad \theta_2 = \frac{\pi}{a} \left(y_p - \frac{W_p}{2} \right); \quad \theta_3 = \frac{\pi}{a} \left(x_q + \frac{W_q}{2\sqrt{2}} \right); \quad \theta_3 = \frac{\pi}{a} \left(x_q - \frac{W_q}{2\sqrt{2}} \right).$$

Using equations (8A.4.6), (8A.4.7) and (8A.4.9) in equation (8A.4.5) eliminates the term $W_p W_q / k^2 a^2$ to give

$$Z_{pq} = -\frac{j2\omega\mu h}{W_p W_q} \left[\frac{2 W_p W_q}{k^2 a} + \frac{\sqrt{2} \ W_p \left(\sin A(\pi - \theta_3) - \sin A(\pi - \theta_4) \right)}{k^2 a \pi \sin ka} - \frac{\sqrt{2} \left(\sin A\theta_1 - \sin A\theta_2 \right) \left(\sin A\theta_3 - \sin A\theta_4 \right)}{k^2 a \sin ka} \right.$$

$$- \frac{W_q \left(\sin \frac{A}{\sqrt{2}} \theta_1 - \sin \frac{A}{\sqrt{2}} \theta_2 \right)}{k^2 a \sin \frac{ka}{\sqrt{2}}} + \frac{a^2 \sqrt{2}}{2\pi^4} \sum_{m=1}^{\infty} \frac{(-1)^m (\sin m\theta_1 - \sin m\theta_2)(\sin 2\theta_3 - \sin 2\theta_4)}{m^2 \ (m^2 - A^2/2)}$$

$$+ \frac{2\sqrt{2} \ a^2}{\pi^4} \sum_{n=1}^{\infty} \sum_{m=n+1}^{\infty} \frac{(-1)^m (\sin m\theta_1 - \sin m\theta_2)}{m \ (m^2 + n^2 - A^2)} \left[\frac{\sin(m+n)\theta_3 - \sin(m+n)\theta_4}{m+n} \right.$$

$$\left. + \frac{\sin(m-n)\theta_3 - \sin(m-n)\theta_4}{m-n} \right] (8A.4.11)$$

In the formula (8A.4.11), it appears that the single summation, on m, could be obtained in closed form. An investigation has revealed that while this is mathematically possible it is however computationally impractical. This is because in detail, the procedure generates EIGHT infinite series, and, each series has two closed forms depending on the required interval of convergence. The result is that it is computationally more efficient to evaluate directly the small number of series terms required for convergence.

A8.5 Case (d) : Ports at Centres $\left(x_p, a - x_p\right)$, $\left(x_q, a - x_q\right)$

A : Integrations

$$Z_{pq} = \frac{2j\omega\mu h}{W_p W_q \pi^2} \int_l^u \int_L^U \left\{ \frac{\pi^2}{a^2 k^2} + \sum_{m=1}^{\infty} \frac{\left[\cos m\frac{\pi}{a}x_p + (-1)^m \cos m\frac{\pi}{a}\left(a - x_q\right)\right]\left[\cos m\frac{\pi}{a}x_q + (-1)^m \cos m\frac{\pi}{a}\left(a - x_q\right)\right]}{m^2 - A^2} \right.$$

$$+ \sum_{m=1}^{\infty}\sum_{n=1}^{\infty}\left[\cos m\frac{\pi}{a}x_p \cos n\frac{\pi}{a}\left(a - x_q\right) + (-1)^{m+n} \cos n\frac{\pi}{a}x_q \cos m\frac{\pi}{a}\left(a - x_q\right)\right] \times$$

$$\left. \frac{\left[\cos m\frac{\pi}{a}x_q \cos n\frac{\pi}{a}\left(a - x_q\right) + (-1)^{m+n} \cos n\frac{\pi}{a}x_q \cos m\frac{\pi}{a}\left(a - x_q\right)\right]}{m^2 + n^2 - A^2} \right\} 2\, dx_p dx_q \quad (8A.5.1)$$

where, $U = x_p + \dfrac{W_p}{2\sqrt{2}}$, $L = x_p - \dfrac{W_p}{2\sqrt{2}}$, $u = x_q + \dfrac{W_q}{2\sqrt{2}}$, $l = x_q - \dfrac{W_q}{2\sqrt{2}}$

Integration for FIRST TERM

$$I_1 = \int_l^u \int_L^U 2 \cdot dx_p dx_q = W_p W_q \qquad (8A.5.2)$$

Integration for SECOND TERM

$$I_2 = \int_l^u \int_L^U \left[\cos m\frac{\pi}{a}x_p + (-1)^m \cos m\frac{\pi}{a}\left(a - x_q\right)\right]\left[\cos m\frac{\pi}{a}x_q + (-1)^m \cos m\frac{\pi}{a}\left(a - x_q\right)\right] 2\, dx_p dx_q$$

$$= \frac{8a^2}{m^2 \pi^2}\left(\sin m\theta_1 - \sin m\theta_2\right)\left(\sin m\theta_3 - \sin m\theta_4\right)$$

$$= \frac{8a^2}{m^2 \pi^2} fm_1 fm_2 \qquad (8A.5.3)$$

Where, $\theta_1 = \dfrac{\pi U}{a}$, $\theta_2 = \dfrac{\pi L}{a}$, $\theta_3 = \dfrac{\pi u}{a}$, $\theta_4 = \dfrac{\pi l}{a}$,

$fm_1 = \sin m\theta_1 - \sin m\theta_2$, $fm_2 = \sin m\theta_3 - s\, \text{in}\, m\theta_4$.

Integration for THIRD TERM

$$I_3 = \int_l^u \int_L^U \left\{ \left[\cos m\frac{\pi}{a}x_p \cos n\frac{\pi}{a}(a-x_p) + (-1)^{m+n} \cos n\frac{\pi}{a}x_p \cos m\frac{\pi}{a}(a-x_p) \right] \times \right.$$

$$\left. \left[\cos m\frac{\pi}{a}x_q \cos n\frac{\pi}{a}(a-x_q) + (-1)^{m+n} \cos n\frac{\pi}{a}x_q \cos m\frac{\pi}{a}(a-x_q) \right] \right\} 2\, dx_p dx_q$$

$$= \frac{2a^2}{\pi^2} \left[\frac{\sin(m+n)\theta_1 - \sin(m+n)\theta_2}{m+n} + \frac{\sin(m+n)\theta_1 - \sin(m+n)\theta_2}{m+n} \right] \times$$

$$\left[\frac{\sin(m+n)\theta_3 - \sin(m+n)\theta_4}{m+n} + \frac{\sin(m-n)\theta_3 - \sin(m-n)\theta_4}{m-n} \right] \qquad (8A.5.4)$$

B: Summations

From the integrations, therefore,

$$Z_{pq} = \frac{j2\omega\mu h}{W_p W_q} \left[-\frac{W_p W_q}{k^2 a^2} + \frac{8}{\pi^4}\frac{a^2}{} Sm_1 + \frac{a^2}{4\pi^4} Sm_2 + \frac{a^2 W_p}{2\sqrt{2}\pi^4} Sm_3 + \frac{a^2 W_q}{2\sqrt{2}\pi^4} Sm_4 + \frac{a^2 W_p W_q}{2\pi^4} Sm_5 \right.$$

$$\left. + \frac{4a^2}{\pi^4} Smn_6 \right] \qquad (8A.5.5)$$

where,

$$Sm_1 = \sum_{m=1}^{\infty} \frac{F_1(m:\theta_1,\theta_2,\theta_3,\theta_4)}{m^2(m^2 - A^2)}$$

$$= \sum_{m=1}^{\infty} \frac{(\sin m\theta_1 - \sin m\theta_2)(\sin m\theta_3 - \sin m\theta_4)}{m^2(m^2 - A^2)}$$

$$= \frac{1}{2}\sum_{m=1}^{\infty} \left\{ \sum_{i=1,4,6,7} \frac{\cos m\alpha_i}{m^2(m^2 - A^2)} - \sum_{i=2,3,5,8} \frac{\cos m\alpha_i}{m^2(m^2 - A^2)} \right\}$$

where α_i is given in Case (c).

Then,

$$Sm_1 = \frac{1}{2A^2} \left\{ \left[\pi\alpha_1 - \frac{\alpha_1^2}{2} - \frac{\pi \cos A(\pi - \alpha_1)}{A \sin A\pi} - \frac{\pi^2}{3} + \frac{1}{A^2} \right] \pm \left(\begin{array}{l} \text{Duplicate terms in } \alpha_2, \alpha_3, \ldots \ldots \alpha_8 \\ \text{a total of 40 terms.} \end{array} \right) \right\}$$

From the extensive algebraic detail it is found that 24 of the 40 terms cancel along with the terms $-\pi^2/3$, and, $1/A^2$. Hence,

$$Sm_1 = \frac{1}{2A^2}\left\{\left[-\frac{\alpha_1^2}{2} - \frac{\pi\cos A(\pi-\alpha_1)}{A\sin A\pi}\right] \pm \left(\begin{array}{l}\text{Duplicate terms in } \alpha_2,\alpha_3,......\alpha_8 \\ \text{a total of 16 terms.}\end{array}\right)\right\}$$

Further,

$$\sum_{i=1,4,6,7}\alpha_i^2 - \sum_{i=2,3,5,8}\alpha_i^2 = 4(\theta_1-\theta_2)(\theta_3-\theta_4) = \frac{\pi^2 W_p W_q}{a^2}$$

and,

$$\sum_{i=1,4,6,7}\cos A(\pi-\alpha_i) - \sum_{i=2,3,5,8}\cos A(\pi-\alpha_i) = \left[\sin A(\pi-\theta_1) - \sin A(\pi-\theta_2)\right]\left[\sin A\theta_3 - sinA\theta_4\right]$$

therefore the expression for $S_1(m)$ simplifies to

$$Sm_1 = \frac{\pi^4 W_p W_q}{2k^2 a^4} + \frac{\pi^4\left(\sin A(\pi-\theta_1) - \sin A(\pi-\theta_2)\right)\left(\sin A\theta_3 - \sin A\theta_4\right)}{k^3 a^3 \sin ka} \qquad (8A.5.6)$$

$$Sm_2 = \sum_{m=1}^{\infty}\frac{(\sin m2\theta_1 - \sin m2\theta_2)(\sin m2\theta_3 - \sin m2\theta_4)}{m^2\ (m^2 - A^2/2)} \qquad (8A.5.7)$$

$$Sm_3 = \sum_{m=1}^{\infty}\frac{(\sin m2\theta_3 - \sin m2\theta_4)}{m\ (m^2 - A^2/2)}$$

$$= \frac{\pi^3 W_q}{\sqrt{2}\ k^2 a^3} + \frac{\pi^3\left(\sin\frac{A}{\sqrt{2}}(\pi-2\theta_3) - \sin\frac{A}{\sqrt{2}}(\pi-2\theta_4)\right)}{k^2 a^2\ \sin ka/\sqrt{2}} \qquad (8A.5.8)$$

$$Sm_4 = \sum_{m=1}^{\infty}\frac{(\sin m2\theta_1 - \sin m2\theta_2)}{m\ (m^2 - A^2/2)}$$

$$= \frac{\pi^3 W_q}{\sqrt{2}\ k^2 a^3} + \frac{\pi^3\left(\sin\frac{A}{\sqrt{2}}(\pi-2\theta_1) - \sin\frac{A}{\sqrt{2}}(\pi-2\theta_2)\right)}{k^2 a^2\ \sin ka/\sqrt{2}} \qquad (8A.5.9)$$

$$Sm_5 = \sum_{m=1}^{\infty}\frac{1}{(m^2 - A^2/2)}$$

$$= \frac{\pi^2}{k^2 a^2} - \frac{\sqrt{2}\ \pi\cot ka/\sqrt{2}}{2ka} \qquad (8A.5.10)$$

$$Smn_6 = \sum_{n=1}^{\infty}\sum_{m=n+1}^{\infty}\left[\frac{\left(\sin(m+n)\theta_1 - \sin(m+n)\theta_2\right)}{(m+n)\ (m^2+n^2-A^2)} + \frac{\left(\sin(m-n)\theta_1 - \sin(m-n)\theta_2\right)}{(m-n)\ (m^2+n^2-A^2)}\right]\left[\frac{\left(\sin(m+n)\theta_3 - \sin(m+n)\theta_4\right)}{(m+n)}\right.$$

$$\left. + \frac{\left(\sin(m-n)\theta_3 - \sin(m-n)\theta_4\right)}{(m-n)}\right] \qquad (8A.5.11)$$

where, $F_1(m : \theta_1, \theta_2, \theta_3, \theta_4)$ is   defined   as   in   Section   A8.2   ,

$$\theta_1 = \frac{\pi}{a}\left(x_p - \frac{W_p}{2\sqrt{2}}\right), \theta_2 = \frac{\pi}{a}\left(x_p + \frac{W_p}{2\sqrt{2}}\right), \theta_3 = \frac{\pi}{a}\left(x_q - \frac{W_q}{2\sqrt{2}}\right), \theta_4 = \frac{\pi}{a}\left(x_q - \frac{W_q}{2\sqrt{2}}\right).$$

Using equations (8A.5.7), (8A.5.8), (8A.5.9) and (8A.5.10) in equation (8A.5.5) eliminates the term $W_p W_q / k^2 a^2$ to give

$$Z_{pq} = -\frac{j2\omega\mu h}{W_p W_q}\left[\frac{W_p W_q}{k^2 a^2} + \frac{W_p W_q}{4\pi k^2 a} + \frac{W_q^2}{4\pi^2 ka} + \frac{W_p W_q}{2\pi^2 k^2} + \frac{4\left(\sin A(\pi - \theta_1) - \sin A(\pi - \theta_2)\right)\left(\sin A\theta_3 - \sin A\theta_4\right)}{k^3 a \sin ka}\right.$$

$$+ \frac{W_p\left(\sin\frac{A}{\sqrt{2}}(\pi - 2\theta_3) - \sin\frac{A}{\sqrt{2}}(\pi - 2\theta_4)\right)}{2\sqrt{2}\,\pi\,k^2\,\sin\,ka/\sqrt{2}} + \frac{W_q\left(\sin\frac{A}{\sqrt{2}}(\pi - 2\theta_1) - \sin\frac{A}{\sqrt{2}}(\pi - 2\theta_2)\right)}{2\sqrt{2}\,\pi\,k^2\,\sin\,ka/\sqrt{2}}$$

$$+ \frac{a^2}{4\pi^4}\sum_{m=1}^{\infty}\frac{(\sin m2\theta_1 - \sin m2\theta_2)(\sin m2\theta_3 - \sin m2\theta_4)}{m^2\,(m^2 - A^2/2)}$$

$$+ \frac{4a^2}{\pi^4}\sum_{n=1}^{\infty}\sum_{m=n+1}^{\infty}\left[\frac{\left(\sin(m+n)\theta_1 - \sin(m+n)\theta_2\right)}{(m+n)\,(m^2 + n^2 - A^2)} + \frac{\left(\sin(m-n)\theta_1 - \sin(m-n)\theta_2\right)}{(m-n)\,(m^2 + n^2 - A^2)}\right]\left[\frac{\left(\sin(m+n)\theta_3 - \sin(m+n)\theta_4\right)}{(m+n)}\right.$$

$$\left.\left. + \frac{\left(\sin(m-n)\theta_3 - \sin(m-n)\theta_4\right)}{(m-n)}\right] \right] \quad (8A.5.12)$$

The possible closed form for the single summation on 'm', above, is not used for the reasoning described in the previous Case(c).

APPENDIX 9A

The Mathcad Program Listing for the Impedance Evaluation

Define:

$\varepsilon_0, \varepsilon_r, \mu_0, \mu_r, c, f_0, h, k_0, \delta, W, N, N1, M1.$

$$\Delta f := \frac{fo}{2 \cdot Q_0}$$

$$fH := fo + \Delta f$$

$$fr := fH$$

$$b1 := \frac{1}{2 \cdot fr \cdot \sqrt{\mu \cdot \varepsilon}} \cdot \sqrt{\frac{2}{\varepsilon r + 1}}$$

$$\varepsilon eff := \frac{\varepsilon r + 1}{2} + \frac{\varepsilon r - 1}{2} \cdot \left(1 + 12 \cdot \frac{h}{b1}\right)^{-\frac{1}{2}}$$

$$\Delta L := 0.412 h \cdot \frac{(\varepsilon reff + 0.3) \cdot \left(\frac{b1}{h} \cdot 0.264\right)}{(\varepsilon reff - 0.258) \cdot \left(\frac{b1}{h} + 0.8\right)}$$

$$a1 := \frac{c}{2 \cdot fr \cdot \sqrt{\varepsilon eff}} - \Delta L$$

$$Zo := \frac{120 \pi}{\sqrt{\varepsilon eff} \cdot \left[\frac{b1}{h} + 1.393 + \left(0.667 \ln\left(\frac{b1}{h} + 1.444\right)\right)\right]}$$

$$I1 := \int_0^\pi \left(\frac{\sin\left(\frac{k0 \cdot b1}{2} \cdot \cos(\theta)\right)}{\cos(\theta)}\right) \cdot \sin(\theta)^3 \, d\theta$$

$$G1 := \frac{I1}{120 \pi^2}$$

218

$$G12 := \frac{1}{120\,\pi^2} \cdot \int_0^{\pi} \left(\frac{\sin\left(\frac{k0 \cdot b1}{2} \cdot \cos(\theta)\right)}{\cos(\theta)} \right) \cdot J0\big(k0 \cdot a1 \cdot \sin(\theta)\big) \cdot \sin(\theta)^3 \, d\theta$$

$$Rin := \frac{1}{(G1 + G12) \cdot 2}$$

$$Qd := \frac{1}{\tan \delta}$$

$$Qc := h \cdot \sqrt{\mu \cdot \pi \cdot f \cdot \sigma c}$$

$$Qr := \frac{\pi}{4 \cdot Gr \cdot Zo}$$

$$\frac{1}{Q_0} := \frac{1}{Qd} + \frac{1}{Qc} + \frac{1}{Qr}$$

$$S := a1^2$$

$$\Delta s := \frac{S}{2 \cdot Q}$$

$$a2 := \sqrt{\Delta s}$$

$$\omega := 2 \cdot \pi \cdot fo$$

$$k := \sqrt{(\omega)^2 \cdot \mu \cdot \varepsilon 0 \cdot \varepsilon r \cdot (1 - i \cdot \delta)}$$

$$A := \frac{k \cdot a1}{\pi}$$

$$B := \frac{k \cdot b1}{\pi}$$

$$A2 := \frac{k \cdot a2}{\pi}$$

$$T := \frac{b1}{2}$$

For Zppγ

$$\theta 1 := \frac{\pi}{b1} \cdot \left(T + \frac{w}{2} \right) \qquad \theta 2 := \frac{\pi}{b1} \cdot \left(T - \frac{w}{2} \right) \qquad \theta 3 := \theta 1 \qquad \theta 4 := \theta 2$$

$$D := \frac{\big(\sin(n \cdot \theta 1) - \sin(n \cdot \theta 2)\big) \cdot \big(\sin(n \cdot \theta 3) - \sin(n \cdot \theta 4)\big)}{n^2 \cdot \sqrt{n^2 - (B)^2}}$$

$$E := \coth\left[\pi\cdot\left[\frac{a1}{b1}\cdot\sqrt{n^2 - (B)^2}\right]\right]$$

$$Zpp\gamma := \frac{i\cdot\omega\cdot\mu\cdot h}{a1\cdot b1}\cdot\left[\left(\frac{-a1}{k}\cdot\cot(k\cdot a1)\right)\ldots + \frac{2\cdot b1^3\cdot a1}{\pi^3\cdot w^2}\cdot\left[\sum_{n=1}^{10}(D\cdot E)\right]\right]$$

For Zpqγ

$$\theta1 := \frac{\pi}{b1}\cdot\left(T + \frac{w}{2}\right) \qquad \theta2 := \frac{\pi}{b1}\cdot\left(T - \frac{w}{2}\right)$$

$$D := \frac{\left(\sin(n\cdot\theta1) - \sin(n\cdot\theta2)\right)\cdot\left(\sin(n\cdot\theta3_r) - \sin(n\cdot\theta4_r)\right)}{n^2\cdot\sqrt{n^2 - (B)^2}}$$

$$E := \coth\left[\pi\cdot\left[\frac{a1}{b1}\cdot\sqrt{n^2 - (B)^2}\right]\right]$$

$$Zpq1 := \begin{vmatrix} r \leftarrow 0 \\ \text{for } j \in 1,2..N \\ \quad\begin{vmatrix} \theta3_r \leftarrow \frac{\pi}{b1}\cdot\left[\left[(b1 - a2) + \left(j\cdot\frac{a2}{N+1}\right)\right] + \frac{w}{2}\right] \\ \theta4_r \leftarrow \frac{\pi}{b1}\cdot\left[\left[(b1 - a2) + \left(j\cdot\frac{a2}{N+1}\right)\right] - \frac{w}{2}\right] \\ Z_r \leftarrow \frac{i\cdot\omega\cdot\mu\cdot h}{a1\cdot b1}\cdot\left[\left(\frac{-a1}{k}\cdot\cot(k\cdot a1)\right)\ldots + \frac{2\cdot b1^3\cdot a1}{\pi^3\cdot w^2}\cdot\left[\sum_{n=1}^{10}(D\cdot E)\right]\right] \\ r \leftarrow r + 1 \\ Zi \leftarrow Z^T \end{vmatrix} \\ Zi \end{vmatrix}$$

$$F := \left(\sin(m\cdot\theta2_r) - \sin(m\cdot\theta1_r)\right)$$

$$G := \left[\sinh\left[\left[\sqrt{\frac{b1^2}{a1^2}\cdot\left[m^2 - (A)^2\right]}\right]\cdot(\pi - \theta4)\right] - \sinh\left[\left[\sqrt{\frac{b1^2}{a1^2}\cdot\left[m^2 - (A)^2\right]}\right]\cdot(\pi - \theta3)\right]\right]$$

$$Zpq2 := \begin{array}{|l} r \leftarrow 0 \\[4pt] \text{for } j \in N+1, N+2..2\cdot N \\[4pt] \quad \begin{array}{|l} \theta 1_r \leftarrow \dfrac{\pi}{a1}\cdot\left[\left[(j-N)\cdot\dfrac{a2}{N+1}\right]+\dfrac{w}{2}\right] \\[10pt] \theta 2_r \leftarrow \dfrac{\pi}{a1}\cdot\left[\left[(j-N)\cdot\dfrac{a2}{N+1}\right]-\dfrac{w}{2}\right] \\[10pt] \theta 3 \leftarrow \dfrac{\pi}{b1}\cdot\left(T+\dfrac{w}{2}\right) \\[10pt] \theta 4 \leftarrow \dfrac{\pi}{b1}\cdot\left(T-\dfrac{w}{2}\right) \\[10pt] Z_r \leftarrow \dfrac{1i\cdot\omega\cdot\mu\cdot h}{w^2\cdot a1\cdot b1}\cdot\left[\left[\dfrac{b1\cdot w}{(k)^2\cdot\sin(\pi\cdot B)}\cdot\Big[\sin[B\cdot(\pi-\theta 4)]-\sin[B\cdot(\pi-\theta 3)]\Big]\right] \ldots \right.\\[12pt] \qquad\qquad \left.+\left[\dfrac{2\cdot a1^3\cdot b1}{\pi^3}\cdot\sum_{m=1}^{10}\dfrac{F\cdot G}{m\cdot\left[m^2-(A)^2\right]\cdot\sinh\left[\pi\cdot\sqrt{\dfrac{b1^2}{a1^2}\cdot\left[m^2-(A)^2\right]}\right]}\right]\right] \\[14pt] r \leftarrow r+1 \\[4pt] Zi \leftarrow Z^T \end{array} \\[4pt] Zi \end{array}$$

$$Zpq3 := \begin{array}{|l} r \leftarrow 0 \\[4pt] \text{for } j \in 2\cdot N+1, 2\cdot N+2..3\cdot N \\[4pt] \quad \begin{array}{|l} \theta 1 \leftarrow \dfrac{\pi}{b1}\cdot\left(T-\dfrac{w}{2}\right) \\[10pt] \theta 2 \leftarrow \dfrac{\pi}{b1}\cdot\left(T+\dfrac{w}{2}\right) \\[10pt] \theta 3_r \leftarrow \dfrac{\pi}{b1}\cdot\left[\left[a2-\left[(j-2\cdot N)\cdot\dfrac{a2}{N+1}\right]\right]-\dfrac{w}{2}\right] \\[10pt] \theta 4_r \leftarrow \dfrac{\pi}{b1}\cdot\left[\left[a2-\left[(j-2\cdot N)\cdot\dfrac{a2}{N+1}\right]\right]+\dfrac{w}{2}\right] \\[10pt] Z_r \leftarrow \dfrac{1i\cdot\omega\cdot\mu\cdot h}{b1\cdot w^2}\cdot\left[\left[\dfrac{w^2}{(k)\cdot\sin(k\cdot a1)}\right]\ldots\right.\\[12pt] \qquad\qquad \left.+\dfrac{-2\cdot b1^2\cdot a1}{\pi^3}\cdot\sum_{n=1}^{10}\dfrac{1}{n^2}\cdot\dfrac{\big(\sin(n\cdot\theta 1)-\sin(n\cdot\theta 2)\big)\cdot\big(\sin(n\cdot\theta 3_r)-\sin(n\cdot\theta 4_r)\big)}{\left[\dfrac{a1}{b1}\cdot\sqrt{n^2-(B)^2}\right]\cdot\sinh\left[\pi\cdot\left[\dfrac{a1}{b1}\cdot\sqrt{n^2-(B)^2}\right]\right]}\right] \\[14pt] r \leftarrow r+1 \\[4pt] Zi \leftarrow Z^T \end{array} \\[4pt] Zi \end{array}$$

$$H := \left(\sin\left(m \cdot \theta 2_r\right) - \sin\left(m \cdot \theta 1_r\right) \right)$$

$$I := \left[\sinh\left[\left[\sqrt{\frac{b1^2}{a1^2} \cdot \left[m^2 - (A)^2 \right]} \right] \cdot (\pi - \theta 4) \right] - \sinh\left[\left[\sqrt{\frac{b1^2}{a1^2} \cdot \left[m^2 - (A)^2 \right]} \right] \cdot (\pi - \theta 3) \right] \right]$$

$$Zpq4 := \begin{vmatrix} r \leftarrow 0 \\ \text{for } j \in 3 \cdot N + 1, 3 \cdot N + 2 .. 4 \cdot N \\ \begin{vmatrix} \theta 1_r \leftarrow \frac{\pi}{a1} \cdot \left[\left[a1 - \left[(j - 3 \cdot N) \cdot \frac{a2}{N+1} \right] \right] + \frac{w}{2} \right] \\ \theta 2_r \leftarrow \frac{\pi}{a1} \cdot \left[\left[a1 - \left[(j - 3 \cdot N) \cdot \frac{a2}{N+1} \right] \right] - \frac{w}{2} \right] \\ \theta 3 \leftarrow \frac{\pi}{b1} \cdot \left(T + \frac{w}{2} \right) \\ \theta 4 \leftarrow \frac{\pi}{b1} \cdot \left(T - \frac{w}{2} \right) \\ Z_r \leftarrow \frac{i \cdot \omega \cdot \mu \cdot h}{w^2 \cdot a1 \cdot b1} \cdot \left[\left[\frac{b1 \cdot w}{(k)^2 \cdot \sin(\pi \cdot B)} \cdot \left[\sin\left[B \cdot (\pi - \theta 4) \right] - \sin\left[B \cdot (\pi - \theta 3) \right] \right] \right] ... \\ + \left[\frac{2 \cdot a1^3 \cdot b1}{\pi^3} \cdot \sum_{m=1}^{10} \frac{H \cdot I}{m \cdot \left[m^2 - (A)^2 \right] \cdot \sinh\left[\pi \cdot \sqrt{\frac{b1^2}{a1^2} \cdot \left[m^2 - (A)^2 \right]} \right]} \right] \right] \\ r \leftarrow r + 1 \\ Zi \leftarrow (Z)^T \\ Zi \end{vmatrix} \end{vmatrix}$$

$$Zpq := \text{augment}(Zpq1, Zpq2, Zpq3, Zpq4)$$

$$Zqp\gamma := Zpq^T$$

222

For Zqqγ

$$D := \frac{\left(\sin\left(n \cdot \theta 1_r\right) - \sin\left(n \cdot \theta 2_r\right)\right) \cdot \left(\sin\left(n \cdot \theta 3_{rr}\right) - \sin\left(n \cdot \theta 4_{rr}\right)\right)}{n^2 \cdot \sqrt{n^2 - (B)^2}}$$

$$E := \coth\left[\pi \cdot \left[\frac{a1}{b1} \cdot \sqrt{n^2 - (B)^2}\right]\right]$$

$$
\text{Zqq}\gamma 1 := \begin{vmatrix}
r \leftarrow 0 \\
\text{for } i \in 1, 2 .. N \\
\quad \begin{vmatrix}
rr \leftarrow 0 \\
\text{for } j \in 1, 2 .. N \\
\quad \begin{vmatrix}
\theta 1_r \leftarrow \dfrac{\pi}{b1} \cdot \left[\left[(b1 - a2) + \left(i \cdot \dfrac{a2}{N+1}\right)\right] + \dfrac{w}{2}\right] \\[2mm]
\theta 2_r \leftarrow \dfrac{\pi}{b1} \cdot \left[\left[(b1 - a2) + \left(i \cdot \dfrac{a2}{N+1}\right)\right] - \dfrac{w}{2}\right] \\[2mm]
\theta 3_{rr} \leftarrow \dfrac{\pi}{b1} \cdot \left[\left[(b1 - a2) + \left(j \cdot \dfrac{a2}{N+1}\right)\right] + \dfrac{w}{2}\right] \\[2mm]
\theta 4_{rr} \leftarrow \dfrac{\pi}{b1} \cdot \left[\left[(b1 - a2) + \left(j \cdot \dfrac{a2}{N+1}\right)\right] - \dfrac{w}{2}\right] \\[2mm]
Z_{r, rr} \leftarrow \dfrac{i \cdot \omega \cdot \mu \cdot h}{a1 \cdot b1} \cdot \left[\left(\dfrac{-a1}{k} \cdot \cot(k \cdot a1)\right) \cdots \right. \\
\qquad\qquad \left. + \dfrac{2 \cdot b1^3 \cdot a1}{\pi^3 \cdot w^2} \cdot \left(\sum_{n=1}^{10} D \cdot E\right)\right] \\
\end{vmatrix} \\
\quad\quad rr \leftarrow rr + 1 \\
\quad r \leftarrow r + 1 \\
Z
\end{vmatrix}
$$

$$F := \left(\sin\left(m \cdot \theta 2_{rr}\right) - \sin\left(m \cdot \theta 1_{rr}\right)\right)$$

$$G := \left[\sinh\left[\left[\sqrt{\frac{b1^2}{a1^2} \cdot \left[m^2 - (A)^2\right]}\right] \cdot \left(\pi - \theta 4_r\right)\right] - \sinh\left[\left[\sqrt{\frac{b1^2}{a1^2} \cdot \left[m^2 - (A)^2\right]}\right] \cdot \left(\pi - \theta 3_r\right)\right]\right]$$

$$H := m \cdot \left[m^2 - (A)^2\right] \cdot \sinh\left[\pi \cdot \sqrt{\frac{b1^2}{a1^2} \cdot \left[m^2 - (A)^2\right]}\right]$$

223

$$\text{Zqq}\gamma 12 := \begin{array}{|l} r \leftarrow 0 \\ \text{for } i \in 1,2..N \\ \quad \begin{array}{|l} rr \leftarrow 0 \\ \text{for } j \in N+1, N+2..2 \cdot N \\ \quad \begin{array}{|l} \theta 1_{rr} \leftarrow \dfrac{\pi}{a1} \cdot \left[\left[(j-N) \cdot \dfrac{a2}{N+1}\right] + \dfrac{w}{2}\right] \\[2mm] \theta 2_{rr} \leftarrow \dfrac{\pi}{a1} \cdot \left[\left[(j-N) \cdot \dfrac{a2}{N+1}\right] - \dfrac{w}{2}\right] \\[2mm] \theta 3_{r} \leftarrow \dfrac{\pi}{b1} \cdot \left[\left[a2 - (i) \cdot \dfrac{a2}{N+1}\right] + \dfrac{w}{2}\right] \\[2mm] \theta 4_{r} \leftarrow \dfrac{\pi}{b1} \cdot \left[\left[a2 - (i) \cdot \dfrac{a2}{N+1}\right] - \dfrac{w}{2}\right] \\[2mm] Z_{r, rr} \leftarrow \dfrac{1i \cdot \omega \cdot \mu \cdot h}{w^2 \cdot a1 \cdot b1} \cdot \left[\left[\dfrac{b1 \cdot w}{(k)^2 \cdot \sin(\pi \cdot B)} \cdot \left[\sin\left[B \cdot (\pi - \theta 4_r)\right] - \sin\left[B \cdot (\pi - \theta 3_r)\right]\right]\right] \dots \\ \qquad + \left(\dfrac{2 \cdot a1^3 \cdot b1}{\pi^3} \cdot \sum_{m=1}^{10} \dfrac{F \cdot G}{H}\right)\right] \\[2mm] rr \leftarrow rr + 1 \end{array} \\ r \leftarrow r + 1 \end{array} \\ Z \end{array}$$

$$I := \left(\sin(n \cdot \theta 1_r) - \sin(n \cdot \theta 2_r)\right) \cdot \left(\sin(n \cdot \theta 3_{rr}) - \sin(n \cdot \theta 4_{rr})\right)$$

$$J := \left[\sqrt{\dfrac{a1^2}{b1^2} \cdot \left[n^2 - (B)^2\right]}\right] \cdot \sinh\left[\pi \cdot \left[\sqrt{\dfrac{a1^2}{b1^2} \cdot \left[n^2 - (B)^2\right]}\right]\right]$$

$$\text{Zqq}\gamma 13 := \begin{array}{|l} r \leftarrow 0 \\ \text{for } i \in 1,2.. \, N \\ \quad \begin{array}{|l} rr \leftarrow 0 \\ \text{for } j \in 2 \cdot N + 1, 2 \cdot N + 2.. \, 3 \cdot N \\ \quad \begin{array}{|l} \theta 1_r \leftarrow \dfrac{\pi}{b1} \cdot \left[\left[\left[(b1 - a2) + \left[(i) \cdot \dfrac{a2}{N+1}\right]\right]\right] - \dfrac{w}{2}\right] \\[2em] \theta 2_r \leftarrow \dfrac{\pi}{b1} \cdot \left[\left[\left[(b1 - a2) + \left[(i) \cdot \dfrac{a2}{N+1}\right]\right]\right] + \dfrac{w}{2}\right] \\[2em] \theta 3_{rr} \leftarrow \dfrac{\pi}{b1} \cdot \left[\left[a2 - \left[(j - 2 \cdot N) \cdot \dfrac{a2}{N+1}\right]\right] - \dfrac{w}{2}\right] \\[2em] \theta 4_{rr} \leftarrow \dfrac{\pi}{b1} \cdot \left[\left[a2 - \left[(j - 2 \cdot N) \cdot \dfrac{a2}{N+1}\right]\right] + \dfrac{w}{2}\right] \\[2em] Z_{r,rr} \leftarrow \dfrac{1 i \cdot \omega \cdot \mu \cdot h}{b1 \cdot w^2} \cdot \left[\left[\dfrac{w^2}{(k) \cdot \sin(k \cdot a1)}\right] \cdots \\ \qquad + \dfrac{-2 \cdot b1^2 \cdot a1}{\pi^3} \cdot \displaystyle\sum_{n=1}^{10} \dfrac{1}{n^2} \cdot \dfrac{I}{J}\right] \end{array} \\ \quad rr \leftarrow rr + 1 \end{array} \\ r \leftarrow r + 1 \\ Z \end{array}$$

$$O := \left(\sin\left(m \cdot \theta 2_{rr}\right) - \sin\left(m \cdot \theta 1_{rr}\right)\right)$$

$$P := \left[\sinh\left[\left[\sqrt{\dfrac{b1^2}{a1^2} \cdot \left[m^2 - (A)^2\right]}\right] \cdot \left(\pi - \theta 4_r\right)\right] - \sinh\left[\left[\sqrt{\dfrac{b1^2}{a1^2} \cdot \left[m^2 - (A)^2\right]}\right] \cdot \left(\pi - \theta 3_r\right)\right]\right]$$

$$R := m \cdot \left[m^2 - (A)^2\right] \cdot \sinh\left[\pi \cdot \sqrt{\dfrac{b1^2}{a1^2} \cdot \left[m^2 - (A)^2\right]}\right]$$

$$\text{Zqq}\gamma14 := \begin{array}{|l} r \leftarrow 0 \\ \text{for } i \in 1,2..\,N \\ \quad \begin{array}{|l} rr \leftarrow 0 \\ \text{for } j \in 3\cdot N + 1, 3\cdot N + 2..\,4\cdot N \\ \quad \begin{array}{|l} \theta1_{rr} \leftarrow \dfrac{\pi}{a1}\cdot\left[\left[a1 - \left[(j - 3\cdot N)\cdot\dfrac{a2}{N+1}\right]\right] + \dfrac{w}{2}\right] \\[4mm] \theta2_{rr} \leftarrow \dfrac{\pi}{a1}\cdot\left[\left[a1 - \left[(j - 3\cdot N)\cdot\dfrac{a2}{N+1}\right]\right] - \dfrac{w}{2}\right] \\[4mm] \theta3_{r} \leftarrow \dfrac{\pi}{b1}\cdot\left[\left[(b1 - a2) + \left[(i)\cdot\dfrac{a2}{N+1}\right]\right] + \dfrac{w}{2}\right] \\[4mm] \theta4_{r} \leftarrow \dfrac{\pi}{b1}\cdot\left[\left[(b1 - a2) + \left[(i)\cdot\dfrac{a2}{N+1}\right]\right] - \dfrac{w}{2}\right] \\[4mm] Z_{r,rr} \leftarrow \dfrac{1\cdot i\cdot\omega\cdot\mu\cdot h}{w^2\cdot a1\cdot b1}\cdot\left[\left[\dfrac{b1\cdot w}{(k)^2\cdot\sin(\pi\cdot B)}\cdot\left[\sin\left[B\cdot(\pi - \theta4_r)\right] - \sin\left[B\cdot(\pi - \theta3_r)\right]\right]\right] \dots \right. \\[4mm] \qquad\qquad \left. + \left(\dfrac{2\cdot a1^3\cdot b1}{\pi^3}\cdot\displaystyle\sum_{m=1}^{10}\dfrac{O\cdot P}{R}\right)\right] \\[4mm] rr \leftarrow rr + 1 \end{array} \\ r \leftarrow r + 1 \end{array} \\ Z \end{array}$$

$\text{Zqq}\gamma2 := \text{Zqq}\gamma1$ $\text{Zqq}\gamma23 := \text{Zqq}\gamma14$ $\text{Zqq}\gamma21 := \text{Zqq}\gamma12^T$ $\text{Zqq}\gamma32 := \text{Zqq}\gamma14^T$

$\text{Zqq}\gamma3 := \text{Zqq}\gamma1$ $\text{Zqq}\gamma24 := \text{Zqq}\gamma13$ $\text{Zqq}\gamma31 := \text{Zqq}\gamma13^T$ $\text{Zqq}\gamma42 := \text{Zqq}\gamma24^T$

$\text{Zqq}\gamma4 := \text{Zqq}\gamma1$ $\text{Zqq}\gamma34 := \text{Zqq}\gamma12$ $\text{Zqq}\gamma41 := \text{Zqq}\gamma14^T$ $\text{Zqq}\gamma43 := \text{Zqq}\gamma34^T$

$\text{Zqq}\gamma t1 := \text{augment}(\text{Zqq}\gamma1, \text{Zqq}\gamma12, \text{Zqq}\gamma13, \text{Zqq}\gamma14)$

$\text{Zqq}\gamma t2 := \text{augment}(\text{Zqq}\gamma21, \text{Zqq}\gamma2, \text{Zqq}\gamma23, \text{Zqq}\gamma24)$

$\text{Zqq}\gamma t3 := \text{augment}(\text{Zqq}\gamma31, \text{Zqq}\gamma32, \text{Zqq}\gamma3, \text{Zqq}\gamma34)$

$\text{Zqq}\gamma t4 := \text{augment}(\text{Zqq}\gamma41, \text{Zqq}\gamma42, \text{Zqq}\gamma43, \text{Zqq}\gamma4)$

$\text{Zqq}\gamma := \text{stack}(\text{Zqq}\gamma t1, \text{Zqq}\gamma t2, \text{Zqq}\gamma t3, \text{Zqq}\gamma t4)$

For Zqqβ

$$D := \frac{\left(\sin\left(m\cdot\theta 1_r\right) - \sin\left(m\cdot\theta 2_r\right)\right)\cdot\left(\sin\left(m\cdot\theta 3_{rr}\right) - \sin\left(m\cdot\theta 4_{rr}\right)\right)}{m^2\cdot\left[\sqrt{m^2 - (A2)^2}\right]}$$

$$E := \coth\left[\pi\cdot\sqrt{m^2 - (A2)^2}\right]$$

$$F := \left(\sin\left(m\cdot\theta 1_r\right) - \sin\left(m\cdot\theta 2_r\right)\right)\cdot\left[\sinh\left[\sqrt{m^2 - (A2)^2}\cdot\theta 3_{rr}\right] - \sinh\left[\sqrt{m^2 - (A2)^2}\cdot\theta 4_{rr}\right]\right]$$

$$G := m\cdot\left[m^2 - (A2)^2\right]\cdot\sinh\left[\pi\cdot\sqrt{m^2 - (A2)^2}\right]$$

$$Zqq\beta 11 := \begin{array}{|l}
r \leftarrow 0 \\
\text{for } i \in 1,2.. N \\
\quad\begin{array}{|l}
rr \leftarrow 0 \\
\text{for } j \in 1,2.. N \\
\quad\begin{array}{|l}
\theta 1_r \leftarrow \dfrac{\pi}{a2}\cdot\left[\left(i\cdot\dfrac{a2}{N+1}\right) + \dfrac{w}{2}\right] \\[2mm]
\theta 2_r \leftarrow \dfrac{\pi}{a2}\cdot\left[\left(i\cdot\dfrac{a2}{N+1}\right) - \dfrac{w}{2}\right] \\[2mm]
\theta 3_{rr} \leftarrow \dfrac{\pi}{a2}\cdot\left[\left(j\cdot\dfrac{a2}{N+1}\right) + \dfrac{w}{2}\right] \\[2mm]
\theta 4_{rr} \leftarrow \dfrac{\pi}{a2}\cdot\left[\left(j\cdot\dfrac{a2}{N+1}\right) - \dfrac{w}{2}\right] \\[2mm]
Z_{r,rr} \leftarrow \dfrac{i\cdot\omega\cdot h\cdot\mu}{w^2}\cdot\left[\begin{array}{l}\left[\dfrac{-w^2}{(k)\cdot a2}\cdot\cot(\pi\cdot A2)\right] + \left[\dfrac{w\cdot\left(\sin\left(A2\cdot\theta 4_{rr}\right) - \sin\left(A2\cdot\theta 3_{rr}\right)\right)}{(k)^2\cdot a2\cdot\sin(\pi\cdot A2)}\right]\ldots \\[3mm] + \left[\dfrac{a2^2\cdot 2}{\pi^3}\cdot\displaystyle\sum_{m=1}^{10}(D\cdot E)\right]\ldots \\[3mm] + \left[\dfrac{2\cdot a2^2}{\pi^3}\cdot\displaystyle\sum_{m=1}^{10}(-1)^m\cdot\left(\dfrac{F}{G}\right)\right]\end{array}\right] \\
\end{array} \\
\quad rr \leftarrow rr + 1 \\
r \leftarrow r + 1 \\
Z
\end{array}$$

$$H := \frac{w \cdot \left[\sin\left[A2 \cdot \left(\pi - \theta 3_{rr} \right) \right] - \sin\left[A2 \cdot \left(\pi - \theta 4_{rr} \right) \right] \right]}{(k)^2 \cdot a2 \cdot \sin\left(\pi \cdot A2 \right)}$$

$$I := \frac{(-1)^m \cdot \left(\sin\left(m \cdot \theta 1_r \right) - \sin\left(m \cdot \theta 2_r \right) \right) \cdot \left(\sin\left(m \cdot \theta 3_{rr} \right) - \sin\left(m \cdot \theta 4_{rr} \right) \right)}{m^2 \cdot \left[\sqrt{m^2 - (A2)^2} \right] \cdot \sinh\left[\pi \cdot \sqrt{m^2 - (A2)^2} \right]}$$

$$J := \frac{\left(\sin\left(m \cdot \theta 1_r \right) - \sin\left(m \cdot \theta 2_r \right) \right) \cdot \left[\sinh\left[\sqrt{m^2 - (A2)^2} \cdot \left(\pi - \theta 3_{rr} \right) \right] - \sinh\left[\sqrt{m^2 - (A2)^2} \cdot \left(\pi - \theta 4_{rr} \right) \right] \right]}{m^2 \cdot \left[m^2 - (A2)^2 \right] \cdot \sinh\left[\pi \cdot \sqrt{m^2 - (A2)^2} \right]}$$

$Zqq\beta12 :=$

$r \leftarrow 0$

for $i \in 1, 2 .. N$

$\quad rr \leftarrow 0$

$\quad$ for $j \in N + 1, N + 2 .. 2 \cdot N$

$$\theta 1_r \leftarrow \frac{\pi}{a2} \cdot \left[\left(i \cdot \frac{a2}{N + 1} \right) + \frac{w}{2} \right]$$

$$\theta 2_r \leftarrow \frac{\pi}{a2} \cdot \left[\left(i \cdot \frac{a2}{N + 1} \right) - \frac{w}{2} \right]$$

$$\theta 3_{rr} \leftarrow \frac{\pi}{a2} \cdot \left[\left[(j - N) \cdot \frac{a2}{N + 1} \right] + \frac{w}{2} \right]$$

$$\theta 4_{rr} \leftarrow \frac{\pi}{a2} \cdot \left[\left[(j - N) \cdot \frac{a2}{N + 1} \right] - \frac{w}{2} \right]$$

$$Z_{r, rr} \leftarrow \frac{i \cdot \omega \cdot h \cdot \mu}{w^2} \cdot \left[\frac{w^2}{(k) \cdot a2 \cdot \sin(k \cdot a2)} - (H) \; ... \right.$$
$$\left. + \left(\frac{-a2^2 \cdot 2}{\pi^3} \cdot \sum_{m = 1}^{10} I \right) \; ... \right.$$
$$\left. + \left(\frac{2 \cdot a2^2}{\pi^3} \cdot \sum_{m = 1}^{10} J \right) \right]$$

$\quad\quad rr \leftarrow rr + 1$

$\quad r \leftarrow r + 1$

Z

$$\text{Zero} := \begin{array}{|l} r \leftarrow 0 \\ \text{for } i \in 1,2.. \text{ N-2} \\ \quad \begin{array}{|l} rr \leftarrow 0 \\ \text{for } j \in 1,2.. \text{ N-2} \\ \quad \begin{array}{|l} Z_{r,rr} \leftarrow i \cdot j \cdot 0 \\ rr \leftarrow rr + 1 \end{array} \\ r \leftarrow r + 1 \end{array} \\ Z \end{array}$$

$Zqq\beta21 := Zqq\beta12^{T}$

$Zqq\beta1t1 := \text{augment}(Zqq\beta11, Zqq\beta12)$

$Zqq\beta1t2 := \text{augment}(Zqq\beta21, Zqq\beta11)$

$Zqq\beta1 := \text{stack}(Zqq\beta1t1, Zqq\beta1t2)$

$Zqq\beta2 := Zqq\beta1$

$Zqq\beta t1 := \text{augment}(Zqq\beta1, \text{Zero})$

$Zqq\beta t2 := \text{augment}(\text{Zero}, Zqq\beta2)$

$Zqq\beta := \text{stack}(Zqq\beta t1, Zqq\beta t2)$

$Zpp\alpha := Zpp\gamma - \left[Zpq \cdot (Zqq\gamma - Zqq\beta)^{-1} \cdot Zqp\gamma \right]$

$$\text{Zero} := \begin{vmatrix} r \leftarrow 0 \\ \text{for } i \in 1,2.. \text{ N}\cdot 2 \\ \begin{vmatrix} rr \leftarrow 0 \\ \text{for } j \in 1,2.. \text{ N}\cdot 2 \\ \begin{vmatrix} Z_{r,rr} \leftarrow i\cdot j\cdot 0 \\ rr \leftarrow rr + 1 \end{vmatrix} \\ r \leftarrow r + 1 \end{vmatrix} \\ Z \end{vmatrix}$$

$$Zqq\beta 21 := Zqq\beta 12^{T}$$

$$Zqq\beta 1t1 := \text{augment}(Zqq\beta 11, Zqq\beta 12)$$

$$Zqq\beta 1t2 := \text{augment}(Zqq\beta 21, Zqq\beta 11)$$

$$Zqq\beta 1 := \text{stack}(Zqq\beta 1t1, Zqq\beta 1t2)$$

$$Zqq\beta 2 := Zqq\beta 1$$

$$Zqq\beta t1 := \text{augment}(Zqq\beta 1, \text{Zero})$$

$$Zqq\beta t2 := \text{augment}(\text{Zero}, Zqq\beta 2)$$

$$Zqq\beta := \text{stack}(Zqq\beta t1, Zqq\beta t2)$$

$$Zpp\alpha := Zpp\gamma - \left[Zpq\cdot(Zqq\gamma - Zqq\beta)^{-1}\cdot Zqp\gamma \right]$$